

The importance of benthic-pelagic coupling and spatial variability for deep-sea meiofauna

Cover illustration: Freija Hauquier

Cover digitalization: Torben Riehl

Illustrations between chapters: Autun Purser

Photographs between chapters: Guy de Smet, Torben Riehl, Ivan Voltski, Freija Hauquier, and Lidia Lins Pereira

Printed by:



Reproduct nv,
Voskenslaan 205
9000 Gent

Marine Biology Research Group
Campus Sterre – S8
Krijgslaan 281
B – 9000 Gent

Belgium

Academic Year 2016 – 2017

Publically defended on December 16th, 2016

Chairman at the defense: Prof. Dr. Koen Sabbe

For citation to published work reprinted in this thesis, please refer to the original publications.

Lins Pereira, L. (2016) The importance of benthic-pelagic coupling and spatial variability for deep-sea meiofauna. Ghent University (UGent), 290 pp.

The research leading to this thesis received funding from the Bijzonder Onderzoeksfonds (BOF, project number 12/DOS/006) and by fundação CAPES (grant number 11595/13-2)

Faculty of Sciences

The importance of benthic-pelagic coupling and spatial variability for deep-sea meiofauna

Lidia Lins Pereira

Supervisors:

Prof. Dr. Ann Vanreusel

Prof. Dr. André Morgado Esteves

Academic Year 2016 – 2017

Thesis submitted in partial fulfilment of the requirements for the degree of

Doctor in Science: Marine Sciences

Supervisors: Prof.Dr. Ann Vanreusel
Prof. Dr. André Morgado Esteves

MEMBERS OF THE COMMITTEE:

Prof. Dr. Koen Sabbe – Chairman, Ghent University

Prof. Dr. Angelika Brandt – University of Hamburg, Hamburg

Dr. Daniel Leduc – NIWA, Wellington

Prof. Dr. Magda Vincx – Ghent University

Dr. Jan Vanaverbeke – Ghent University

Dr. Ellen Pape – Ghent University

Prof. Dr. Ann Vanreusel – Ghent University *

Prof. Dr. André Morgado Esteves*

*non-voting member

THESIS DEFENDED IN PUBLIC:

Friday, 16 December 2016 at 17:00 h

Leszaal Jans Jacob Berzelius – Ghent University

Sterrecampus S3 – Krijgslaan 281 – B-9000 Ghent

20,0 μm



Table of contents

Acknowledgements	XIV
Samenvatting	XXII
Summary	XXXIV
List of Figures	XLIV
List of Tables	LII
Chapter 1: General Introduction	1
1.1 A glimpse of the deep-sea environment.....	1
1.1.1. The meiobenthos and nematodes.....	6
1.2 Main factors driving biodiversity, abundance, and biomass in the deep sea	8
1.2.1 Benthic-pelagic coupling	8
1.2.2 Spatial variability and patch-mosaic dynamics.....	12
1.2.3 Dispersal and distribution in the deep sea	16
1.3 Study areas	
1.3.1 The Western Iberian Margin (300–1000 m)	21
1.3.2 The Vema Fracture Zone (4900–5700 m).....	23
1.3.3 The Atlantic sector of the Southern Ocean (3700–4100 m).....	25
1.4 International Framework	27
1.5 Aims and Outline of the thesis	30
Chapter 2: The link between meiofauna and surface productivity in the Southern Ocean	37
2.1 Abstract.....	37

2.2 Introduction.....	38
2.3 Material and methods.....	41
2.3.1 Study area and sampling procedure	41
2.3.2 Meiofauna sample processing	43
2.3.3 Environmental parameters	44
2.3.4 Data analysis	45
2.4 Results.....	46
2.4.1 Trends in NPP and estimated POC flux	46
2.4.2 Benthic environment and metazoan meiofauna	48
2.4.3 Relation between environmental data and meiofaunal densities	51
2.5 Discussion	52
2.5.1 Trends in NPP and estimated POC flux	52
2.5.2 Benthic-pelagic coupling	54
2.6 Supplementary data.....	57
Chapter 3: Nematode community composition and feeding shaped by contrasting productivity regimes in the Southern Ocean.....	65
3.1 Abstract.....	65
3.2 Introduction.....	66
3.3 Material and methods.....	70
3.3.1 Sampling and study area	70
3.3.2 Sediment analyses.....	72
3.3.3 Surface environmental parameters.....	74
3.3.4 Nematodes	74

3.3.5 Nematode respiration.....	76
3.3.6 Data analysis.....	76
3.4 Results.....	80
3.4.1 Environmental variables.....	80
3.4.2 Nematode community and biomass	81
3.4.3 Nematode species	84
3.4.4 Nematode fatty acids.....	86
3.4.5 Structural and functional nematode diversity and nematode respiration rates	88
3.4.6 Correlation between environmental variables and nematode community structure, biomass and total FA	88
3.5 Discussion	91
3.5.1 Surface primary productivity, sedimentary pigments and nematode standing stocks	91
3.5.2 Nematode community structure	93
3.5.3 Nematode fatty acids.....	95
3.5.4 Nematode function, taxon diversity and respiration.....	99
3.5.5 Environmental drivers of nematode standing stocks	100
3.6 Conclusions	101
3.7 Supplementary data	102
Chapter 4: Testing deep-sea biodiversity paradigms on abyssal nematode genera and <i>Acantholaimus</i> species	115
4.1 Abstract.....	115

4.2 Introduction.....	116
4.3 Material and methods.....	120
4.3.1 Sampling and study area	120
4.3.2 Environmental variables.....	124
4.3.3 Nematode sampling processing.....	125
4.3.4 Data analyses	126
4.4 Results.....	128
4.4.1 The deep sea is diverse at a local scale, but turnover is limited	128
4.4.2 Benthic-pelagic coupling and patch-mosaic dynamics.....	137
4.5 Discussion	141
4.5.1 The deep sea is diverse at a local scale, while turnover can be restricted	141
4.5.2 Deep-sea diversity does not increase with increasing organic matter input at a local scale.....	145
4.5.3 Increased patch dynamics (does not) increase local diversity	149
4.6 Conclusions	151
4.7 Supplementary data.....	153
Chapter 5: Evaluating environmental drivers of spatial variability in free-living nematode assemblages along the Portuguese margin.....	169
5.1 Abstract.....	169
5.2 Introduction.....	170
5.3 Material and methods.....	174
5.3.1 Sampling and study area	174
5.3.2 Sediment analyses.....	177

5.3.3 Nematode sample processing for community analyses	178
5.3.4 Data analysis.....	179
5.3.5 Molecular phylogenetic analyses of nematodes	181
5.4 Results.....	183
5.4.1 Environmental variables.....	183
5.4.2 Nematode community structure	185
5.4.3 Correlation between nematode community structure and environmental variables	189
5.4.4 Nematode molecular phylogenetic analyses	191
5.5 Discussion	193
5.5.1 Sediment heterogeneity in combination with increased amount and patchiness of food resources contributes to a higher beta diversity.....	194
5.5.2 Beta diversity between different bathymetric transects is higher than beta diversity across similar depths	198
5.5.3 Absence of depth-specific clades.....	199
5.6 Conclusions	202
5.7 Supplementary data	205
Chapter 6: General discussion on patterns and processes elucidating nematode assemblage structure	231
6.1 Patterns of nematode diversity, density and biomass in the deep sea.....	231
6.1.1 Local and regional diversity, density, and biomass.....	231
6.2 What drives alpha and beta diversity in the deep sea?	239
6.2.1 Environmental factors.....	239

6.2.2 Spatial variation in nematode composition (bathymetrical and geographical patterns) 246

6.2.3 Non-ecological drivers of nematode diversity 250

6.3 Research constraints and future perspectives 252

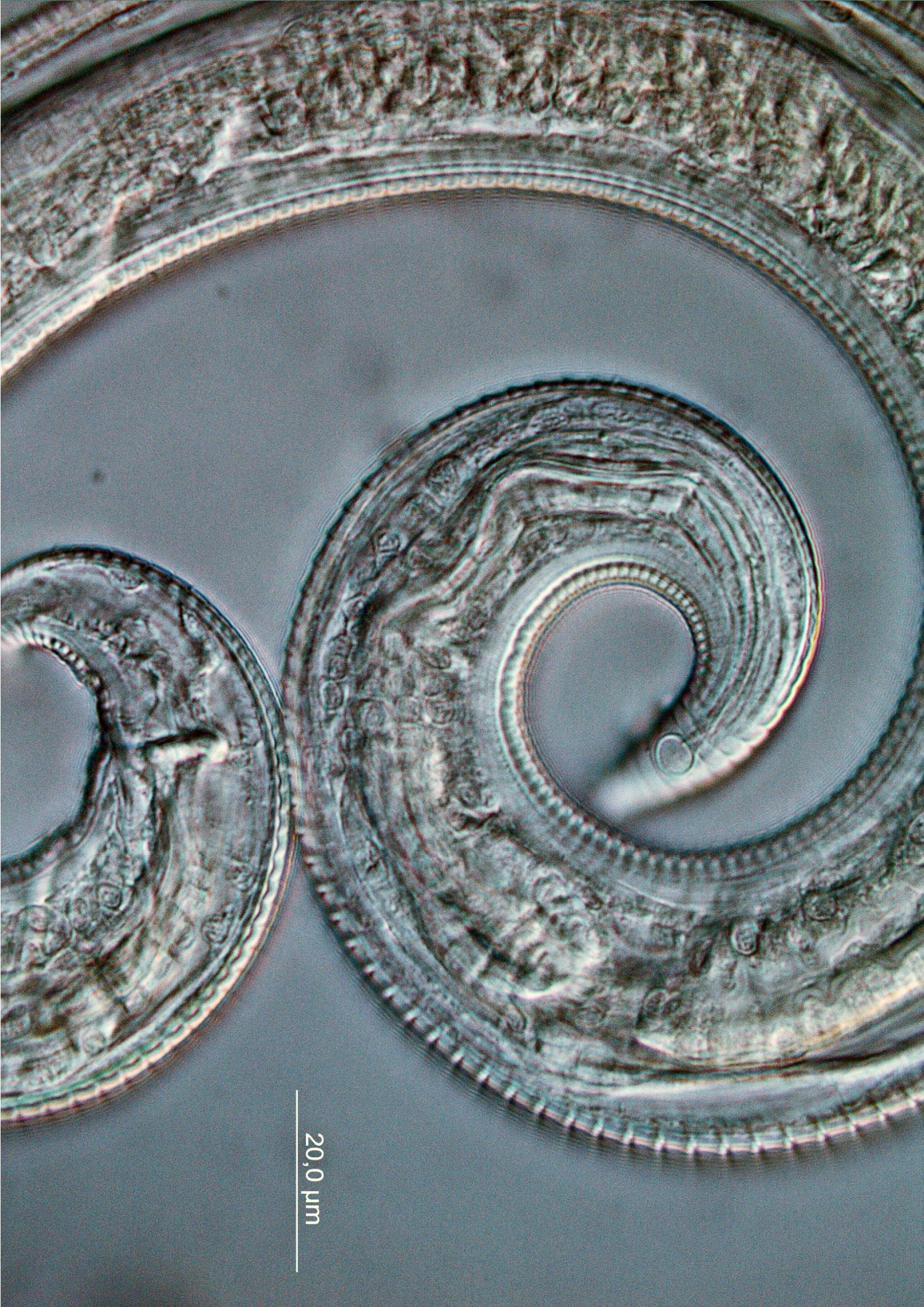
Cited literature..... 260

List of publications 286

A1 Publications 287

C2 Publications (Dissertations, essays, internal reports, and conference abstracts) . 288

Websites 290



20,0 μ m

Acknowledgements

“Working hard for something we don’t care about is called stress; working hard for something we love is called passion” Simon Sinek

Many people live FOR their PhD. Instead, I decided to live my PhD. Living my PhD not only implied that I would need good scientific skills as I thought before, but also many other aspects and fields of my life were involved. In my case, coming from another extreme end country, where culture and temperature were extremely different, I also had to adapt to the lack of hugs by introducing them into my new world. Therefore, a PhD for me was not only to develop new ideas and execute them, and also write about them. A PhD for me was also to meet new people from all over the world, travel everywhere and work with people from everywhere, participate in many campaigns, learn 3 languages, hate myself, love myself, hate myself again. A PhD for me was to discover that wool is warmer than cotton, that the snow is beautiful and that the difference between different cultures and different people is something amazing. Living my PhD was evolving as a human being, knowing more about myself, rediscover myself, and adding a bit of Belgium and of the world into myself. I will carry all of this with me for the rest of my life.

Ann. Meer dan een promotor, mijn leermeester. Voor bazen doe je gewoon wat ze willen, zonder het recht te hebben om hen in vraag te stellen, voor een leermeester heb je respect en bewondering. Sinds het begin heeft Ann altijd mijn suggesties en ideeën gerespecteerd en aangemoedigd met groot enthousiasme. Ik voelde me thuis bij haar, die steeds openstond voor discussies reikend van wetenschap tot familie aangelegenheden. Ze heeft me ook geleerd wat eerlijke wetenschap is, om samen te werken met andere mensen, om me beter te voelen toen ik ontdekte dat de wetenschappelijke wereld niet zo mooi is als ik dacht. Heel erg bedankt voor alles!

André. Desde o bacharelado sempre ao meu lado apoiando (quase) todas as minhas decisões e me incentivando a voar cada vez mais alto à procura de meus sonhos. Obrigada

por me respeitar, por sempre fazer tudo o que estava ao seu alcance e por me deixar livre para decidir o que me deixa mais feliz.

Jury. I would like to thank all the jury members who dedicated their valuable time to read this thesis. I feel very honoured for your acceptance to be part of this jury and for contributing significantly to a much improved thesis. Thank you Dr. **Daniel Leduc** for your very detailed and helpful comments, I admire you a lot as a scientist. Thank you Prof. Dr. **Angelika Brandt**, for your comments, your kindness, and your great strength as a scientist which inspire us women to look forward. I am also grateful to Dr. **Ellen Pape**, for seeing all the small mistakes I have not noticed before, and Prof. Dr. **Magda Vincx**, for asking those questions which challenge us scientists to think thirty minutes before an answer is able to come to mind. I am also thankful to Dr. **Jan Vanaverbeke**, whom I respect for his great intelligence, but also ‘to the point’ questions and openness in science, and to the chairman Prof. Dr. **Koen Sabbe**, for being an excellent chairman.

Laboratório de Meiofauna. Gostaria de agradecer à Prof. **Verônica** Genevois por ter acreditado em mim desde o início. Seu entusiasmo será sempre lembrado com carinho. Às minhas mães **Rita** e **Cris**, que me ensinaram desde a lavar amostras até identificar Nematoda. Meu carinho por vocês é muito especial e me faz um bem danado quando as vejo. Ao meu pai **Neyvan**, por todas as lasanhas e o apoio desde que cheguei ao laboratório. À **Patrícia**, compartilhar o laboratório com você é sempre mais divertido, obrigada também por todo o apoio científico. Queria agradecer também à **Tarci, Mário, Paulo, Vivi, Rafa, Iza, Neide, Ju, Alex, Alexandre, Beta e Virág**.

Mijn vijf engelen. **Dirk** van Gansbeke en **Bart** Beuselinck, die me geholpen hebben met (bijna) al mijn abiotische analyses. Zonder jullie zou mijn doctoraat een paar maanden later klaar geweest zijn. Mijn derde engel is **Annelien** Rigaux. Bedankt voor de hulp met mijn moleculair werk en ook voor jouw vriendschap (en voor jouw taartjes). De laatste twee hadden een antwoord op al mijn vragen: **Annick** van Kenhove en **Guy** de Smet. Als de ene het antwoord niet wist, kon ik zeker terecht bij de andere. Ze hebben me niet alleen geholpen met het labo werk, maar ze waren er altijd, in goed en kwade tijden. Steeds met de juiste woorden of met een knuffel. Jullie hebben een grote hart.

Co-authors. A work conducted together has always more power than doing it alone. I appreciate a lot the outstanding skills of **Renata** Alves, **Frederik** Leliaert, **Cristina** Silva, **Katja** Guilini, **Torben** Riehl, **Gritta** Veit-Köhler, **Sofia** Ramalho, **Nico** Augustin, and **Eliana** Cordova. Without you my work would never have the same quality. Thank you for your collaboration.

Marbiol. This is a big chapter of my life. Many people went away, many new people arrived. I would like to thank my colleagues for all the good and bad moments we spent together, each of you had a significant impact on who I am now. Thanks to **Isolde**, **Quang**, **Iván**, **Elise**, **Jeroen**, **Delphine**, **Rasha**, **Francesca**, **Jelle**, **Annelies**, **Mohammed**, **Ulrike**, **Tom**, **Marleen**, **Thibaud**, **Niels**, **Eva**, **Lara**, **Lisa**, **Kenny**, **Xiuqin**, **Nele**, **Freija**, **Sebastian**, **Pieterjan**, **Jan Reubens**, **Jan Vanaverbeke**, **Carl**, **Ana-Maria**, **Christoph**, **Eezin**, and **Yana**. Especial thanks to **Bart**, **Liesbet**, **An-Sofie**, **Luana**, **Freija**, and **Ellen**, for sharing more than a dance with me. **Ellen**, you are the craziest friend I have by far. I love the fact that I can always tell you what I think about something. This gives me the freedom to always be honest with you without the feeling that you will

misunderstand me. **Freija**, thank you so much for your friendship this beautiful drawing, now I can say I have the most beautiful PhD cover ever! **An-Sofie**, you have an unbelievable good heart, I am very happy I found such a good person like you in this World. Thank you **Katja**, for sharing an office, coffee, chocolates, children drawings, and laughs, with this crazy Brazilian. And lastly I would like to thank **Tânia**, for your friendship and for accepting me as a drama queen. Everything we shared in this last seven years I will never forget, you were there for me since my first birthday in the snow. Obrigada por tudo! **Nic Smol** and Prof. **Wilfrida Decraemer**, thank you for your guidance and sharing your heart with the nematology students.

Karina. Some people will have an impact on your life that will be remembered forever. Karina, without you I don't know if I would have made it so peacefully to where I am now. You are one of the few persons who made me find who I am, accept myself and be happy with it. With you I can talk for hours and be 100 % myself without expecting judgements and critics in return. It is difficult to express in words how much I appreciate our talks and views of the world. You and **Niel** are an exception in this world, you two make the world more beautiful.

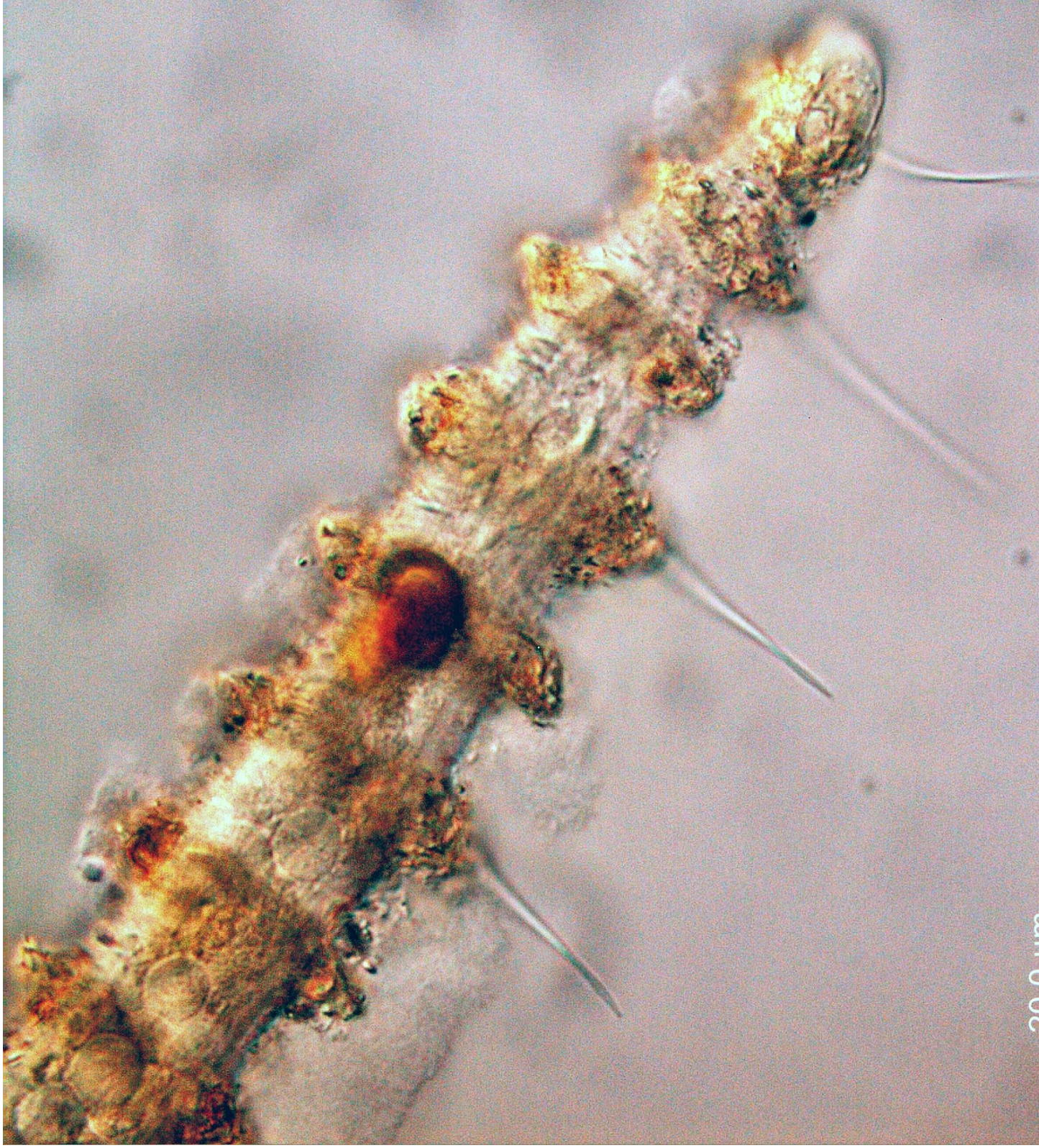
Friends (other). I am really grateful for having **Inge** and **Daniel** in my life. They were ALWAYS there for me, celebrating my successes but also taking care of me when I was sick or had to move all my stuff to another flat (by bus). I am lucky to have you two in my life. I also want to thank the 'dinsdagbende', **Jamie**, **Michael**, **Sofietje**, **Soph**, **Andries**, **Elisa**, **Bréandan**, **Roderic**, **Bartje**, **Liselotte**, **Pieter** and **Charlotte**. A special thanks to **Charlotte**, my first and long lasting Belgian friend. Whom I could always count on and laugh together. I would like to thank my friend **Tom Mockett**, for all the long and funny

conversations we had together. **Yirina**, you made my adaptation phase here in Belgium smoother and happier. I love your food and the many moments we shared together. Even being far away, **Tadeu, Lucas, Luiza e Priscilinha**, pra mim foi sempre bom saber que vocês estavam sempre comigo mesmo de longe. Thank you **Sara** and **Laetitia** for our laughs and baby monkey songs. Thank you **Autun** for your very beautiful drawings and for the unforgettable moments we spend together on the Sonne.

Aikido family. Je voudrais remercier de tout mon cœur ma deuxième famille ici en Belgique. Elle était avec moi dès le début de tout. L'Aikido était longtemps le seul endroit où j'ai trouvé l'amour, les sourires, les amis. Quand j'y allais, j'avais toujours le sourire sur le visage. Un grand merci à mon professeur **Stéphane** Goffin, pour tous les enseignements et pour l'amitié. Merci **Laetitia**, pour toujours me faire sentir accueillie. **Jean-Christophe** et **Stany**, merci pour votre amitié, pour m'avoir fait rire, pour la pratique et pour venir me chercher à la gare toutes les semaines. Merci aussi à **Anne, Gilles, Julie, Eric, Laurence, Alexandre** et **Jean**.

Family. Minhas pérolas, meus tesouros. Eu amo vocês mais do que tudo nessa vida. **Laís, Sandra e Aguinaldo**. Sempre comigo, sempre ao meu lado nos bons e menos bons momentos. Cada dia eu me sinto agradecida por tê-los em minha vida, por terem me apoiado e por terem me aceitado do jeito que eu sou, com ou sem pijama dentro de casa. Vocês me fazem sentir que não estou sozinha nesse mundo, que a qualquer momento eu posso voltar para um lugar chamado lar se algo imprevisto acontecer. Vocês estão sempre no meu coração. Também queria agradecer aos outros membros da família buscapé: **Simmone, Shirley, Luiz Carlos, Toninho, Wagner, Jairo, Aline, Arthur e Babi**. Aos meus irmãos **Ana e André**, e aos meus avôs e avós, **Lucy, Carlos, Sebastiana e Euclides**

Schnuki. Du bist recht spät gelandet! Ich habe dich eher erwartet. Seit deiner Ankunft war ich von Gefühlen überwältigt, die ich nie zuvor für jemanden gespürt habe. Ich hätte nie gedacht, dass ein Deutscher so lieb und einfühlsam sein kann, wie du. Ich liebe jede Seite an dir, von deinen Qualitäten bis hin zu deinen Fehlern. Wirklich, seit du da bist, hast du mir gezeigt, dass jemanden lieben heißt, ein Wegbegleiter zu sein, gemeinsam (köstliche) Mahlzeiten zu genießen, zusammen zu reisen, gemeinsam Artikel zu besprechen (das konnten wir nicht verhindern) und sogar zusammen am Wochenende zu arbeiten, weil du eine verrückte Freundin hast, die ihre Promotion schreiben muss. Ich bin so dankbar, dich in meinem Leben zu haben, du bist mehr als etwas Besonderes, du hast ein großes Herz.



20,0 μm

Samenvatting

De diepzee die een overgroot deel van onze oceanen omvat, reikt tot 11000 m diep en is daarmee één van de grootste leefgebieden op aarde. Alhoewel dit afgelegen gebied reeds 150 jaar uitgebreid onderzocht wordt, is onze kennis van de verschillende ecosystemen in de diepzee en hun biodiversiteit relatief beperkt en het onderzoek ernaar uitdagend. Met toenemende waterdiepte stijgt de druk, daalt de temperatuur en neemt de lichtintensiteit en daarmee ook de fotosynthese af. In het begin van de negentiende eeuw achtte men deze barre omstandigheden verantwoordelijk voor het bemoeilijken van het leven in de diepzee en het verhinderden van onderzoek. Dat idee lag aan de basis van de “Azoic theory” (Edward Forbes, 1844), in die tijd algemeen geaccepteerd door de wetenschappelijke gemeenschap. Pas tijdens de laatste decennia zagen we een snelle evolutie in het wetenschappelijk onderzoek in de diepzee, mede dankzij de technologische vooruitgang die de ontdekkingen van deze nieuwe omgevingen en bijzondere organismen mogelijk heeft gemaakt.

In de jaren '60 gooide men het idee van een azoïsche omgeving compleet overboord en beschouwde men de biodiversiteit in de diepzee veel groter dan in ondiepe gebieden. De vraag die echter bleef gesteld worden was: Hoe kunnen zoveel soorten overleven in deze diepzee-omgeving? De co-existentie van soorten in de diepzee wordt verondersteld vooral gevormd te worden door de beschikbaarheid van voedsel, heterogeniteit van sedimenten, hydrodynamische regimes, beschikbaarheid van zuurstof en verstoring. Het effect van elk van deze omgevingsfactoren hangt echter af van het onderzochte organisme en de schaal waarop het effect onderzocht wordt. Voor meiofauna ($< 1\text{mm}$), bijvoorbeeld, wordt aangenomen dat kleinschalige processen een grote rol te spelen in het reguleren van de gemeenschap en de co-existentie van soorten in de diepzee. Nematoden, de meest abundante meercellige meiofauna groep, vertonen een grote soortendiversiteit in de diepzee, terwijl verschillende daartoe behorende taxa ook wijdverspreid voorkomen. Door hun kosmopolitisme en aanwezigheid in relatief hoge abundantie en diversiteit, vormen

nematoden de ideale organismen om de link te bestuderen tussen diversiteit en omgevingsprocessen die de bodem van de diepzee beïnvloeden.

De algemene doelstelling van dit doctoraatsonderzoek was het verkrijgen van meer inzicht in de distributie van nematodentaxa, trofische interacties, en de benthopelagische koppeling in de diepzee, alsook om na te gaan welke omgevingsfactoren het meest bepalend zijn in het structureren van nematodengemeenschappen en de co-existentie van soorten. De belangrijkste onderzoeksvragen die gesteld werden zijn: Is de diepzee divers in termen van meiofauna? Is er een link tussen primaire productie aan het wateroppervlak en meiofauna densiteit, diversiteit en biomassa? Wordt deze potentiële link ook gereflecteerd in de samenstelling van de nematodengemeenschap? Voeden nematoden selectief in de diepzee afhankelijk van de verschillende concentraties en de kwaliteit van het organische materiaal dat beschikbaar is in hun directe omgeving? Zijn er verschillen in nematodengemeenschappen tussen oligotrofe en eutrofe regio's? Indien dit het geval is, op welke schaal stellen we die verschillen vast? Veroorzaakt waterdiepte een verschil in de samenstelling van nematodengemeenschappen? Veroorzaken verschillen in *patch-mosaic dynamics* verschillen in de diversiteit van de nematodengemeenschap?

Het antwoord op deze vragen werd gezocht op basis van onderzoek die in drie regio's: twee in de Noord-Atlantische Oceaan (Westelijke Iberische Rand en Vema Fracture Zone) en één in de Zuidelijke Oceaan. Het onderzoek in het gebied in de Zuidelijke Oceaan werd uitgevoerd tijdens twee wetenschappelijke campagnes aan boord van de RV Polarstern (ANT-XXIV/2 en ANT-XXVIII/3 cruises), en vond plaats op waterdieptes tussen 1951 en 5323 m, langsheen een noord-zuid en oost-west transect. Het onderzoeksgebied werd gekarakteriseerd door slib-klei sedimenten en gepulste voedseltoevoer. Negen stations werden onderzocht (in totaal 27 MUC corers) in het kader van de projecten ANDEEP-SYSTCO en SYSTCO II. Het gebied op de Westelijke Iberische Rand werd onderzocht tijdens twee wetenschappelijke campagnes aan boord van de RV Belgica (B2013/17 en

B2014/15 cruises), en omvatte waterdieptes tussen 290 en 1006 m en twee isobatische transecten parallel met de kust. De twee onderzochte transecten (één op de rand van het continentaal plat en de ander bovenaan de continentale helling) vertoonden verschillende omgevingskenmerken. Het transect bovenaan de continentale helling werd gekenmerkt door slib-kleiige sedimenten en lage toevoer aan organisch materiaal, terwijl the transect langs de rand van het continentaal plat gekenmerkt werd door hoge heterogeniteit in de sedimentsamenstelling en hoge beschikbaarheid aan voedsel. Er werden tien stations onderzocht (34 MUC corers in totaal) in het kader van dit doctoraatsproject dankzij de BOF toelage 12/DOS/006. Het derde onderzochte gebied maakt deel uit van de Vema Fracture Zone en de Vema Transform Fault, die de Mid-Atlantische Rug kruisen op circa 10°N. Dit gebied werd onderzocht tijdens één wetenschappelijke campagne aan boord van de RV Sonne (SO 237 cruise) en omvat waterdieptes tussen 4998 en 5771 m. Kenmerkend voor dit onderzoeksgebied zijn de voornamelijk slib-kleiige sedimenten, alhoewel ook zeer fijn, fijn en grof zand werd gerapporteerd, en de lage toevoer aan voedsel door het gebrek aan seizoenale periodes van hoge productiviteit aan het wateroppervlakte. Zes stations werden onderzocht (17 MUC corers in totaal) in het kader van het Vema-TRANSIT project.

In **Hoofdstuk 1** wordt een overzicht geboden aan relevante achtergrondinformatie gerelateerd aan de diepzee-omgeving, het meiobenthos en nematoden, en de belangrijkste structurerende factoren voor benthische biodiversiteit in de diepzee.

In **Hoofdstuk 2** onderzoeken we op macroschaal niveau wat de link is tussen meiofauna diversiteit, densiteit en biomassa op hoger taxon niveau en de omgevingsvariabelen die gelinkt zijn aan voedselbeschikbaarheid. De gegevens rond de structuur van de meiobenthische gemeenschap waren afkomstig van twee transecten in het Atlantische deel van de Zuidelijke Oceaan. Het eerste Noord-Zuid transect was gelegen langs de nulmeridiaan en het tweede Oost-West transect langs het Polaire Front. In deze studie testten we in welke mate de structuur van de meiofauna gemeenschap (1951 – 5323 m

waterdiepte) geassocieerd was met omgevingsvariabelen die gerelateerd zijn aan de input aan organisch materiaal zoals de primaire productiviteit aan het wateroppervlak, de chlorofyl a concentratie, en de flux aan deeltjes organische koolstof (POC) naar de zeebodem. De resultaten toonden aan dat nematoden domineren (84.4–92.4 %) op elk site en dat er een significante toename is in relatieve abundantie en densiteit van deze groep in westelijke richting, geassocieerd met een parallelle toename in primaire productie in het wateroppervlak en chlorofyl a. Langsheen het Noord-Zuid transect werden geen significante correlaties gevonden tussen meiofauna densiteit of biomassa en omgevingsvariabelen, terwijl hogere geschatte POC fluxen in de sites ten zuiden van het Polaire Front gerelateerd waren aan hogere meiofauna diversiteit en densiteit in vergelijking met sites ter hoogte van het Polaire Front. Deze studie concludeert dat densiteiten van meiofauna mogelijks deels afhankelijk zijn van de primaire productiviteit aan het wateroppervlak als hun primaire voedselbron, ongeacht de grote waterdiepte. Alhoewel de POC flux niet algemeen gerelateerd was aan de toename in meiofaunadensiteiten, is er een duidelijk onderscheid tussen sites ten zuiden van het Polaire Front gekenmerkt door hogere meiofauna abundanties en POC fluxen, en de sites ter hoogte van het Polaire Front gekenmerkt door lagere meiofauna abundanties en POC fluxen.

Langsheen hetzelfde Oost-West transect in de Zuidelijke Oceaan, exploreer ik in **Hoofdstuk 3** in welke mate de primaire productiviteit aan het wateroppervlak en de benthische omgevingsvariabelen gereflecteerd zijn in de standing stock en de gemeenschapsstructuur van nematoden. Deze bentisch-pelagische koppeling werd ook onderzocht aan de hand van vetzuurtechnieken, waarbij de voedselselectiviteit van “bulk” nematoden en specifieke nematoden taxa (*Desmodora* en Desmoscolecidae) werd getest. De resultaten tonen aan dat het South Georgia site (NW van South Georgia Island en de meest westelijke locatie in deze studie) niet enkel de hoogste primaire productiviteit aan

het wateroppervlak kende, maar ook de hoogste concentraties aan chlorofyl a en vetzuren bevatte in het sediment, alsook hogere densiteiten en biomassa van nematoden. Vetzuurresultaten voor “bulk” nematoden, het genus *Desmodora*, en de family Desmoscolecidae suggereren een planktonisch dieet vooral gebaseerd op diatomeeën in South Georgia. Nematoden vanuit andere sites ten oosten van South Georgia, gekenmerkt door lagere primaire productiviteit aan het wateroppervlak en lage chlorofyl a concentraties in het sediment, vertoonden geen voorkeur voor verse diatomeeën op basis van hun vetzuurcompositie. Het genus *Desmodora*, die gekenmerkt wordt als een epistratumvoeder en gewoonlijk niet vaak gevonden wordt in de typische zachte sedimenten in de diepzee, werd in deze studie in hoge densiteiten gevonden in South Georgia, waarschijnlijk als een reactie op de verhoogde primaire productiviteit aan het wateroppervlak, wat de benthopelagische koppeling bevestigt, zelf op grote diepte. In conclusie, deze studie suggereert dat veranderingen in *standing stocks* en de gemeenschapssamenstelling van nematoden, alsook voedselselectiviteit van nematoden, positief geassocieerd zijn en beïnvloed worden door primaire productiviteitsregimes aan het wateroppervlak.

In de daaropvolgende studie wilden we nagaan of de aanwezigheid van een eerder ongewone diepzeenematodengemeenschap (bijvoorbeeld dominantie van *Desmodora*) in de Zuidelijke Oceaan gerelateerd was aan de primaire productie aan het wateroppervlak.

Hoofdstuk 4 richt zich op de vergelijking van nematodengemeenschappen tussen eutrofe en oligotrofe abyssale omgevingen, de Zuidelijke en de Noord-Atlantische Oceaan, respectievelijk, om na te gaan of verschillen in biodiversiteit gevormd kunnen worden door omgevingsfactoren aan het wateroppervlak en de zeebodem en op welke schaal dit van toepassing is. Drie hoofdzaken werden getest: (1) de diepzee is een zeer diverse omgeving op lokale schaal, maar ruimtelijke turnover is gelimiteerd op genus- en soortenniveau; (2) veranderingen in biodiversiteit worden gedreven door veranderingen in de aard en de

hoeveelheid aan input van organisch materiaal; (3) *patch-mosaic dynamics* drijven lokale diversiteit. Om deze hypothesen te testen bestudeerden we de diversiteit en densiteit van de nematodengemeenschap en de diversiteit van een typisch diepzeegenus *Acantholaimus*. Biodiversiteit werd vergeleken op vier verschillende niveaus: tussen stalen (m.a.w. alfa-diversiteit), tussen sites (m.a.w. beta-diversiteit), tussen sites van dezelfde regio, en tussen regio's. De resultaten bevestigen een hoge lokale alfa diversiteit zoals eerder geobserveerd voor de diepzee, terwijl regionale diversiteit verschillend was voor beide transecten, wat erop wijst dat turnover beïnvloed kan worden door verschillende omgevingsfactoren. Hoge primaire productie in oppervlaktewateren was positief gecorreleerd met de densiteit van nematoden, terwijl diversiteit geen relatie vertoonde met toenemende input aan organisch materiaal. Nematodengemeenschappen in gebieden die gekenmerkt werden door een constante maar lage voedseltoevoer vertonen sterke overeenkomsten die uit andere abyssale gebieden (bv. Noord-Atlantische Oceaan), terwijl de gemeenschappen uit hoogproductieve regio's gekenmerkt werden door verschillende dominante genera en *Acantholaimus* soorten en door een over het algemeen lagere lokale diversiteit. Deze resultaten stemmen overeen met de soorten-energie hypothese, die suggereert dat productiviteit een grens kan stellen aan de diversiteit van een ecosysteem. Tenslotte werd geen positieve correlatie vastgesteld tussen sedimentheterogeniteit en lokale diversiteit wat erop wijst dat alhoewel tussen de sites significante verschillen gevonden waren in granulometrie, die als onbelangrijk beschouwd konden worden in het bepalen van de structuur van de nematoden gemeenschappen in abyssale regio's.

In **Hoofdstuk 5** testen we of voedselbeschikbaarheid en heterogeniteit van het sediment de diversiteit van nematoden op lokale en regionale schaal beïnvloeden, op basis van een vergelijking tussen gemeenschappen bemonsterd langsheen twee parallelle transecten op de shelf break (300-400 m) en de upper slope (1000 m) van de westelijke Iberische

continentale rand (600 m waterdiepte en onderlinge afstand ~30 km). Veranderingen in diversiteit werden onderzocht op vier niveaus: binnen een staal (alfa-diversiteit), in een site (beta-diversiteit), tussen sites van hetzelfde dieptetransect, en tussen transecten. Hoge variabiliteit in voedselbeschikbaarheid en hoge heterogeniteit van het sediment in de sites op de shelf break waren sterk gerelateerd aan de hoge diversiteit binnen de sites, en hogere variatie in gemeenschapsstructuur tussen sites in vergelijking met het *upper slope* transect. De omgevingsfactoren (voedselbeschikbaarheid en sedimentsheterogeniteit), daarentegen, varieerden niet significant tussen sites op de *upper slope*. Dit gebrek aan verschil werd ook gereflecteerd in lage lokale diversiteit en turnover van de gemeenschap tussen de sites op de *upper slope*. Tenslotte waren de verschillen in nematodengemeenschappen tussen transecten groter dan de verschillen binnen ieder transect, en gingen de verschillen gepaard met veranderingen in de omgeving. Deze resultaten suggereren dat veranderingen in gemeenschapsstructuur eerder beïnvloed worden door omgevingsvariabelen dan door ruimtelijke verschillen op de Westelijke Iberische rand. Deze resultaten wijken af van de algemene trend van hoge diversiteit op de *slope* zoals eerder geobserveerd in andere studies.

Hoofdstuk 6 integreert en bediscussieert de belangrijkste bevindingen en inzichten in de ecologie van nematoden die verworven werden in de loop van dit doctoraatsonderzoek in een brede wetenschappelijke context. Daarnaast belichten we ook de belangrijkste beperkingen waarmee we tijdens deze studie geconfronteerd werden en de toekomstperspectieven voor het verder ontwikkelen van diepzee-onderzoek. Op basis van de resultaten werd een hogere lokale en regionale diversiteit vastgesteld op de westelijke Iberische rand en een lagere relatieve abundantie van de meest algemene genera, wat wijst op een gedeelde dominantie tussen vele verschillende genera. Diversiteit, densiteit en biomassa waren lager op de abyssale sites, waar de meest algemeen geobserveerde diepzeegenera domineerden. Veranderingen in diversiteit, densiteit en biomassa werden

toegeschreven aan veranderingen in omgevingsvariabelen. De heterogeniteit van het sediment stimuleerde diversiteit, terwijl de aanvoer aan organisch materiaal diversiteit bevorderde tot op zekere hoogte, waarna de afname in diversiteit toegeschreven werd aan de toename in dominante genera.

Tot slot biedt dit doctoraatsonderzoek nieuwe inzichten in de ecologie van meiofauna in de diepzee in termen van de distributie van meiofauna biodiversiteit, benthopelagische koppeling, en voedselselectiviteit. De belangrijkste verwezenlijkingen van dit werk zijn een overzicht van de distributie van nematodengemeenschappen in de diepzee op zowel grote (~1000 km) als kleine schaal (~100 m) en inzicht in hoe die beïnvloed worden door verschillen in omgevingsfactoren. We observeerden dat nematodengemeenschappen die voorkomen in voedselrijke omgevingen die gereguleerd worden door verstoring verschillen van degene die onderworpen zijn aan de gewoonlijke lage en constante voedseltoevoer. In onze onderzoeksgebieden nam de diversiteit af van de *shelf break* naar de *slope*, wat contrasteert met eerdere studies. Die afname werd toegeschreven aan de potentiële invloed van tijdelijke verstoring op de *shelf break*, die afgeleid werd uit de heterogeniteit van het sediment langsheen het transect. Daarenboven verschilde de regionale diversiteit langsheen de abyssale transecten, in die zin dat lage betadiversiteit geobserveerd werd in oligotrofe regio's en hoge betadiversiteit in eutrofe regio's; een bevinding die in contrast staat met resultaten uit eerdere studies. Deze verschillen in turnover trends werden mogelijk geregeld door verschillen in productiviteit aan het wateroppervlak, waarbij minder productieve regio's een typische diepzeegemeenschap voor zachtere sedimenten ondersteunt terwijl productieve regio's vooral gekenmerkt worden door een hogere turnover en onverwachte dominantie van atypische diepzeegenera. Bovendien suggereert het onderzoek naar de voedselselectiviteit van nematoden in de Zuidelijke Oceaan dat productiviteit de nematoden beïnvloedt, in die zin dat ze in staat zijn om zich te voeden met vers organisch materiaal wanneer dit voorhanden is, maar dat ze over het algemeen

afhankelijk zijn van refractorisch organisch materiaal wanneer vers materiaal schaars is. In conclusie, de resultaten van deze thesis stellen het al dan niet standhouden van enkele gevestigde paradigma's in diepzee onderzoek in vraag, tenminste met betrekking tot nematoden.

100 μm



Summary

Covering a vast proportion of the oceans and reaching water depths up to 11000 m lies one of the greatest habitats on Earth, the deep sea. Although this remote zone has been studied extensively since about 150 years ago, the comprehension of the various deep-sea ecosystems and their biodiversity is still a challenge. With increasing water depth, pressure increases and light begins to wane, together with a decrease in photosynthesis, temperature, and food resources. These considered “harsh” conditions were once thought to impede the blooming of life in the deep sea, and postponed deep-sea studies in the beginning of the nineteenth century, supported by the at that time widely accepted ‘Azoic theory’ (1844) of Edward Forbes. It was only during the last decades that deep-sea research has evolved at a fast pace, with the development of new technologies which have facilitated discoveries of new environments and peculiar organisms.

In the 1960’s, the idea of a faunal depauperate environment was completely abandoned and diversity in the deep sea was found to be much greater than in shallow-water environments. However, the question that remained was: How do so many species thrive in this ‘extreme’ environment? Species coexistence in the deep sea is believed to be mostly shaped by the same factors as observed in shallow waters: resource availability, sediment heterogeneity, hydrodynamic regimes, oxygen availability, and disturbance. However, the effect of these environmental drivers depends on the organism studied and at which spatial scale effects are investigated. For meiofauna (< 1mm), for instance, small-scale (mm to ~1000 m) processes are believed to play a major role in regulating community and species coexistence. Nematodes, the most abundant metazoan meiofauna group, exhibit high species diversity in the deep sea, and several taxa show a wide distribution. Due to their cosmopolitanism and high relative abundance and diversity, nematodes represent ideal organisms to study the link between diversity and environmental processes influencing the deep-sea bed.

The general objectives of this PhD were to gain further insight in nematode taxon distribution, trophic interactions, and benthic-pelagic coupling in the deep sea, as well as to investigate which environmental drivers are important in shaping nematode communities and species diversity. The main research questions tested were: Is the deep sea diverse at a local scale and turnover limited? is there a link between surface primary productivity and meiofauna density, biomass, and diversity? Is this potential link also reflected in the nematode community composition? Do nematodes feed selectively in the deep sea according to the different concentration and quality of organic matter present in their environment? Are there nematode community differences between oligotrophic and eutrophic regions? And if so, at which scale do these changes occur? Are there links between water depth and nematode community composition? Do changes in patch-mosaic dynamics shape nematode biodiversity?

In order to answer these questions, three studied regions were considered: two in the North Atlantic (Western Iberian Margin and Vema Fracture Zone) and one in the Southern Ocean. The Southern Ocean area was investigated based on two research campaigns on board of the RV Polarstern (ANT-XXIV/2 and ANT-XXVIII/3 cruises), and covered water depths between 1951 and 5323 m along a north-south and east-west transect. The studied area was characterized by silt-clay sediments and pulsed food input. Nine stations were investigated (in total 27 MUC cores) in the framework of the projects ANDEEP-SYSTCO and SYSTCO II. The Western Iberian Margin area was examined based on two research campaigns on board of the RV Belgica (B2013/17 and B2014/15 cruises), and covered water depths between 290 and 1006 m and two isobathic transects parallel to the coast. The two investigated transects (one on the shelf break and the other on the upper slope) exhibited divergent environmental characteristics. While the upper slope transect possessed silt-clay sediments and low organic matter input, the shelf break transect was represented by high sediment heterogeneity and high food availability. Ten

stations were investigated (34 MUC cores in total) in the framework of this PhD project through the BOF grant 12/DOS/006. The last investigated area was part of the Vema Fracture Zone and the Vema transform fault, which cross the Mid-Atlantic Ridge at about 10° N. This area was studied based on one research campaign on board of the RV Sonne (SO 237 campaign) and covered water depths between 4998 and 5771 m. This studied area is characterized by predominantly silt-clay sediments, although very fine, fine, and coarse sand were also reported, and by a low food input without seasonal surface productivity events. Six stations were investigated (17 MUC cores in total) in the framework of the project Vema-TRANSIT.

An overview of the background information about the deep-sea environment, the meiobenthos and nematodes, and the main factors driving benthic biodiversity in the deep sea is presented in **Chapter 1**.

In **Chapter 2**, I investigated at a macro-scale (~1000 km) level the link between meiofauna diversity, density, and biomass at higher taxon level, and environmental variables linked to food availability. Data on meiobenthic community structure was obtained from two transects situated in the Atlantic part of the Southern Ocean. A latitudinal transect was located along the prime meridian, and a longitudinal transect along the Polar Front. In this study, it was tested to what extent the meiofaunal community attributes dwelling the deep-sea floor between 1951 and 5323 m water depth was associated with environmental variables related to organic matter input, such as surface primary productivity, chlorophyll a concentration in the sediment, and estimated particulate organic carbon (POC) flux to the seabed. Results revealed a dominance of nematodes (84.4–92.4 %) at all sites, and a significant westward increase in relative abundances and density for this group, associated with an increase in surface primary productivity and chlorophyll a. Along the North-South transect, no significant correlation was observed between meiofauna density and biomass and environmental variables, but higher estimated POC

fluxes at the sites south of the Polar Front were associated with higher meiofauna diversity and density in comparison to the sites located at the Polar Front. This study concludes that densities of meiofauna might be partially dependant on the surface primary productivity as their primary food source, despite the great water depth. Although POC flux was not related to densities of meiofauna in general, there is a clear separation between sites south of the Polar Front, which yielded higher meiofauna abundances and estimated POC fluxes, and sites at the Polar Front, harbouring lower meiofauna abundances and estimated POC fluxes.

Along the same East–West transect in the Southern Ocean, in **Chapter 3** I explore to what extent the surface primary productivity and benthic environmental variables were linked with nematode standing stocks and community structure. In addition, the nature of the benthic-pelagic coupling process was also investigated through the use of fatty acid analysis, with which feeding selectivity of “bulk” nematodes and particular nematode taxa (*Desmodora* and Desmoscolecidae) was tested. Results revealed that the South Georgia site (NW of South Georgia island and the most western site in this study), exhibited not only highest surface primary productivity, but also highest sediment Chlorophyll a concentration and total sediment fatty acids, together with elevated nematode densities and biomass. Fatty acid results for “bulk” nematodes, the genus *Desmodora*, and the family Desmoscolecidae suggest a plankton-based diet mainly composed of diatoms in South Georgia. Nematodes present in the other sites located east of South Georgia, characterized by low surface primary productivity and low sediment Chlorophyll a, showed no preference for fresh diatom material based on the fatty acid composition. Although not commonly found in typical deep-sea soft sediment environments, the nematode genus *Desmodora*, originally classified as an epistratum feeder, exhibited high densities in South Georgia. This occurred probably as a response to the increased surface primary productivity at this site, confirming the presence of benthic-pelagic coupling

events even at great depths. In conclusion, this study suggests that changes in standing stocks and nematode community composition, together with feeding selectivity, can be shaped by surface primary productivity regimes.

In the subsequent study I wanted to test whether the occurrence of a rather unusual deep-sea nematode community (i.e. one dominated by *Desmodora*) in the Southern Ocean was related to changes in surface primary productivity. **Chapter 4** deals with the comparison of nematode communities between eutrophic and oligotrophic abyssal environments, i.e. the Southern Ocean and the North Atlantic, respectively, in order to investigate whether differences in biodiversity and composition can be shaped by surface and bottom environmental drivers and at which scale it occurs. Three main hypotheses were tested: (1) the deep sea is a highly diverse environment at a local scale, but spatial turnover is limited at small and large scales at genus and species level; (2) diversity changes occur in response to changes in the nature and amount of organic matter input; (3) patch-mosaic dynamics drive local diversity. To test these hypotheses, nematode genus diversity and density, and diversity of species belonging to the dominant deep-sea genus *Acantholaimus* were studied. Biodiversity was compared at four nested scales: within sampled cores (i.e. alpha diversity at core level), within sites (i.e. beta diversity between cores from the same site), between sites from the same region, and between regions. Results confirmed the high local alpha diversity observed for the deep sea, but regional diversity differed for both transects, indicating that turnover can be shaped by different environmental drivers. High surface primary productivity was positively correlated with nematode densities, while diversity responses to increased organic matter input showed no trend. Areas under constant and low food input revealed similar nematode communities to other abyssal areas (e.g. North Atlantic), while sites under high productivity were characterized by different dominant genera and *Acantholaimus* species, and by a generally lower local diversity. These results are in agreement with the species-energy hypothesis, which suggests that

productivity can set a limit to the diversity of an ecosystem. Lastly, no positive correlation was observed between sediment variability and local diversity, indicating that, although sediment differences were significant across sites, these were unimportant to shape the nematode community structure in abyssal areas.

After comparing biodiversity at a macro-scale level between abyssal regions which were subjected to different productivity regimes, in **Chapter 5**, sites sampled at the Western Iberian margin were investigated along two isobathic parallel transects located at the shelf break (300–400 m water depth) and upper slope (1000 m water depth) to test if food availability and sediment heterogeneity at a local and regional scale affect bathyal nematode diversity. Changes in diversity were also here investigated at three levels: within sites (i.e. beta diversity between cores from the same site), between sites from the same depth transect, and between transects. High variability in food availability and high sediment heterogeneity at the shelf-break sites were directly linked to high genus diversity within sites, and a higher variability in nematode community structure across sites compared to the upper slope transect. In contrast, environmental factors (food availability and sediment heterogeneity) did not vary significantly between sites at the upper slope, and this lack of differences was reflected in low local diversity and community turnover between upper slope sites. Finally, differences in nematode communities between transects were higher than differences within each of the isobathic transects, but these shifts were paralleled by environmental changes. These results suggest that changes in community structure are mainly shaped by environmental drivers rather than spatial differences at the Western Iberian margin and diverge from the general trends of highest diversity at the slope observed in other studies.

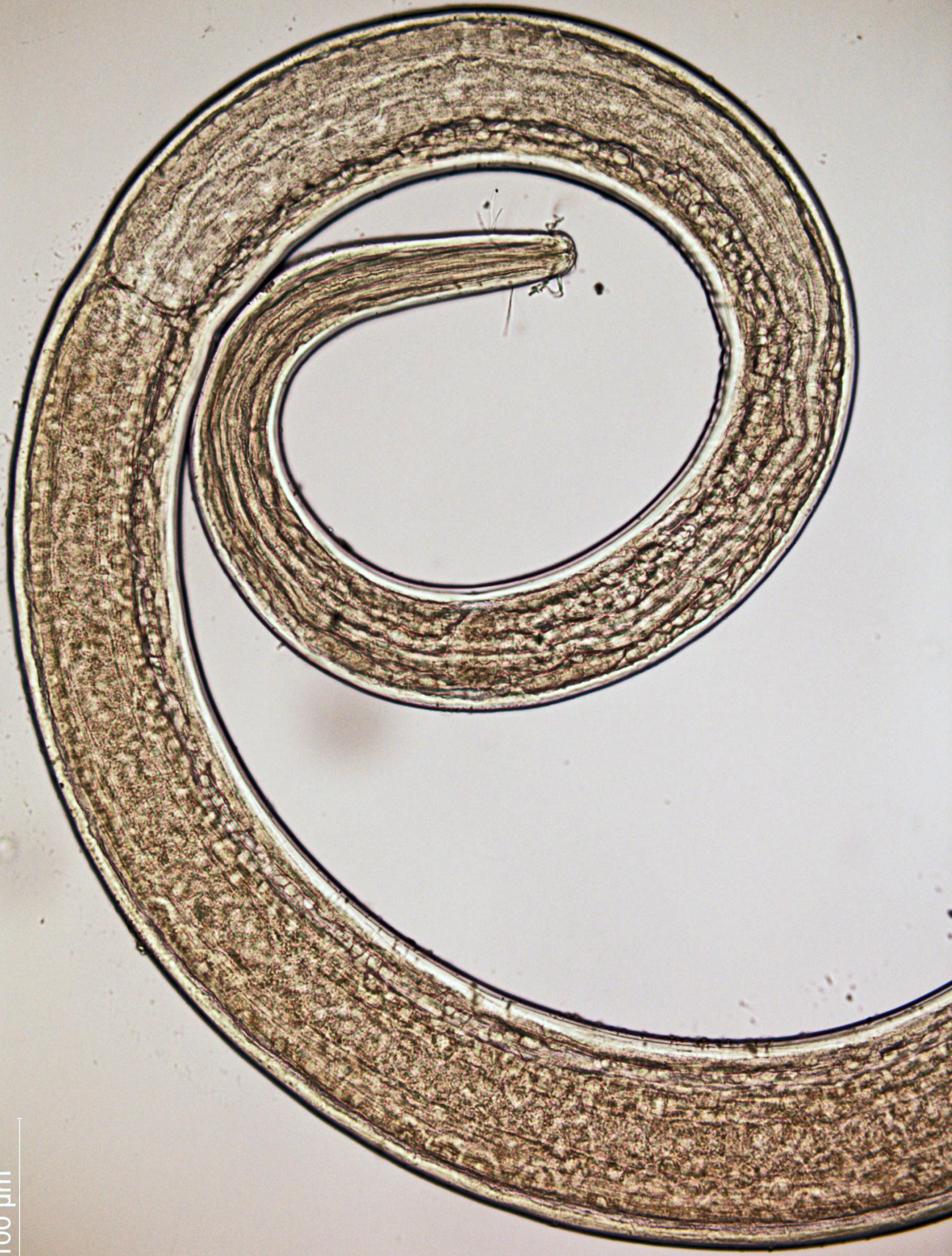
Chapter 6 integrates and discusses the main findings and insights obtained in nematode ecology provided by this doctoral thesis in the context of the current knowledge, as well as the main research constraints faced during this study and future perspectives to further

development of deep-sea meiofaunal research. Based on the results, higher local and regional diversity were observed at the Western Iberian Margin when compared to the other studied areas, as well as a lower relative abundance of the most common genera, indicating shared dominance between many different genera. Diversity, density, and biomass were lower at the abyssal sites, and were represented by high dominance of commonly observed deep-sea genera. Changes in diversity, density, and biomass were attributed to alterations in environmental drivers. Therefore, sediment heterogeneity promoted diversity, while organic matter input was only able to enhance diversity up to a certain extent, where after a certain point decreases in diversity were attributed to increases in dominant genera.

In conclusion, this PhD provides new insights regarding the ecology of deep-sea meiofauna in terms of biodiversity distribution, benthic-pelagic coupling, and feeding selectivity in the deep sea. The main achievements of this work include an overview of how deep-sea nematode communities are distributed on a large and small scale and insights in how they are driven by environmental differences. I have observed that nematode communities dwelling below food-enriched environments and regulated by disturbance events differ from those subjected to the usual low and constant food input. Here, diversity decreased from the shelf break to the slope, in contrast to other studies. This decrease was attributed to the potential positive influence of disturbance events at the shelf break, inferred by the high sediment heterogeneity probably derived from currents in this transect. In addition, regional diversity differed at the abyssal transects, where low turnover was observed for oligotrophic environments and high beta diversity for eutrophic environments. These differences in turnover trends were possibly regulated by differences in surface productivity, where less productive regions showed a typical deep-sea soft sediment community, while productive regions were mainly characterized by a higher turnover and unexpected dominance of atypical deep-sea genera. Moreover, the investigation of feeding

selectivity in the Southern Ocean for bulk and specific taxa suggested that productivity can affect nematodes, which are able to feed on fresh organic matter from the surface when this is available, but that they generally rely on refractory organic matter when food is scarce. In conclusion, results presented in this thesis question whether some established paradigms of deep-sea research are valid for nematodes.

100 μm



List of Figures

- Figure 1.1. . Examples of organisms dwelling the deep-sea floor: A) *Metadasynemella* sp.; B) *Molgolaimus* sp.; C) Thoracostomopsidae (Enoplida); D) *Proberbeeii mirabilis* (Decapoda, Parapaguridae); E) Elpidiidae (Holothuroidea); F) Gastropoda (Mollusca); G) Lophoenteropneusta (Hemichordata) ; H) Asteroidea (Echinodermata) ; I) Cephalopoda (Mollusca); J) Nudibranchia (Gastropoda) ; K) *Coryphaenoides* sp. (Osteichthyes); L) ; Funnel-like sponge (Porifera) ; M) *Paropsurus* sp. (Isopoda, Munnopsidae) and a cup-like sponge (Porifera). A-B: from the Western Iberian Margin; C: from the Vema fracture zone; D-M: taken at the Peru Basin, Pacific Ocean (© GEOMAR). Scale bars: A-C: 20 μ m, D-M: 64.2 mm. 2
- Figure 1.2. Profile of a typical passive continental margin (Adapted from Gage and Tyler, 1991) 4
- Figure 1.3. Various deep-sea bottom types observed at the North Atlantic VEMA Fracture Zone: A) Flat sea bottom covered with almost intact *Sargassum* leaves (~5000 m); B) Flat sea bottom showing bioturbation caused by benthic animals; C) Seabed covered with manganese nodules; D) Basalt rocks at the Mid-Atlantic Ridge area; E,F) Seafloor exhibiting non-regular ridges; G) Regular ridges, which can be an indication of bottom hydrodynamics. © Nils Brenke. 14
- Figure 1.4. Longhurst biogeographical provinces Longhurst, 1998 covered in this study. CNRY = Eastern (canary) Coastal Province; NATR = North Atlantic Tropical Gyral Province; WTRA = Western Tropical Atlantic Province; SANT = Subantarctic Water Ring Province; ANTA = Antarctic Province; APLR = Austral Polar Province. 21
- Figure 1.5. Sampling sites located at the Western Iberian Margin. The map displays the sampled sites and black lines the bathymetry contours. Depth increases from light blue to purple. 22
- Figure 1.6. Bathymetry map showing the sampling sites located in the North Atlantic, along the Vema Fracture Zone. The Vema Transform Fault is located at station A4. 23
- Figure 1.7. A transform fault offsets the Mid Atlantic Ridge at 11° N forming the eastern and western Vema Fracture zone (from Morozov et al. (2010)). 24
- Figure 1.8. Westward flow in the VEMA fracture zone by the Antarctic Bottom Water (AABW) for waters below 4300 m (blue). Red lines represent the North Atlantic Deep Water (NADW), which are located above 4300 m water depth. White areas are deeper than 4700 m, light grey areas are between 4700 m and 4300 m deep, dark grey areas between 4300 m and 3500 m, and black areas represent depths shallower than 3500 m. Green Xs show the location of composite section that has estimated the southward geostrophic flow (<http://www.whoi.edu/page.do?pid=30735>). 25
- Figure 1.9. Sampling sites located at the Southern Ocean. The map displays features of the Antarctic Circumpolar Current (Orsi and Harris, 2001): Subtropical front (STF), Subantarctic front (SAF), Polar Front (PF), southern Antarctic Circumpolar Current front (sACCf), and southern boundary of the Antarctic Circumpolar Current (sbACC). 26
- Figure 2.1. Location of ANT-XXIV/2 and ANT-XXVIII/3 sites. Coordinates are given in Table 1. The map displays features of the Antarctic Circumpolar Current (Orsi and Harris, 2001): Subtropical Front (STF), Subantarctic Front (SAF), Polar Front (PF), southern Antarctic Circumpolar Current Front (sACCf) and southern boundary of the Antarctic Circumpolar Current (sbACC). Bathymetry data provided by ETOPO1 and world boundaries by ESRI (Amante and Eakins, 2009). Sampling sites are represented by symbols: SG (South Georgia), HC_BEP (High Chlorophyll before Eddy Pump),

HC_AEP (High Chlorophyll after Eddy Pump), sPF (South Polar Front), LC (Low Chlorophyll), cWS (central Wedell Sea), MR (Maud Rise) and LS (Lazarev Sea). 39

Figure. 2.2. Satellite-based estimates of Net Primary Productivity (NPP) monthly variation in the Southern Ocean for the NS 2007/8 (bottom) and EW-2012 (top) sites. Grey zones represent the sampling period. Months without a value refer to the data which could not be extracted due to ice coverage. 48

Figure. 2.3. Meiofauna densities (ind/10cm²) and seafloor Particulate Organic Carbon (POC) fluxes (mg g⁻² Month⁻¹) for the ANT-XXIV/2 and ANT- XXVIII/3 sites, and Chlorophyll a (Chla, µg g⁻¹) for the EW-2012 sites. 49

Figure. 3. 1. Location of ANT-XXVIII/3 sites. The map displays features of the Antarctic Circumpolar Current (Orsi and Harris, 2001): Subtropical Front (STF), Subantarctic Front (SAF), Polar Front (PF), southern Antarctic Circumpolar Current Front (sACCf) and southern boundary of the Antarctic Circumpolar Current (sbACC). Bathymetry data provided by ETOPO1 and world boundaries by ESRI (Amante and Eakins, 2009). Sampling sites are represented by symbols: SG (South Georgia), HC_BEP (High Chlorophyll_before Eddy Pump), HC_AEP (High Chlorophyll_after Eddy Pump) and LC (Low Chlorophyll). 70

Figure. 3. 2. Environmental variables used in this study for SG (South Georgia), HC_BEP (High Chlorophyll before Eddy Pump), HC_AEP (High Chlorophyll before Eddy Pump), and LC (Low Chlorophyll) sites: Chla (Chlorophyll a), Chla:Phaeo (Chlorophyll a: phaeopigments), Chla: % TOC (Chlorophyll a: % Total Organic Carbon), CPE (Chloroplastic Pigment Equivalent), TN (Total Nitrogen), TOC (Total Organic Carbon), MGS (Mean Grain Size), NPP (Net Primary Productivity), Total sedFA (Total Fatty Acid of the sediment) and relative abundance (% of total fatty acid) for SFA (Saturated Fatty Acid) in the sediment, MUFA (Monounsaturated Fatty Acid) in the sediment and PUFA (Polyunsaturated Fatty Acid) in the sediment. Black lines represent the median, lower box indicates the first quartile and upper box the third quartile. Upper line shows the maximum value and lower line the minimum value. 79

Figure. 3. 3. Total nematode density (ind/10 cm²) of the five most abundant genera expressed per sediment layer and per site. 83

Figure. 3.4. Density (10 cm²) and Total Biomass (µg/g) per site of nematodes. Thick black lines represent the median, lower box indicates the first quartile and upper box the third quartile. Upper line on the boxes shows the maximum value and lower line the minimum value. 84

Figure. 3.5. Total *Desmodora* (SG_D1), Desmoscolecidae (SG_D2) and “bulk” nematode fatty acids represented per site in pg/g (Total nemFA) and relative concentrations (% of total fatty acid) of nemSFA (nematode Saturated Fatty Acid), nemMUFA (nematode Monounsaturated Fatty Acid), nemPUFA (nematode Polyunsaturated Fatty Acid), nemPlanktonic FA (nematode Planktonic Fatty Acid) and nemBacterial FA (nematode Bacterial Fatty Acid). Thick black lines represent the median, lower box indicates the first quartile and upper box the third quartile. Upper line of the boxes shows the maximum value and lower line the minimum value. 86

Figure. 3. 6. Non-metric MDS plot (Bray-Curtis similarity) based on nematode fatty acid profiles. Upper figure represent total nematode fatty acid for the “bulk” nematodes. Lower figure include both total nematode “bulk” fatty acid as well as total fatty acid for *Desmodora* and Desmoscolecidae. 87

- Figure 3. 7. Distance-based redundancy (dbRDA) illustrating the DISTLM model based on genera assemblage data (A) and genus individual biomass (B), and fitted environmental variables with their vector (strength and direction of effect of the variable on the ordination plot). AVPP= Average Net Primary Productivity, Chla= Chlorophyll a, Chla:%TOC= Chlorophyll a: Total Organic Carbon, %TOC= Total Organic Carbon, %TN= Total Nitrogen. 90
- Figure 4. 1. Location of ANT-XXVIII/3 and SO 237 sites. Exact coordinates are given in Table 4.1. Bathymetry data was provided by GEBCO. Sampling sites are represented by symbols: SG (South Georgia), HC_BEP (High Chlorophyll_Before Eddy Pump), HC_AEP (High Chlorophyll_After Eddy Pump), LC (Low Chlorophyll); A1, A2, and A3 (East Mid-Atlantic Ridge), A4 (at the Mid-Atlantic Ridge), and B1, B2 (West of the Mid-Atlantic Ridge). 122
- Figure 4. 2. Univariate nematode boxplots data for (a) total density (ind/10 cm²), (b) genus richness (S), and (c) Shannon-Wiener (H') diversity. Blue boxplots represent Southern Ocean sites and green boxplots represent North Atlantic sites. Black lines represent the median, empty circles represent the mean, lower box indicates the first quartile and upper box the third quartile. Upper line shows the maximum value and lower line the minimum value. 129
- Figure 4. 3. Univariate boxplots data for *Acantholaimus* (a) relative abundance (%), (b) species richness (S), and (c) Shannon-Wiener diversity (H'). Blue boxplots represent Southern Ocean sites and green boxplots represent North Atlantic sites. Thick black lines represent the median, empty circles represent the mean, lower box indicates the first quartile and upper box the third quartile. Upper line shows the maximum value and lower line the minimum value. 130
- Figure 4. 4. Relative abundances of *Acantholaimus* species per site for each transect. MAR= Mid-Atlantic Ridge. 131
- Figure 4. 5. Dissimilarities between nematode genus composition (a) and *Acantholaimus* species (c) in relation to geographical distance (km). Black circles represent dissimilarities between regions, grey triangles stand for dissimilarities between SO sites, and dark grey squares exhibit dissimilarities between NA sites. Stacked columns (b and d) represent the additive partitioning per transect (Southern Ocean (SO) and North Atlantic (NA)) of species richness (S) and the Shannon index of diversity across three sampling scales: α = within each core, β_1 = within sites, and β_2 = between sites from the same transect. 133
- Figure 4. 6. Species occurrences for *Acantholaimus* species found in this study combined with records from the literature (Table S2). 136
- Figure 4. 7. Depth distribution of the *Acantholaimus* species found in this study combined with previous records from the literature (Table S2). Sp 9 in this study is referred as morphotype 5 by Lins et al. (2015). 137
- Figure 4. 8. Environmental variables used in this study per site: (a) SED (sediment grain size diversity), (b) TOM (Total Organic Matter), (c) TOC (Total Organic Carbon), (d) TN (Total Nitrogen), (e) CPE (Chloroplastic Pigment Equivalents), (f) NPP (average Net Primary Productivity). Blue boxplots represent Southern Ocean sites and green boxplots represent North Atlantic sites. Black lines represent the median, empty circles represent the mean, lower box indicates the first quartile and upper box the third quartile. Upper line shows the maximum value and lower line the minimum value. 139

- Figure 4. 9. Values of net primary productivity (NPP) per month for the SO (a) and NA (b) sites during the years 2011/2012 and 2014/2015, respectively. 140
- Figure 4. 10. Line drawings of the *Acantholaimus* species found at the Southern Ocean and the North Atlantic transects. Only species for which male specimens were found are presented. 148
- Figure 5.1. Location of B2013/17 and B2014/15 sites. Sampling sites are represented by black circles. 176
- Figure 5.2. Environmental variables used in this study per site: Chla (Chlorophyll a), CPE (Chloroplastic Pigment Equivalent), Carotenes, SED (sediment diversity), Silt-Clay, Very fine sand, Fine sand, Medium sand, and Coarse sand. Green boxplots represent shallow sites and blue boxplots represent deep sites. Black lines represent the median, empty circles represent the mean, lower box indicates the first quartile and upper box the third quartile. Upper line of the boxes shows the maximum value and lower line the minimum value. 185
- Figure 5.3. Most abundant nematode genera (> 4 %) per site. Inner circles indicate average genus density (ind/ 10 cm²) and outer circles genus standard deviation. Green circles represent shallow sites and blue circles deep sites. 187
- Figure 5.4. Nematode Shannon-Wiener (H') diversity, nematode density (individuals/10 cm²), Expected number of genera (EG(80)) and trophic diversity (TD) per site. Green boxplots represent shallow sites and blue boxplots represent deep sites. Black lines represent the median, empty circles represent the mean, lower box indicates the first quartile and upper box the third quartile. Upper line shows the maximum value and lower line the minimum value. 188
- Figure 5.5. Dissimilarity values in nematode genus composition among geographical distance (A), sediment composition (B), and chloroplastic pigment equivalents (CPE). Green squares represent dissimilarities between shallow sites, dark blue circles between deep sites and light blue triangles show dissimilarities between shallow and deep. 189
- Figure 5.6. Correlations between (A) Sediment particle-size diversity (SED) and Expected genus diversity (EG (80)), (B) between SED and Trophic diversity (TD), (C) between EG (80) and Chloroplastic Pigment Equivalents (CPE) and (D) between TD and CPE. Green triangles represent correlations for shelf-break sites and dark blue circles between slope sites. R indicate correlation values of Spearman. * shows significant correlations. 190
- Figure 5.7. Distance-based redundancy analysis (dbRDA) illustrating the DistLM model based on the genera assemblage data for slope (blue) and shelf-break (green) sites (A) and only between shelf-break sites (B). Fitted environmental variables are shown with their vectors (strength and direction of effect of the variable on the ordination plot). 191
- Figure 5.8. Consensus of Bayesian inference of phylogeny of the genus *Halalaimus* based on 18S rDNA sequence fragments generated in this study and from Bik et al. (2010); node support is given as posterior probabilities (PP); nodes with PP smaller than 0.50 were collapsed. The outgroup was set to *Wieseria*. The tree shows multiple instances of close relationships between individuals collected at different depth zones. 193
- Figure 5.9. Scheme showing (a) how beta diversity varied across sites and between bathymetrical transects. The green bar represents the 'shallow' transect and the light blue bar the 'deep' transect. Grey circles inside the bars represents the sites sampled at each transect. Coloured circles inside grey

circles refer to the variability in nematode genus composition within site and across sites. It illustrates the higher densities and patchiness found at the 'shallow' sites and the lower turnover found at the 'deep' sites. The (b) figure reveals the main environmental factors responsible for beta diversity between both depth transects. Upwelling effects, primary production, currents, and decrease of POC (particulate organic carbon) with increasing depth are considered to be correlated with both local and regional diversity. The fate of organic matter produced at the surface varies with depth, where deeper areas will receive lower labile organic matter (OM) when compared to shallower areas. This figure also illustrates the higher variability in sediment at the 'shallow' transect when compared to the deeper transect. The green bar represents the 'shallow' transect and the light blue bar the 'deep' transect.

204

Figure 6.1. Levels of biodiversity used in this thesis: (α), alpha diversity at core level; (β1) turnover between cores and within a site; (β2) turnover between sites in the same transect; (β3) turnover between areas.

233

Figure 6. 2. Total nematode density per 10 cm² (A), total nematode biomass (B), and Shannon-Wiener diversity (C) of nematode genera per core found in all studied regions in this thesis. (D) shows the percentage of the common (abundances > 2 %) versus the rare genera found per core. Red line indicate threshold of 50 %. The sites SG (South Georgia), HC_AEP (high chlorophyll after eddy pump), HC_BEP (high chlorophyll before eddy pump), and LC (low chlorophyll) were part of the Southern Ocean (SO) transect; sites A1, A2, A3, A4, B1, and B2 were the sites sampled in the North Atlantic (NA), along the Vema fracture zone. Sites D1, D2, D3, and D4 were part of the slope at the Western Iberian Margin (WIM), while sites S1, S4, S7, S2, and S6 represent sites sampled at the shelf break of the WIM.

234

Figure 6.3. Total nematode density (A), biomass (B), and Shannon-Wiener diversity (C) of nematode genera per site for all studied areas. (D) shows the contribution of genera shared per site. "One core" represents the genera found only in one core, "Shared (2)" through "Shared (4)" signifies genera present in two–four cores respectively. The * symbol indicates sites where only three cores were sampled and ** sites with only two cores. The sites SG (South Georgia), HC_AEP (high chlorophyll after eddy pump), HC_BEP (high chlorophyll before eddy pump), and LC (low chlorophyll) were part of the Southern Ocean transect; sites A1, A2, A3, A4, B1, and B2 were the sites sampled in the North Atlantic, along the Vema Fracture Zone. Sites D1, D2, D3, and D4 were part of the slope at the Western Iberian Margin, while sites S1, S4, S7, S2, and S6 represent sites sampled at the shelf break of the Western Iberian Margin.

236

Figure 6.4. Total nematode density (A), total biomass (B), and Shannon-Wiener diversity (C) of nematode genera per region studied in this thesis. (D) represents a Venn diagram based on genus richness, where the overlap shows the number of shared genera between the different regions for all studied areas. SO= Southern Ocean, NA= North Atlantic, WIM= Western Iberian Margin.

237

Figure 6.5. Nematode Shannon-Wiener diversity in relation to sediment grain size for five different sediment fractions: silt-clay, very fine sand, fine sand, medium sand, and coarse sand. Values on top of each graph refer to the Spearman rank correlation values for each correlation coefficient. All correlations are statistically significantly ($p < 0.05$).

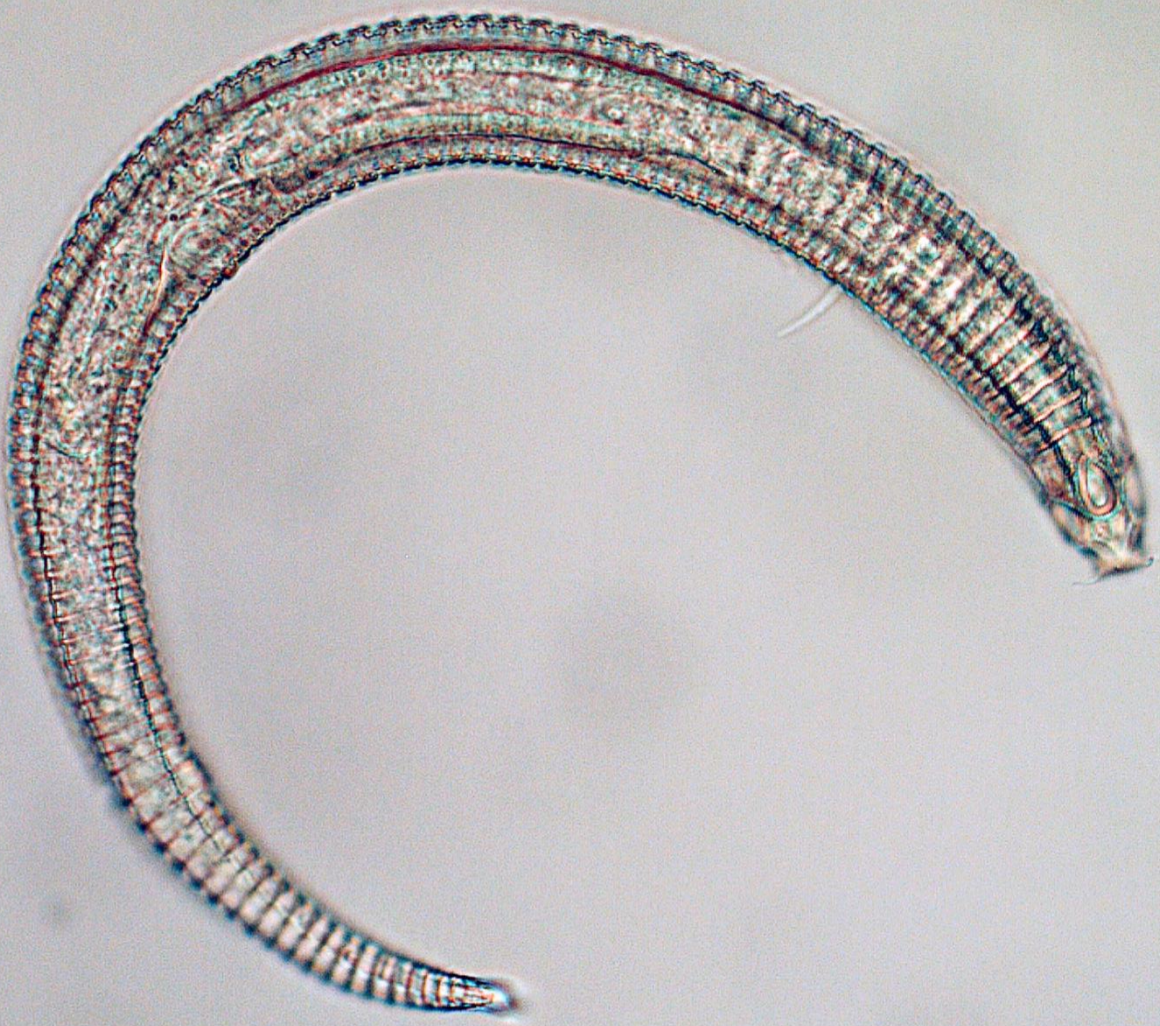
246

Figure 6.6. Preliminary results from the partial COI phylogeny of the nematode family Phanodermatidae. The inferred relationships support no clear separation of clades into groups restricted to east or west of the Mid-Atlantic Ridge (MAR). Generally, clades are intermingled between sites and regions. However, on species level (i.e., sequences with separation < 0.05) a clear geographic clustering was found. Nodes deep within the family have no statistical support. Reconstruction of Phanodermatidae COI relationships was conducted using Maximum Likelihood. Bootstrap support values were generated using 1000 replicates. The analyses were performed by means of Randomized Accelerated Maximum likelihood (RAxML). Due to the poor description of the genera from this family, an attempt was made to separate groups by the presence of teeth (pink star). This morphological character is distributed over several major clades in the tree. Due to the unsupported deeper nodes,

inference of origins of teeth were not always possible, however, this character appears to be generally conservative as it is present in all specimens of several well-supported clades, while it is completely absent in others. West represents sites west of the MAR, East sites east of the MAR, and PRT Abyssal, sites from the same depth collected at the adjacent Porto Rico Trench. 255

Figure 6.7. Preliminary results from the metabarcoding analysis for the Western Iberian Margin (WIM) and North Atlantic along the Vema Fracture Zone. This figure shows that for some groups low refinement (e.g. Enoplida is only kept at order level) and wrong BLAST results due to the low amount of sequences available in the database (e.g. *Wilsonema*, a soil nematode) can still hamper the broad use of this technique. Some groups are identified with the same colour, this means that the BLAST did not exhibit clear results, i.e. that matches could be one group or the other. The y axis shows the relative abundance of each group. 256

Figure 6.8. Nematode oxygen consumption in function of time for nematodes collected at the 1000 m upper slope sites at the Western Iberian Margin campaign (B2014/15). 257



50,0 μm

List of Tables

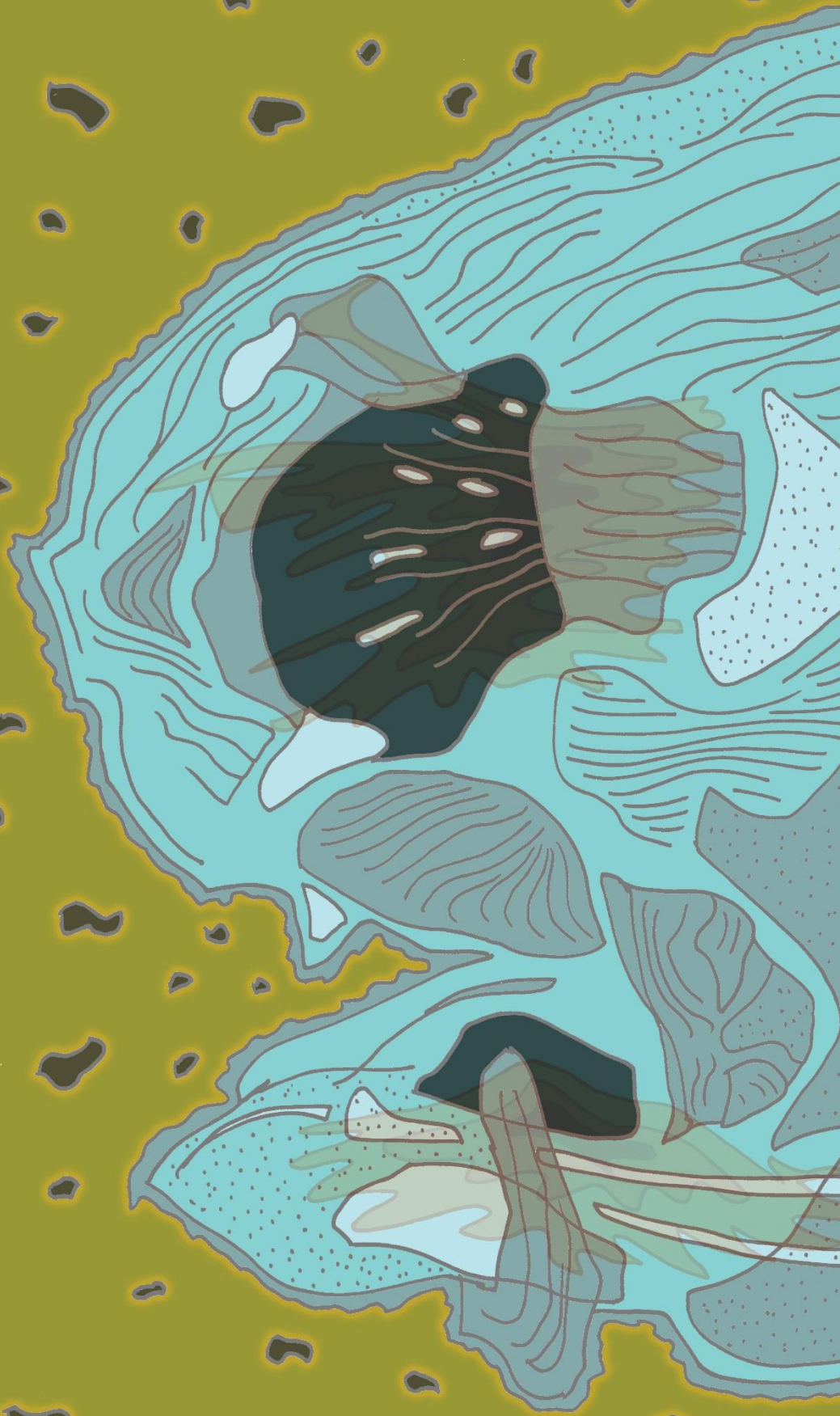
- Table 2. 1. Sampling details. Each deployment is treated as one replicate. In the deployment column, number in brackets represent the core codes, thus the replicates. Core numbers not in bold represent the cores sampled for the meiofauna analyses, while core codes in bold refer to cores used for environmental analyses. PF = Polar Front. 43
- Table 2.2. Overview per site of taxon richness (number of groups), meiofauna density (ind/10cm²), nematode density (ind/10cm²) and total nematode biomass (µg dwt), and nematode relative abundance (%) ± standard deviation for NS-2007/8 and EW-2012 sites. The station cWS was only represented by one replicate. 51
- Table 2.3. Results from multivariate PERMANOVA analyses for differences in meiofauna density, nematode density, and nematode biomass. 51
- Table 3.1. Sampling details from each sampled site. Each deployment code (and core number in brackets) refers to one replicate (four replicates per site in total). Core numbers in bold were used for community analyses while non-bold core codes were used for nematode fatty acids and environmental analyses. 72
- Table 3.2. Mean relative abundance of dominant genera (≥ 2 %) and feeding type (FT) per site over 5 cm depth. 82
- Table 4. 1. Sampling details for the ANT-XVIII/3 and SO 237 campaigns. PF (Polar Front), E MAR (East Mid-Atlantic Ridge), MAR (Mid-Atlantic Ridge), W MAR (West Mid-Atlantic Ridge). Replicate numbers represent the number of cores used for nematode community analyses and * represent the cores used for environmental analyses. 123
- Table 4. 2. Most abundant nematode genera (> 2 %) per site (average ± st.dev.). 134
- Table 4. 3. PERMANOVA results for the environmental variables used in this study. SED (sediment grain size diversity), TOM (Total Organic Matter), TOC (Total Organic Carbon), TN (Total Nitrogen), CPE (Chloroplastic Pigment Equivalents), NPP (average Net Primary Productivity). Main *p* perm represents *p*-values for the 2-factor nested design test. Significantly different *p*-values are displayed in bold. Pairwise *t*-test results are only shown if values were significant. When all differences between sites pairs were not significant, pairwise *t*-tests were displayed as ND. 138
- Table 5.1. Sampling details. St codes refer to sites sampled at the 'Shallow transect', while Deep codes refer to sites sampled at the 'Deep transect'. Each St site is characterized by three independent replicates obtained from three different deployments (three cores), while the Deep stations are characterized by four independent replicates obtained from four different deployments (four cores). 177
- Table 6. 1. DistLM (Distance-based Linear Model) results for marginal tests and sequential tests showing the influence of environmental (food availability and sediment characteristics) and spatial (depth and spatial structure) factors on the nematode multivariate community beta diversity. Food availability refers to the following variables: chloroplastic pigment equivalents, total nitrogen, total carbon, total organic matter, net primary productivity, and estimated particulated organic carbon flux. Sediment characteristics include: silt-clay, very fine sand, fine sand, medium sand, and coarse sand. Geographical distances include: latitude, longitude, latitude², longitude², latitude³, and longitude³.

Prop. = proportion of total variation explained; Prop. (cumul) = proportion of total accumulative variation. Only variables with $p < 0.05$ were added. 248

Table 6. 2. Main environmental factors and diversity scales studied in this thesis. The grey tringle illustrates the continental margin (bathymetrical difference), and the grey square the abyssal plain (geographical difference). WIM = Western Iberian Margin; NA = North Atlantic, VEMA transect; SO= Southern Ocean transect. OM = organic matter. 249

General Introduction

1







Chapter 1: General Introduction

1.1 A glimpse of the deep-sea environment

We may speak of the deep sea as the largest environment on Earth, since it comprises approximately 90 % of the seabed (Gage and Tyler, 1991; Ramirez-Llodra et al., 2010). However, only 5 % of this environment has been explored until 2010 (Ramirez-Llodra et al., 2010) due to its remoteness and difficulties in observing and sampling organisms (Gage and Tyler, 1991). In the nineteenth century, the theory of a lifeless deep ocean (Forbes, 1844) created by Edward Forbes was not only disproved but also spectacular life forms inhabiting the deep sea were discovered (Fig. 1.1). It is now known that the deep-sea bottom contains a high local diversity¹ of organisms (Hessler and Sanders, 1967; Ramirez-Llodra et al., 2010), while at the same time it shows similar species spread throughout the large distances of abyssal plains (> 4000 m depth) (Etter and Bower, 2015; Havermans et al., 2013). However, it is not just the newly discovered deep-sea organisms that are responsible for generating interest in the bathyal and abyssal environments. The high habitat heterogeneity, such as those formed by canyons, seamounts, and cold water coral reefs have also contributed to a growing awareness of deep-sea biodiversity. Generally characterised by low densities and biomass, deep-sea chemosynthetic-driven and reduced environments, such as hydrothermal vents, cold seeps, and oxygen minimum zones, may

¹ Diversity throughout this thesis is considered at both genus and species level and it is represented by the Shannon-Wiener, species/genus richness, expected number of genera, and Pielou's indices.

harbour outstanding levels of metazoan densities and biomass (Levin, 2003; Vanreusel et al., 2010a).



Figure 1.1. Examples of organisms dwelling the deep-sea floor: A) *Metadasynemella* sp.; B) *Molgolaimus* sp.; C) Thoracostomopsidae (Enoplida); D) *Proberbeeii mirabilis* (Decapoda, Parapaguridae); E) Elpidiidae (Holothuroidea); F) Gastropoda (Mollusca); G) Lophoenteropneusta (Hemichordata) ; H) Asteroidea (Echinodermata) ; I) Cephalopoda (Mollusca); J) Nudibranchia (Gastropoda) ; K) *Coryphaenoides* sp. (Osteichthyes); L) ; Funnel-like sponge (Porifera) ; M) *Paropsurus* sp. (Isopoda, Munnopsidae) and a cup-like sponge (Porifera). A-B: from the Western Iberian Margin; C: from the Vema fracture zone; D-M: taken at the Peru Basin, Pacific Ocean (© GEOMAR). Scale bars: A-C: 20 μ m, D-M: 64.2 mm.

Previously thought to be a stable environment in terms of temperature, salinity, oxygen, light, sedimentation rates, and food supply. (Hessler and Sanders, 1968), we now know that the deep sea is anything but regular for many of these factors. The deep-sea benthos is subjected to benthic storms, variations in temperature, tidal regimes, and deep-water masses with high speed, such as the Antarctic Bottom Water and the Deep Atlantic Bottom Water (Ercilla et al., 2016; Gage, 1997; Thistle, 2003; Thistle et al., 1985; Tyler, 1995). Moreover, high resolution imagery of the seabed topography has shown that the deep seafloor is structured by various morphological features and deposits (Ercilla et al., 2016), which influence the distribution of benthic organisms (Zeppilli et al., 2016).

Beginning in 1844 with the discovery of deep-sea fine sediments (Forbes, 1844), 27 other habitats have since been revealed (Ramirez-Llodra et al., 2010). Furthermore, the deep-seabed topography is also characterized by the balancing between seafloor sedimentation and spreading parameters (Gage and Tyler, 1991; Menard, 1967). Usually, the seabed is divided into four benthic depth zones: the subtidal (until 200 m), the bathyal (200–4000 m), the abyssal (4000–6000 m), and the hadal (> 6000 m) zone. The subtidal and bathyal zones together compose the continental margins (Gage and Tyler, 1991). The continental margins, where the ocean extends until the deep sea, comprise the continental shelf (not actually characterized as deep sea), the continental slope, and continental rise (Levin and Dayton, 2009) (Fig. 1.2). Continental shelves (0 – 200 m) extend from the low-water line and usually end at the shelf break, where the deep sea generally starts (Levin and Sibuet, 2012; Wiseman and Ovey, 1953). A clear increase in declivity (200 – 3000 m) characterises the continental slope, which marks the underlying border between oceanic and continental crust (Gage and Tyler, 1991; Levin and Sibuet, 2012). The continental slope can be interrupted by terraces and submarine canyons (Gage and Tyler, 1991). Submarine canyons are of significant importance since they act as carbon traps, as well as channels for organic material transport between slopes and abyssal plains (McClain and Hardy,

2010). Following the base of the continental slope, a thick wedge of slope-derived sediment characterises the continental rise (3000–4000 m), which is usually smoother than the continental slope (Gage and Tyler, 1991; Levin and Sibuet, 2012) (Fig. 1.2). In general, continental margins are considered extremely important due to their heterogeneity of habitats, which are responsible for harbouring high species diversity, as well as essential ecosystem functions and services (e.g. oil, gas, and methane hydrates), and carbon burial (Levin and Dayton, 2009). They are also considered to be highly dynamic environments not only in terms of topography, but also in their distinct water masses, strong gradients in pressure, temperature, oxygen, food supply, and substrate stability (Levin and Dayton, 2009).

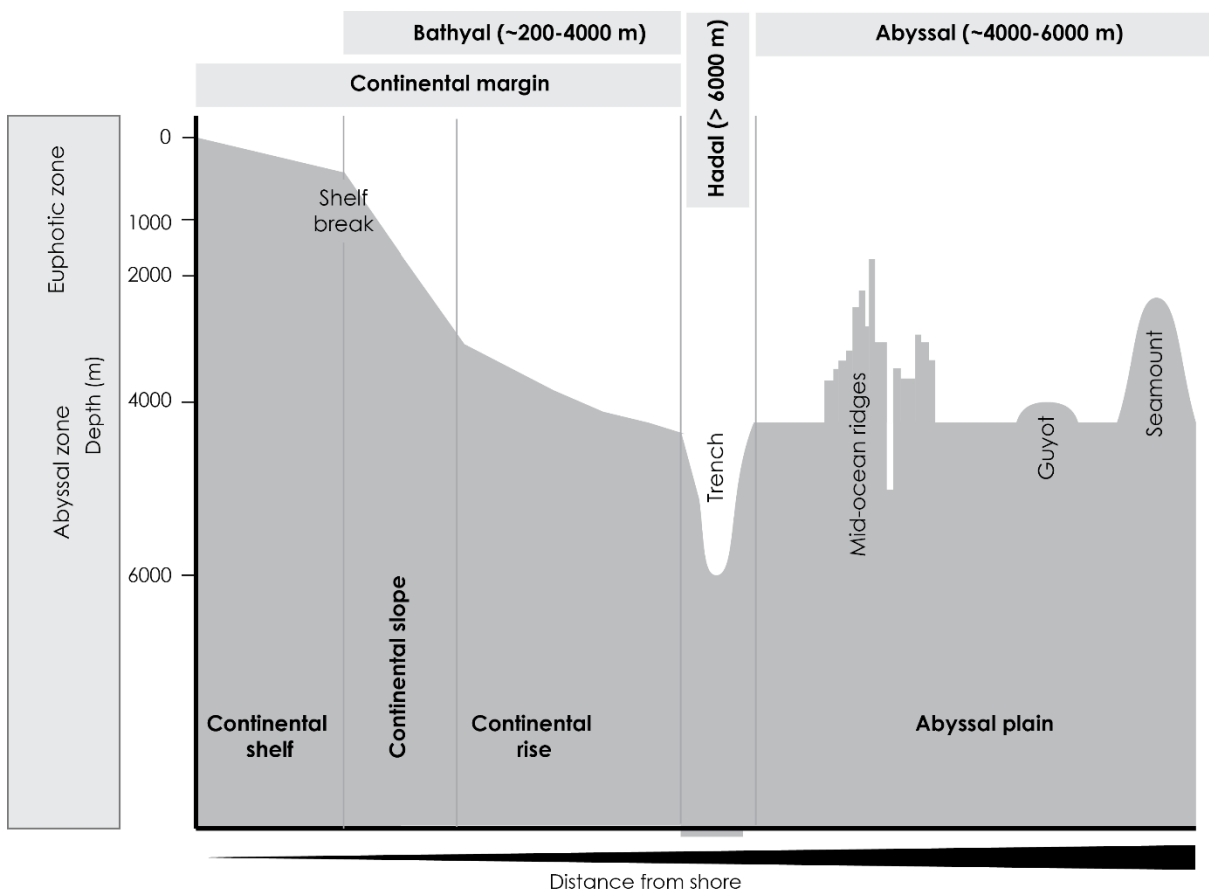


Figure 1.2. Profile of a typical passive continental margin (Adapted from Gage and Tyler, 1991)

Below 4000 m and covering 54 % of the Earth's surface lie the abyssal plains, where slopes and ridge flanks flatten (Ramirez-Llodra et al., 2010) (Fig 1.2). The sediment in abyssal plains is mostly confined to fine sediments which can be thousands of meters thick (Ramirez-Llodra et al., 2010; Smith et al., 2008), but hard substrates associated with manganese nodules and fault scarps can also occur (Smith et al., 2008; Vanreusel et al., 2016). Actually, the concept of an abyssal 'plain', without major topographic features should be abandoned. Abyssal plains are frequently interrupted by guyots (undersea mountains with a flat top) and seamounts, which are essentially topographically-isolated peaks able to rise up to 1000 m above the seafloor (Abelmann et al., 2006; Gage and Tyler, 1991; Ramirez-Llodra et al., 2010). Moreover, on abyssal plains, when the oceanic crust bends and deepens, there can originate mid-ocean ridges and also trenches, which are seismically active areas deeper than 6000 m and up to 11000 m (Gage and Tyler, 1991). Thus, abyssal plains are heterogeneous and not at all flat as previously thought (Smith et al., 2008). Different from continental margins, abyssal plains are considered energy-poor environments due to the complete lack of photosynthesis and high dependence on detrital organic material derived from the surface waters (Smith et al., 2008).

Overall, the rate and nature of the organic matter (OM) input in the deep sea, together with particular bottom processes of the divergent deep-sea habitats, such as bottom currents, tidal events, and OM distribution on the seabed, affect the deep-sea floor dwelling benthic communities in different ways. Moreover, different factors operate at different spatial scales, where small-scale² processes tend to occur at faster rates and are integrated hierarchically in larger-scale³ processes (Levin et al., 2001). Processes affecting benthic organisms at different scales are directly related to organism size and tend to become more or less important depending on the organism's dimensions. On a large scale,

² cm to 10 m.

³ 100s to 1000s of m.

processes associated with regional diversity⁴, such as environmental gradients, dispersal, metapopulation dynamics, and gradients in habitat heterogeneity, are all considered important (Levin et al., 2001). On a small scale (1 – 10 m), processes which regulate the benthic community tend to occur on shorter time scales, and involve biotic and abiotic factors, such as predation, facilitation, and exclusion, as well as resource partitioning, physical disturbances, and physiological tolerances (Levin et al., 2001).

1.1.1. The meiobenthos and nematodes

Benthic metazoans are divided into three different groups according to their size: Megafauna, Macrofauna, and Meiofauna⁵ (Giere, 2009; Mare, 1942), the latter of which is the focus group of this thesis. The study of the small organisms called meiofauna started before the term “meiofauna (meiobenthos)” was coined for this group (Higgins and Thiel, 1988; Mare, 1942). It includes both metazoans, as well as the small one-celled protists, for e.g. Foraminifera (Gage and Tyler, 1991). The ecology of deep-sea meiofauna beyond the continental shelf (up to 567 m water depth) was studied for the first time by Wigley and McIntyre (1964). Since then, intensive research on the deep-sea meiofauna has been conducted, allowing scientists to have a broader view of how this group is distributed along all ocean basins and water depths, and better understand what drives their coexistence (Mokievskii et al., 2007; Soetaert and Heip, 1995; Vanreusel et al., 2010b; Vincx et al., 1994).

In the deep sea, the metazoan meiofauna in soft sediments is dominated by nematodes and copepods, where nematode relative abundance can reach > 85 % (Mokievskii et al.,

⁴ Regional diversity can be the diversity at the level of site, between sites, and between studied areas.

⁵ The definition of megafauna, macrofauna, and meiofauna vary according to different environments and studies.

2007). While meiofaunal abundances tend to decrease with increasing water depth (similar to other size classes), its relative biomass increases with increasing water depth, surpassing that of macro- and megafauna, which show a steeper decrease in biomass with depth (Rex et al., 2006).

Due to their small size, meiofaunal organisms are dependent on the biogeochemical characteristics of the sediment, such as sediment composition, and oxygen availability (Ingels and Vanreusel, 2013; Leduc et al., 2012c; Tyler, 1995; Vanreusel et al., 1995). Together with food input from the surface, these factors are believed to be the most important drivers of meiofaunal community attributes (Levin et al., 2001; Smith et al., 2008). Nevertheless, due to the scarce food supply faced in the deep sea, competition for food and other biotic interactions, such as bioturbation and predation, could also affect species coexistence (Gallucci et al., 2008). In the case of food-depleted patches or as an effect of intra-/interspecific competition, nematodes are able to actively disperse in their search for better conditions (de Meester et al., 2012). Nevertheless, meiofauna dispersal in the deep sea probably occurs primarily through passive dispersal via bottom currents (Thistle et al., 1985), as, due to their size, it seems improbable that they could actively disperse over large distances.

The relative abundance of nematodes increases with increasing water depth (Mokievskii et al., 2007). Many nematode genera in the deep sea have been reported in various ocean basins and depths, and are thus considered cosmopolitan (Vanreusel et al., 2010b; Vincx et al., 1994). Some genera show increasing diversity with increasing water depth, such as *Acantholaimus* and *Halalaimus* (Soetaert and Heip, 1995; Vanreusel et al., 2010b). These genera can also be found in shallow waters, and increase in importance with increasing water depth due to the disappearance of other shallow-water genera (Soetaert and Heip, 1995). Nevertheless, the question still remains, why do some genera increase in abundance and diversity in the generally food-depleted deep sea? And, what drives their distribution?

Patterns in nematode diversity and the processes responsible for these trends are still not well understood.

It is also important to mention that most nematode studies have been mainly limited to genus level (Ingels et al., 2011; Netto et al., 2005; Pape et al., 2013b; Sebastian et al., 2007; Somerfield and Clarke, 1995; Vanreusel et al., 2010b). Because of the time-consuming investment necessary to describe new species, efforts made in nematode taxonomic identification, especially towards macro-ecological approaches remains at genus level. It has been observed that studies dedicated to answering ecological questions and the effect of environmental factors on nematode biodiversity, identification down to genus level may be sufficient as most deep-sea nematode genera have low environmental specificity (Leduc et al., 2012a). Nonetheless, the dearth of information up to species level can restrict comparisons between studies in terms of species distribution and biodiversity estimates. Moreover, the phylogenetic relationships between the different genera, whether they are or not monophyletic, and the implications of those relationships for ecological studies when nematodes are compared at genus level, are still not being measured.

1.2 Main factors driving biodiversity, abundance, and biomass in the deep sea

1.2.1 Benthic-pelagic coupling

While some environmental variables fluctuate relatively little on an ocean-basin scale, such as temperature, salinity, and oxygen, the deep sea-bottom can be subjected to an array of variations in other physical and biological features on different scales. In general, deep-sea communities are driven by the same basic mechanisms of energy availability, biological interactions, disturbance, and heterogeneity, the same as those found in other

major marine ecosystems (Levin et al., 2001). However, communities in the deep sea appear to be primarily regulated by the rate and quality of food flux to the seafloor (Company et al., 2008; Danovaro et al., 2008, 1999; Gooday, 2002; Levin et al., 2001; Rex, 1981; Ruhl et al., 2008; Sachs et al., 2009). The input of phytodetritus to the seafloor can shape benthic communities by creating patchiness and increasing habitat heterogeneity, thereby enabling species coexistence through niche differentiation and facilitation (Cardinale et al., 2000; Tyler, 1995).

Surface primary productivity and the subsequent sedimentation of phytoplankton to the seabed through the biological pump is the main source of carbon to the deep sea (Billett et al., 1983; Woolley et al., 2016). Although most of the new OM production is consumed in the water column and commonly only 1–3 % reaches the sea bottom, generally 70–95 % of the particulate OM that arrives there is believed to be composed of labile compounds (Boon and Duineveld, 1996; Lampitt et al., 2010; Sachs et al., 2009). Nevertheless, surface primary productivity varies regionally and seasonally (Lutz et al., 2002). Up to 90 % of the overall new OM production is concentrated at continental margins (Levin and Dayton, 2009) and upwelling areas, while offshore regions in the open ocean (e.g. western North Atlantic) can be strongly oligotrophic (Jochem and Zeitzschel, 1993). Beside regional differences, benthic-pelagic coupling in the deep sea can be heavily affected by seasonality, which results in low resource availability in particular regions during most parts of the year (Gooday, 2002; Peck et al., 2006). Such a pronounced pattern of seasonality in food supply to the deep seabed can be observed mostly at high latitudes, where seasonality is strongest (Griffiths, 2010). In these regions, the amount of OM arriving at the seafloor not only depends on water depth and distance from land, and on the composition and activity of plankton communities, but is also determined by current regimes and ice coverage, leading to intricate effects on the benthos (Arrigo and Thomas, 2004; Gutzmann et al., 2004; Peck et al., 2006). In the Southern Ocean (SO), the presence of the strong Antarctic

Circumpolar Current is linked to lateral advection and consequently to east-west differences in primary productivity (Demidov et al., 2012). These differences have an impact on the benthic community dwelling beneath the Antarctic Circumpolar Current and adjacent areas, as lateral advection can transport OM to other areas (Brandão et al., 2014).

Together with the production of OM in the upper water layers, sea surface oceanographical processes (e.g. upwelling events, gyres), water depth, activity of plankton communities, and distance from land, determine the OM flux to the seabed (Fischer et al., 2000; Middelburg et al., 1997; Wei et al., 2010). Bathymetric trends and the influence of water depth on benthic standing stocks and diversity have been extensively studied (Smith et al., 2006; Rex et al., 2006). While density and biomass tend to decrease with increasing water depth, patterns in diversity have showed either an unimodal trend, a positive trend, or no correlation with increasing depth (Gray, 1994; Muthumbi et al., 2011; Rex, 1981). As observed for the production of OM, the flux of particulate organic carbon (POC) to the sea bottom is also dependent on region and seasonal variability (Lampitt, 1985; Lampitt and Antia, 1997; Smith et al., 2008). The high seasonality observed for the polar regions is reflected in a greater amplitude of flux to the bottom when compared to non-polar areas (Lampitt and Antia, 1997). Thus, while in polar areas seasonality is the major factor causing enhanced POC sinking speed in summer (up to 200 m d^{-1}) and decreased sinking speed in winter (Closset et al., 1992), other areas are mainly influenced by wind stress, currents, and interannual variation of those factors (Crespo et al., 2011; Figueiras et al., 2002; Lampitt et al., 2010; Relvas et al., 2007).

During its descent and after its settlement at the bottom, OM undergoes mineralization processes. At the seafloor, this process is mainly mediated by the benthic biota (Jamieson et al., 2013; Serpetti et al., 2013). The responses of sea-floor communities to variations in particle fluxes are commonly dominated by bacteria, which show high increases in

abundance and biomass as a reaction to OM input, followed by protists, such as foraminifera, and subsequently metazoans (Gooday, 2002; Moodley et al., 2008). Accordingly, microbial degradation seems to be the major regulator of mineralization processes in the deep sea (Jamieson et al., 2013). In addition, mega- and macrofauna enhance mineralization processes through feeding (i.e. mechanic fragmentation and digestion) as well as burrowing activities (Levin et al., 1997; Serpetti et al., 2013). The role of meiofauna in OM mineralization has been indirectly shown through increases in bacterial respiration during an enrichment experiment with and without the presence of meiofauna, suggesting that mineralization of organic matter by bacteria can be facilitated by the presence of meiofauna at least in shallow-water marine environments (Nascimento et al., 2012). Increases in meiofauna body mass were also observed in response to OM input, as were assimilations of specific fatty acids derived from diatoms and/or dinoflagellates (Fabiano and Danovaro, 1999; Guilini et al., 2013; Vanreusel et al., 1995). Concurrently, fatty acid assimilation from surface-derived diatom deposits were observed in macrofauna and meiofauna (Guilini et al., 2013; Leduc et al., 2014; Würzberg et al., 2011), thus confirming the idea of a food web directly dependent on fresh food input. In conclusion, all benthic size classes seem to contribute to OM mineralization, and consequently to the functioning of deep-sea ecosystems (Smith et al., 2008).

Biochemical techniques, such as fatty acid analysis, represent an important tool to track the carbon flow in deep-sea meiofauna (Duros et al., 2011; Ginger et al., 2001). The recent use of fatty acid analysis in nematodes (Guilini et al., 2013; Leduc, 2009; Leduc et al., 2014) has shown that they can selectively feed on food sources which contain specific fatty acid groups. Fatty acids can firstly be grouped into phytoplankton-derived and bacterial-derived fatty acids. Secondly, the higher the unsaturation, the more food-rich a fatty acid is considered (Dalsgaard et al., 2003). Thus, feeding on polyunsaturated fatty acids (PUFAs) would mean feeding on a richer food source, while feeding on saturated fatty

acids would represent a diet mostly based on refractory organic matter (Dalsgaard et al., 2003). Specific fatty acid groups or ratios thereof can also be used as biomarkers, such as the ratio $\frac{\Sigma 16:1\omega 7}{\Sigma 16:0} > 1$, which indicates a diatom-based diet or $\frac{22:6\omega 3 (DHA)}{20:5\omega 3 (EPA)} = 1$, related to a dinoflagellate diet (Dalsgaard et al., 2003). However, fatty acid ratios to estimate the diet of an organism should still be interpreted with caution when conducted in natural environments, since bioconversion pathways, for instance in nematodes, can occur. PUFAs can be, for example, affected by temperature (lower temperatures increase the level of unsaturation) and nematodes may also biosynthesise PUFAs from other fatty acids, interfering in the correct interpretation of exact PUFA concentrations of the studied organism (Dalsgaard et al., 2003; Leduc et al., 2014).

Similarly, fatty acids can be an central instrument in the study of trophic interactions in marine habitats (Kelly and Scheibling, 2012). Most components of mega-, macro- and meiofauna have shown to be dependent on ‘labile’ organic matter as a food source (Ginger et al., 2001; Würzberg et al., 2011). This can be seen in the high relative abundance of PUFAs in many organisms, which are indicators of either a diatom-based or a dinoflagellate diet, as most metazoans are not able to synthesize these macromolecules themselves (Dalsgaard et al., 2003). However, the seasonality of the food input in the deep sea requires benthic organisms to change their feeding habits when fresh food is scarce. Thus, when food is limited, refractory detritus provides an important and regulating food component for the benthos (Ginger et al., 2001).

1.2.2 Spatial variability and patch-mosaic dynamics

In the previous section, we have seen which aspects influence benthic-pelagic coupling in the deep sea and how it occurs. The food input to the seafloor is thus influenced by the

quality and quantity of OM, as well as by how fast this OM reaches the sea bottom and how much of it is consumed in the water column (Lampitt and Antia, 1997; Levin et al., 2001; Tyler, 1995). Besides food input, other mechanisms responsible for shaping density, biomass, and diversity of deep-sea benthic communities include such physical factors, seabed topography, disturbance, boundary constraints, and hydrodynamics (McClain and Schlacher, 2015), as well as the biological factors of bioturbation, population dynamics, and dispersal (Gage, 1997). Commonly, the ecological impact of physical factors depend primarily on the strength of the factor and the susceptibility of organisms (McClain and Schlacher, 2015).

How OM is distributed when arriving at the sea bottom might also influence species coexistence. It was in 1965, that R.J. Menzies stated abandoning the idea of a flat deep-sea floor (Menzies, 1965). We now know that seabed topography can be highly heterogeneous, exhibiting ripples, mounds, and hard rock substrata which can cause uneven distribution of OM on the seabed (Menzies, 1965; Tyler, 1995; Zeppilli et al., 2016) (Fig. 1.3).

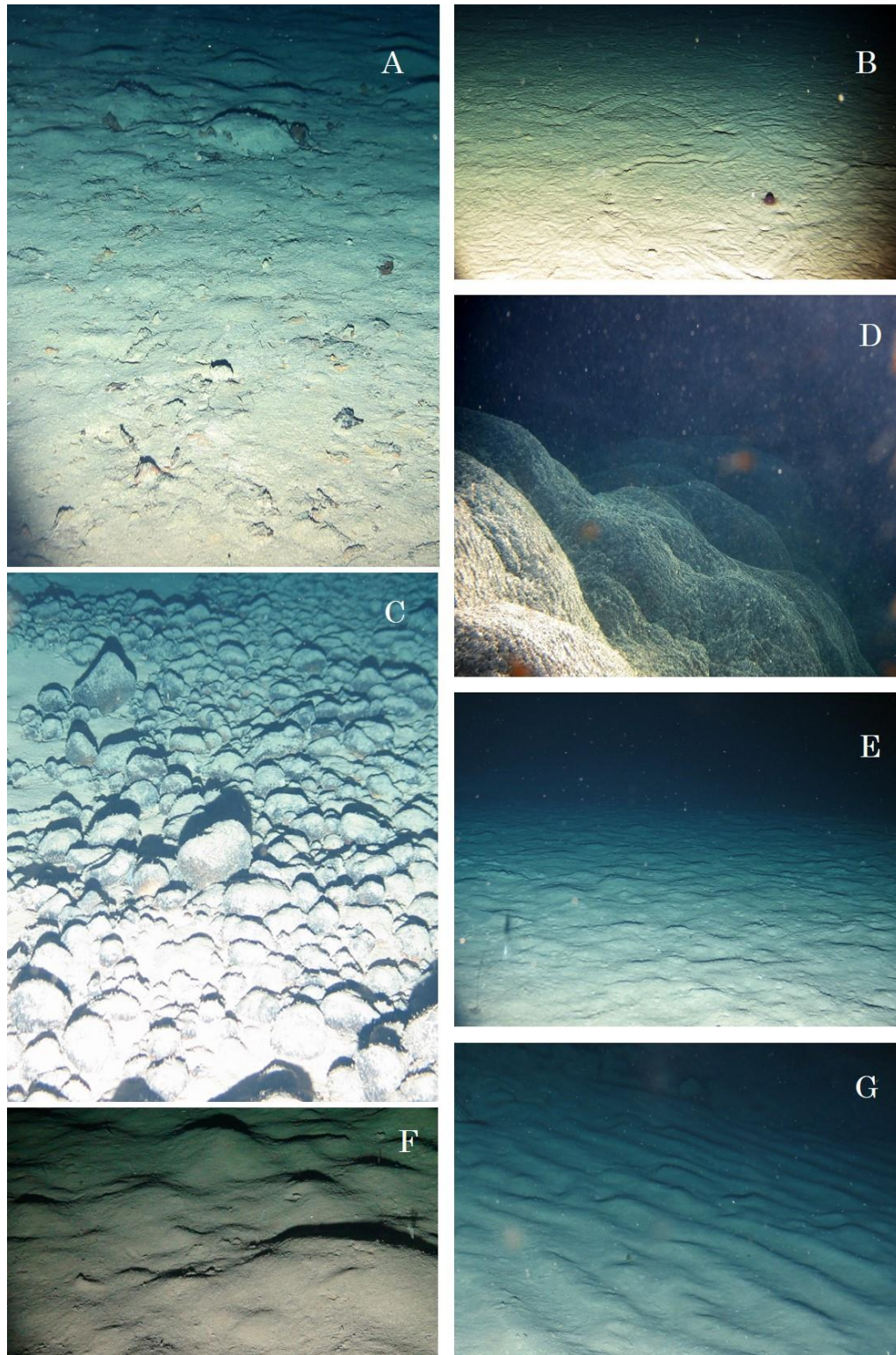


Figure 1.3. Various deep-sea bottom types observed at the North Atlantic Vema Fracture Zone: A) Flat sea bottom covered with almost intact *Sargassum* leaves (~5000 m); B) Flat sea bottom showing bioturbation caused by benthic animals; C) Seabed covered with manganese nodules; D) Basalt rocks at the Mid-Atlantic Ridge area; E,F) Seafloor exhibiting non-regular ridges; G) Regular ridges, which can be an indication of bottom hydrodynamics. © Nils Brenke.

While sediment topography can determine the uneven distribution of OM on the seafloor, sediment composition can influence how OM is trapped, depending on whether it is for instance, dominated by silt-clay or coarser particles, since coarser grain size allows more OM to penetrate deeper (Leduc et al., 2012c; Tyler, 1995). This heterogeneity in OM accumulation and distribution creates patches, which in turn result in the patchy meiofauna distribution at small scales (1 – 10 m), already reported for the deep sea (Danovaro et al., 2013; Grassle, 1989; Leduc et al., 2012c). Sediment heterogeneity is thus, believed to be a crucial factor shaping benthic-community dynamics and promoting species coexistence in the deep sea (Leduc et al., 2012c; McClain and Rex, 2015).

Patterns of diversity depend on spatial scales (Crist et al., 2003; Gambi et al., 2014). This means that small-scale community patterns can be different from patterns found over large areas or regions (Crist et al., 2003). For example, small-scale (cm to 10 m) heterogeneity differences in sediment depth in meiofaunal communities seem to be regulated by the oxygen concentration within the sediment (Ingels and Vanreusel, 2013; Steyaert et al., 2005). At a broader scale (100s to 1000s of m), however, higher species diversity turnover can be observed in environments subjected to a pulsed OM in comparison to oligotrophic areas (Lamshead, 2004). Increased surface productivity is thus responsible for augmenting patchiness and consequently diversity at a regional scale (Shorrocks and Sevenster, 1995).

There has been considerable interest in determining spatial variation in deep-sea species diversity, and which environmental factors are responsible to affect species coexistence at different spatial scales (Danovaro et al., 2013; Levin et al., 2001). In general, diversity in this thesis was assessed on three different scales which are nested within each other in the following order: alpha (α), i.e. the diversity at the core level, beta (β), regional diversity within a site, between sites, and between studied areas, and gamma (γ) diversity, i.e. the total diversity of an area (Whittaker, 1960; Whittaker et al., 2001). In 1996, Lande

developed a statistical method to test the null hypothesis that partitions of species richness or diversity differs from those expected by chance (Lande, 1996). The so-called additive partitioning method, brings alpha, beta, and gamma diversity to the same scale. Called additive components, it helps determine which type of diversity contributes most to total diversity in a given area (Crist et al., 2003; Lande, 1996). This method also tests whether species diversity is based on a non-random distribution of individuals, such as specific aggregation, resource partitioning, and community saturation (Crist et al., 2003; Shorrocks and Sevenster, 1995). The randomization (null hypothesis) is tested using a ‘reshuffling algorithm to place individuals in samples randomly while preserving the original species-abundance and sample-size distributions’ (Crist et al., 2003). The use of the additive method can help unravel spatial patterns of diversity distribution, which can provide important information on those mechanisms which regulate diversity and the complexity of ecosystems (Levin, 1992).

1.2.3 Dispersal and distribution in the deep sea

Food availability and biological interactions are considered main factors in driving small-scale (cm to 10 m) patterns of diversity (Levin et al., 2001). Small-scale differences modulate alpha diversity and are thought to be especially important in the deep sea due to the extraordinary patchiness characterizing this environment (Danovaro et al., 2013; Kaiser et al., 2007). However, near-bottom currents, sediment composition, habitat heterogeneity, besides other abiotic factors driven by hydrodynamics, are considered responsible for large-scale differences in local diversity in the deep sea (Gage, 1997; Levin et al., 2001). Accordingly, these factors determine beta diversity along bathymetrical gradients and across geographical distances (Easton and Thistle, 2016; Havermans et al.,

2013; Strugnell et al., 2008). Beta diversity patterns are furthermore affected by the dispersal of organisms and connectivity between areas (Derycke et al., 2013; Etter and Bower, 2015; Gallucci et al., 2008).

The dispersal of organisms is generally defined as the movement of individuals from one place to another with potential consequences for gene flow (Ronce, 2007). If organisms disperse, then connectivity, here defined as the exchange of organisms across habitat patches which lead to gene flow (Calabrese and Fagan, 2004), increases. While some species possess pelagic larval stages, which commonly have relatively high dispersal capabilities (Etter and Bower, 2015), others disperse by passive/active transport of adults through the water column (Gallucci et al., 2008). Dispersal in the deep sea can generate connectivity at different scales, integrating local heterogeneity and regional-scale dynamics (Etter and Bower, 2015). Woolley et al. (2016) observed that connectivity in the deep sea appears to decrease with increasing distance from the continental margin. However, low genetic divergence has been observed in abyssal organisms across large distances (Etter et al., 2011; Etter and Bower, 2015; France and Kocher, 1996; Havermans et al., 2013; Strugnell et al., 2008), while pronounced genetic divergences were correlated with bathymetry (Etter et al., 2011; Havermans et al., 2013). Primarily, dispersal may result in the increase of diversity as well as connectivity if new patches are colonized by pioneers. Secondly, where communities are established, dispersal can lead to intra- as well as inter-specific competition (especially for food, as space is not a limiting factor), and consequently to competitive exclusion (Whittaker et al., 2001). Whether either intra- or inter-specific competition occurs in the deep sea leading to species exclusion is unclear.

In the meiofauna, copepods have been demonstrated to be the first meiofaunal organism to colonize a habitat after a disturbance event, due to their strong swimming capabilities (Boeckner et al., 2009; da Fonseca-Genevois et al., 2006; Thistle et al., 1991). Nematodes, lacking a pelagic larval stage and unable to swim, are shown to be passively transported

through the water column, arriving later than copepods in a disturbed site, but demonstrating strong resistance to disturbance and gradually increasing in abundance until they become the dominant group (Boeckner et al., 2009). Throughout their complete life cycle, nematodes can disperse over large distances either passively in the water column (Palmer, 1988) or actively, using a variety of cues to choose preferential spots (Palmer, 1988; Ullberg and Olafsson, 2003). This could explain the success of this group in colonizing different environments and the existence of cosmopolitan species (Decraemer et al., 2001; Zeppilli et al., 2011).

Dispersal leads to connectivity between areas or genetic structuring at small spatial scales (Bik et al., 2010; Derycke et al., 2013; Van Campenhout et al., 2014). Consequently, connectivity ‘links dynamics at different scales and integrates local heterogeneity, affecting regional-scale dynamics and long-term persistence’ (Etter and Bower, 2015). Shallow-water studies showed that connectivity can exist in nematodes across large geographic scales (Derycke et al., 2013), but data are still scarce for deep-sea meiofauna in general and especially across-depth connectivity in this taxon (Bik et al., 2010). The physical uniformity of the deep sea may evoke assumptions regarding the lack of barriers to dispersal, especially in abyssal plains, but bathymetric stratification has been revealed for genotypes and phenotypes of several molluscs and crustaceans on small (~ 300 m) bathymetrical scales (Etter and Bower, 2015; France and Kocher, 1996; Havermans et al., 2013; Wilson, 1983). The genetic divergence across smaller bathymetrical gradients was more prominent than differences across larger geographical distances, for instance in the cosmopolitan amphipod *Eurythenes gryllus* (Havermans et al., 2013). Contrastingly, nematode and isopod studies indicate a homogeneous gene pool between deep sea and shallow water habitats through the analyses of nuclear (18s rDNA) and mitochondrial (COI) markers (Bik et al., 2010; Hessler and Thistle, 1975; Riehl and Kaiser, 2012). These

findings suggest that dispersal across depths and/or geographic distance may be taxon specific.

Current understanding of cosmopolitanism, dispersal, and connectivity in deep-sea dwelling meiofauna is still in its infancy (Bik et al., 2010; Decraemer et al., 2001; Gallucci et al., 2008; Zeppilli et al., 2011). Studies based on morphological taxonomy suggested that cosmopolitanism can exist in the deep sea (Menzel et al., 2011; Zeppilli et al., 2011), but one's flea in the ear might find it at least questionable. In this sense, questions which arise point towards problems concerning morphological identification and means of dispersal: Are there cryptic species? How can species disperse over such long distances considering their small size? Cryptic species, meaning species which are morphologically indistinguishable but still genetically different, suggesting independent evolutionary entities, have been repeatedly reported for many taxa (Bik et al., 2010; Moura et al., 2012; Nygren et al., 2010; Pawlowski et al., 2007). Until present, only a few studies were published concerning deep-sea nematodes using classic DNA sequencing (Bik et al., 2010; Van Campenhout et al., 2014). Bik et al. (2010) reported low endemism for nematodes over large distances. However, a relatively conservative marker, 18S rDNA, was used in this research.

Nevertheless, it indicates that DNA markers can help to elucidate many questions still unanswered by traditional morphological taxonomy (Derycke et al., 2005). Nowadays, a variety of markers can be used to test evolutionary relationships at different time scales and hierarchy levels between organisms (Blaxter and Floyd, 2003; Blaxter et al., 1998). Nevertheless, the use of more variable markers for nematodes (e.g. microsatellites), which could be more adequate to separate recent species or investigate gene flow, is still challenging due to failure in selecting appropriate markers and in obtaining successful PCR amplifications. The current solution has been to combine the use of DNA methods, such as phylogenetics, and population genetics, with morphological taxonomy, called

integrative taxonomy (Janssen et al., 2015; Miljutin and Miljutina, 2016a). By vouchering specimens, one can always go back to the morphology of an organism to clarify doubts left by the molecular results. Additionally, since molecular tools can be used to detect spatial differences between organisms, their use can indicate connectivity and dispersal in the deep sea at various levels and time scales (Bik et al., 2010).

1.3 Study areas

The study areas of this thesis were situated along continental margins and abyssal plains in the Atlantic and the Southern Ocean. They were located within six different biogeographical provinces according to Longhurst (1998): samples collected at the Western Iberian margin were situated in the Eastern (canary) Coastal Province (CNRY), while samples collected in the North Atlantic were part of the North Atlantic Tropical Gyral Province (NATR) and Western Tropical Atlantic Province (WTRA); finally, samples collected in the Southern Ocean were derived from the Subantarctic Water Ring Province (SANT), Antarctic Province (ANTA) and Austral Polar Province (APLR) (Fig. 1.4). In the following subsections, general oceanographic features of each area are presented.

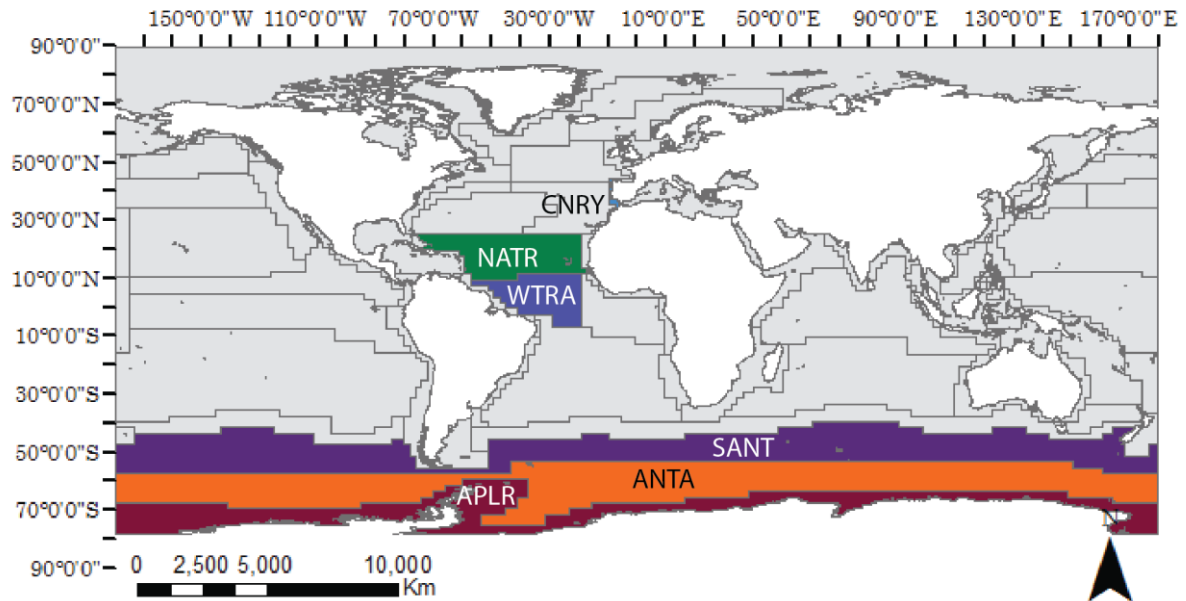


Figure 1.4. Longhurst biogeographical provinces (Longhurst, 1998) covered in this study. CNRY = Eastern (canary) Coastal Province; NATR = North Atlantic Tropical Gyral Province; WTRA = Western Tropical Atlantic Province; SANT = Subantarctic Water Ring Province; ANTA = Antarctic Province; APLR = Austral Polar Province.

1.3.1 The Western Iberian Margin (300–1000 m)

Sampling at the Western Iberian Margin (WIM) occurred aboard the *RV Belgica* (B2013/17 and B2014/15). The WIM is part of the CNRY province (Fig. 1.5), which comprises the Portugal to Senegal eastern boundary current (Longhurst, 1998). The WIM is characterized by a narrow shelf (10–65 km wide) and a steep slope fragmented by canyons extending from the shelf to the abyssal plains (Garcia and Thomsen, 2008; Nolasco et al., 2013; Pinheiro et al., 1996; Relvas et al., 2007).

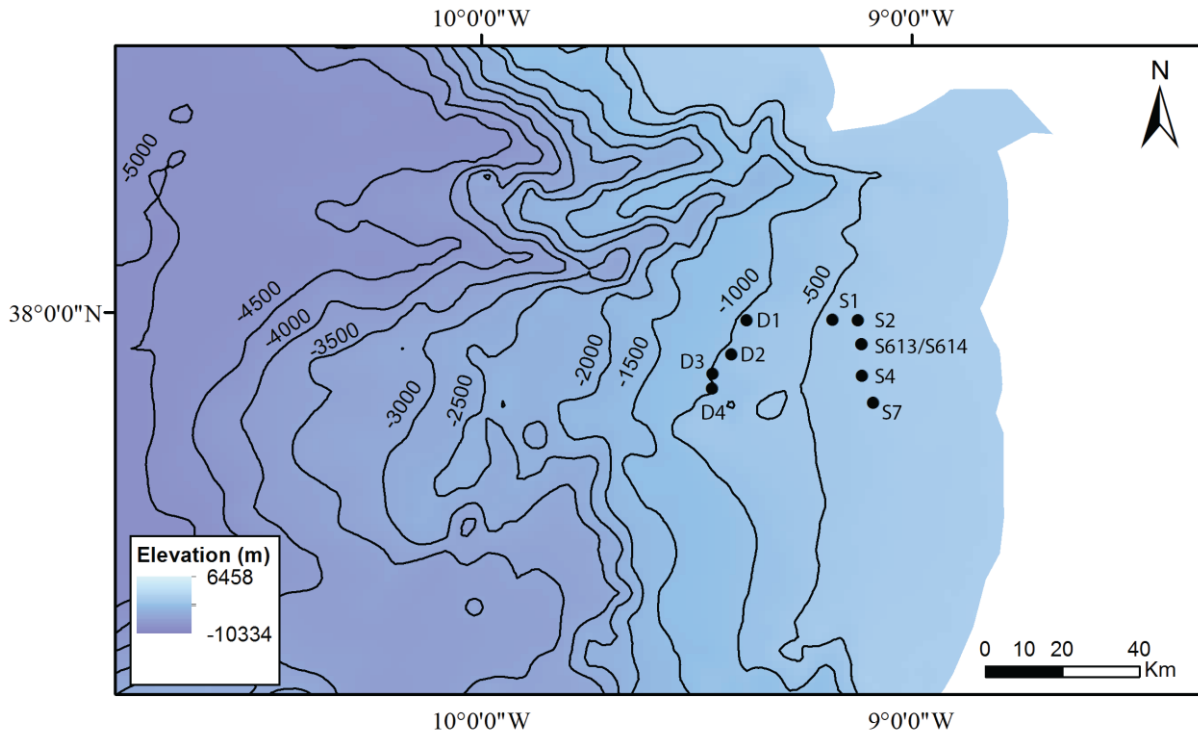


Figure 1.5. Sampling sites located at the Western Iberian Margin. The map displays the sampled sites and black lines the bathymetry contours. Depth increases from light blue to purple.

At the WIM, there is a broad and continuous equatorward surface-water flow that extends from Portugal to Senegal with typical velocities of a few centimetres per second (Nolasco et al., 2013). The coastal regime at the WIM is mainly regulated by the seasonal meridional migration of the trade wind system, which drives upwelling events in the area (Longhurst, 1998). With increased primary productivity between May and June, yearly primary production can reach up to 90 g C m^{-2} (Salgueiro et al., 2014). Along the coast, upwelling events and intensive flow can enhance both vertical as well as horizontal transport of particles from near shore to the open ocean (Crespo et al., 2011; Figueiras et al., 2002; Relvas et al., 2007).

Wind-driven variation in this area is the main factor responsible for a mixed-layer of nutrients at the surface waters, and consequently for a dominance of algal blooms during upwelling processes (Longhurst, 1998). Because of this mixed layer and due to high wind

stress, and enhanced seasonal upwelling, organic matter produced at the surface sinks unconsumed to the seafloor, ensuring benthic utilisation and consequently high mineralisation rates (Longhurst, 1998).

1.3.2 The Vema Fracture Zone (4900–5700 m)

Sampling in the North Atlantic was performed aboard the *RV Sonne* (SO237) (Fig. 1.6). The sampling area covered two distinct biogeographical provinces, the NATR and the WTRA (Longhurst, 1998). Along the Vema fracture zone and the Vema transform, five sites were sampled east and west of the Vema transform fault, as well as one site within the Vema transform fault, situated on the Mid-Atlantic Ridge.

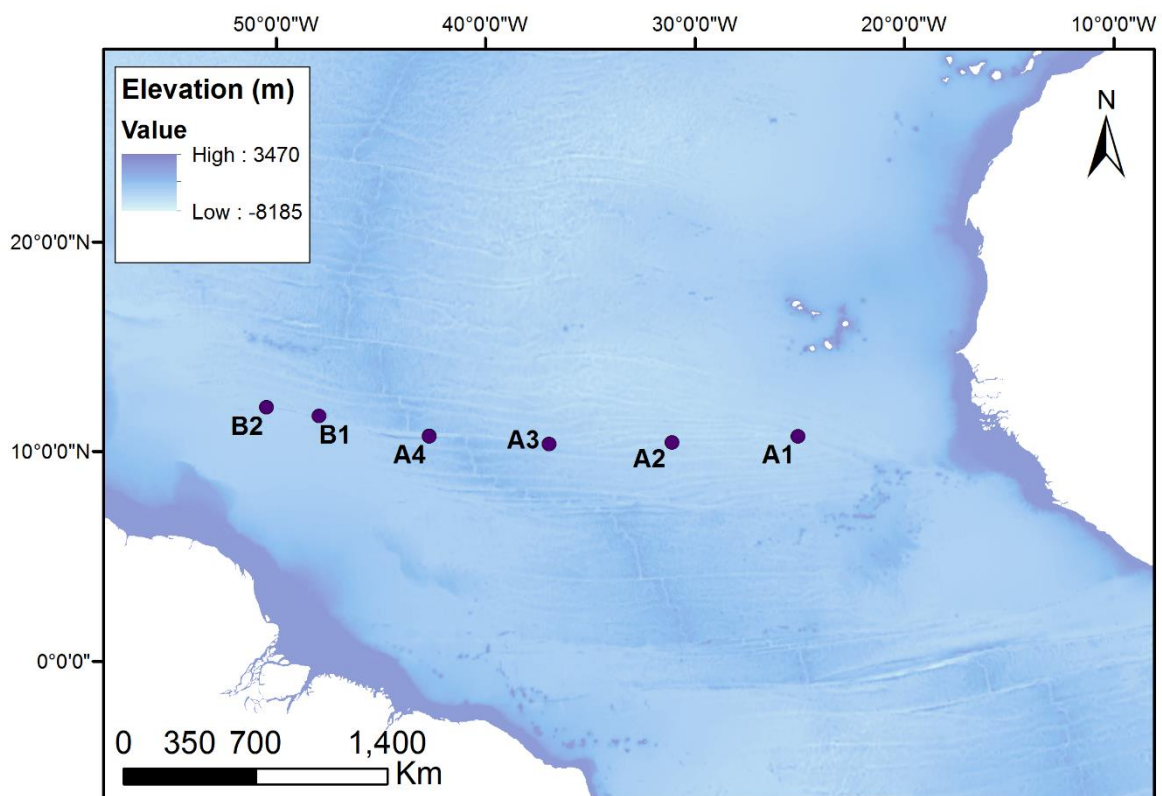


Figure 1.6. Bathymetry map showing the sampling sites located in the North Atlantic, along the Vema Fracture Zone. The Vema Transform Fault can be identified as the horizontal line at station A4.

The Vema fracture zone, located at 11° N, is part of a group of transform faults which offset the Mid-Atlantic Ridge by 320 km (Cannat et al., 1991; Louden et al., 1986). It is composed by a flat transform valley bounded by steep walls with some peaks reaching as high as 500 m below the surface (Morozov et al., 2010) (Fig. 1.7).

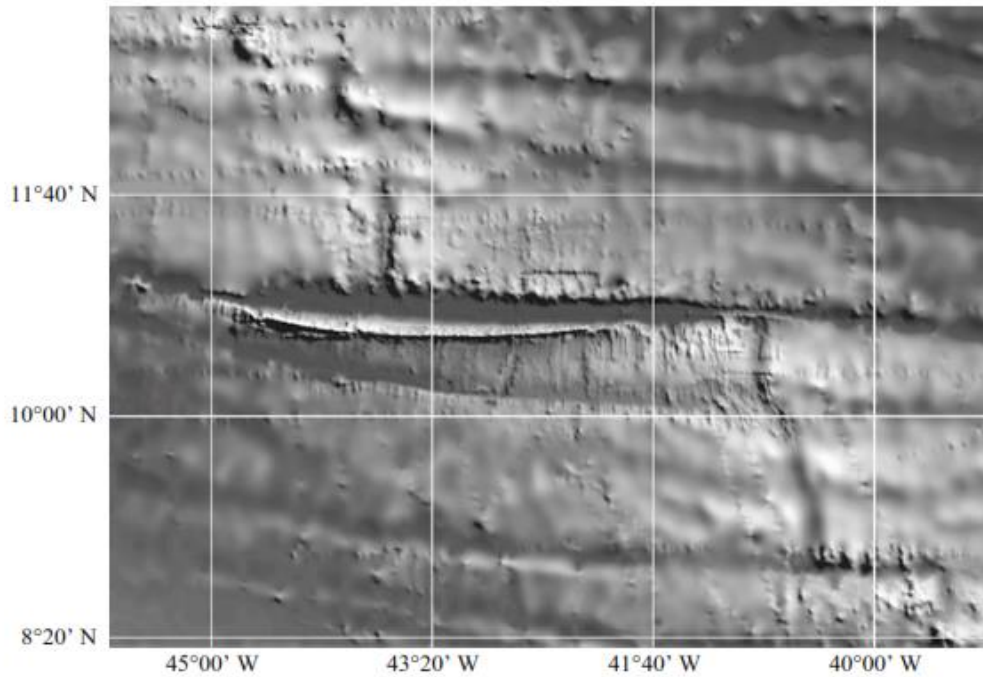


Figure 1.7. A transform fault offsets the Mid Atlantic Ridge at 11° N forming the eastern and western Vema Fracture zone (from Morozov et al. (2010)).

The Vema fracture zone and Vema transform are strongly affected by the advection of the Antarctic Bottom Water (AABW), which penetrates the Vema transform from the western side of the Mid-Atlantic Ridge. The AABW is characterized by low temperature, low salinity, and high nutrient content in comparison to the North Atlantic deep water (NADW), and flows near the seabed with bottom currents of up to 34 cm/s (Morozov et al., 2015, 2010) (Fig. 1.8).

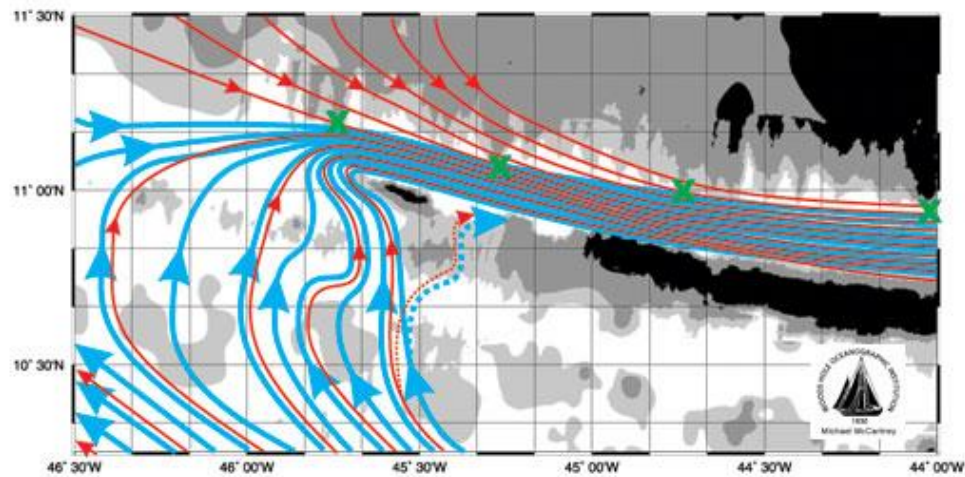


Figure 1.8. Westward flow in the VEMA fracture zone by the Antarctic Bottom Water (AABW) for waters below 4300 m (blue). Red lines represent the North Atlantic Deep Water (NADW), which are located above 4300 m water depth. White areas are deeper than 4700 m, light grey areas are between 4700 m and 4300 m deep, dark grey areas between 4300 m and 3500 m, and black areas represent depths shallower than 3500 m. Green Xs show the location of composite section that has estimated the southward geostrophic flow (<http://www.whoi.edu/page.do?pid=30735>).

Surface productivity in both NATR and WTRA is mainly wind-driven and seasonal (Longhurst, 1998). In both regions, winter convective mixing is considered weak and highly influenced by the North Equatorial Countercurrent (NECC), which induces vertical motion within cyclonic edges (Longhurst, 1998). Moreover, the productivity regime in these two areas lack bloom events and is mainly dominated by picoplankton, which is believed to exhibit negligible sedimentation rates (Jochem et al., 1993).

1.3.3 The Atlantic sector of the Southern Ocean (3700–4100 m)

Sites sampled at the Atlantic part of the Southern Ocean were collected during two campaigns (ANT-XXIV/2 and ANT-XXVIII/3) onboard of the *RV Polarstern* (Fig. 1.9). The nine sampled sites were spread along three biogeographical provinces according to Longhurst (1998): the SANT, ANTA, and APLR.

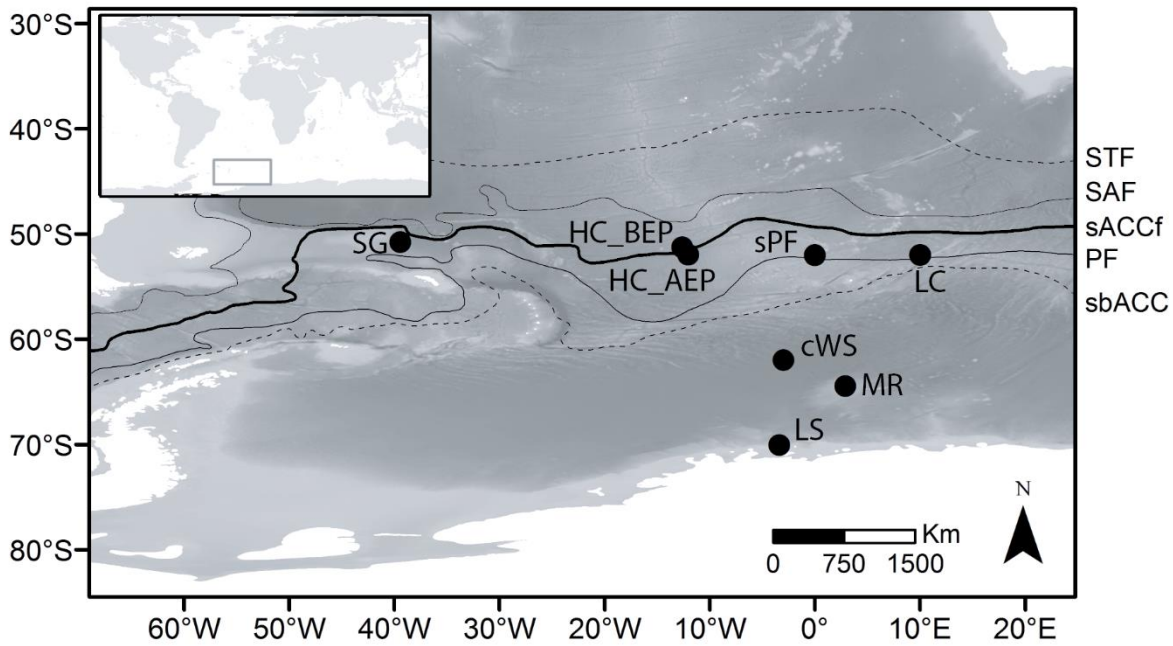


Figure 1.9. Sampling sites located at the Southern Ocean. The map displays features of the Antarctic Circumpolar Current (Orsi and Harris, 2001): Subtropical front (STF), Subantarctic front (SAF), Polar Front (PF), southern Antarctic Circumpolar Current front (sACCf), and southern boundary of the Antarctic Circumpolar Current (sbACC).

Most of the studied sites (SG, HC_AEP, HC_BEP, sPF, and LC) were located in the SANT province. This province is bordered to the south by the Polar Front, which marks the extent of low salinity and cold water (Knox, 1994). The seabed topography along the main path of the Polar Front is believed to exert a strong influence on the Polar Front course. This is a complex region under the influence of the Antarctic Circumpolar Current (ACC) and is characterised by a highly seasonal surface primary productivity (Fischer et al., 2000). Nevertheless, east-west differences in productivity are also observed along the Polar Front, leading to asymmetric primary productivity throughout the year (Demidov et al., 2012).

The most pronounced differences in productivity in the SANT province are observed around the island of South Georgia, where one site of this thesis is located (SG). This site lies under the so-called *Chaetoceros* spp. region, which is named after a major diatom group important for carbon export from the surface to the seabed in this area (Sachs et al., 2000).

2009), characterised by iron and nutrient-rich surface waters. The other sites sampled at the SANT province were located in the *Flagilariopsis kerguelensis* region, which is an iron-depleted ecosystem (Sachs et al., 2009).

The ANTA province, where the sites cWS and MR were sampled, differs from the SANT province by possessing both an open water zone as well as a seasonally ice-covered zone (Longhurst, 1998). The permanently open-water zone of this province is mainly characterised by the dominance of small-cell heterotrophic protists and bacteria in the surface waters (Longhurst, 1998). Nevertheless, the sampled site MR, located at the Maud Rise seamount, is considered to be a region different from the adjacent ocean basins in terms of induced sea-ice formation and mixed-layer anomalies (Beckmann et al., 2001; Brandt et al., 2011a). In general, seamounts perform important roles in ocean circulation through enhanced flow and current speeds (Beckmann et al., 2001). Enhanced currents are directly related to an increase in turbulence and vertical mixing of nutrients, augmenting the downward transport of organic matter produced at the surface and consequently benthic biodiversity and biomass in the area (Beckmann et al., 2001; Brandt et al., 2011a).

Represented by only one site (LS), the APLR province is seasonally ice-covered and exhibits a deep continental shelf (200–500 m). Moreover, this province is characterised by a westward flow of the Antarctic surface water, confluent with the southern branch of the ACC in the ANTA province Longhurst, 1998. This area exhibits a high productivity due to the ice-melted blooms in the surface layers.

1.4 International Framework

Flemish and Brazilian funding provided the necessary support which permitted me to conduct this doctoral study with a multidisciplinary approach, and establish meaningful collaborations with various laboratories and establish valuable sampling partnerships.

In the framework of the projects ANDEEP-SYSTCO (ANtartic DEEP-sea benthic diversity – SYSTem Coupling in the deep Southern Ocean) and SYSTCO II (SYSTem Coupling in the deep Southern Ocean II), starting in summer 2007/08 and 2012, respectively, processes regulating benthic communities in the Southern Ocean were studied (Bathmann, 2010; Brandt et al., 2011). The ANDEEP-SYSTCO project focused on the role of the Southern Ocean in global energy budgets, climate change and functioning of atmospheric, pelagic and benthic systems of the Southern Ocean. Considering the benthic environment, ANDEEP-SYSTCO aimed to investigate the biology of abyssal key species, the role of the bottom-nepheloid layer for the recruitment of benthic animals, as well as the influence of the quality and quantity of food sinking through the water column on abyssal life, feeding ecology, and trophic relationships of abyssal animals (Bathmann and Herrmann, 2010). This doctoral research addressed the latter aim of the project, which investigated nematode communities and their link to the net primary productivity at the surface, as well as their link to the flux of organic matter to the seafloor.

The ANDEEP_SYSTCO II project targeted coupling processes, such as those found during changes in the phytoplankton bloom through the water column and their impact on benthic communities. It comprised investigations of diversity, distribution of abundance of deep-sea benthic organisms and their impact on the biological productivity, as well as the ecology of deep-sea fauna (Wolf-Gladrow, 2012). This doctoral research addressed both objectives of ANDEEP_SYSTCO II, where meiofauna and specifically nematode community characteristics are linked to surface primary productivity and other environmental variables potentially affecting community distribution. Moreover,

techniques to assess carbon flow, such as fatty acid analysis, were also incorporated to test benthic-pelagic coupling and functional diversity in the deep Southern Ocean.

A third project involved the research campaign named Vema-Transit, which lasted from December 2014 until January 2015. The aim of this project was to sample and survey the Vema Fracture zone and Vema Transform fault in the following aspects: generate a high resolution map of the entire length of the eastern Vema Fracture Zone, determine whether it poses a barrier for the dispersal of benthic organisms from east to west, determine whether the benthic fauna from the adjacent Porto Rico Trench differs from that of the Vema Fracture Zone, perform a detailed mapping of the megafauna using AUV images, analyse sediment and pore water, and measure the intensity of turbulent mixing in the near-bottom waters (Devey et al., 2015). This doctoral research targeted the ecological aspects of the Vema Fracture Zone as a physical barrier for the potential dispersal of meiobenthic organisms through the Vema transform fault, and how diversity at the Vema varies spatially when compared to other regions.

The Flemish fund for scientific research (FWO) through this project promoted increased international collaboration: **the enigma of the success of nematodes in the deep sea** (Project number: G083512N). The aim of this project was to investigate why nematodes are so successful in terms of high diversity and cosmopolitanism in the deep sea. This project comprised diverse deep-sea regions and involved innovative tools, such as molecular barcoding and metagenomics, as well as traditional techniques, i.e. traditional morphological taxonomy and additive partitioning analysis, to further investigate the role of nematode communities in the deep sea. This thesis comprised investigations of connectivity in the deep sea, as well as benthic-pelagic coupling that were linked to the aforementioned project.

1.5 Aims and Outline of the thesis

The aim of this thesis was to gain new understanding about the potential factors shaping deep-sea meiobenthic communities. As its main aspects, it addressed benthic-pelagic coupling, particulate OM flux to the seafloor, and OM input in the seabed. Moreover, new insights in spatial turnover, patch-mosaic dynamics and habitat heterogeneity, as well as bottom dynamic effects based on sediment heterogeneity were studied in different deep-sea habitats, such as continental margins and abyssal plains. Finally, nematode distribution patterns were analysed across different spatial scales and linked to environmental factors potentially responsible for their dispersal. Accordingly, this thesis treated a vast and interdisciplinary array of topics addressing deep-sea meiobenthic communities, including taxonomy, molecular genetics, phylogenetics, sedimentology, and oceanography.

This thesis is based on field observational studies at the continental slope of the Western Iberian Margin (**Chapter 5**) and Southern Ocean (**Chapter 2**), at the Maud Rise seamount located in the Southern Ocean (**Chapter 2**), and on abyssal plains in the Southern Ocean and North Atlantic (**Chapters 2, 3, and 4**). Each chapter, apart from the general introduction (**Chapter 1**) and discussion (**Chapter 6**), is either published or under review. Therefore, each chapter is intended to be autonomous, and can be read on its own. Unavoidably, there might be some overlap between the different chapters, especially in the Introduction and Material and Methods sections.

Each chapter of this thesis deals addresses the influence of environmental drivers on meiofauna density, biomass, and diversity, together with spatial heterogeneity. **Chapter 1** focuses on the main aspects covered in this thesis and how they could help in bringing new insight to still unanswered questions concerning deep-sea ecology. In the first study

(**Chapter 2**), surface primary productivity, estimated POC flux, and sediment chlorophyll *a* concentration were used as proxies for food availability in different environments in the Southern Ocean. This study aimed to test the extent meiofaunal communities were dependent on the organic matter input derived from surface waters and how they were related. Moreover, this study attempted to observe if macro-ecological oceanographic features could have an influence on meiofaunal organisms on a small spatial scale. This work was published as: *Lins L., Guilini K. Veit-Köhler G., Hauquier F., Alves R.M.S., Esteves A.M., Vanreusel A., 2014. The link between meiofauna and surface primary productivity in the Southern Ocean. Deep-sea Research II 108, 60-68.*

While an indirect link between detritus and benthic meiofauna could be observed in Chapter 2, in **Chapter 3** a direct link between organic matter input and meiofauna was measured through the use of fatty acid analysis of nematodes. Fatty acid content in bulk nematodes, as well as in the family Desmoscolecidae and the genus *Desmodora* was investigated to first test if their fatty acids were derived from fresh food input and if so, could they feed selectively on rich food sources. Moreover, macro-ecological variables, such as surface primary productivity, in combination with small-scale sediment characteristics, such as chlorophyll *a*, granulometry, and total organic matter content, were correlated to differences in nematode community composition and to their contribution to benthic-pelagic coupling. The changes in abundance of specific genera adapted to feed on fresh labile organic material were also studied in relation to variability in primary productivity. This study was published as: *Lins L., Silva M.C., Hauquier F., Esteves A.M., Vanreusel A., 2015. Nematode community composition and feeding shaped by contrasting productivity regimes in the Southern Ocean. Progress in Oceanography, 134, 356-369.*

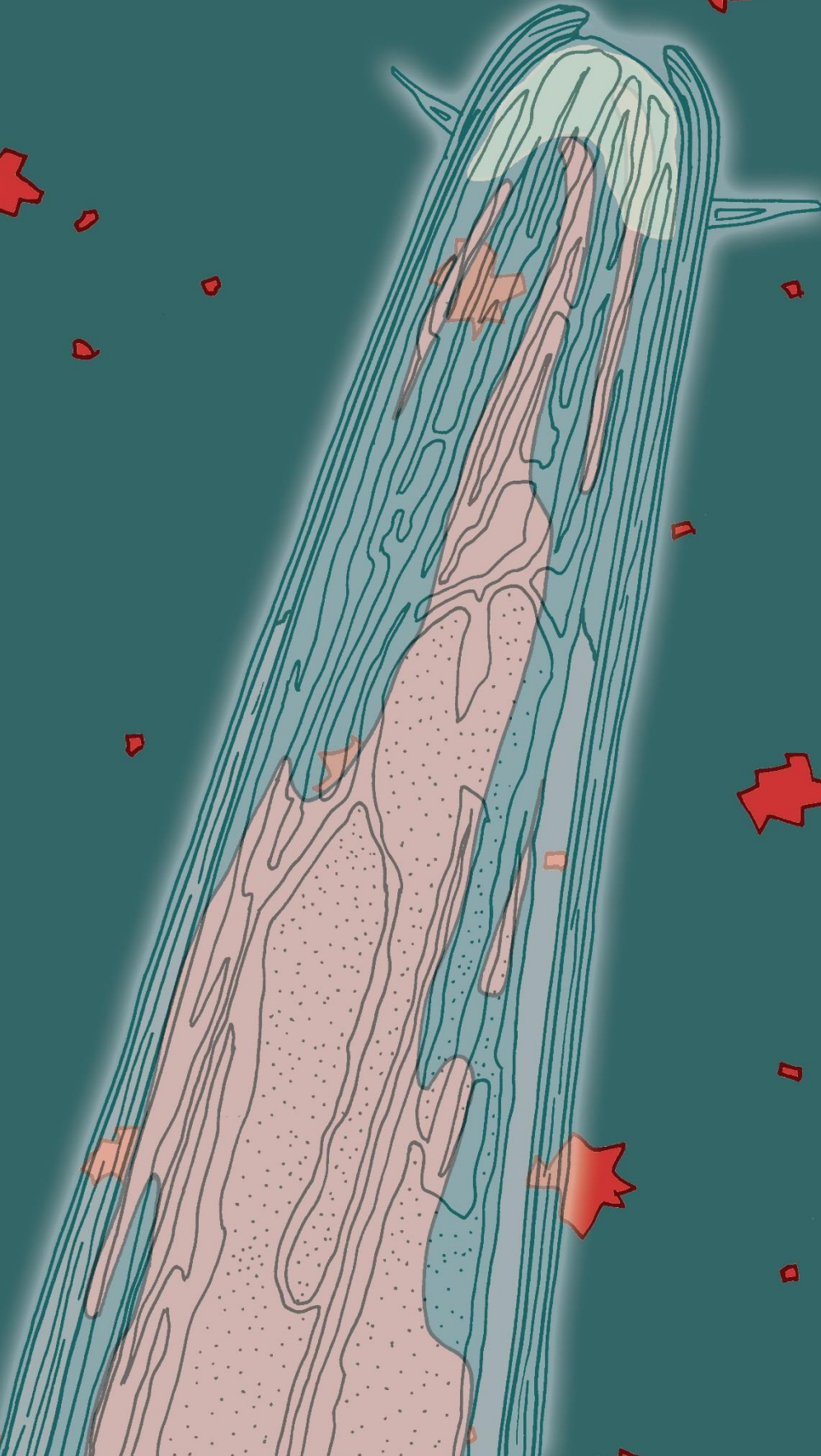
In order to gain more insight in how nematode communities inhabiting oligotrophic regions differ in terms of turnover, standing stocks (biomass and density), and diversity, nematode communities from the Southern Ocean were compared to the oligotrophic region

along the abyssal Vema Fracture Zone, located in the North Atlantic (**Chapter 4**). Responses to organic matter input and multispatial scale variability through additive partitioning of local and regional diversity were investigated. Additionally, the nematode genus *Acantholaimus*, typically found in the deep sea and increasing in importance (relative abundance) with increased water depth, was also investigated on species level. These results are accepted for publication as: *Lins L., Silva M.C., Neres P., Esteves A.M., Vanreusel A., 2016. Testing deep-sea biodiversity paradigms on abyssal nematode genera and Acantholaimus species. Deep-sea research II.*

Going from the abyssal plains of the Southern Ocean and North Atlantic with contrasting productivity regimes to the upper-shelf and slope in the Western Iberian Margin, **Chapter 5** presents the consequences of not only OM, but also of sediment heterogeneity on the marine benthos. Under the same productivity regime, small- and regional-scale variations in nematode community structure were observed in this region. Along bathymetrical and geographical transects, integrative approaches using molecular and morphological techniques were used. In addition, not only the effect of resources arriving at the seafloor were investigated, but also the indirect effect of disturbance on nematode beta diversity. We have further examined the potential effects of connectivity between patches across depth transects. The results of this study are currently under review as: *Lins L., Leliaert F., Riehl T., Ramalho S.P., Cordova E. A., Esteves A.M., Vanreusel A., 2016. Species variability and connectivity in the deep sea: evaluating effects of spatial heterogeneity and hydrodynamics. Biogeosciences Discussions.*

In **Chapter 6**, results from the previous chapters were integrated and discussed in a broader context. Macro-scale patterns of nematode biodiversity were inferred and future directions emphasized.

The link between meiofauna and surface productivity in the Southern Ocean



2





Chapter 2: The link between meiofauna and surface productivity in the Southern Ocean

Manuscript published in modified form as:

Lidia Lins, Katja Guilini, Gritta Veit-Köhler, Freija Hauquier, Renata Mamede da Silva Alves, André Morgado Esteves, and Ann Vanreusel. "The Link between Meiofauna and Surface Productivity in the Southern Ocean." **Deep Sea Research Part II: Topical Studies in Oceanography** 108 (2014): 60–68.

2.1 Abstract

Particulate organic carbon (POC) export fluxes generally reflect patterns of primary production in the upper ocean, sinking to the seabed and acting as a food source for benthic organisms. Data on meiobenthic communities from two SYSTem COUpling cruises (SYSTCO) in the deep Southern Ocean (RV Polarstern ANT-XXIV/2, north-south transect along the prime meridian, and ANT-XXVIII/3, east-west transect along the Polar Front) were combined with surface and benthic environmental variables, as well as POC flux estimates based on satellite measurements. It was tested to what extent meiofaunal communities were determined by prevailing conditions of an east-west increase in net primary productivity (NPP) and bottom chlorophyll *a* (Chl*a*) concentration, and a westwards, divergently decreasing estimated POC flux. Nematodes dominated the meiofauna (84.4% - 92.4%) and occurred with a westward increase in relative abundances and density for the ANT-XXVIII/3 stations, associated with a parallel increase in NPP and Chl*a*. Nematode biomass was negatively correlated with the estimated POC flux. Along the north-south transect no significant correlation was found but higher estimated POC fluxes at stations south of the Polar Front were associated with higher meiofauna diversity and density at higher taxon level, while stations located at the Polar Front, which were associated with lower POC fluxes, contained communities with lower diversity and density.

2.2 Introduction

Surface-water productivity in the Southern Ocean (SO) is largely determined by the unique environmental features of this region. The SO consists of water masses south of the Polar Front (PF), which marks the northern extent of low salinity and cold water (Knox, 1994). Due to its vastness, the SO plays an important role in the global ocean circulation system and possesses the fastest surface ocean current in the world, the Antarctic Circumpolar Current (Griffiths, 2010; Knox, 1994). Generally, the SO receives low terrestrial input and its prevailing flow of energy is defined by phytoplankton surface productivity, followed by sinking and breakdown in the pelagic and benthic microbial loop (Griffiths, 2010; Rowe et al., 2008). Nevertheless, benthic–pelagic coupling is strongly influenced by the high seasonality of primary production resulting in rather low resource availability during most parts of the year (Gooday, 2002; Peck et al., 2006). Surface primary production, together with varying water depth, current regimes, and seasonal ice coverage over large parts of the SO, lead to complex interactions with the benthos, the richest element of the food web in terms of number of species (Griffiths, 2010; Gutzmann et al., 2004; Peck et al., 2006).

Export fluxes of particulate organic matter (POM) through the vertical water column frequently reflect general patterns of primary production (Lutz et al., 2002), and are considered an important process for the benthic–pelagic coupling, as most of the POM consists of labile carbon compounds (Sachs et al., 2009). However, the transport of POM to the deep sea is considered relatively inefficient, with only about 1 % to 3 % of the primary production reaching the deep seabed and the rest being broken down on its way to the bottom by organisms living in the water column (Lutz et al., 2002).

Numerous variables determine the intensity of these export fluxes, including photosynthetic production, zooplankton grazing, oxidative depth-dependent remineralization rates and water depth (Lutz et al., 2002). In addition, sea-ice formation and lateral advection linked mainly to the Antarctic Circumpolar Current may regulate primary production and affect the fate of surface-produced organic matter in the SO (Abelmann et al., 2006; Griffiths, 2010). Seasonal sea ice has been suggested to be an important environment for algal photosynthesis, providing suitable light and nutrient levels, as well as contributing to organic carbon export to the deep sea, favouring benthic organisms' establishment (Brandt et al., 2011b; Brandt and Ebbe, 2009; Guilini et al., 2013; Sachs et al., 2009; Vancoppenolle et al., 2013; Veit-Köhler et al., 2013).

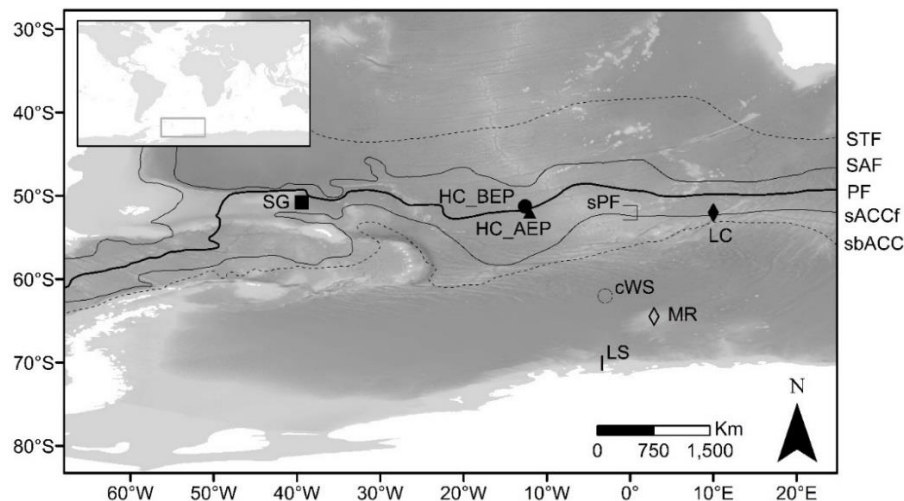


Figure 2.1. Location of ANT-XXIV/2 and ANT-XXVIII/3 sites. Coordinates are given in Table 1. The map displays features of the Antarctic Circumpolar Current (Orsi and Harris, 2001): Subtropical Front (STF), Subantarctic Front (SAF), Polar Front (PF), southern Antarctic Circumpolar Current Front (sACCf) and southern boundary of the Antarctic Circumpolar Current (sbACC). Bathymetry data provided by ETOPO1 and world boundaries by ESRI (Amante and Eakins, 2009). Sampling sites are represented by symbols: SG (South Georgia), HC_BEP (High Chlorophyll before Eddy Pump), HC_AEP (High Chlorophyll after Eddy Pump), sPF (South Polar Front), LC (Low Chlorophyll), cWS (central Wedell Sea), MR (Maud Rise) and LS (Lazarev Sea).

Declines in standing stocks with depth are generally attributed to a decrease in food availability (e.g. particulate organic carbon flux, Rex et al., 2006), although other factors such as predation, competition and/or life history traits may also play a role (Levin et al.,

2001; Ramirez-Llodra et al., 2010; Soetaert et al., 2002). A few studies report on the link between surface primary production and benthic communities in the SO (Brandão et al., 2014; Brandt et al., 2011b; Guilini et al., 2013; Veit-Köhler et al., 2013; Würzberg et al., 2011). Moreover, in combination with direct measurements, Wei et al. (2010) used models to predict which factor contributed most to benthic–pelagic coupling worldwide. Shallow-water as well as deep-sea communities were found to be positively linked to surface primary productivity and estimated particulate organic carbon (POC) flux.

Two recent papers compared the fatty acid composition of deep-sea nematodes to that of the sediment in the studied region (Guilini et al., 2013), and they have investigated the short-term response of nematode community structure to a natural phytodetritus pulse (Veit-Köhler et al., 2011). Both studies suggested a fresh phytodetritus diet based on (1) the relatively high proportion of fatty acids indicative of phytodetritus in nematodes and (2) a vertical movement in the sediment towards surface layers as a response to food input. No studies in the SO, however, integrated seasonally-based surface primary production or estimated POC flux data with meiofauna standing stocks and seafloor labile organic matter in order to link those variables. Estimated POC fluxes reflect primary productivity processes and might be a better predictor of labile organic matter which arrives at the sea bottom than net primary productivity (NPP). Together with sediment Chlorophyll *a* (Chl*a*), estimated seafloor POC fluxes can reflect how much organic matter reaches the deep seabed, since the algorithm takes into account both NPP and water depth.

Metazoan meiofauna provide a good tool for studying standing stock patterns in the SO deep sea relative to surface productivity mainly due to their omnipresence and low mobility. Among the metazoan meiofaunal groups, nematodes usually dominate both in abundance and biomass, occurring frequently in percentages higher than 90 % (Giere, 2009).

In order to assess differences in meiofauna standing stocks (i.e. density and biomass) according to different surface-water productivity regimes in the SO, we integrated data from two sampling campaigns along a north–south (N–S) and an east–west (E–W) transect in the Atlantic part of the Southern ocean, covering different water depths, to test the following hypotheses:

- (1). Variation in meiofauna standing stocks and diversity in the SO are related to variation in surface primary productivity.
- (2). Estimated POC fluxes and sea-floor labile organic matter (depth-related variables) determine small-scale (i.e. within a site) patterns of meiofauna standing stocks and diversity.

2.3 Material and methods

2.3.1 Study area and sampling procedure

During the RV Polarstern ANT-XXIV/2 (28.11.2007–04.02.2008) and ANT-XXVIII/3 07.01.2012–07.03.2012) cruises to the SO (Bathmann and Herrmann, 2010; Wolf-Gladrow, 2012), deep-sea sediment samples were collected in the framework of the ANDEEP-SYSTCO and SYSTCO II projects, respectively. The study area comprises of nine sites distributed along a N–S (Prime Meridian between 49°S and 70°S) and an E–W (between 10°E and 39°W) transect, covering depths ranging from 1935 m to 5323 m (Fig. 2.1 and Table 2.1). Samples from the ANT-XXVIII/3 campaign comprised both spatially different sites as well as one site which was sampled before and after an eddy event (Eddy Pump project) (Table 2.1). These eddy events are supposed to stimulate the pumping of organic matter to the seabed. Eddy Pump was a parallel project which intended to identify eddy

structures between 50° and 60°S, where the upwelled deep-water masses interact with the atmosphere, in order to study the effect of circulation and carbon pumps.

Sampling was conducted using a Multicorer (MUC) equipped with twelve Plexiglass cores to retrieve virtually undisturbed sediment cores. During the ANT- XXIV/2 campaign (henceforth referred to as NS-2007/8) the inner core diameter was 9.4 cm (equivalent to 69.4 cm² cross-sectional surface area) while for the ANT-XXVIII/3 (EW-2012) campaign it was 6 cm (25.5 cm² cross-sectional surface area).

Table 2. 1. Sampling details. Each deployment is treated as one replicate. In the deployment column, number in brackets represent the core codes, thus the replicates. Core numbers not in bold represent the cores sampled for the meiofauna analyses, while core codes in bold refer to cores used for environmental analyses. PF = Polar Front.

Site	Deployment (core code)	Date	Depth (m)	Latitude	Longitude	Geographical area
SG	175-5 (7-8)	04/03/2012	4154.2	50°46.69'S	39°25.35'W	South Georgia
SG	175-6 (5-6)	04/03/2012	4155.2	50°46.59'S	39°25.33'W	South Georgia
SG	175-7 (2-3)	04/03/2012	4154.2	50°46.60'S	39°25.38'W	South Georgia
SG	175-8 (1-10)	04/03/2012	4154	50°46.60'S	39°25.39'W	South Georgia
SG	175-9 (3-6)	04/03/2012	4152.1	50°46.57'S	39°25.33'W	South Georgia
HC_AEP	141-6 (3-4)	18/02/2012	4113	51°15.98'S	12°37.04'W	PF(After Eddy Pump)
HC_AEP	141-9 (6-8)	18/02/2012	4114	51°16.03'S	12°37.06'W	PF(After Eddy Pump)
HC_AEP	141-10 (3-6)	19/02/2012	4113	51°15.97'S	12°36.94'W	PF(After Eddy Pump)
HC_AEP	141-11 (3-5)	19/02/2012	4113.2	51°16.02'S	12°37.12'W	PF(After Eddy Pump)
HC_BEP	086-26 (4-8)	01/02/2012	3966.2	51°58.87'S	12°3.76'W	PF(Before Eddy Pump)
HC_BEP	086-28 (6-8)	01/02/2012	3968	51°58.74'S	12°2.11'W	PF(Before Eddy Pump)
HC_BEP	086-29 (3-5)	01/02/2012	3970.8	51°58.78'S	12°1.95'W	PF(Before Eddy Pump)
HC_BEP	086-30 (1-3)	02/02/2012	3965.4	51°58.91'S	12°2.16'W	PF(Before Eddy Pump)
LC	081-8 (3-4-6)	19/01/2012	3760.5	51°59.99'S	9°59.99'E	PF(Low Chlorophyll)
LC	081-9 (8-10)	19/01/2012	3760.7	52°0.01'S	10°0.05'E	PF(Low Chlorophyll)
LC	081-12 (6-8)	19/01/2012	3757.5	51°59.93'S	10°0.06'E	PF(Low Chlorophyll)
LC	081-13 (6-7)	19/01/2012	3760.5	52°0.042'S	9°59.90'E	PF(Low Chlorophyll)
sPF	013-12 (2-6-12)	06/12/2007	2963	52° 2.22' S	0° 1.04' W	South PF
sPF	013-14 (1-4-9)	06/12/2007	2970	52° 2.25' S	0° 1.11' W	South PF
sPF(2nd)	085-5 (2-3-11)	26/01/2008	2965	52° 1.20' S	0° 0.20' E	South PF (second visit)
sPF(2nd)	085-7 (1-4-8)	27/01/2008	2964	52° 1.53' S	0° 0.16' E	South PF (second visit)
cWS	033-10 (3-4)	30/12/2007	5323	62° 0.80' S	2° 59.05' W	Wedell Sea
MR	039-10 (5)	03/01/2008	2116	64° 28.83' S	2° 52.48' E	Maud Rise
MR	039-12 (8)	03/01/2008	2123	64° 28.83' S	2° 52.53' E	Maud Rise
MR	039-14 (11)	03/01/2008	2119	64° 28.84' S	2° 52.49' E	Maud Rise
LS	017-12 (6-8-11)	22/12/2007	1935	70° 4.86' S	3° 22.59' W	Lazarev Sea
LS	017-14 (1-11-12)	22/12/2007	1951	70° 4.80' S	3° 22.71' W	Lazarev Sea

2.3.2 Meiofauna sample processing

At every site, cores for community analysis were sliced into 1-cm layers down to 5 cm and together with the supernatant water (added to the first layer) preserved in a 4–7 % borax-buffered formaldehyde solution. Samples were washed over stacked sieves with a 1000 µm

mesh and a 32 µm mesh to retain the meiofauna fraction and remove smaller particles. The 32 µm fraction was then elutriated and centrifuged three times (G-force=6056.12 g, RPM=4000, NS-2007/8, and RPM=5421, EW-2012) with colloidal silicagel Levasil (specific gravity 1.17), for the NS-2007/8 sites, and LUDOX HS40 Dupont (specific gravity 1.19), for the EW-2012 sites, as a flotation medium (Heip et al., 1985). After being stained with Rose Bengal, all metazoan organisms were classified at higher taxon level following Higgins and Thiel (1988) and counted under a stereomicroscope (50x magnification).

Nematodes were hand-picked and mounted on glass slides. The length (excluding filiform tail tips) and maximum body width of nematodes (100 specimens per layer if possible) were measured using the compound microscope Leica DMR and Leica LAS 3.3 imaging software. Nematode total biomass was then calculated according to Andrassy's formula $G = \frac{a^2 \times b}{1.6 \times 10^6}$, where G = wet weight in µg, a = maximum body diameter (µm) and b = total length (µm) (Andrássy, 1956). A dry-to-wet ratio of 0.25 was assumed (Heip et al., 1985).

2.3.3 Environmental parameters

Cores for environmental analyses were obtained from the same MUC deployment as cores for meiofauna analysis (Table 2.1). Previously frozen at -80 °C, each 1 cm-thick slice was subsampled and subsequently analysed for biochemical parameters down to 5 cm sediment depth. For total sedimentary organic carbon (%TOC) and nitrogen (%TN), samples were lyophilized, homogenized and acidified with 1 % HCl and the %TOC and %TN contents were measured using a Flash EA 1112 + Mas 200 Elemental Analyser. Samples for sediment Chla were lyophilized, homogenized and the pigments extracted in 90 % acetone, after which they were separated using reverse-phase HPLC, and measured with a Gibson fluorescence detector (Wright and Jeffrey, 1997). Net primary productivity (NPP) values were extracted from the Vertically Generalized Production Model (VGPM,

resolution: 1°) described by Behrenfeld and Falkowski (1997). The VGPM model is a chlorophyll-based algorithm that estimates NPP values using satellite measurements of sea surface temperature, surface Chla and photosynthetically active radiation.

The available HDF (Hierarchical Data Format) format data were extracted using the Marine Geospatial Ecology Tools for ArcGIS and converted to raster using the software ArcGIS. Due to the long ice-coverage period in the Southern Ocean, some NPP values could not be obtained from the satellite VGPM data. The values for Seasonal Variation Index (SVI) measurements were derived from the yearly NPP values (i.e. calculated based on the month of sampling and the eleven months before it), and consequently for NPP and POC were then restricted to the ice-free months. The POC flux to the ocean floor was estimated based on the export water depth (z_e), and seasonal variation in NPP calculated as the standard deviation divided by the mean of monthly NPP values (Lutz et al., 2002, 2007):

$$SVI = \frac{\sigma(NPP)}{NPP}, \text{ and } POC = pr_d \exp\left(\frac{-z_e}{rld}\right) + pr_r.$$

Pr_d , rld and pr_r are functional forms of coefficient algorithms and are calculated as follows:

$$pr_d = (31 * SVI^2 + 49 * SVI + 7.8) 10^{-3};$$

$$rld = 1400 \exp(-0.54 * SVI);$$

$$pr_r = (2.6 * SVI^2 - 4.2 * SVI + 4.8) 10^{-3}.$$

2.3.4 Data analysis

The untransformed univariate data (i.e. density, richness, and biomass) and multivariate assemblage data (density of each group) on higher taxon level were analysed by means of non-parametric permutational ANOVA based on Euclidean distances and Bray–Curtis

similarities, respectively (Anderson et al., 2008), to assess N–S and E–W differences. The dataset was investigated using either a fully crossed three-factor model design (Site [ST]:fixed; Slice [SL]: fixed, Replicates [Rep]: random, nested within [ST]), to investigate differences between sediment layers, or a one-factor model design ([ST]: fixed) using the software PERMANOVA+ for PRIMER (Anderson et al., 2008). The one-factor design ([ST]: fixed) was used to compare differences between sites.

A PERMDISP analysis was conducted to test for homogeneity of multivariate dispersions using distances among centroids. Pair-wise t-tests were performed between all pairs of levels to determine where the differences between each combination were located. This was followed by a SIMPER analysis to identify which meiofauna taxa were responsible for the dissimilarities between sites.

The set of seafloor and surface environmental data (%TOC, %TN, Chla/%TOC, Chla, average estimated POC, average estimated NPP, SVI, and Depth) was tested for collinearity with Draftsman plots and partial Spearman correlations (given depth) using R (Kim, 2013). Benthic variable analyses (%TOC, %TN, Chla/%TOC, and Chla) were only conducted for the EW-2012 samples due to the lack of a complete environmental dataset for the NS2007/8 campaign. DISTLM (distance-based linear model) routines were performed to analyse the relationship between meiofaunal assemblage structure and biomass, and the environmental variables. The DISTLM was built on ‘step-wise’ selection procedure and adjusted R^2 was chosen as the selection criterion (Anderson et al., 2008).

2.4 Results

2.4.1 Trends in NPP and estimated POC flux

NPP monthly average values ranged from $84.7 \text{ g C m}^{-2} \text{ month}^{-1}$ to $574.2 \text{ g C m}^{-2} \text{ month}^{-1}$ (Fig. 2.2). An increase in average monthly NPP was observed along the E–W transect for all sites (EW-2012) from the LC to the SG site. This longitudinal gradient was particularly more pronounced at the end of Antarctic summer (January/ February) (Fig. 2.2). In addition, the monthly NPP values at the LC site fell within the range of the south PF sites values of the NS-2007/8 campaign, while NPP values at the MR site grouped together with SG site values. Throughout most of the Antarctic summer, SG exhibited the most elevated NPP values when compared to the other sites, with monthly NPP values up to $972.3 \text{ g C m}^{-2} \text{ month}^{-1}$. Additionally, seasonal variability in NPP (SVI) was greatest at MR (0.9), followed by HC_AEP (0.74), and SG (0.69). The longest ice-coverage period was observed for the southernmost site LS (11 months) followed by MR (9 months) and cWS (8 months).

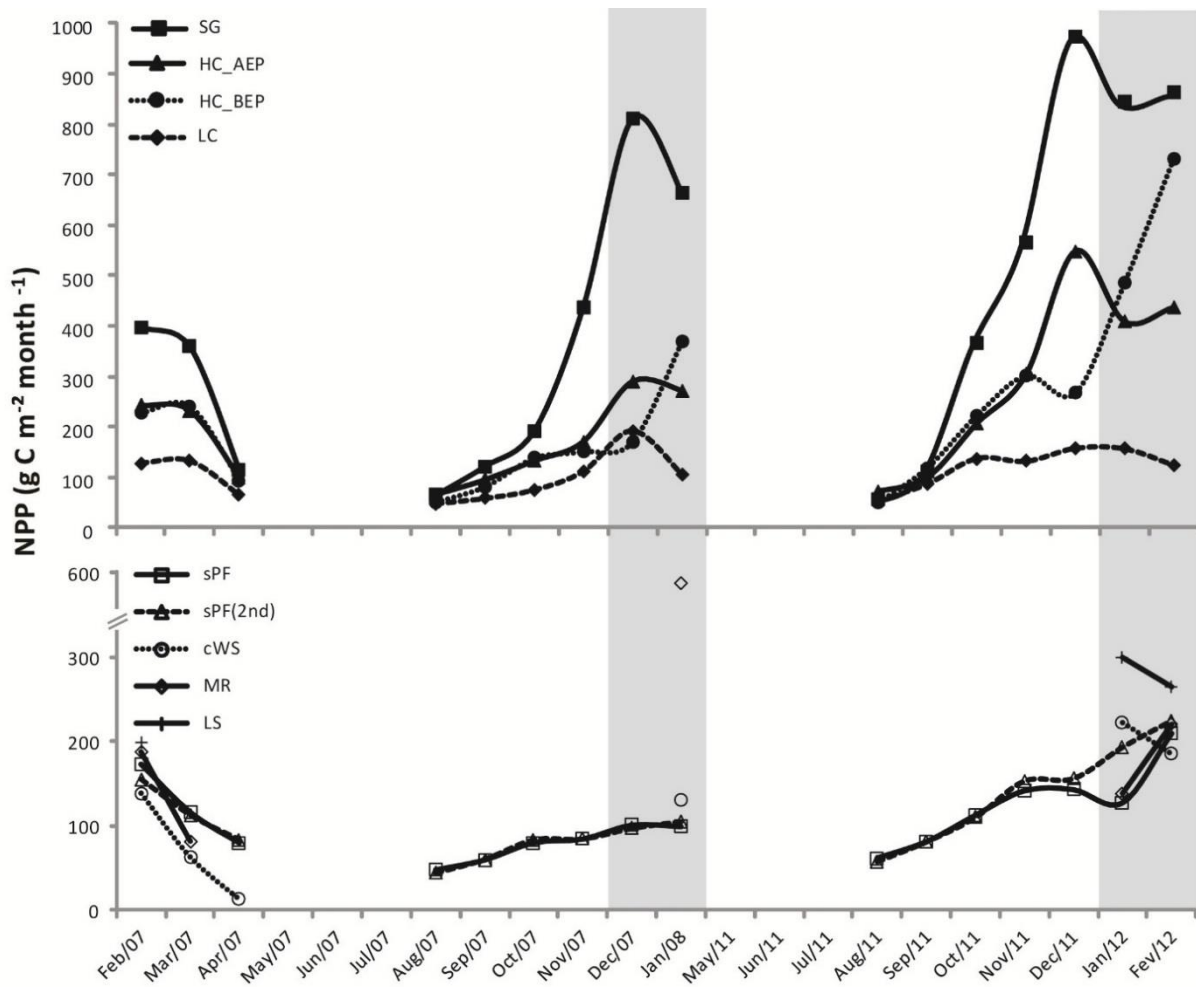


Figure. 2.2. Satellite-based estimates of Net Primary Productivity (NPP) monthly variation in the Southern Ocean for the NS 2007/8 (bottom) and EW-2012 (top) sites. Grey zones represent the sampling period. Months without a value refer to the data which could not be extracted due to ice coverage.

Average estimated POC fluxes to the seafloor varied from $3.4 \text{ mg m}^{-2} \text{ month}^{-1}$ up to $13.6 \text{ mg m}^{-2} \text{ month}^{-1}$ (Fig. 2.3). They slightly increased eastwards (Fig. 2.3) and overall declined with depth ($r = -0.76$, NS-2007/8, and $r = -0.99$, EW-2012, Spearman rank correlation). Fluxes at site MR were at least two times higher than at all other sites whilst cWS displayed the lowest values (Fig. 2.3).

2.4.2 Benthic environment and metazoan meiofauna

Total Sediment Chla concentrations (only measured for the EW-2012 sites) significantly differed between sites along the E–W transect (one-way PERMANOVA, $p < 0.0003$, pair-wise t-test, $p < 0.001$, Table S1). There was a westward increase towards SG, where Chla concentrations reached $18.8 \mu\text{g g}^{-1}$ sediment (Fig. 2.3).

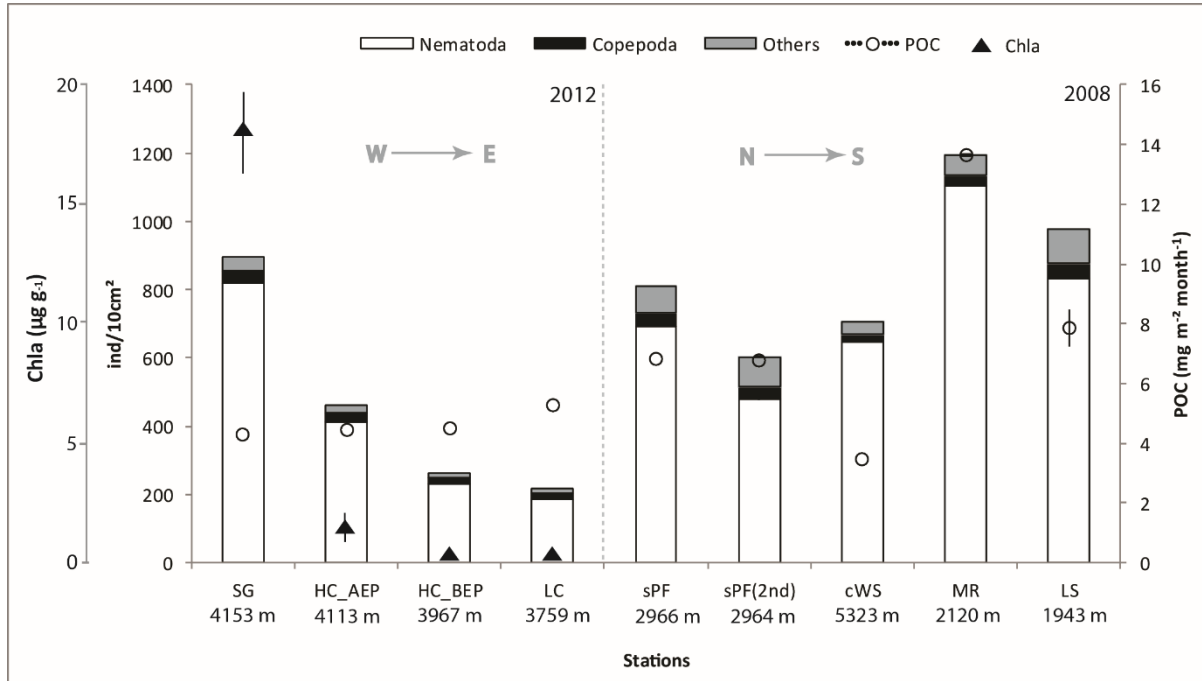


Figure. 2.3. Meiofauna densities (ind/10cm²) and seafloor Particulate Organic Carbon (POC) fluxes ($\text{mg g}^{-2} \text{Month}^{-1}$) for the NS-2007/8 and EW-2012 sites, and Chlorophyll a (Chla, $\mu\text{g g}^{-1}$) for the EW-2012 sites.

The highest meiofauna densities were detected in MR and LS, while at LC and HC_BEP lowest densities were found (Table 2.2). At all sites, nematodes were consistently the dominant taxon (84.4–92.4 %), followed by copepods (2.6–8.2 %) and nauplius larvae, here considered as a separate group (2.1–10.1 %). Densities of all three taxa followed the same pattern, with higher densities found at MR and LS and lower densities at LC (Table 2.2). Meiofauna densities significantly differed between sites (one-way PERMANOVA, $p < 0.001$, Table 2.3) and pair-wise comparisons can be found in Table S2. Nematode densities between sites were significantly different as shown by PERMANOVA tests ($p < 0.001$, Table 2.3) and pair-wise comparisons revealed significant differences between most EW-2012 sites (except for HC_BEP and LC). Nematode densities for sites HC_AEP, HC_BEP,

and LC were also significantly distinct from MR and LS sites, and HC_BEP and LC from sPF site. SIMPER analyses revealed that the dissimilarities between sites were mainly a result of differences in the relative abundance of nematodes, copepods and nauplii. When only the first sediment layer (0–1 cm) was considered (one-way PERMANOVA, $p < 0.001$) pairwise comparisons for EW-2012 revealed significant differences for meiofauna between all sites except for the pairs SG and HC_AEP, and HC_BEP and LC. Three-factor PERMANOVA results revealed significant differences for the interaction of factors Site x Slice ($p < 0.0001$). PERMDISP results were significant for total nematode densities ($p > 0.0002$), indicating that part of the differences observed was due to dispersion of the data. The results for the three-way PERMANOVA based on the multivariate matrix relative abundances revealed significant differences between the interaction of factors Site x Slice ($p < 0.001$). Pair-wise t-tests can be observed in Table S2.

PERMANOVA analysis of total nematode biomass indicated significant differences between sites ($p < 0.001$, Table 2.3). Pair-wise t-tests revealed significantly higher nematode biomass for SG, compared to the other EW-2012 sites. Nematode biomass at the NS-2007/8 sites did not diverge significantly as shown by the pairwise tests. Nevertheless, higher biomass values for all sites were present in cWS and LS (Table 2.2).

A total of 23 higher metazoan meiofauna groups were identified. Taxon richness (S) varied from five to sixteen taxa and differed significantly between sites (one-way PERMANOVA, $p < 0.001$, Table 2.2). Nevertheless, pair-wise comparisons revealed only significant differences between MR and EW-2012 sites (SG, HC_AEP, HC_BEP, and LC), and between SG and the sites LS and sPF (2nd). The taxa Crinoidea and Gastropoda (originally not belonging to the meiofauna), and Loricifera and Tantulocarida were restricted to NS-2007/8 sites. Results from the three-factor PERMANOVA design revealed significant differences between the interaction Site x Slice ($p < 0.0141$). PERMDISP results for meiofauna richness were not significant ($p > 0.05$).

Table 2.2. Overview per site of taxon richness (number of groups), meiofauna density (ind/10cm²), nematode density (ind/10cm²) and total nematode biomass (µg dwt), and nematode relative abundance (%) ± standard deviation for NS-2007/8 and EW-2012 sites. The station cWS was only represented by one replicate.

Site	Taxon Richness	Meiofauna density	Nematode Density	Nematode biomass	Nematode relative abundance
SG	8.5 ± 1.8	893.3 ± 218.0	819.6 ± 197.4	8.15 ± 1.7	85.8 ± 3
HC_AEP	8.0 ± 1.1	461.5 ± 103.9	410.1 ± 99.8	3.48 ± 2.3	85.3 ± 4.4
HC_BEP	6.0 ± 0.8	263.6 ± 87.9	230.3 ± 76.2	0.80 ± 0.5	63.7 ± 3.4
LC	6.7 ± 1.3	219.2 ± 86.1	185.1 ± 78.4	3.07 ± 0.6	71.5 ± 8.6
sPF	16.0 ± 0	807.4 ± 184.3	693.8 ± 173.5	6.70 ± 0.2	77.1 ± 2.4
sPF(2nd)	16.5 ± 0.7	599.8 ± 40.4	480.1 ± 17.2	7.35 ± 2.3	75.1 ± 1.2
cWS	11.0	704.2	648.4	11.7	92.7
MR	14.3 ± 1.1	1192.5 ± 248.1	1102.4 ± 232.5	4.9 ± 1.5	78.4 ± 3.1
LS	18.0 ± 1.4	978.1 ± 110.4	833.1 ± 101.6	12.4 ± 3.0	79.4 ± 3.2

Table 2.3. Results from multivariate PERMANOVA analyses for differences in meiofauna density, nematode density, and nematode biomass.

Meiofauna community structure						
Source	df	SS	MS	Pseudo-F	P(perm)	perms
Site	8	19238	2404.7	10.111	<i>0.0001</i>	9915
Res	18	4280.8	237.82			
Total	26	23518				
Nematode density						
Source	df	SS	MS	Pseudo-F	P(perm)	perms
Site	8	18564	2320.5	9.376	<i>0.0001</i>	9932
Res	18	4454.8	247.49			
Total	26	23019				
Nematode biomass						
Source	df	SS	MS	Pseudo-F	P(perm)	perms
Site	8	25604	3200.5	98.058	<i>0.0001</i>	9934
Res	141	46020	326.38			
Total	149	71624				
Total	149	71624				

2.4.3 Relation between environmental data and meiofaunal densities

Partial Spearman Rank correlations (Fig. S1) between seafloor environmental variables and meiofauna densities (0–5 cm) for the EW-2012 samples revealed significant ($p < 0.05$) positive relationships between meiofauna densities and Chla ($r = 0.79$) and Chla/ %TOC ($r = 0.94$), and significant negative correlations with estimated POC fluxes ($r = -0.67$). In addition, nematode densities were positively correlated with estimated POC fluxes ($r = 0.92$) for the NS-2007/8, and densities of surface-dwelling nematode densities (0–1 cm) had strong correlations with Chla ($r = 0.96$). Correlations between NPP and seasonal variation (SVI) on one hand and meiofauna and nematode densities on the other hand were not significant. Nematode biomass for the N–S sites was negatively correlated with estimated POC flux ($r = -0.71$).

Significant correlations occurred between depth and densities of meiofauna ($r = 0.82$) for the E–W sites, and between depth and nematode densities for both E–W and N–S sites ($r = 0.71$ and $r = -0.73$, respectively). No taxa richness-depth trend was observed. DISTLM analyses showed a significant effect of the estimated POC fluxes ($p < 0.0016$, Tables S3 and S4) on the meiofauna and nematode densities when just the first-centimetre layer was analysed (both adjusted $R^2 = 0.228$). These tests revealed that estimated POC fluxes were responsible for 18 % of the total meiofauna density significant variation. For the nematode total density over 5 cm sediment depth, POC and average NPP accounted for 43 % of total variation (Table S3).

2.5 Discussion

2.5.1 Trends in NPP and estimated POC flux

The east–west increase in NPP in the Atlantic part of the Southern Ocean is in agreement with previous *in situ* and satellite-based measurements for the SO (Atkinson et al., 2001;

Demidov et al., 2012), whilst NPP values were higher than those reported previously for the SO (Lutz et al., 2007). An elevated NPP at SG was expected, as this region is characterized by local nutrient resupply due to upwelling processes which supports high phytoplankton productivity (Brandon et al., 2000; Orsi et al., 1995; Whitehouse et al., 1996). The low NPP values found for the cWS and LS sites were possibly underestimated as a result of the long ice coverage period during which Chla satellite measurements were not available. As such, sea-ice algal productivity is not taken into account although it can be considered an important food source in sea-ice ecosystems, accounting for 25 % of total primary production (Arrigo and Thomas, 2004).

A high NPP peak at the MR site was reported by other studies (Beckmann et al., 2001; Brandt et al., 2011a) and surface-water sampling at this site indicated a vigorous pelagic food web associated with a rich ice-edge bloom (Brandt et al., 2011a). These ice-covered areas are also favoured during sea-ice decay in summer, which creates a shallow mixed layer that significantly enhances primary production (Flores et al., 2011). Therefore, the high NPP peak observed for the MR site in January 2008 could be a response to ice melting and subsequent ice-algae sedimentation in the form of dissolved or particulate organic carbon, living cells or aggregations of dead and living cells (Arrigo and Thomas, 2004).

A slight increase in estimated POC deposition was associated with strongly decreasing benthic Chla concentrations and surface NPP values for the EW-2012 sites. However, NPP and POC are highly correlated since estimated POC is derived from NPP values. Particularly for site SG, higher estimated POC values were expected since NPP values are higher than for other sites. So far, however, the processes influencing actual seafloor POC fluxes are not quantitatively understood (De La Rocha and Passow, 2007). POC flux estimates are water-depth dependent but they do not take into account small-scale patterns nor do they include biological-pump interrelated processes, such as (dis)aggregation of organic-rich particles (De La Rocha and Passow, 2007; Lutz et al.,

2007). Its values are highly dependent on depth differences, which play a crucial role in the transfer efficiency of POC (De La Rocha and Passow, 2007; Lutz et al., 2007). This is possibly the reason why estimated POC values do not vary as greatly for the EW-2012 sites (3760.5–4155.5 m) as they do for the NS-2007/8 sites (1935–5323 m).

2.5.2 Benthic-pelagic coupling

At the highly productive SG site (highest average monthly NPP), highest sediment Chla values were in accordance with the E–W NPP increase. Meiofauna and nematode densities and nematode relative abundance also increased westwards and were thus highest in the most western station SG. The nematode densities observed for SG were higher than those reported in other abyssal plain studies (Sebastian et al., 2007; Vanreusel et al., 1995). Based on the observed patterns for NPP and Chla in this study, we can conclude that the meiofauna is partially directly reliant on the surface primary productivity as its primary food source, despite the great water depth. The same outcome observed here was already reported in other studies for other areas (Danovaro et al., 1999; Gooday, 2002; Pape et al., 2013b; Smith et al., 2008; Vanreusel et al., 1995). This hypothesis is corroborated by recent fatty acid and stable isotope studies (Guilini et al., 2013; Veit-Köhler et al., 2013), which clearly show the dependency of meiofauna on fresh phytodetritus at the NS-2007/8 sites. Sediment Chla concentrations measured at the NS-2007/8 sites by Veit-Köhler et al. (2011, 2013) revealed higher Chla values at the sPF sites, followed by LS and cWS. Nevertheless, these values may reflect local blooming and settlement events. The high meiofauna densities observed at the MR and LS sites could be then explained by seasonal ice coverage and elevated primary production at the seasonal ice edge (Flores et al., 2011; Froneman et al., 2004; Hunt et al., 2011; Soreide et al., 2010). Increases in benthic densities in areas covered by sea ice were not considered in previous studies. However, heavy carbon isotope

signatures found for nematodes (-21.5–19.3 ‰) from the Weddell Sea might indicate that rapidly sinking ice algae may be a significant food source for metazoan meiobenthos (Moens et al., 2007). Likewise, enriched carbon isotope values for the meiofauna from the LS site (-25.4 – -24.9 ‰), influenced by ice most of the year, were observed by Veit-Köhler et al. (2013), indicating the possible inclusion of isotopically enriched ice-algae in the meiofauna diet.

Although POC fluxes estimated from satellite images by means of the VGPM algorithm must be interpreted with caution, large-scale patterns can be inferred from this algorithm. There is a clear separation between sites south of the PF, which yielded higher meiofauna densities and estimated POC fluxes (except for the cWS site), and sites at the PF, with lower meiofauna densities and POC fluxes. The lower densities observed for SG in comparison with the MR and LS sites (located closer to the continent and with much lower, though underestimated, NPP values) were not expected. This divergent pattern emphasizes the potential contribution of ice algae to POC fluxes and the fact that MR, as a seamount, exhibit particular characteristics in terms of diversity and local hydrodynamics (Abelmann et al., 2006; Brandt et al., 2011a). Conversely, great interannual variability of nutrients in the PF region could also play a role (Demidov et al., 2012). This high instability might be caused by the magnitude of phytoplankton nutrient utilization and the extent to which nutrients are recycled in the mixed layer. In addition, S-shaped meanders formed in this area by the influence of two water masses, the South Georgia Shelf Water and the Antarctic Zone Water, create a turbulent environment (Brandon et al., 2000; Peterson and Stramma, 1991). These meanders have different surface temperatures and, together with strong currents, create a very complex area which can stimulate the pump of organic matter to the seabed that is difficult to model by the algorithm used in this research (Lutz et al., 2002, 2007). Thus, these particular features

present at SG could have been responsible for the high meiofauna densities and biomass observed at this site.

Taxon richness significantly differed between the NS-2007/8 and EW-2012 sites, with the former yielding higher diversity index. The considerable variation in NPP observed at the PF sites and pulse nutrient loading can restrict resource exploitation to part of the annual cycle of production and consequently suppress diversity (Pape et al., 2013b). Moreover, the great variation in depth between the NS and the EW transects might also have been responsible for the higher density and diversity found at the south PF sites. Conversely, constant NPP levels observed at sites south of the PF potentially favour feeding over a longer time period and can thus support more taxa (Rex and Etter, 2010). The southern sites are likely to be more stable due to less influence of strong currents, proximity to the continent and ice coverage in the winter, potentially favouring more diverse and steady communities, as well as higher standing stocks.

The lack of differences in nematode biomass linked to primary production and sediment Chla between sites contrasts with studies conducted elsewhere in deep-sea environments (Billett et al., 2013; Gontikaki et al., 2011; Gooday, 2002; Pape et al., 2013a; Thistle, 2003; Wei et al., 2010; Wolff et al., 2011). Although the link between productivity and standing stocks is well established for shallow water and deep-sea environments (Rex et al., 2006; Wei et al., 2010), it is less clear how standing stocks are partitioned among species. Food supply can be foraged by a single species so that differences are masked when higher-group comparisons are made (Rex and Etter, 2010). Nevertheless, although no nematode biomass gradient was observed in this study, SG displayed the highest biomass for the PF-located sites, as well as the highest PF-NPP and sediment Chla values. Importantly, south of the PF, cWS, and LS displayed the highest nematode biomass values as well as the highest observed taxon richness thereby supporting the biomass-diversity stability hypothesis of Cardinale et al. (2013), who suggests that more diverse communities are

generally more efficient in capturing resources and thus able to produce more biomass than less diverse communities.

Although marine benthos reflect patterns in surface net primary production and POC fluxes on a worldwide scale, meiobenthic communities in the SO display strong density heterogeneity or patchiness along a broad scale range. This high patchiness is the main factor causing high alpha and beta diversity at small spatial scale in the deep sea and thus enhancing deep-sea biodiversity (Danovaro et al., 2013). No significant link was found between meiofauna standing stocks and NPP. In addition, POC flux was negatively correlated with the meiofauna densities for the EW-2012 sites and positively correlated with nematodes for the NS-2007/8 sites. This implies that the use of estimated POC fluxes might not reflect the actual benthic food influx and consumption, as was also observed by Wei et al. (2010).

2.6 Supplementary data

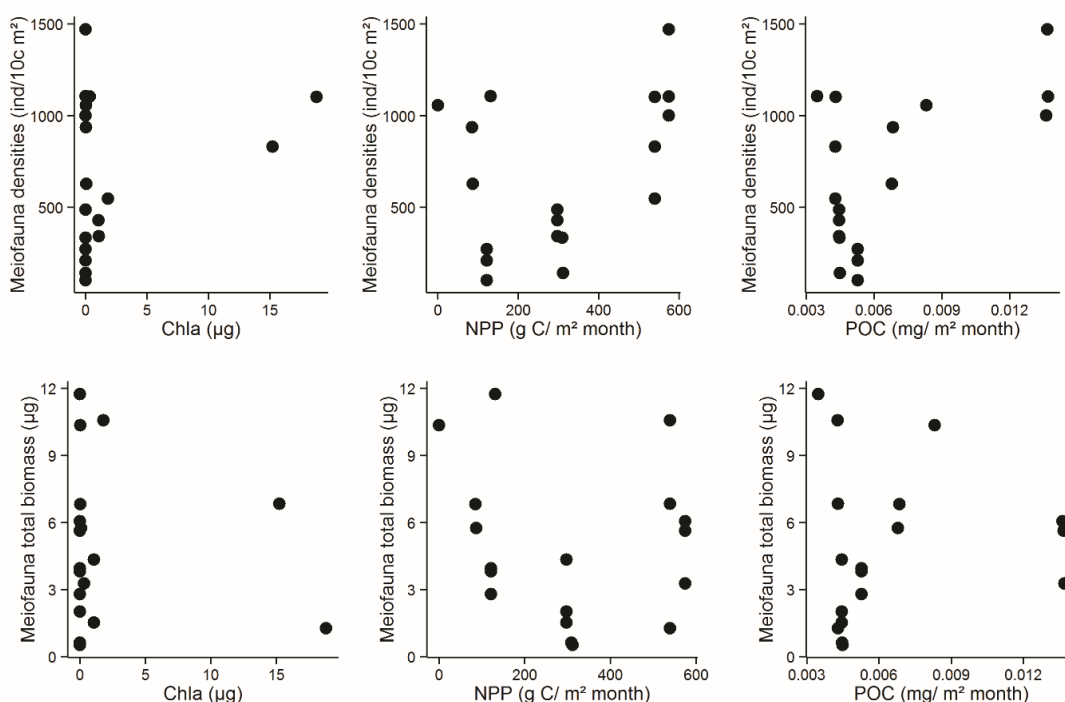


Fig. S1. Scatter plots between meiofauna total densities and biomass, and total Chla, estimated particulate organic carbon (POC) flux, and average net primary productivity (NPP) for all stations from both NS-2007/8 and EW-2012 transects.

Table S1. Results of univariate PERMANOVA analyses for Chla.

Chla						
Source	df	SS	MS	Pseudo-F	P(MC)	perms
Site	3	418.01	139.34	87.199	0.0003	10
Res	4	63.917	15.979			
Total	7	424.4				

Table S2. Results from pair-wise multivariate PERMANOVA analysis for differences in meiofauna community structure (total densities and relative abundances). When permutation values P(perm) were lower than 100, then P Monte Carlo (MC) was used. Values in bold represent $p < 0.05$.

Total densities (ind/ 10 cm ²)					Relative abundances (%)			
Groups	t	P(perm)	perms	P(MC)	t	P(perm)	perms	P(MC)
SG, HC_AEP	35.082	0.0238	126		0.83357	0.6556	126	
SG, HC_BEP	46.774	0.008	126		7.087	0.0071	126	
SG, LC	4.672	0.0106	126		3.3688	0.0091	126	
SG, sPF	10.253		21	0.3535	2.5552		21	0.0172
SG, sPF(2nd)	24.414		21	0.05	3.1259		21	0.0068
SG, MR	1.557		56	0.1424	2.6222		56	0.0111
SG, LS	0.86279		21	0.4659	2.039		21	0.0409
HC_AEP, HC_BEP	23.523		35	0.0359	6.3052		35	0.0007
HC_AEP, LC	26.901		35	0.0189	2.8015		35	0.0232
HC_AEP, sPF	26.004		15	0.0438	2.2014		15	0.059
HC_AEP, sPF(2nd)	15.986		15	0.1513	2.7895		15	0.0248
HC_AEP, MR	50.228		35	0.0016	2.1934		35	0.0514
HC_AEP, LS	37.977		15	0.012	1.5419		15	0.1534
HC_BEP, LC	0.70897		35	0.5363	1.6906		35	0.11
HC_BEP, sPF	3.205		15	0.0142	4.0722		15	0.0057
HC_BEP, sPF(2nd)	26.592		15	0.0368	4.1867		15	0.0037
HC_BEP, MR	49.663		35	0.0012	4.8934		35	0.0001
HC_BEP, LS	38.368		15	0.008	4.9188		15	0.0031
LC, sPF	30.985		15	0.0152	1.1192		15	0.3166
LC, sPF(2nd)	26.716		15	0.0285	1.1976		15	0.2923
LC, MR	46.277		35	0.0017	1.5017		35	0.1699
LC, LS	35.739		15	0.0078	1.7101		15	0.1354
sPF, sPF(2nd)	18.413		3	0.1867	1.2617		3	0.3108
sPF, MR	22.123		10	0.0853	0.43016		10	0.7957
sPF, LS	11.447		3	0.3703	1.731		3	0.1851
sPF(2nd), MR	46.293		10	0.009	1.4149		10	0.2104
sPF(2nd), LS	53.091		3	0.0259	2.3193		3	0.1106
MR, LS	17.177		10	0.1539	1.4133		10	0.2235

Table S3. Distance-based linear model (DistLM) marginal tests for higher taxonomical groups and nematode densities, and selected environmental variables. NPP= Average net primary productivity, SVI= Seasonal variation, POC= Particulate organic carbon

Meiofauna density				
Variable	SS(trace)	Pseudo-F	P	Prop.
NPP	2556	30.483	0.0627	0.10868
SVI	672.33	0.73571	0.45	2.86E-02
POC	4199.3	54.342	0.0102	0.17855
Nematoda density				
Variable	SS(trace)	Pseudo-F	P	Prop.
NPP	6.43E+09	71.845	0.0129	0.22323
SVI	2.14E+09	20.092	0.163	7.44E-01
POC	1.02E+09	13.645	0.0006	0.35308
Meiofauna density (0-1cm)				
Variable	SS(trace)	Pseudo-F	P	Prop.
NPP	1835.5	15.042	0.2109	5.68E-02
SVI	450.31	0.35299	0.7251	1.39E-02
POC	8335.9	86.806	0.0015	0.25773
Nematoda density (0-1cm)				
Variable	SS(trace)	Pseudo-F	P	Prop.
NPP	1835.5	15.042	0.2187	5.68E-02
SVI	450.31	0.35299	0.7258	1.39E-02
POC	8335.9	86.806	0.0022	0.25773
Meiofauna density E-W 2012				
Variable	SS(trace)	Pseudo-F	P	Prop.
Chl a	2697.8	30.154	0.1015	0.33447
Chla/%TOC	4866.2	9.125	0.0007	0.60331
% TN	392.64	0.30702	0.6905	4.87E-02
% TOC	532.6	0.4242	0.6299	6.60E-02
Nematoda density E-W 2012				
Variable	SS(trace)	Pseudo-F	P	Prop.
Chl a	4.62E+09	98.029	0.025	0.62032
Chla/%TOC	6.73E+09	56.522	0.0009	0.90403
% TN	33185	0.27983	0.6157	4.46E-01
% TOC	46016	0.39515	0.5436	6.18E-02

Table S4. Distance-based linear model (DistLM) sequential tests for higher taxonomical groups and nematode densities, and selected environmental variables. NPP= Average net primary productivity, SVI= Seasonal variation, POC= Particulate organic carbon

Meiofauna density							
Variable	Adj R ²	SS(trace)	Pseudo-F	P	Prop.	Cumul.	res.df
+POC	0.1457	4199.3	54.342	0.0116	0.17855	0.17855	25
+NPP	0.17859	1486.9	20.012	0.1385	6.32E+02	0.24178	24
+SVI	0.21218	1441.8	20.232	0.1443	6.13E+02	0.30308	23
Nematoda density							
Variable	Adj R ²	SS(trace)	Pseudo-F	P	Prop.	Cumul.	res.df
+POC	0.32721	1.02E+09	13.645	0.0016	0.35308	0.35308	25
+NPP	0.43166	3.52E+09	55.949	0.0268	0.1223	0.47538	24
+SVI	0.48506	1.99E+09	34.888	0.0787	6.91E+02	0.54448	23
Meiofauna density (0-1cm)							
Variable	Adj R ²	SS(trace)	Pseudo-F	P	Prop.	Cumul.	res.df
+POC	0.22804	8335.9	86.806	0.0018	0.25773	0.25773	25
Nematoda density (0-1cm)							
Variable	Adj R ²	SS(trace)	Pseudo-F	P	Prop.	Cumul.	res.df
+POC	0.22804	8335.9	86.806	0.0026	0.25773	0.25773	25
Meiofauna density E-W 2012							
Variable	Adj R ²	SS(trace)	Pseudo-F	P	Prop.	Cumul.	res.df
+Chla/%TOC	0.53719	4866.2	9.125	0.0007	0.60331	0.60331	6
+% TOC	0.54618	585.08	11.189	0.3273	7.25E+02	0.67584	5
+Chla	0.57055	635.21	12.837	0.3153	7.88E+02	0.7546	4
Nematoda density E-W 2012							
Variable	Adj R ²	SS(trace)	Pseudo-F	P	Prop.	Cumul.	res.df
+Chla/%TOC	0.88804	6.73E+09	56.522	0.0006	0.90403	0.90403	6
+% TOC	0.90151	19080	18.209	0.2319	2.56E+01	0.92965	5

Nematode community composition and feeding shaped by contrasting productivity regimes in the Southern Ocean



3





Chapter 3: Nematode community composition and feeding shaped by contrasting productivity regimes in the Southern Ocean

Manuscript published in slightly modified form as: Lidia Lins, Maria Cristina da Silva, Freija Hauquier, André Morgado Esteves, and Ann Vanreusel. “Nematode Community Composition and Feeding Shaped by Contrasting Productivity regimes in the Southern Ocean.” *Progress in Oceanography* 134 (2015): 356–69.

3.1 Abstract

In the Southern Ocean, during the ANT-XXVIII expedition (RV Polarstern), four stations contrasting in terms of surface primary productivity were studied along the Polar Front from 39° W and 10° E. We investigated to what extent differences in surface primary productivity, together with benthic environmental variables (concentration of Chlorophyll *a* and its derivatives, and sediment fatty acid composition) mirrored in nematode standing stocks (i.e. density and biomass) and differences in community composition. Moreover, nematode fatty acid (FA) analyses were performed to unravel feeding selectivity patterns on “bulk” nematodes and particular nematode taxa (*Desmodora* and Desmoscolecidae). South Georgia station, located NW of South Georgia island, possessed not only highest surface primary productivity, but also highest chlorophyll *a* (and its derivatives) and total sediment FA concentrations, also reflected in up to 10-fold higher nematode standing stocks. FA composition from “bulk” nematodes, *Desmodora* and desmoscolecids revealed a planktonic-based diet, as revealed by diatom biomarkers ($\frac{16:1\omega7}{16:0} > 1$) for “bulk” nematodes and *Desmodora* from South Georgia. Nematodes at the other stations situated more to the east showed non-selectivity for fresh diatom material based on the FA composition, associated with low surface primary productivity and low labile carbon concentrations (low

chlorophyll a values) in these areas. Uncommonly found in typical deep-sea environments, the nematode genus *Desmodora* exhibited high numbers at South Georgia station, probably as a response to the high primary productivity at the surface, confirming the strong benthic-pelagic coupling even at great depths. This study suggests that alterations in nematode standing stocks and community composition, together with selective feeding reflected by distinct FA composition, can be positively associated and shaped by surface productivity regimes.

3.2 Introduction

Marine sediments are considered major carbon reservoirs in the global carbon cycle (Jamieson et al., 2013; Killops and Killops, 2005; Serpetti et al., 2013). In general, surface primary productivity by phytoplankton, together with water depth and distance from land, is one of the main determinants of the flux of organic matter (OM) to the seabed, which in turn regulates rates of carbon mineralization and/or burial of organic matter in deeper sediment layers (Fischer et al., 2000; Middelburg et al., 1997). Although most of the OM (> 90%) produced by the phytoplankton is directly consumed in the water column, 70 – 95% of the particulate OM arriving at the seafloor is still composed of labile carbon compounds (Boon and Duineveld, 1996; Sachs et al., 2009). Part of the phytoplanktonic remains, together with zooplanktonic faecal pellets, form fluffy aggregates of marine snow, which can rapidly sink to the sea bottom (Killops and Killops, 2005). After reaching the bottom, OM mineralization occurs mainly at the sediment surface (Killops and Killops, 2005; Nascimento et al., 2012).

Upon arrival at the seabed, microbial degradation becomes the dominant process directly or indirectly regulating different OM mineralization pathways (Jamieson et al., 2013;

Thullner et al., 2009). Additionally, mega- and macrofauna may act as ecosystem engineers, altering habitat structure via their feeding and burrowing activities, which allow freshly deposited OM to penetrate deeper into the sediment (Levin et al., 1997; Serpetti et al., 2013). The role of macrofauna (between 1 mm and 1 cm) for the microbiology and biogeochemistry of aquatic sediments and their response to OM input is relatively well established (Hughes and Gage, 2004; Jeffreys et al., 2013; Levin et al., 1997; Rex et al., 2006; Ruhl et al., 2008). In contrast, few studies report on the function of meiofauna (< 1 mm) in OM recycling, although this group become numerically dominant (in terms of densities and biomass) with increasing water depth (Danovaro et al., 2008; Thiel, 1975). Nascimento et al. (2012) clearly show that the presence of meiofauna enhances OM mineralization in shallow marine sediments through a significant increase in respiration rates observed in an enrichment experiment with and without the presence of meiofauna. Nevertheless, the interaction between nematodes and microbes and their roles in enhancing mineralization processes and, moreover, their interaction in the food web remains unclear so far (Moens and Vincx, 1997), especially in the deep sea (Ingels et al., 2010). On the other hand, fatty acid and stable isotope analyses have shown that deep-sea meiofauna, especially nematodes, are mainly dependent on freshly-derived organic material from the surface, which constitutes a high quality food source for benthic organisms (Guilini et al., 2013; Leduc et al., 2014; Veit-Köhler et al., 2011).

A decrease in benthos-mediated mineralization occurs with an increase in water depth (Glud, 2008; Middelburg et al., 1997). In the abyss, many aspects of ecosystem function and structure are chiefly modulated by the rate and nature of food (in the form of aggregates) flux to the seabed (De La Rocha and Passow, 2007; Sachs et al., 2009; Smith et al., 2008). Therefore, naturally occurring diatom blooms in the surface generally lead to very high benthic fluxes (Sachs et al., 2009). In addition, because sinking velocities of organic aggregates are predominantly determined by aggregate size, and other factors,

such as stickiness and porosity, these features can also play a role in determining particle settlement (Iversen and Ploug, 2013; Karakas et al., 2009). When settled, these aggregates will potentially act as food source for the fauna dwelling at the deep-sea bottom. This benthic-pelagic coupling between food supply from the photic zone and its settlement to the seafloor was demonstrated in many bathyal and abyssal studies (Billett et al., 1983; Lampadariou and Tselepides, 2006; Lins et al., 2014; Pape et al., 2013b; Rex et al., 2006; Smith et al., 2008, 2006; Wei et al., 2010). On the contrary, differences in benthic community structure, diversity and biomass in conjunction with differences in surface primary productivity are poorly studied in the deep sea (Guilini et al., 2013 cf. revisited site at Polar Front; Jeffreys et al., 2013; Pape et al., 2013; Ruhl et al., 2008; Sebastian et al., 2007).

The Southern Ocean, characterized by extreme seasonality in sea-ice cover and surface primary production, is considered a major driver in ocean circulation, connecting deep waters from the Pacific, Atlantic and Indian oceans (Griffiths, 2010). In the Atlantic sector of the Southern Ocean, east-west differences in primary productivity are observed (Demidov et al., 2012). These regional differences in primary productivity could affect patterns of community composition and biomass at the sea bottom (Brandão et al., 2014; Würzberg et al., 2014).

For many benthic taxa, including both meio- and macrobenthic groups, there is evidence that maximum body size significantly decreases with increasing depth, possibly due to diminishing food supply (Ramirez-Llodra et al., 2010; Smith et al., 2008; Thiel, 1975). Nevertheless, aspects of energy flow concerning the meiofauna are still not well-understood and remain mainly focused on standing stock quantification (Duros et al., 2011; Ingels et al., 2011; Vanreusel et al., 1995). Recently used techniques, such as fatty acid (FA) analyses, could potentially provide more insights in meiofauna ecosystem functioning through the study of dietary intakes and food constituents to sequestering of

lipid reserves (Dalsgaard et al., 2003; Leduc et al., 2014; Leduc and Probert, 2009). This technique was already used for nematodes (“bulk”) from the Southern Ocean (Guilini et al., 2013) as a trophic marker and indicated a fresh-food feeding behaviour within this group. The presence of polyunsaturated fatty acids (PUFAs) in the analysed organisms indicates a rich phytoplankton-based diet (as these FAs are only produced by few bacteria species) (Dalsgaard et al., 2003), which might have originated from direct grazing or indirect consumption of certain microorganisms (e.g. foraminiferans) or even small metazoans. This nutritious diet emphasizes the potential role of nematodes as high-quality food for higher trophic levels (Leduc et al., 2014; Leduc and Probert, 2009). The use of fatty acids in nematodes should, however, be interpreted with caution. PUFAs can be, for instance, affected by temperature (lower temperatures increase the level of unsaturation) and nematodes may also biosynthesise PUFAs from other fatty acids, interfering in the correct interpretation of exact PUFA concentrations of the studied organism (Dalsgaard et al., 2003; Leduc et al., 2014).

Based on analyses of nematode assemblages from four sites in the Southern Ocean characterized by strong differences in surface primary productivity the following hypotheses are tested:

Differences in surface primary productivity regulate nematode standing stocks (i.e. abundance and biomass) and respiration in the Southern Ocean;

Nematode community composition mirrors increases in surface primary productivity through the increase in densities of specific genera adapted to feed on fresh material (e.g. *Desmodora* and *Microlaimus*), as well as alterations in algal-derived fatty acids (PUFAs) in nematodes;

Different nematode taxa feed selectively on specific food sources as reflected by their different FA composition.

3.3 Material and methods

3.3.1 Sampling and study area

During the RV Polarstern ANT-XXVIII/3 (07.01.2012 – 11.03.2012) cruise (Wolf-Gladrow, 2012) to the Southern Ocean, sediment samples for nematode analyses were taken in the framework of the SYSTCO II project. The study area comprised four sites at the Polar Front situated along an E-W (between 10° E and 39° W) gradient, and covering depths from 3760.5 m to 4155.2 m (Fig. 3.1, Table 3.1). Sampling was performed using a Multicorer (MUC) equipped with 12 Plexiglass tubes yielding samples with a virtually undisturbed sediment-surface (inner core diameter 6 cm, cross-sectional area 25.5 cm²).

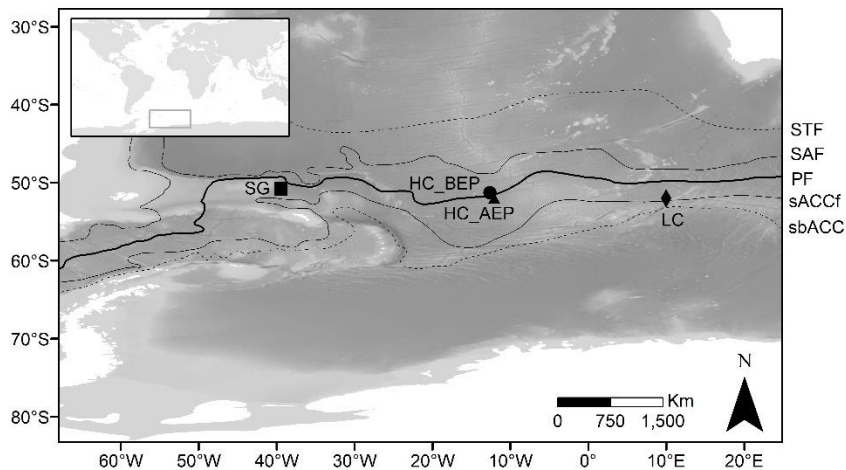


Figure. 3.1. Location of ANT-XXVIII/3 sites. The map displays features of the Antarctic Circumpolar Current (Orsi and Harris, 2001): Subtropical Front (STF), Subantarctic Front (SAF), Polar Front (PF), southern Antarctic Circumpolar Current Front (sACCf) and southern boundary of the Antarctic Circumpolar Current (sbACC). Bathymetry data provided by ETOPO1 and world boundaries by ESRI (Amante and Eakins, 2009). Sampling sites are represented by symbols: SG (South Georgia), HC_BEP (High Chlorophyll_before Eddy Pump), HC_AEP (High Chlorophyll_after Eddy Pump) and LC (Low Chlorophyll).

The Polar Front marks the northern extent of low salinity and cold water (Knox, 1994). Sampling locations were chosen based on previously available surface chlorophyll *a* (Chl*a*) concentrations data provided by the University of Bremen. South Georgia site (SG), located northwest of South Georgia Island, is considered a highly productive region during austral summer, supporting high phytoplankton biomass (Atkinson et al., 2001). The second region comprised two different sites located at the same transition zone and characterized by high annual primary production: HC_BEP (High Chlorophyll_Before Eddy Pump) and HC_AEP (High Chlorophyll_After Eddy Pump), which is the same position re-sampled after 13 days of a phytoplankton bloom in the area. Although a higher Chl*a* concentration was expected after the bloom, this was not visualized in the surface Chl*a* maps. This area was also supposed to exhibit eddies between sampling periods, which were tracked before and during the cruise using satellite remote sensing of sea surface high anomalies and ocean colour. Therefore, these sites received the name before and after Eddy Pump due to collaboration with the Eddy Pump project during the same campaign. The most eastern site (LC; Low Chlorophyll) exhibited low surface chlorophyll values throughout the year (Fig. 3.1).

Table 3.1. Sampling details from each sampled site. Each deployment code (and core number in brackets) refers to one replicate (four replicates per site in total). Core numbers in bold were used for community analyses while non-bold core codes were used for nematode fatty acids and environmental analyses.

Site	Deployment (core code)	Date	Depth (m)	Latitude	Longitude	Remarks
SG	175-5 (7-8)	04/03/2012	4154.2	50°46.69'S	39°25.35'W	South Georgia
SG	175-6 (5-6)	04/03/2012	4155.2	50°46.59'S	39°25.33'W	South Georgia
SG	175-7 (2-3)	04/03/2012	4154.2	50°46.60'S	39°25.38'W	South Georgia
SG	175-8 (1-10)	04/03/2012	4154	50°46.60'S	39°25.39'W	South Georgia
SG	175-9 (3-6)	04/03/2012	4152.1	50°46.57'S	39°25.33'W	South Georgia
HC_AEP	141-6 (3-4)	18/02/2012	4113	51°15.98'S	12°37.04'W	PF(After Eddy Pump)
HC_AEP	141-9 (6-8)	18/02/2012	4114	51°16.03'S	12°37.06'W	PF(After Eddy Pump)
HC_AEP	141-10 (3-6)	19/02/2012	4113	51°15.97'S	12°36.94'W	PF(After Eddy Pump)
HC_AEP	141-11 (3-5)	19/02/2012	4113.2	51°16.02'S	12°37.12'W	PF(After Eddy Pump)
HC_BEP	086-26 (4-8)	01/02/2012	3966.2	51°58.87'S	12°3.76'W	PF(Before Eddy Pump)
HC_BEP	086-28 (6-8)	01/02/2012	3968	51°58.74'S	12°2.11'W	PF(Before Eddy Pump)
HC_BEP	086-29 (3-5)	01/02/2012	3970.8	51°58.78'S	12°1.95'W	PF(Before Eddy Pump)
HC_BEP	086-30 (1-3)	02/02/2012	3965.4	51°58.91'S	12°2.16'W	PF(Before Eddy Pump)
LC	081-8 (3-4-6)	19/01/2012	3760.5	51°59.99'S	9°59.99'E	PF(Low Chlorophyll)
LC	081-9 (8-10)	19/01/2012	3760.7	52°0.01'S	10°0.05'E	PF(Low Chlorophyll)
LC	081-12 (6-8)	19/01/2012	3757.5	51°59.93'S	10°0.06'E	PF(Low Chlorophyll)
LC	081-13 (6-7)	19/01/2012	3760.5	52°0.042'S	9°59.90'E	PF(Low Chlorophyll)

3.3.2 Sediment analyses

Samples for granulometric and geochemical analyses (1 g of sediment) were divided per 1 cm-layer down to 5 cm and frozen at -80° C. Grain size distribution was measured with a Malvern Mastersizer 2000 (0.02 – 2000 µm size range) and divided from silt-clay to coarse sand fractions (Buchanan, 1984). Total sedimentary organic carbon (% TOC) and nitrogen (% TN) were determined with a Carlo Erba elemental analyser on freeze-dried and homogenized samples after acidification with 1% HCl to eliminate carbonates. Total organic matter (% TOM) content was determined after combustion of the sediment samples at 550° C.

Chla, chlorophyll degradation products and carotenes in the sediment were measured with a Gibson fluorescence detector (Wright and Jeffrey, 1997) after lyophilisation, homogenization and extraction in 90% acetone, and separation of the samples via reverse-phase HPLC (High-Performance Liquid Chromatography). Chloroplastic Pigment Equivalents (CPE: sum of Chla and its degradation products) was used to estimate surface-produced OM. The ratio Chla: phaeopigments served to estimate the freshness of photosynthetically derived OM (Thiel, 1978).

Hydrolysis of total lipids and methylation to fatty acid methyl esters for FA analysis on the sediment was performed on 3 g sediment based on a modified one-step derivatization method in which lipid extraction and esterification were combined (Abdulkadir and Tsuchiya, 2008). Sediment was lyophilized for 24h and the extraction performed with 2.5% sulfuric acid in methanol, which replaced boron trifluoride-methanol since BF_3 -methanol can create loss of PUFAs.

The FA methylnonadecanoate C19:0 (0.1mg/ml, Fluka 74208) was used as internal standard. Each vial was mixed for 30 seconds and heated (using a warming bath) up to 80° C for 1h30 after which they were treated with hexane and centrifuged for 10 minutes at 1000 RPM (Eppendorf centrifuge 5810R). Replicate extracts were analysed using a gas chromatograph (Hewlett Packard 6890N) coupled to a mass spectrometer (HP 5973). Samples were run in splitless mode, with a 5 μL injection per run at 250° C, using a HP88 column (60 m x 25 mm internal diameter, Df = 0.20; Agilent J&W; Agilent Co., USA). Fatty acid methyl esters were identified based on retention times and mass spectra's comparisons with authentic standards and available ion spectra in different libraries (WILEY, Niest and a self-made mass spectral library from 37 FA), and determined with the software MSD ChemSite (Agilent Technologies).

3.3.3 Surface environmental parameters

Annual average Net Primary Production (avNPP) values were extracted from the Vertically Generalised Production Model (resolution: 1°) (Behrenfeld and Falkowski, 1997). The Vertically Generalised Production Model is a chlorophyll-based algorithm that estimates average values (avNPP) values based on sea surface temperature, surface Chla and photosynthetically active radiation via satellite measurements. The available HDF format data were extracted using the Marine Geospatial Ecology Tools for ArcGIS and converted to raster using the software ArcGIS (Lutz et al., 2002, 2007).

3.3.4 Nematodes

At each site, four replicate samples (SG possessed five replicates) used for community analysis were sliced per 1 cm down to 5 cm sediment depth and fixed in seawater buffered 4% formalin. Samples were washed over a 1000 µm sieve and the meiofauna was retained on a 32 µm sieve. The meiofauna was centrifuged three times using LUDOX HS40 Dupont (specific gravity 1.19) as flotation medium and then stained with Rose Bengal. Nematodes were counted under a stereomicroscope (50x magnification) and 100 individuals (whenever enough present) were picked out. The individuals were gradually transferred to glycerine (De Grisse, 1969), mounted on glass slides and identified to genus level using pictorial keys (Warwick et al., 1998). The most abundant genera present in all stations were identified to species level.

Functional diversity of nematode assemblages was assessed using individual trophic levels based on buccal morphology according to Wieser (1953): selective deposit feeders (1A), non-selective deposit feeders (1B), epistratum feeders (2A), and predators (2B),

complementing the 2B group (predators) with the notion of ‘scavengers’ (Jensen, 1987). Taxonomic diversity was calculated using Shannon-Wiener diversity (H'), Pielou’s evenness (J') and total number of genera (S).

The length (excluding filiform tails) and the maximum body width were measured for all identified nematodes (32%–100% of the total nematode abundance) with the compound microscope Leica DMR and Leica LAS 3.3 imaging software. Biomass was then calculated per genus through the volumetric method according to Andrassy’s formula $G = a^2 \times b / 1.6 \times 10^6$, with G = wet weight in μg , a = maximum body diameter (μm) and b = total length (μm) (Andrássy, 1956).

Fatty acid methyl esters for FA of nematodes were measured on previously frozen samples (-80°C) at cm resolution to 5 cm sediment depth. Samples were centrifuged one time using LUDOX HS40 Dupont (specific gravity 1.19) and all individuals were picked out while kept on ice and immediately frozen at -20°C . The effect of thawing was, thus, regarded as negligible. From 2–4 replicate extracts from “bulk” nematodes (240–903 individuals, excluding desmoscolecids and *Desmodora*), the nematode family Desmoscolecidae (163 – 258 individuals) and the genus *Desmodora* (175 – 302 individuals) were performed following the same method as for the sediment FA. The last two groups were chosen because they were highly dominant in SG and easy to recognize under a stereomicroscope in the samples. A few FA served as biomarkers in order to unravel the relative contributions of possible food sources (phyto- and/or zooplankton) to the animals’ diets.

Firstly, the phytoplankton-derived FA were divided in microalgae-derived planktonic (16:1 ω 7, 18:1 ω 9, 18:2 ω 6, 20:PUFA, 22:PUFA) and bacterial (15:0, 17:0, 17:1 and *iso* and *anteiso* saturated FA [SFA] and monosaturated FA [MUFA]) markers. *Iso* + *anteiso* 15:0/ 15:0, *iso* + *anteiso* 15:0/ 16:0 and Σ *iso* + *anteiso* 15:0 +17:0 were also used to infer a bacterial-derived diet (Dalsgaard et al., 2003 and references therein). Then, specific

biomarker ratios were used to verify diatom (if $\frac{16:1\omega7}{16:0} > 1$ and $\frac{\Sigma 16:0}{\Sigma 18:0}$ positively correlated with diatom biomass) or dinoflagellate-based (if $\frac{22:6\omega3(DHA)}{20:5\omega3(EPA)} \geq 1$) diet. Σ SFAs, Σ MUFAs and Σ PUFAs contents were compared between sites.

3.3.5 Nematode respiration

Nematode respiration rates (Resp) based on individual dry weight (DWT) were estimated according to de Bovée and Labat (1993), where $Q_{10} = 2$ and T = Temperature at the seabed (°C):

$$\text{Resp (T)} = 0.0449 \text{ DWT}^{0.8544} \exp^{(\ln Q_{10}/10) * (T-20)} \text{ (de Bovée and Labat, 1993).}$$

This respiration formula was preferred instead of Shirayama (1992) respiration values measured for deep-sea nematodes at 2-4° C because the second suggests no temperature dependence of respiration rates in the deep sea, while de Bovée and Labat (1993) incorporate temperature in their formula. Moreover, considering that the temperatures of the seabed measured in this study remained below 2-4° C, we have considered the de Bovée and Labat (1993) formula as the most appropriate method.

3.3.6 Data analysis

Trends in environmental predictor variables (Chla, Chla: phaeopigments, Chla: %TOC, CPE, % TN, % TOC, median grain size, total FA, avNPP, SFAs, MUFAs and PUFAs) and univariate nematode response variables (total biomass, total respiration, H', J', S, and total FA) were investigated by means of Spearman rank correlations in R (R Core Team, 2013) and Draftsman plots in PRIMER (Anderson et al., 2008).

The %TOM and its vertical profile in the sediment was used according to Soetaert et al. (1997) to estimate how food is drawn into the sediment. The %TOM can be used as a measure of bioturbation, where subsurface peaks are expected when OM from the superficial layers is brought to deeper layers by organisms' activities.

The untransformed nematode community structure data on genus level (and on species level for the most dominant genera) based on a Bray-Curtis similarity matrix was analysed by means of non-parametric permutational ANOVA (PERMANOVA; Anderson et al., 2008) to assess differences between sites (1-factor design) and whenever possible between sediment layers (3-factor nested design). The one-factor model design comprised site (ST) as a fixed factor. The three-factor model design included as factors site (ST: fixed), slice (SL: fixed) and replicate (REP: random, nested in site). The interaction ST x SL informs about the difference in depth profiles of uni- or multivariate nematode measures or environmental variables among sites. Non-metrical multi-dimensional scaling (MDS) was used to visualize the results. Subsequent pairwise t-tests were performed between all pairs of levels to determine where the differences between each combination were located.

In addition, PERMDISP routines were executed in order to test for homogeneity of multivariate dispersions. The PERMDISP results were never significant, indicating location differences through equally dispersed distances to centroids. SIMPER routines were performed on the nematode community structure with a cut-off of 90% for low contributions. The same PERMANOVA design used for the nematode multivariate community structure data was applied to all other univariate and multivariate data using resemblance matrices based on Euclidean distances and Bray-Curtis similarities, respectively. Analyses were performed on nematode biomass, respiration, c-p matrix (colonizer-persister matrix calculated based on nematode trophic group), trophic groups,

gender and life stage, as well as nematode FA profiles (including the sum of FA groups and FA ratios).

The multivariate environmental data was first normalized (subtracted mean divided by the standard deviation) and resemblance matrices calculated based on Euclidean distances. Then, PERMANOVA tests were performed using the same design as described for the multivariate community data. DISTLM (distance-based linear model) routines were performed to analyse and model the relationship between nematode community structure, biomass, and FA profile on one hand, and the environmental variables with correlations lower than 0.9 (Chla, Chla:phaeopigments, Chla: % TOC, CPE, % TN, % TOC, total FA and avNPP) on the other hand. Highly correlated variables (*i.e.* $r > 0.9$) were first transformed to cosine (Chla: % TOC, CPE, medium grain size and total FA) and if high correlations persisted were excluded from the DISTLM analysis (medium grain size). The DISTLM was built using a step-wise selection procedure and adjusted R^2 as selection criterion. Results were visualized using dbRDA (distance-based redundancy analysis) plots.

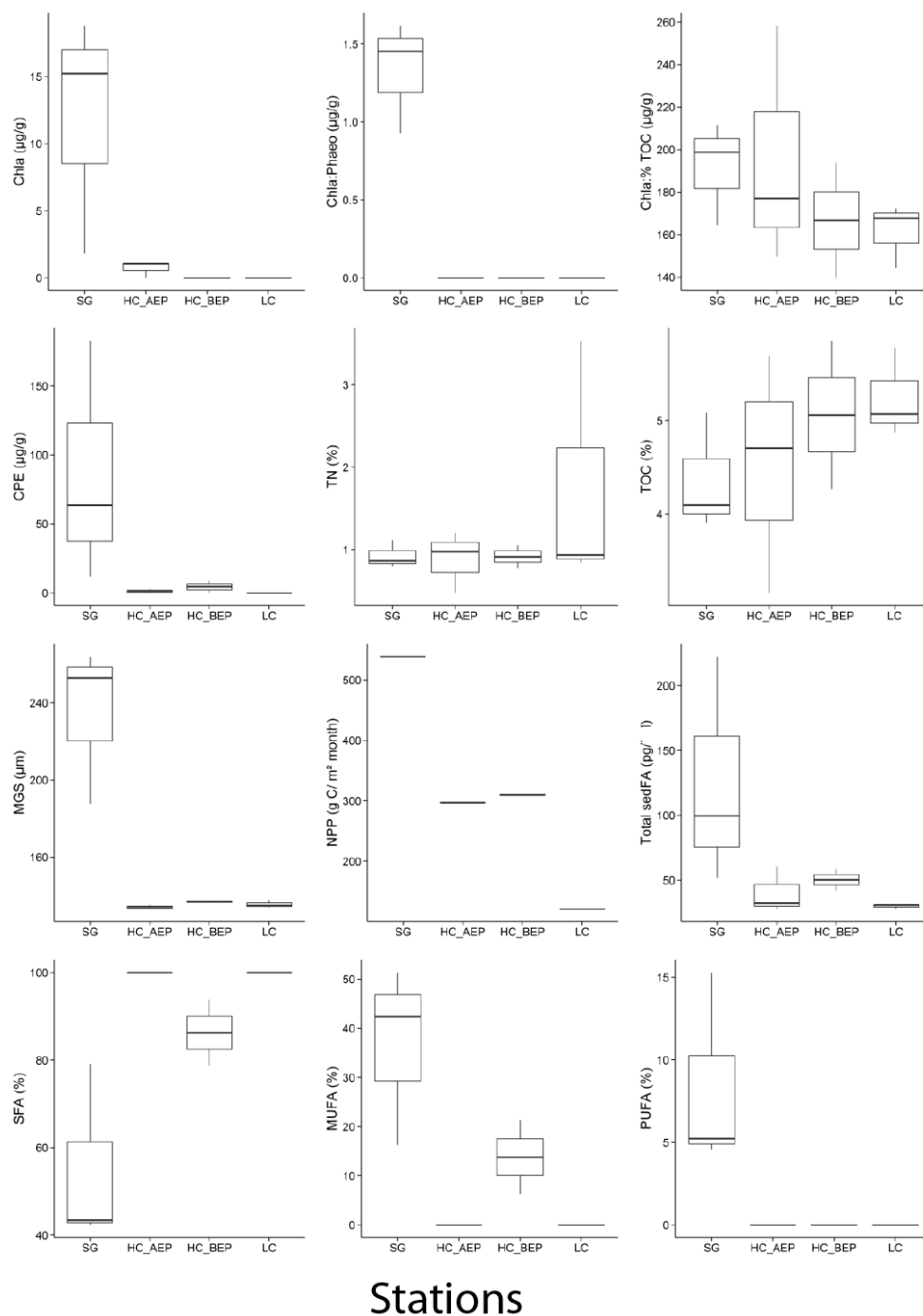


Figure. 3.2. Environmental variables used in this study for SG (South Georgia), HC_BEP (High Chlorophyll before Eddy Pump), HC_AEP (High Chlorophyll before Eddy Pump), and LC (Low Chlorophyll) sites: Chla (Chlorophyll a), Chla:Phaeo (Chlorophyll a: phaeopigments), Chla: % TOC (Chlorophyll a: % Total Organic Carbon), CPE (Chloroplastic Pigment Equivalent), TN (Total Nitrogen), TOC (Total Organic Carbon), MGS (Mean Grain Size), NPP (Net Primary Productivity), Total sedFA (Total Fatty Acid of the sediment) and relative abundance (% of total fatty acid) for SFA (Saturated Fatty Acid) in the sediment, MUFA (Monounsaturated Fatty Acid) in the sediment and PUFA (Polyunsaturated Fatty Acid) in the sediment. Black lines represent the median, lower box indicates the first quartile and upper box the third quartile. Upper line on the boxes shows the maximum value and lower line the minimum value.

3.4 Results

3.4.1 Environmental variables

Biogeochemical properties of the sediment are shown in Fig. 3.2. The sediment at all sites was mainly composed of silt-clay fractions (82% - 92%), followed by very fine sand. However, mean grain size was significantly higher at SG (PERMANOVA, $p = 0.02$), with higher relative contribution of fine (0.2% - 3.2%) and medium (2.2% - 4.7%) sand. Sedimentary % TOC and % TN did not differ between sites ($p > 0.05$) (Fig. 3.2). A significant eastwards increase in % TOC was observed, as well as a decrease towards deeper sediment layers ($p = 0.003$) but only for HC_AEP, HC_BEP and LC sites (Fig. S1). Sediment Chla ($p = 0.005$), as well as Chla: phaeopigments ($p < 0.0002$) and CPE ($p = 0.02$) decreased eastwards, with SG displaying significantly higher values in comparison with the other sites (Fig. 3.2). Chla: % TOC concentrations, although decreasing eastwards, did not exhibit significant differences between sites ($p > 0.05$). Total sediment FA was lower at the eastern sites (Fig. S1), but due to the high variation between samples (Fig. 3.2) these differences were not significant ($p > 0.05$, Table S2). Neither sediment FA profiles ($p > 0.05$) nor Σ SFAs ($p > 0.05$) or Σ MUFAs ($p > 0.05$) significantly differed between sites. On the other hand, Σ PUFAs were significantly more abundant at SG ($p = 0.003$) than at the other sites (Fig. 3.2). Accordingly, when bacterial FA and planktonic FA were considered, SG clearly exhibited significantly higher values for both categories than the other sites ($p = 0.001$), except for HC_BEP. Surface average NPP followed the same eastward decrease as observed for the other environmental variables, with higher concentrations (538.9 ± 0 g C m⁻² month⁻¹) displayed at SG ($p < 0.0001$) (Fig 3.2).

3.4.2 Nematode community and biomass

Nematodes were the dominant meiofaunal group at all sites (78% - 94%) and their mean abundance varied from 185 to 819 ind/10 cm². The most abundant genera per site ($\geq 2\%$) are represented in Table 3.2 and the vertical profile of the five most abundant genera per site is visualized in Fig. 3.3. Nematode total densities (Fig. 3.4) and total number of genera (S) were significantly higher at SG ($p < 0.0001$ and $p = 0.005$, respectively; Table S3) and decreased eastwards. A total of 130 nematode genera were found over all sites. All sites differed in genus structure based on the relative abundances ($p < 0.0001$), whereas SIMPER test revealed that SG was more dissimilar to other sites when average dissimilarities were compared. Dissimilarities between SG and the other sites varied from 66 – 75 %, while differences between other pairs of stations varied between 62 and 64 %. The genera *Desmodora* De Man, 1989, *Cervonema* Wieser, 1954, and *Tricoma* Cobb, 1893, with higher abundances in SG, together with *Acantholaimus* Allgén, 1933 and *Thalassomonhystera* Jacobs, 1987, being more abundant at the three other sites, were the major genera which combined responsible for up to 31% of the dissimilarity between SG and the other sites.

Table 3.2. Mean relative abundance of dominant genera ($\geq 2\%$) and feeding type (FT) per site over 5 cm depth.

SG	%	FT	HC_AEP	%	FT	HC_BEP	%	FT	LC	%	FT
<i>Thalassomonhystera</i>	14.6	1A	<i>Microlaimus</i>	19.5	2A	<i>Microlaimus</i>	26.5	2A	<i>Thalassomonhystera</i>	21.3	1A
<i>Acantholaimus</i>	12.6	2A	<i>Thalassomonhystera</i>	17.3	1A	<i>Thalassomonhystera</i>	19.2	1A	<i>Acantholaimus</i>	19.8	2A
<i>Desmadora</i>	9.8	2A	<i>Acantholaimus</i>	11.8	2A	<i>Daptonema</i>	6	1B	<i>Microlaimus</i>	7.2	2A
<i>Tricoma</i>	7.6	1A	<i>Southerniella</i>	5.3	1A	<i>Acantholaimus</i>	5.9	2A	<i>Desmoscolex</i>	4.8	1A
<i>Cervonema</i>	5.1	1B	<i>Tricoma</i>	5.1	1A	<i>Diplopeltula</i>	4.8	1A	<i>Tricoma</i>	4.7	1A
<i>Microlaimus</i>	4.8	2A	<i>Diplopeltula</i>	4.4	1A	<i>Theristus</i>	3.2	2A	<i>Molgolaimus</i>	3.7	1A
<i>Enchonema</i>	4	1A	<i>Molgolaimus</i>	2.8	1A	<i>Leptolaimus</i>	3	1A	<i>Halalaimus</i>	3.6	1A
<i>Southerniella</i>	3.9	1A	<i>Halalaimus</i>	2.8	1A	<i>Desmoscolex</i>	2.8	1A	<i>Diplopeltula</i>	3.4	1A
<i>Daptonema</i>	2.8	1B	<i>Daptonema</i>	2.7	1B	<i>Pareudesmoscolex</i>	2.5	1A	<i>Daptonema</i>	3.4	1B
<i>Diplopeltula</i>	2.6	1A	<i>Leptolaimus</i>	2.2	1A	<i>Tricoma</i>	2.1	1A			
<i>Dichromadora</i>	2.5	2A	XYALIDAE sp2	2.2	1B						
<i>Halalaimus</i>	2.4	1A									
<i>Actinonema</i>	2.2	2A									
<i>Desmoscolex</i>	2	1A									

Total nematode biomass was significantly greater at SG ($p < 0.0001$) than at the other sites (Fig. 3.4) and decreased towards deeper sediment layers. Lack of differences for the three-way PERMANOVA in biomass between deeper layers (2-5 cm) ($p > 0.05$) among all pairs of sites and significant differences observed at the first sediment layers indicated that differences between sites were mainly due to differences observed in the first centimetres (0-2 cm) ($p < 0.05$).

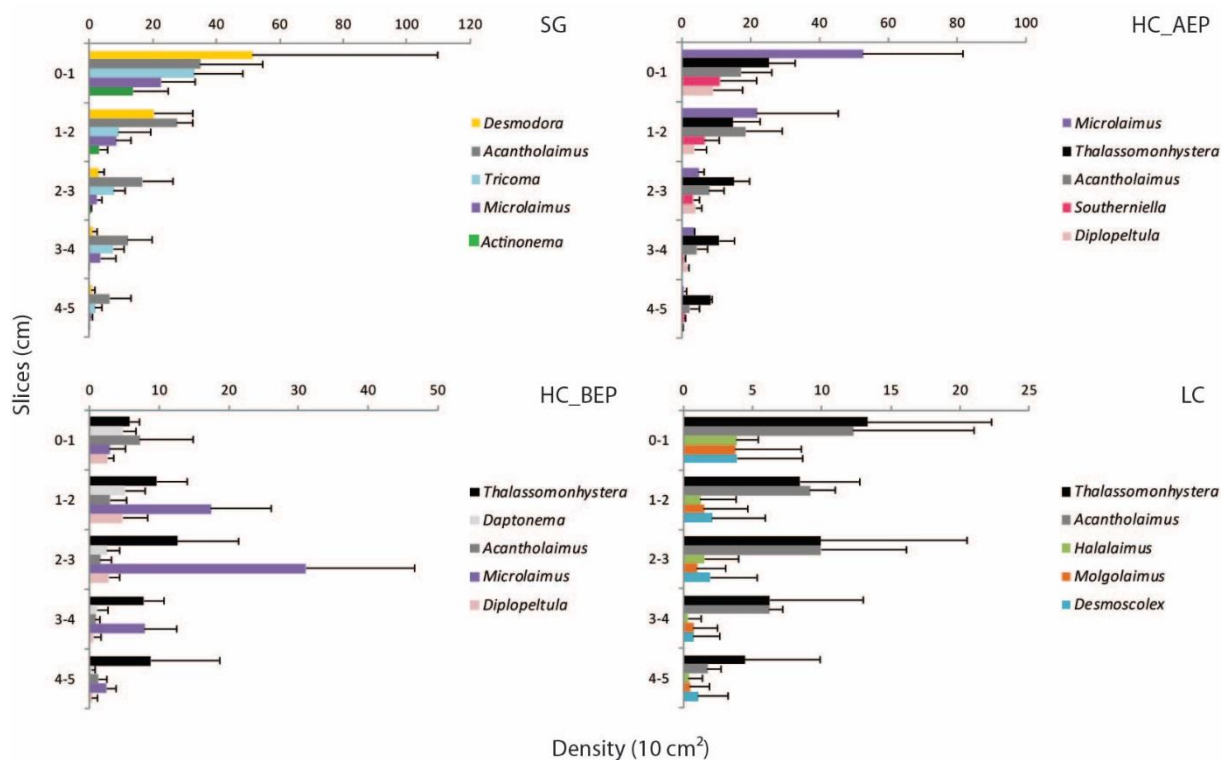


Figure. 3.3. Total nematode density (ind/10 cm²) of the five most abundant genera expressed per sediment layer and per site.

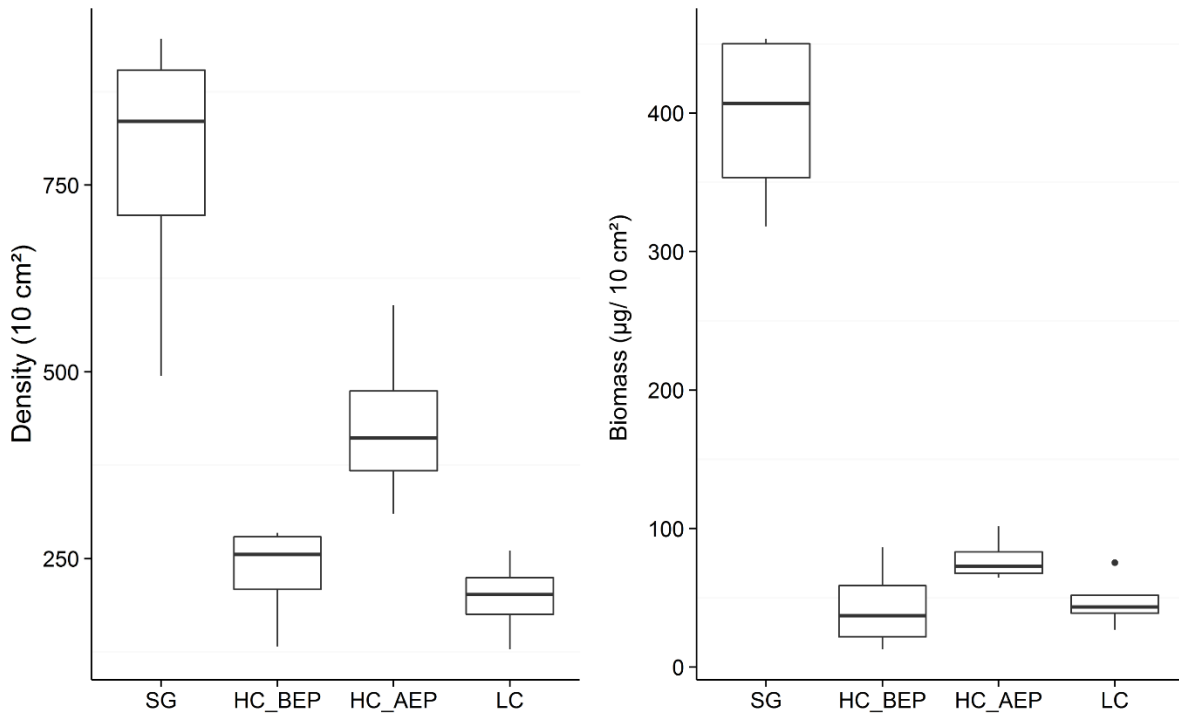


Figure. 3.4. Density (10 cm²) and Total Biomass (µg/g) per site of nematodes. Thick black lines represent the median, lower box indicates the first quartile and upper box the third quartile. Upper line on the boxes shows the maximum value and lower line the minimum value.

3.4.3 Nematode species

Four genera were the most dominant at all sites and therefore identified up to species or morphotype level: *Acantholaimus*, *Desmodora*, *Microaimus* De Man, 1880 and *Thalassomonhystera*. *Thalassomonhystera* showed the highest number of species (33), followed by *Acantholaimus* (20) and *Microaimus* (12). The genus *Desmodora* was represented by only one species, *Desmodora profundum* Moura et al., 2014.

Acantholaimus community structure based on densities significantly differed between sites ($p = 0.02$) and between sediment layers ($p < 0.0001$). HC_AEP showed the highest number of *Acantholaimus* species (13) and also the highest number of unique *Acantholaimus* species (3), followed by HC_BEP (11), with 2 unique *Acantholaimus*

species. SIMPER routines revealed *Acantholaimus elegans* Jensen, 1988 as responsible for dissimilarities between LC (where it possessed higher abundances) and the other sites. Two species contributed most to dissimilarities between sediment layers: *Acantholaimus invaginatum* Muthumbi & Vincx, 1997, which was present in higher abundances in the deeper layers, and *Acantholaimus maks* Gerlach, Schrage & Riemann, 1979, mainly present in superficial layers. *A. invaginatum* was also present in higher abundances in SG than at the other sites. PERMANOVA based on presence-absence of *Acantholaimus* did not reveal significant differences between sites ($p = 0.12$).

Desmodora profundum was present at all sites, but showed highest densities (more than 6 times compared to other sites) at SG ($p < 0.0001$). This species was mainly found in superficial sediment layers (Fig. 3.3). Concerning the *Microlaimus* species, significant differences were observed between sites ($p = 0.01$) but not between slices ($p > 0.05$). HC_AEP exhibited the highest number of *Microlaimus* species (11) and was the only site which possessed a unique *Microlaimus* species (morphotype XII). SIMPER routines revealed differences in the abundance of morphotype VI as the most important factor responsible for dissimilarities between HC_AEP/HC_BEP and the other sites. *Thalassomonhystera* species significantly differed between sites ($p = 0.01$) but not between slices ($p = 0.27$). SG possessed higher species diversity (25) in comparison with other sites, but only one species was unique for this site (morphotype XXIX). LC exhibited four unique species: morphotypes VI and XIII, and *Thalassomonhystera mortalis* Bussau, 1993 and *Thalassomonhystera subtilis* Bussau, 1993, while morphotype XVIII was exclusive at HC_BEP.

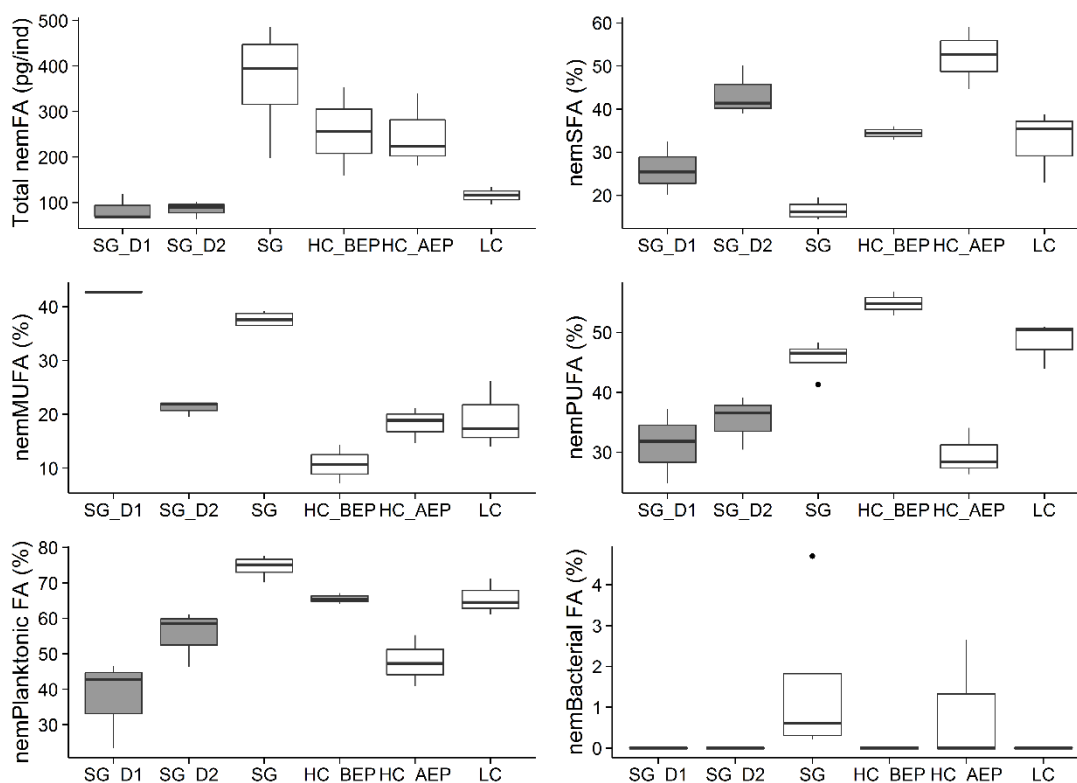


Figure. 3.5. Total *Desmodora* (SG_D1), Desmoscolecidae (SG_D2) and “bulk” nematode fatty acids represented per site in pg/g (Total nemFA) and relative concentrations (%) of nemSFA (nematode Saturated Fatty Acid), nemMUFA (nematode Monounsaturated Fatty Acid), nemPUFA (nematode Polyunsaturated Fatty Acid), nemPlanktonic FA (nematode Planktonic Fatty Acid) and nemBacterial FA (nematode Bacterial Fatty Acid). Thick black lines represent the median, lower box indicates the first quartile and upper box the third quartile. Upper line of the boxes shows the maximum value and lower line the minimum value.

3.4.4 Nematode fatty acids

Total “bulk” nematode FA, as well as Σ MUFAs, exhibited significantly greater concentrations in nematodes from SG compared with other sites (pairwise $p = 0.001$; Fig. 3.5). MDS profiles based on the total FA concentrations on “bulk” nematodes showed SG as a separate cluster apart from the other sites (Fig. 3.6). Comparisons between “bulk” nematode FA content in species of the family Desmoscolecidae, and the genus *Desmodora* (for SG only) exhibited significantly lower amounts of FA for the two last groups in comparison with “bulk” nematode FA, which was composed by all other nematodes except desmoscolecids and *Desmodora* ($p = 0.0002$; Table S2).

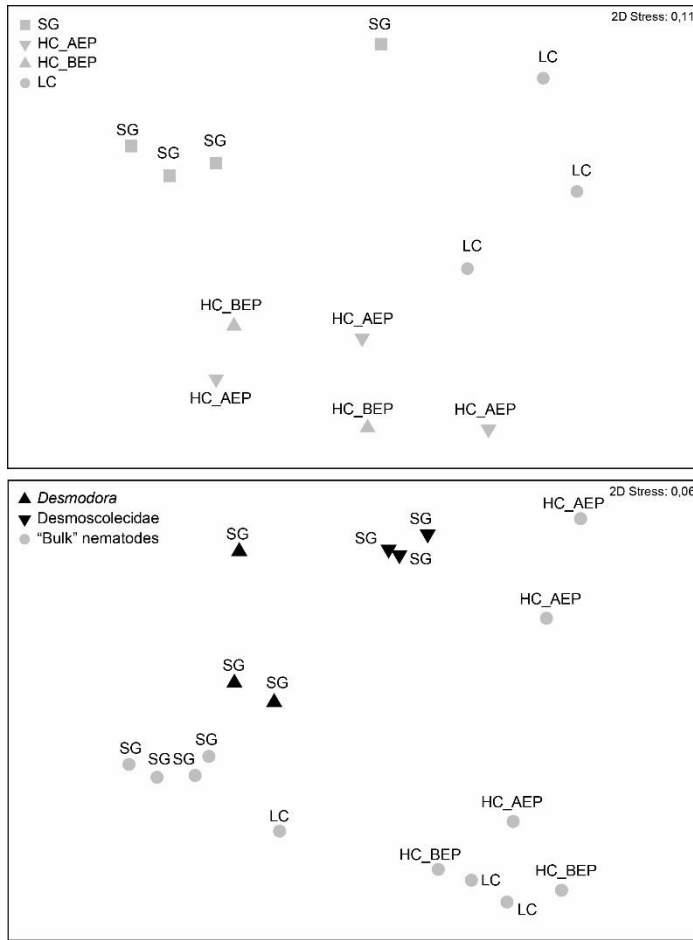


Figure. 3. 6. Non-metric MDS plot (Bray-Curtis similarity) based on nematode fatty acid profiles. Upper figure represent total nematode fatty acid for the “bulk” nematodes. Lower figure include both total nematode “bulk” fatty acid as well as total fatty acid for *Desmodora* and Desmoscolecidae.

MDS based on the FA relative abundances for the three groups showed separate clusters for *Desmodora* and desmoscolecids in comparison with nematode “bulk” FA profiles (Fig. 3.6). SIMPER routines revealed the ratio $\frac{\sum 16:0}{\sum 18:0}$ as the main responsible for dissimilarities between “bulk”

nematode FA, *Desmodora* and desmoscolecids (Table S5). When nematode FA were assigned to potential food sources, plankton-derived FA were dominant in nematodes (including desmoscolecids and *Desmodora*) at all sites (Table S4). The ratio $\frac{\sum 16:1\omega 7}{\sum 16:0}$, considered as a diatom biomarker, was higher than 1 in nematodes (except for the desmoscolecids) from SG (Table S3). The fatty acid 20:4 ω 6, shown to be an important component in foraminiferans (Würzberg et al., 2014), was found in relatively high abundances ($12.7\% \pm 2.0\%$ to $23\% \pm 5.4\%$) in all nematodes (except *Desmodora*) (Table S4). Bacterial FA were rarely present in nematodes, reaching maximum relative amounts of $6.1\% \pm 1.5\%$. PERMANOVA based on the nematode “bulk” FA revealed significant

differences between sites ($p = 0.0003$) and between all pairs of sites except for HC_AEP x HC_BEP and HC_BEP x LC.

3.4.5 Structural and functional nematode diversity and nematode respiration rates

Univariate significant correlations revealed that biomass was only positively correlated with Shannon-Wiener H' diversity ($r = 0.76$, $p = 0.009$, $n = 12$) and Pielou's evenness J' ($r = 0.75$, $p = 0.01$, $n = 12$), as well as with total sediment FA ($r = 0.92$, $p < 0.0001$, $n = 12$). Moreover, Shannon-Wiener was only positively correlated with total sediment FA ($r = 0.63$, $p = 0.04$, $n = 12$).

PERMANOVA analyses based on trophic groups displayed significant differences between sites and slices ($p < 0.0001$). SIMPER analysis revealed that dissimilarities were mainly due to the average abundance of feeding type 1A, which decreased in abundance with increasing sediment depth at HC_AEP and LC sites. Feeding type 2A was mainly concentrated in the superficial layers at SG and HC_AEP. Total nematode respiration estimates exhibited significantly higher values for SG in comparison with other sites ($p < 0.0001$).

3.4.6 Correlation between environmental variables and nematode community structure, biomass and total FA

The DISTLM analysis based on 9 environmental variables explained 49 % of the total nematode community structure based on observed genus densities. Net surface primary productivity (avNPP) accounted for 36% of the total variation and Chla·phaeopigments for 13% (Fig. 3.7A, Tables S6, S7). The other variables did not contribute significantly to

the model and/or added < 5% in explaining assemblage variation. For the DISTLM based on the total nematode biomass, freshness of photosynthesis-derived OM (Chla:phaeopigments) was the only significant variable explaining biomass variability (21%) (Fig 3.7B, Tables S6, S7).

DISTLM based on total nematode FA showed similar results as for nematode community structure variation, with average productivity, avNPP, being responsible for 38 % of the total FA variability and Chla:phaeopigments for 23 %. The other variables did not contribute significantly to the model (Tables S6, S7).

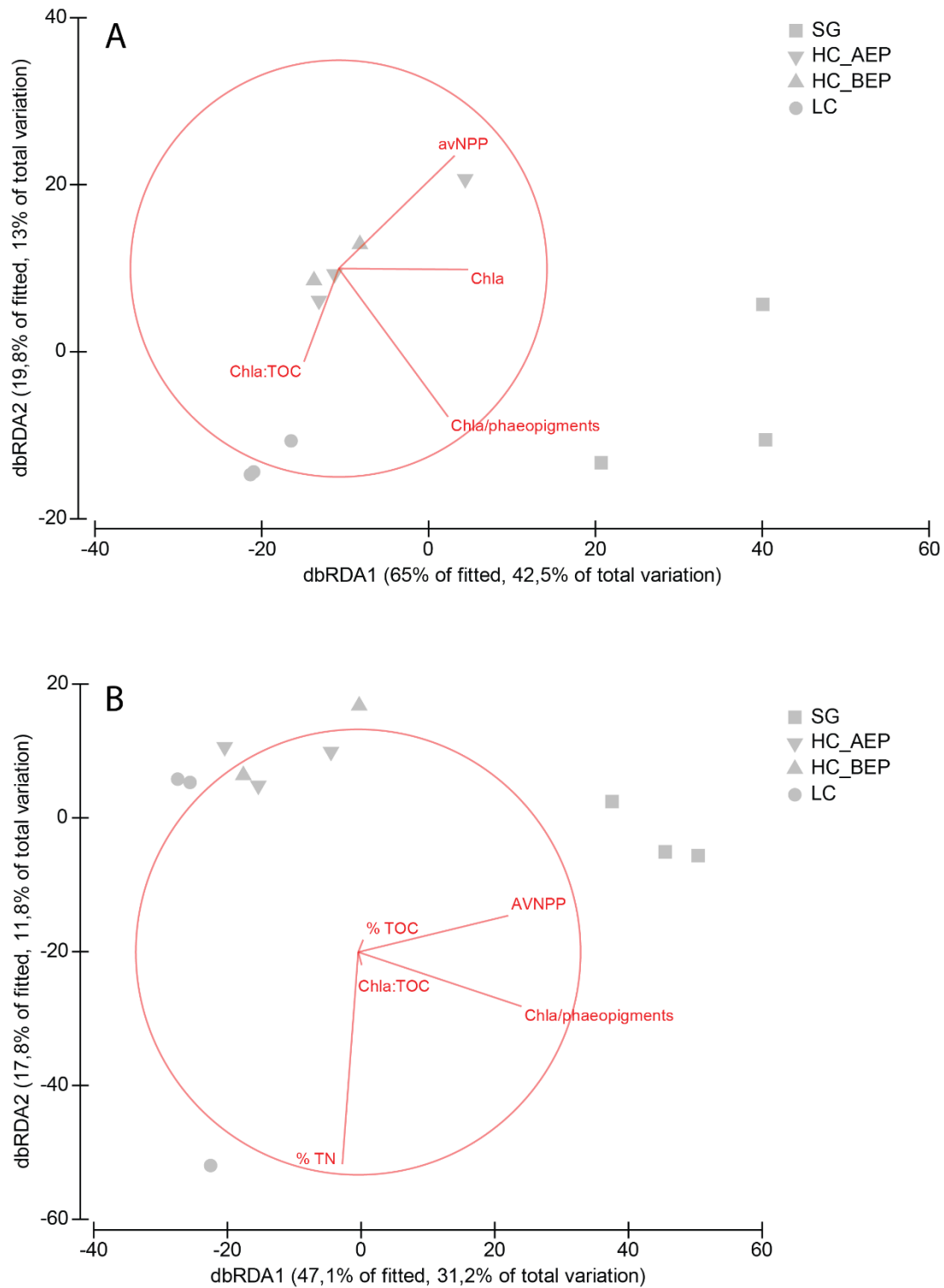


Figure. 3.7. Distance-based redundancy (dbRDA) illustrating the DISTLM model based on genera assemblage data (A) and genus individual biomass (B), and fitted environmental variables with their vector (strength and direction of effect of the variable on the ordination plot).AVPP= Average Net Primary Productivity, Chla= Chlorophyll a, Chla:%TOC= Chlorophyll a: Total Organic Carbon, %TOC= Total Organic Carbon, %TN= Total Nitrogen.

3.5 Discussion

3.5.1 Surface primary productivity, sedimentary pigments and nematode standing stocks

Higher surface productivity at SG compared to the other sites, and its positive correlations with sediment Chla, CPE and total sediment FA values point to a significant sedimentation of labile OM to the seabed at this station. Next to that, highest nematode standing stocks (i.e. density and biomass) observed at SG suggests a strong benthic-pelagic coupling in the studied site, as was expected and already documented in previous studies (Lins et al., 2014; Veit-Köhler et al., 2011). The same link was also reported for the microbial communities (Ruff et al., 2014), megafauna (mainly echinoderms) (Würzberg et al., 2014) and ostracods (Brandão et al., 2014) studied at the same locations, where SG showed elevated abundances and biomass of these organisms compared to the more eastern located sites at the same latitude. Although other factors may play a role in the high standing stocks found at SG (e.g. grain size, bottom currents and bottom topography), nematode densities at SG were up to ten times higher than those previously reported for the Polar Front (Guilini et al., 2013) and other regions in the deep Southern Ocean (Sebastian et al., 2007), while the other sites (HC_AEP, HC_BEP and LC) exhibited a lower OM input and showed densities similar to adjacent abyssal areas (Guilini et al., 2013; Sebastian et al., 2007). The benthic-pelagic coupling effect was not very pronounced at HC_AEP and HC_BEP, which exhibited surface primary productivity values higher than LC, but this difference was barely reflected in the nematode biomass.

According to Sachs et al. (2009), the sites studied here (situated at the Polar Front) are located in the circumpolar “diatom ooze belt”, which constitutes one of the most important

areas of biogenic silica accumulation due to naturally occurring diatom blooms and very high benthic fluxes. This ooze belt can be divided in diatom provinces and SG region is situated within the *Chaetoceros* spp. province, while the other sites are dominated by *Fragilariopsis kergulensis*. *Chaetoceros* spp. is considered of major importance for carbon export and the highest benthic fluxes of the Southern Ocean were observed within this province (Abelmann et al., 2006). Thus, the high labile carbon values (Chla: phaeopigments) displayed at SG are strongly linked to a nutrient-rich and extensive export as observed at the *Chaetoceros* spp. province. On the contrary, *F. kergulensis*, which reflects low labile carbon fluxes (Abelmann et al., 2006), might explain the weaker coupling observed between HC_AEP and HC_BEP relatively high surface primary productivity and the low nematode standing stocks. Hence, lower fresh and lower quality OM export to HC_AEP, HC_BEP and LC sediments were perhaps responsible for the lower nematode densities and biomass found at these sites when compared to SG.

Besides being located in the *Chaetoceros* spp. province, benthic fluxes might also be augmented at SG by the presence of year-round nutrient availability, with amounts twice that of the open water (Whitehouse et al., 1996), enhancing not only quality but also quantity of OM flux to the seabed. The reason for this high productivity at SG might occur by a combination of different factors: the occurrence of island-mass effects, the proximity of the Polar Front, the Weddell-Scotia Confluence, the proximity to the american continent, and the island's subantarctic location (Whitehouse et al., 1996). Additionally, nutrient resupply, such as upwelling at the adjacent shelf break, is also suggested to enhance annual primary production in SG (Ruff et al., 2014). This constantly high nutrient availability is most likely also responsible for the higher meiobenthic standing stocks observed in the region (Lins et al., 2014).

The occurrence of fine, medium and coarse sand fractions (present at > 4000 m) at SG in association with lower and equally distributed % TOM until 5 cm sediment depth provides

a strong indication of the high hydrodynamics in the area, with sediment being flushed down from the slope. In addition, the homogeneous distribution of % TOM in the sediment may reflect bioturbation profiles. As opposed to the other sites where there is a decrease with depth, % TOM at SG expresses a homogeneous vertical distribution up to at least 5 cm depth in the sediment, which may suggest that OM is drawn into the sediment via bioturbation activities (Soetaert et al., 1997). Therefore, high nematode biomass and high density of large nematode genera found at SG, represented mainly by the genera *Acantholaimus*, *Desmodora* and *Cervonema*, could be an indication of sediment reworking at this site through the mixing of OM between sediment layers. At the other sites, the lower nematode biomass and their smaller size, together with the rapid decline of % TOM with depth into the sediment, might indicate low sediment reworking. Nevertheless, nematode bioturbation is generally overruled by macro- and megabenthic bioturbation, following the organic matter reworked by the macro- and megafauna. Unfortunately, the effect of the macro- and megafauna in bioturbation processes in SG could not be inferred since no data are available (Brandt et al., 2014).

3.5.2 Nematode community structure

Thalassomonhystera (except in SG), *Acantholaimus* and *Microlaimus* (except in LC), commonly found in soft bottom deep-sea environments (Vanreusel et al., 2010b), were dominant at all sites and, although possessing a high species diversity, displayed the same dominant species at all locations. The genus *Thalassomonhystera*, here dominated by one morphotype at all sites, is already known to exhibit a wide distribution, dominating many deep-sea environments including abyssal plains (Sebastian et al., 2007; Vanreusel et al., 2010b). Thus, although sites were distant up to 3000 km from each other, the same

morphospecies was responsible for the greater abundances of this genus overall, suggesting potentially high dispersal capability of this morphospecies. With respect to *Acantholaimus* species, *Acantholaimus invaginatum* dominated at all sites, decreasing in abundance with increasing sediment depth, while deeper sediment layers were dominated by *Acantholaimus maks*. The latter is approximately three times longer than *A. invaginatum*. The success of slender nematodes in deeper layers of the sediment was already observed in several studies both from shallow water and the deep sea (Jensen, 1986; Lins et al., 2013; Soetaert et al., 2002). Their slender body is supposed to enhance mobility, enabling them to migrate between anoxic patches of food and parts of the sediment where oxygen is available, and allows to bridge oxic spots, optimising the body volume/surface ratio (Jensen, 1986; Soetaert et al., 2002), what might explain niche segregation observed between these two *Acantholaimus* species.

Microlaimus, dominated by one morphotype at all locations, displayed a typical opportunistic behaviour, suggesting a migration from deeper to superficial layers whenever fresh food supply was provided, as indicated by the high abundances observed in the superficial sediment layers at SG and HC_AEP and in deeper layers at LC. The same behaviour was also observed by Guilini et al. (2013) for the total nematode community and by Jeffreys et al. (2013) for deep dwelling Foraminifera. Unexpectedly, high densities of *Desmodora* and *Tricoma* were found in SG. These two genera are normally not encountered in such high numbers at abyssal depths (Vanreusel et al., 2010b). However, similar to our study, high densities of *Desmodora* in the Southern Ocean were previously described in a study conducted southeast of SG, along the Scotia Arc (Ingels et al., 2006). Although dominated by other species (*Desmodora campbelli*), the presence of *Desmodora* in high abundances along the Scotia Arc was also unexpected, and its omnipresence at other distant sampled sites was attributed to passive transport in the bedload and water column (Ingels et al., 2006). In this study, *Desmodora* dominated at SG

both in density and biomass by a single species, *D. profundum*, previously described by Moura et al. (2014) for the deep south-east Atlantic, but also present at the other Polar Front sites. Its presence both in the south-east Atlantic deep sea, as well as at all sites from this study suggests that this species can be susceptible to erosion and passive transport in the water column. Generally, the genus *Desmodora* is considered as opportunistic, usually found in highly productive environments, such as seamounts, seeps and vents, but it also prefers coarser substrates unlike most nematodes in the deep sea (Vanreusel et al., 2010b). Thus, the high productivity at SG, together with a slightly coarser sediment fraction, may therefore have induced its dominance. Moreover, Gerlach and Schrage (1972) observed that this genus is able to have a life span of approximately 600 days, and probably even longer in the deep sea, being able to persist throughout the year even if productivity is seasonal.

The genus *Tricoma* belongs to the family Desmoscolecidae and its presence is typical, although in lower numbers than observed here, for the abyssal deep sea (Soetaert and Heip, 1989). This genus is mainly found in high abundances in environments dominated by coarser sediments, such as corals and seamounts, and its stout body size might offer advantages for an opportunistic behaviour in relation to other nematodes in environments dominated by coarse sediments.

3.5.3 Nematode fatty acids

Little is known on deep-sea nematode FA composition in general (Leduc, 2009; Leduc et al., 2014; Leduc and Probert, 2009) and in the abyssal Southern Ocean in particular (Guilini et al., 2013). This is mainly due to difficulties in assembling enough material for the analyses, as nematodes are very small organisms and they are even smaller in deep-

sea sediments (Ramirez-Llodra et al., 2010). Moreover, the interpretation of FA results is not straightforward, since it can also involve FA biosynthesis by the studied organism. Thus, research is mainly concentrated on “bulk” analyses, diluting the signal from individual genera or species and muting the potentially high degree of interspecific variability. In this study, we could perform individual analyses on *Desmodora* and desmocoecids due to their high abundance at SG.

When total “bulk” FA content was analysed, nematodes exhibited higher total individual FA concentrations at SG compared to the other sites, as well as higher total sediment FA content. These differences in FA concentrations could have been due to differences in mean body mass of the nematodes. However, within sediment FA, Σ SFA and Σ MUFA were the most abundant groups, while Σ PUFA dominated in nematodes, suggesting a selective uptake behaviour of this group for high quality FA or FA biosynthesis (Leduc et al., 2014). Hence, this study corroborates with the low sediment Σ PUFA concentrations also found by Würzburg et al. (2011) and the high nematode Σ PUFAs revealed by Guilini et al. (2013) in the Southern Ocean. However, the potential of nematodes as high quality food source for higher trophic levels is still under debate (Leduc, 2009), as they generally possess very low FA concentrations when compared to other meiofaunal groups, such as copepods (De Troch et al., 2012). When FA from *Desmodora* and desmoscoecids (for SG) were compared to the “bulk” FA, Σ MUFAs and Σ SFAs dominated in each group, respectively. MUFAs are commonly found in faecal pellets, especially in environments subjected to a high food supply, where residence time of food in the guts of zooplankton is shortened (Reemtsma et al., 1990). The presence of intact faecal pellets in the sediment was observed at SG by Ruff et al. (2014). These authors observed that the presence of intact faecal pellets and chloroplast rRNA at the seafloor “provided evidence for a short transport time of few weeks and suggested a strong benthic-pelagic coupling”. The higher amount of MUFAs in *Desmodora*, characterized as a sediment-surface dwelling epistratum feeder (according to

Wieser, 1953), was clearly associated with elevated water and sediment pigment concentrations, as expressed by a diatom-biomarkers $\frac{16:1\omega7}{16:0}$ with ratio greater than 1, $\frac{DHA}{EPA}$ smaller than 1 and by elevated EPA content. In this study, FA content indicates that *Desmodora* may feed on partially degraded diatoms present in intact faecal pellets, as suggested by their high MUFA concentrations. The lack of 20:4 ω 6 in *Desmodora* (and its presence in all other nematodes) was possibly the reason for the lower PUFA concentration found in this genus. This FA is normally found in high abundances in foraminiferans (Gooday, 2002; Suhr et al., 2003) and the lack of it only in *Desmodora* indicates the potential selective feeding behaviour of this group or a different FA metabolism.

Direct plankton-based FA seem to contribute most to the diet of nematodes. Bacterial FA were scarcely present in nematodes, indicating that their primary food source might be fresh phytoplankton detritus derived from the surface waters. The ratio $\frac{16:1\omega7}{16:0} > 1$, together with high EPA content, indicated a diatom-based diet for nematodes (including *Desmodora*) from SG, while the other sites had $\frac{16:1\omega7}{16:0}$ ratios lower than 1. Nevertheless, when $\frac{DHA}{EPA}$ was compared between sites, the ratio remained around 1, indicating that not only EPA but also DHA (commonly found in dinoflagellates and other microalgae) was present in high concentration in “bulk” nematodes. DHA values reached up to almost 20% of the total FA content and it was already shown that although marine nematodes are able to biosynthesize highly unsaturated FA (HUFAs), they hardly ever biosynthesize DHA (Honnens et al., 2014; Leduc and Probert, 2009), pointing to a selective feeding behaviour. This FA is an important constituent of all organisms and in the benthic system it may represent food sources with high refractory material content (which might be rich in DHA) rather than dietary dinoflagellates. Thus, higher values of markers for “fresh” diatom input (16:1 ω 7 and EPA) were observed at SG, while the other sites exhibited strong indications for a more refractory feeding behaviour (high DHA values at LC and a marked

decrease from HC_BEP to HC_AEP). An important FA that should be mentioned is the PUFA 20:4 ω 6, present in high abundances in foraminiferans but also biosynthesised by nematodes (Gooday, 2002; Suhr et al., 2003). While it lacked completely in *Desmodora*, this FA was present in relatively high abundances in all other “bulk” nematodes and Desmoscolecidae, suggesting a potential input of foraminiferans in their diet. Lejzerowicz et al. (2014) showed single-chambered, soft-walled monothalamous taxa as the most abundant Foraminifera encountered at the same sites of the Southern Ocean sampled as this study. Considering that foraminiferans are ubiquitous and PUFA-rich, their potential inclusion in the general nematode food diet might not be surprising. Hence, we conclude that when there is high quality food available, nematodes will selectively feed on this fresh OM, whereas when food becomes limiting, they will adopt a diet consisting of refractory material, which enables them to feed throughout the year.

Isotope studies conducted on deep-sea nematodes from the Northeast Pacific suggested a sedimentary food source, thus mainly composed of refractory organic matter (Jeffreys et al., 2013). Hitherto, this behaviour would be more expected in food-limited environments, as was observed in the FA analyses for the LC site. Because “fresh” food is limited at this site, foraging might be restricted to refractory material. Next to differences in interspecific isotope composition, differences in prey availability, nematode body size and habitat might be responsible for variation in trophic levels within the same species (Leduc et al., 2014). Consequently, without the combination with stable isotope analyses, results should be interpreted with caution. Studies conducted on pelagic copepods showed that they accumulate large lipid reserves (wax esters, 16:1 ω 7, 18:4 ω 3 and EPA) as an adaptation to the pronounced seasonality and strongly pulsed food supply, but that in the Antarctic they have evolved a more opportunistic feeding behaviour, storing triacylglycerols rather than wax esters (Dalsgaard et al., 2003). FA contents of nematodes are generally much lower than in copepods (De Troch et al., 2012), and together with the dominance of typical

phospholipids of biomembranes (EPA, DHA and 16:0) observed in other studies (Graeve et al., 1997), they possibly do not accumulate lipids as an energy storage. It is improbable then that they would synthesize great amounts of polyunsaturated FA *de novo* without any need for it (Guilini et al., 2013). Thus, PUFA concentrations in nematodes from HC_BEP, HC_AEP and LC might be derived from intermediate food components, such as foraminiferans, or from feeding on refractory material (available all year round), which is poor in PUFA (Guilini et al., 2013).

3.5.4 Nematode function, taxon diversity and respiration

Trophic structure showed a higher number of 1B (non-selective deposit feeders) in SG and this number increased with sediment depth due to the presence of *Cervonema*, *Daptonema* and *Sabatieria* in deeper layers of the sediment. Representatives of these genera were long and big in this study, and could easily dwell in deeper layers to avoid competition and/or feed on refractory material buried deeper down. Moens and Vincx (1997), when analysing feeding behaviour of various species, mentioned that *Daptonema setosum* (1B) had a restless and erratic feeding behaviour, interrupting periods of immobility or slow gliding with abrupt activity. Therefore, although the feeding behaviour of the other 1B genera was not yet tested, we expect low selectivity of this group. Epistratum feeders (2A) dominated the samples at all sites. At HC_BEP they were mainly present in the subsurface layer (1-2 cm), and at HC_AEP they were mostly concentrated in the superficial layers. These differences were mainly due to the genus *Microloaimus* and its migration towards superficial layers after fresh food input, indicating an opportunistic behaviour of this genus. At SG, trophic group 2A was mainly represented by the genus *Desmodora*,

mostly present in the superficial layers. In general, epistratum feeders are often associated with surface sediments due to fresh OM input.

The higher total respiration rates at SG were in accordance with the higher fresh Chla input, as well as with elevated nematode diversity. More diverse communities are generally linked to a higher sediment-community respiration, which in turn is also correlated to higher energy availability (Levin et al., 2001). A more diverse community is believed to be able to mineralise more carbon and optimise resource use (Pape et al., 2013a) and its response to food input can be immediate (Gage and Tyler, 1991), resulting in higher oxygen consumption (enhanced respiratory activity) after a phytoplankton bloom (Veit-Köhler et al., 2011). Sachs et al. (2009) observed a high sedimentary oxygen uptake at the Polar Front for sites underlying areas of high chlorophyll concentration in surface waters. Our results are in accordance with respiration rates observed by Pape et al. (2013a) for the Mediterranean and NE Atlantic, where diversity mirrored respiration rates, and with the general sediment community oxygen consumption results found for nematodes elsewhere (Franco et al., 2010; Levin et al., 2001; Veit-Köhler et al., 2011).

3.5.5 Environmental drivers of nematode standing stocks

DISTLM results for density, biomass and FA composition displayed a significant effect of the average primary productivity (avNPP) on nematode density and FA profiles, and of sediment Chla on nematode biomass. This reflects the importance of surface primary productivity and flux of OM to the seabed as major drivers of nematode community structure. It has been shown before that deep-sea communities appear to be chiefly controlled by energy availability (Karakas et al., 2009; Levin et al., 2001; Pape et al., 2013b; Pfannkuche and Lochte, 1993; Soetaert and Heip, 1989) including diatom

production at the surface (Sachs et al., 2009). Moreover, Ruff et al. (2014) observed for the same SG site a strong benthic-pelagic coupling due to the export of dense, fast-settling particles detected by the presence of intact 16S RNA, a strong indicator for fresh phytoplankton. These results corroborate the previously mentioned “diatom ooze belt” dominated by *Chaetoceros* spp. and their high carbon export capacity in SG site (Sachs et al., 2009). Next to that, in Antarctica, low degradation rates of OM may occur due to the low temperatures and low microbial activity, enabling the accumulation of OM sediments over longer periods of time (Fabiano and Pusceddu, 1998) and, consequently, its availability to the benthic organisms.

3.6 Conclusions

With the use of different approaches concerning surface primary productivity estimates, sediment Chla and the use of FAs in combination with nematode community analysis, we integrated environmental and biological traits to unravel different aspects of benthic-pelagic coupling in the Southern Ocean. We observed that nematode standing stocks from abyssal plains of the Southern Ocean are regulated by fresh plankton-derived food sources, though nematodes may also use refractory material or other food sources indirectly dependent on plankton input (e.g. foraminiferans). Differences in nematode community structure as well as the increase in nematode PUFAs mostly occur in relation to an increase in surface primary productivity, since certain nematode genera (e.g. *Desmodora*) seem to be significantly favoured by the increase in labile organic matter arriving at the seabed.

As nematodes do not have lipid reserves and must feed all-year round, they will predominantly feed on fresh organic matter when present, as shown by the nematode FA

profile in comparison with sediment FA, but change to a poorer diet based on refractory material whenever fresh food becomes scarce. Food selectivity based on FA biomarkers indicated a dietary preference for diatoms in “bulk” nematodes and *Desmodora* from SG, whereas at the other sites feeding on food sources other than diatoms was dominant.

FA analyses on nematodes, as well as other promising techniques, such as compound specific stable isotopes from amino acids, are still restricted by the small size of this group. “Bulk” techniques provided a good insight in this study because very contrasting sites in terms of surface productivity were used and one main feeding type (2A) dominated the samples, providing clear FA signals. Nevertheless, information about each genus feeding habit is still diluted and/or restricted to the most abundant genera.

3.7 Supplementary data

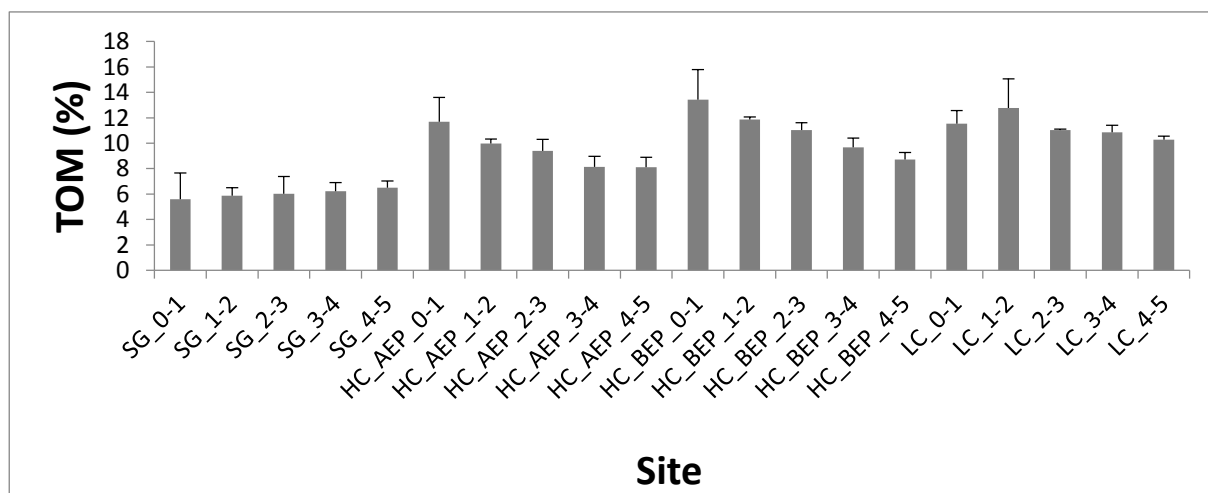


Figure S1. Total organic matter (% TOM) per sediment layer (0-1, 1-2, 2-3, 3-4, and 4-5 cm) in each site. SG = South Georgia; HC_AEP = High Chlorophyll_after Eddy Pump; HC_BEP = High Chlorophyll_before Eddy Pump; LC = Low Chlorophyll.

Table S1. Sediment fatty acid composition for the individual fatty acids, sum of fatty acid groups, and fatty acid ratios per station.

Fatty acids and ratios	SG	HC_AEP	HC_BEP	LC
C:14	4.9 ± 3.9	2 ± 0.5	3 ± 0.3	2 ± 0.6
antei isoC15	1.1 ± 0.3	1.1 ± 0.3	1.6 ± 0.1	1.1 ± 0.3
iso C:15	2.1 ± 0.4	1.7 ± 0.6	2.5 ± 0.7	1.7 ± 0.5
C15:0	0.4 ± 0.3	0.1 ± 0.2	0.2 ± 0.2	0.1 ± 0.2
C:16	11.7 ± 5.4	8.5 ± 6.2	7.2 ± 1	5.3 ± 0.2
C16:1w7	10.5 ± 9.7	0 ± 0	2.1 ± 1.7	0 ± 0
C18:0	2.7 ± 1	2.2 ± 0.6	2.1 ± 0.4	1.8 ± 0.3
C18:1w9trans	1.6 ± 1.8	0 ± 0	0.2 ± 0.3	0 ± 0
C18:1w9cis	8.1 ± 6	0 ± 0	0.9 ± 0.9	0 ± 0
EPA	4.7 ± 5.5	0 ± 0	0 ± 0	0 ± 0
C24:0	0.7 ± 1.2	0.6 ± 0.5	0.5 ± 0.4	0.2 ± 0.2
DHA	0.9 ± 1.4	0 ± 0	0 ± 0	0 ± 0
SUM_FA	48.9 ± 34.6	15.9 ± 7.1	19.8 ± 4.5	11.8 ± 0.8
DHA/EPA	0.2 ± 0.3	0 ± 0	0 ± 0	0 ± 0
EPA/DHA	0.6 ± 1.1	0 ± 0	0 ± 0	0 ± 0
C16:1w7/16:0	1.3 ± 0.9	0 ± 0	0.5 ± 0.2	0 ± 0
iso C:15+antei iso C:15/ 15:0	1.5 ± 2.5	1.1 ± 1.9	0 ± 0	0.4 ± 0.6
iso C:15+antei iso C:15/ 16:0	1.5 ± 0.2	1.8 ± 0.1	2.3 ± 0.2	1.6 ± 0.5
ΣC16/ΣC18	26.3 ± 15.2	8.5 ± 6.2	9.5 ± 2.4	5.3 ± 0.2
C16:1 + EPA	15.2 ± 15.1	0 ± 0	2.1 ± 1.7	0 ± 0
ΣSFA	23.4 ± 11.9	15.9 ± 7.1	16.8 ± 1.8	11.8 ± 0.8
ΣMUFA	20.2 ± 16.9	0 ± 0	3 ± 2.8	0 ± 0
ΣPUFA	5.5 ± 6.9	0 ± 0	0 ± 0	0 ± 0
ΣSFA%	55 ± 21	100 ± 0	86.3 ± 10.7	100 ± 0
ΣMUFA%	36.7 ± 18.3	0 ± 0	13.8 ± 10.7	0 ± 0
ΣPUFA%	8.4 ± 6.1	0 ± 0	0 ± 0	0 ± 0

Table S2. Univariate PERMANOVA table of results for sediment fatty acid profiles based on the relative abundance of each fatty acid (Sediment SFAs = sediment saturated fatty acids; Sediment MUFAs = sediment monounsaturated fatty acids; Sediment PUFAs = sediment polyunsaturated fatty acids; Bacterial + planktonic FA = fatty acid bacterial- or planktonic-derived; avNPP = average net primary productivity). Values in bold and italic indicate significant differences ($p < 0.05$).

Sediment SFAs							
Source	df	SS	MS	Pseudo-F	P(perm)	unique perms	P(MC)
site	3	205.93	68.643	1.2572	0.32	7360	
Res	7	382.2	54.599				
Total	10	588.13					
Sediment MUFAs							
Source	df	SS	MS	Pseudo-F	P(perm)	unique perms	P(MC)
site	3	8980.8	2993.6	4.5469	0.0698	897	
Res	7	4608.7	658.39				
Total	10	13590					
Sediment PUFAs							
Source	df	SS	MS	Pseudo-F	P(perm)	unique perms	P(MC)
site	3	1246.6	415.52	16.572		62	<i>0.0031</i>
Res	6	150.44	25.074				
Total	9	1397					
Bacterial + planktonic FA							
Source	df	SS	MS	Pseudo-F	P(perm)	unique perms	P(MC)
site	3	2401.7	800.57	9.6817	<i>0.0011</i>	4978	
Res	6	496.13	82.689				
Total	9	2897.8					
avNPP							
Source	df	SS	MS	Pseudo-F	P(perm)	unique perms	P(MC)
site	3	2.6443E5	88145	2.0766E5	<i>0.0001</i>	302	
Res	7	2.9713	0.42447				
Total	10	2.6444E5					

Table S3. Multivariate PERMANOVA two-way nested design table of results for nematode density, relative abundance, total number of genera and biomass. Significant results ($p < 0.05$) are represented in bold and italic.

Nematode Density (10 cm²)						
<i>Source</i>	<i>df</i>	<i>SS</i>	<i>MS</i>	<i>Pseudo-F</i>	<i>P(perm)</i>	<i>unique perms</i>
Site	3	37403	12468	59.967	<i>0.0001</i>	9888
Slice	4	26382	6595.6	57.527	<i>0.0001</i>	9875
Replicate (site)	12	24949	2079.1	18.134	<i>0.0001</i>	9742
Site x slice	12	32817	2734.7	23.852	<i>0.0001</i>	9757
Res	48	55033	1146.5			
Total	79	1,7658E5				

Nematode community structure						
<i>Source</i>	<i>df</i>	<i>SS</i>	<i>MS</i>	<i>Pseudo-F</i>	<i>P(perm)</i>	<i>uniauue perms</i>
Site	3	21855	7285	52.691	<i>0.0001</i>	9883
Slice	4	15848	3962.1	48.888	<i>0.0001</i>	9879
Replicate (site)	12	16591	1382.6	1.706	<i>0.0001</i>	9758
Site x slice	12	20848	1737.4	21.437	<i>0.0001</i>	9771
Res	48	38901	810.44			
Total	79	1.14E+09				

Total number of nematode genera (S)						
<i>Source</i>	<i>df</i>	<i>SS</i>	<i>MS</i>	<i>Pseudo-F</i>	<i>P(perm)</i>	<i>unique perms</i>
Site	3	20286	6762	39.356	<i>0.0001</i>	9884
Slice	4	11605	2901.4	33.381	<i>0.0001</i>	9863
Replicate (site)	12	20618	1718.2	19.768	<i>0.0001</i>	9761
Sitexslice	12	12774	1064.5	12.247	<i>0.049</i>	9786
Res	48	41720	869.16			
Total	79	1.07E+05				

Total nematode biomass (µg dwt)						
<i>Source</i>	<i>df</i>	<i>SS</i>	<i>MS</i>	<i>Pseudo-F</i>	<i>P(perm)</i>	<i>unique perms</i>
Site	3	50632	16877	42.716	<i>0.0001</i>	9873
Slice	4	22217	5554.4	21.377	<i>0.0001</i>	9800
Replicate(site)	12	47413	3951.1	15.207	<i>0.0001</i>	9603
Site x slice	12	44751	3729.3	14.353	<i>0.0001</i>	9623
Res	48	1.25E+09	2598.2			
Total	79	2.90E+09				

Table S4. Relative concentrations of individual fatty acid (% of total fatty acid) in “bulk” nematodes (and separate groups *Desmodora* and Desmoscolecidae) from all sampled sites (SG = South Georgia; HC_AEP = High Chlorophyll_After Eddy Pump; HC_BEP = High Chlorophyll_Before Eddy Pump; LC = Low Chlorophyll).

Fatty acids and ratios	SG		"Bulk" nematodes			
	Desmoscolecidae	<i>Desmodora</i>	SG	HC_AEP	HC_BEP	LC
14:0	1.1 ± 2.6	4.1 ± 0.2	2 ± 0.2	1.4 ± 1.7	3.2 ± 3.3	1.1 ± 1.9
antei iso 15:0	-	-	0.3 ± 0.2	-	-	-
iso 15:0	-	-	0.3 ± 0.4	1.2 ± 1.5	-	-
15:0	-	-	0.3 ± 0.9	-	-	-
16:0	26.1 ± 1.6	13.3 ± 3	8.6 ± 0.5	31.6 ± 5.8	20.8 ± 2.4	20.2 ± 6.1
16:1 ω 7	12.4 ± 1.5	26.4 ± 3	12.4 ± 1.8	4.6 ± 1.2	1.2 ± 1.2	2.2 ± 3.8
17:0	-	-	0.2 ± 0.5	-	-	-
17:1 ω 7	-	-	0 ± 0.1	-	-	-
18:0	15.5 ± 2.5	7.4 ± 2.9	4.5 ± 0.5	16.4 ± 4.4	9.8 ± 3.2	11.2 ± 4.2
18:1 ω 9t	0.8 ± 1.8	4 ± 0.2	7.5 ± 1.8	6.2 ± 4.7	4.3 ± 4.4	7.7 ± 0.9
18:1 ω 9c	8.1 ± 2	5.3 ± 0.4	8.9 ± 1.4	8.2 ± 2.2	6.6 ± 0.6	7.5 ± 1.1
18:2 ω 6t	-	-	0.9 ± 2.2	-	-	-
18:2 ω 6c	-	2.4 ± 3.2	0.5 ± 0.2	-	-	-
20:1 ω 9t	0.1 ± 0.2	-	3 ± 0.9	-	-	1 ± 1.7
20:1 ω 9c	-	4 ± 3.2	4 ± 1.4	-	-	1 ± 1.8
20:2 ω 6	-	-	1.5 ± 0.2	-	-	-
20:4 ω 6	17.2 ± 3.5	-	12.7 ± 2	13.7 ± 2.6	23 ± 5.4	19.9 ± 2.4
EPA(20:5 ω 3)	18.7 ± 2.8	18.6 ± 1	15.6 ± 1.8	5.8 ± 4.7	12.9 ± 0.2	13 ± 0.8
24:1 ω 9	-	3 ± 6.4	1.7 ± 0.1	-	-	-
DHA(22:6 ω 3)	-	11.5 ± 9	15.1 ± 1.6	11 ± 2.7	18.2 ± 2.8	15.1 ± 1.8
DHA/EPA	-	0.6 ± 0.6	1 ± 0.1	1.9 ± 0.2	1.4 ± 0.2	1.2 ± 0.3
EPA/DHA	-	1.61 ± 0.6	1 ± 0.1	0.5 ± 0.2	0.7 ± 0.2	0.8 ± 0
16:1 ω 7/16:0	0.5 ± 0	2 ± 0.5	1.4 ± 0.2	0.1 ± 0	0.1 ± 0	0.1 ± 0.2
iso 15:0+antei iso 15:0/ 15:0	-	-	-	-	-	-
Σ C16/ Σ C18	1.6 ± 0	2.1 ± 0	0.9 ± 0.1	1.2 ± 0	1.1 ± 0	0.8 ± 0
Σ SFA	42.7 ± 5.9	24.9 ± 3.3	16.2 ± 2.3	50.6 ± 7.2	33.9 ± 2.2	32.5 ± 8.4
Σ MUFA	21.4 ± 1.4	42.7 ± 12.2	37.5 ± 1.4	18.9 ± 3.3	12.1 ± 5	19.4 ± 6.3
Σ PUFA	35.9 ± 4.5	32.4 ± 14.4	46.3 ± 3.1	30.5 ± 4	54.1 ± 2.8	48.1 ± 3.9
Σ Planktonic FA %	86.4 ± 7.9	64.1 ± 20	79.3 ± 3.3	92.9 ± 7.2	95.6 ± 2.2	95.7 ± 5.0
Σ Bacterial FA %	1.14 ± 0	4.1 ± 0	2.8 ± 2.1	2.5 ± 1.5	3.2 ± 0	1.1 ± 0

Table S5. Dissimilarity (> 5 %) SIMPER routines based on the nematode (including *Desmodora* and Desmoscolecidae) individual fatty acid concentrations.

<i>Desmodora</i> x Desmoscolecidae	%	Desmoscolecidae x Nematoda	%	<i>Desmodora</i> x Nematoda	%
ΣC16/ΣC18	26.15	ΣC16/ΣC18	32.59	ΣC16/ΣC18	18.32
EPA/DHA	8.27	ΣMUFA	8.12	ΣPUFA	12.38
ΣMUFA	7.95	ΣPUFA	7	C16:1w7/16:0	11.8
C16:1w7/16:0	7.64	EPA/DHA	6.94	C20:4w6	6.83
ΣSFA	6.81	DHA/EPA	6.82	EPA/DHA	6.12
C20:4w6	6.05	ΣSFA	6.4		
DHA/EPA	5.86	DHA(22:6w3)	5.54		
C16:1w7	5.04				

Table S6. Marginal tests from the distance-based linear model (DISTLM) for genera assemblages and selected environmental variables. Chla = Chlorophyll a; Chla:phaeo = chlorophyll a: phaeopigments; Chla: TOC = chlorophyll a: total organic carbon; CPE = chloroplastic pigment equivalents; % TN = total nitrogen content; % TOC = total organic carbon content; total sedFA = total sediment fatty acid content; avNPP = average net primary productivity. Values in bold and italic indicate significant differences ($p < 0.05$).

Nematode structure	community	SS(trace)	Pseudo-F	P	Prop.
<i>Chla</i>		4337.5	4.6603	<i>0.0001</i>	0.34115
<i>Chla:phaeo</i>		4334.3	4.655	<i>0.0054</i>	0.3409
<i>Chla:TOC</i>		993.83	0.76315	0.5664	7.8166E-2
<i>CPE</i>		2295.3	1.9828	0.08	0.18053
<i>% TN</i>		1199.2	0.93724	0.4296	9.4316E-2
<i>% TOC</i>		1381.3	1.0969	0.3209	0.10864
<i>total sedFA</i>		2226.7	1.9109	0.0992	0.17514
<i>avNPP</i>		4639.8	5.1717	<i>0.0028</i>	0.36493

Nematode total biomass	SS(trace)	Pseudo-F	P	Prop.
<i>Chla</i>	6443.9	2.6176	<i>0.0027</i>	0.22531
<i>Chla:phaeo</i>	8275.3	3.6644	<i>0.0052</i>	0.28935
<i>Chla:TOC</i>	2064.1	0.70006	0.8581	7.2171E-2
<i>CPE</i>	3806.1	1.3816	0.1018	0.13308
<i>% TN</i>	3405.1	1.2163	0.3035	0.11906
<i>% TOC</i>	2474.5	0.85246	0.5861	8.65E-02
<i>total sedFA</i>	3593	1.2931	0.2474	0.12563
<i>avNPP</i>	8153.2	3.5888	<i>0.0005</i>	0.28508

Total FA concentration	SS(trace)	Pseudo-F	P	Prop.
<i>Chla</i>	2019.2	2.2976	0.0557	0.20337
<i>Chla:phaeo</i>	3536.1	4.9785	<i>0.003</i>	0.35615
<i>Chla:TOC</i>	613.61	0.59286	0.7535	6.1803E-2
<i>CPE</i>	838.99	0.83072	0.5569	8.4502E-2
<i>% TN</i>	636	0.61598	0.7947	6.41E-02
<i>% TOC</i>	494.81	0.47206	0.7446	4.98E-02
<i>total sedFA</i>	826.46	0.81719	0.5744	8.3241E-2
<i>avNPP</i>	3793.5	5.5649	<i>0.0002</i>	0.38208

Table S7. Sequential tests from the distance-based linear model (DISTLM) for genera assemblages and selected environmental variables. Chla = Chlorophyll a; Chla:phaeo = chlorophyll a: phaeopigments; Chla:TOC = chlorophyll a: total organic carbon; CPE = chloroplastic pigment equivalents; % TN = total nitrogen content; % TOC = total organic carbon content; total sedFA = total sediment fatty acid content; NPP = average net primary productivity. Values in bold and italic indicate significant differences ($p < 0.05$).

Nematode structure	community	Adj R ²	SS(trace)	Pseudo-F	P	Prop.	Cumul.	res.df
<i>+NPP</i>		0.29437	4639.8	5.1717	<i>0.0023</i>	0.36493	0.36493	9
<i>+Chla:Phaeo</i>		0.36971	1663.5	2.0758	<i>0.0299</i>	0.13083	0.49576	8
<i>+Chla</i>		0.39028	984.44	1.2699	0.2432	7.7428E-02	0.57319	7
<i>+Chla:TOC</i>		0.42272	1022.7	1.3935	0.2190	8.0441E-02	0.65363	6

Best solution

Adj R ²	RSS	No.Vars
Selections		
0.42272	4403.8	4 1-3; 9

Nematode total biomass ($\mu\text{g}/10 \text{ cm}^2$)	Adj R ²	SS(trace)	Pseudo-F	P	Prop.	Cumul.	res.df
<i>+Chla: Phaeo</i>	0.21039	8275.3	3.6644	<i>0.0047</i>	0.28935	0.28935	9
<i>+% TN</i>	0.25292	3231.4	1.5124	0.1704	0.11299	0.40233	8
<i>+NPP</i>	0.27428	2564.4	1.2355	0.2260	8.9664E-2	0.492	7
<i>+% TOC</i>	0.29803	2482.9	1.2367	0.2649	8.6817E-2	0.57882	6
<i>+Chla:TOC</i>	0.32555	2401.2	1.2448	0.2916	8.3959E-2	0.66277	5

Best solution

Adj R ²	RSS	No.Vars
Selections		
0.32555	9644.6	5 2; 3; 5; 6; 9

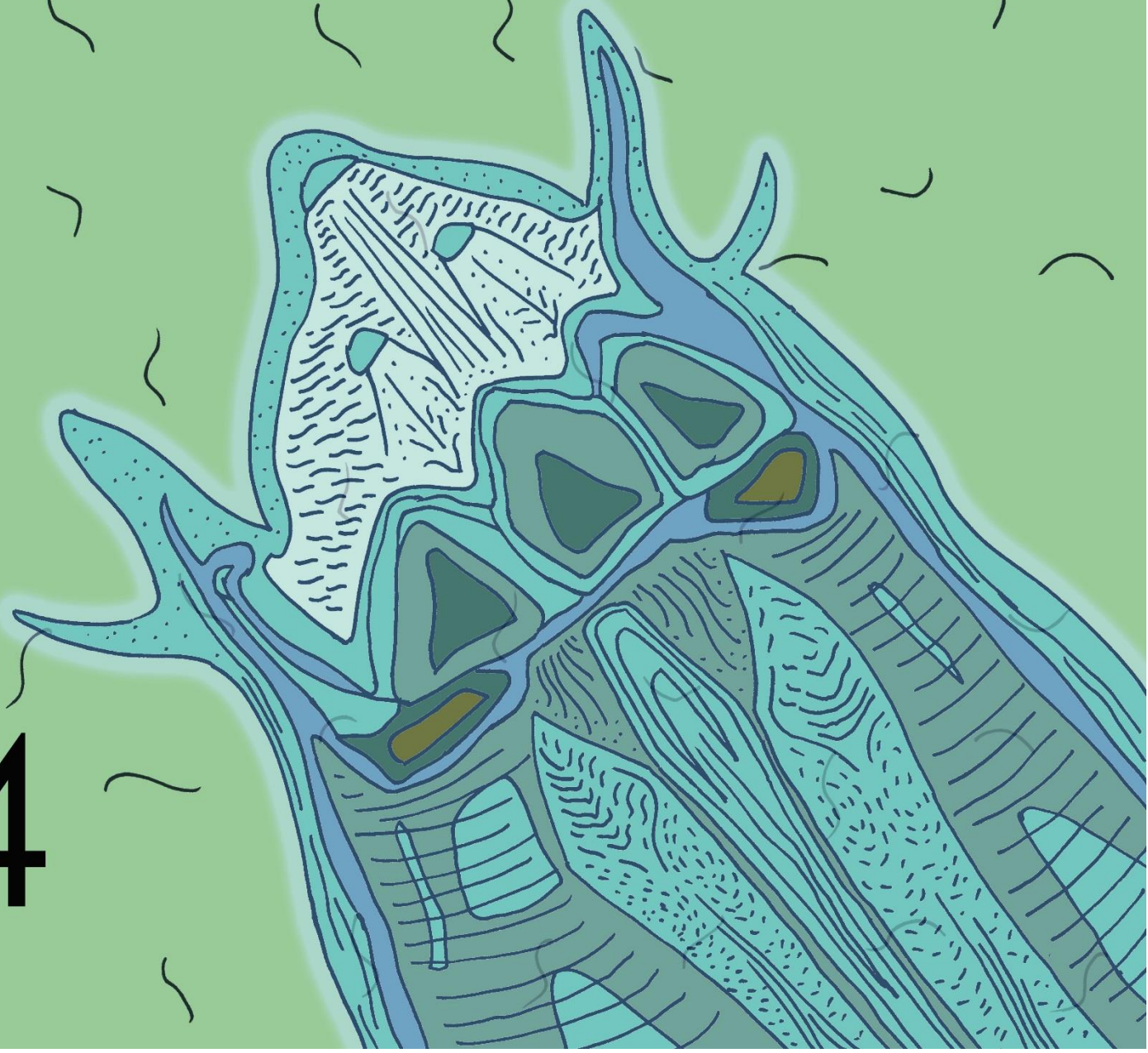
Nematode total FA (pg/ind)	Adj R ²	SS(trace)	Pseudo-F	P	Prop.	Cumul.	res.df
<i>+NPP</i>	0.31342	3793.5	5.5649	<i>0.0002</i>	0.38208	0.38208	9
<i>+Chla: Phaeo</i>	0.5168	2297.1	4.7882	<i>0.0077</i>	0.23137	0.61334	8
<i>+% TOC</i>	0.5498	709.1	1.5864	0.1973	7.142E-2	0.68486	7
<i>+CPE</i>	0.61648	844.18	2.217	0.0956	8.5025E-2	0.76989	6
<i>+total sedFA</i>	0.64372	516.02	1.4588	0.2416	5.1974E-2	0.82186	5

Best solution

Adj R ²	RSS	No.Vars
Selections		
0.64362	1768.7	5 2;
4; 6; 8; 9		

Testing deep-sea biodiversity paradigms on abyssal nematode genera and *Acantholaimus* species

4







Chapter 4: Testing deep-sea biodiversity paradigms on abyssal nematode genera and *Acantholaimus* species

Manuscript currently accepted for publication as:

Lins L., da Silva, M.C., Neres, P., Esteves A.M., Vanreusel A., 2016. "Testing deep-sea biodiversity paradigms and their application to abyssal nematode genera and *Acantholaimus* species". **Deep-Sea Research II**.

4.1 Abstract

Biodiversity patterns in the deep sea have been extensively studied in the last decades. In this study, we investigated whether reputable concepts in deep-sea ecology also explain diversity and distribution patterns of nematode genera and species in the abyss. Among them, three paradigms were tackled: (1) the deep sea is a highly diverse environment at a local scale, while on a regional and even larger geographical scale, species and genus turnover is limited; (2) the biodiversity of deep-sea nematode communities changes with the nature and amount of organic matter input from the surface; and (3) patch-mosaic dynamics of the deep-sea environment drive local diversity. To test these hypotheses, diversity and density of nematode assemblages and of species of the genus *Acantholaimus* were studied along two abyssal E-W transects. These two transects were situated in the Southern Ocean (~50° S) and the North Atlantic (~10° N). Four different hierarchical scales were used to compare biodiversity: within sampled cores, within site, between sites from the same region, and between regions. Results revealed that the deep sea harbours high alpha diversity, but that turnover can be shaped by different environmental drivers. Therefore, these results the second part of the paradigm about limited species turnover in the deep sea. Higher surface primary productivity was correlated to greater nematode

densities, while diversity responses to the augmentation of surface productivity showed no trend at a local scale. Areas subjected to a constant and low food input revealed similar nematode communities to other oligotrophic abyssal areas, while sites under high productivity were characterized by different dominant genera and *Acantholaimus* species, and by a generally low local diversity. Our results corroborate the species-energy hypothesis, where productivity can set a limit to the richness of an ecosystem. Finally, we observed no correlation between sediment variability and local diversity. Although differences in sediment variability were significant across sites, these had to be considered without effect on the nematode community structure in the studied abyssal areas.

4.2 Introduction

Recent advances in deep-sea research have tested established paradigms of deep-sea diversity (McClain and Schlacher, 2015). Among them, productivity effects on benthic diversity, patch-mosaic dynamics structuring assemblages, and the high local diversity encountered in the deep sea have been discussed extensively (Gage, 1996; Grassle and Sanders, 1973; Lamshead and Boucher, 2003; Levin et al., 2001; McClain and Schlacher, 2015). The increasing interest in ecosystem functioning and ecosystem services and their relation to biodiversity has not only brought new insights on the interactions between abiotic and biotic elements of different habitats, but also on carbon sequestration and burial in the deep sea (Levin and Dayton, 2009; Thurber et al., 2014). Nevertheless, to provide information about functions and services of an ecosystem, background evidence on the ecosystem structure is essential to understand the consequences of biodiversity loss (Danovaro et al., 2008; Frid and Caswell, 2016; Thurber et al., 2014).

Reduced diversity may lead to a reduction of functions in an ecosystem (Danovaro et al., 2008; Thurber et al., 2014). However, particularly for small-sized taxa, such as those comprising the meiofauna, deep-sea species remain largely undescribed (Ramirez-Llodra et al., 2010), hampering estimates of diversity and consequently the costs of biodiversity loss. Nematodes, which frequently represent more than 90 % of the meiofauna, are considered to be rich in species in the deep sea (Danovaro et al., 2010; Mokievskii et al., 2007). Due to the time-consuming investment required for describing new species, effort in nematode taxonomic identification, especially towards macro-ecological approaches, is often limited to genus level (Ingels et al., 2011; Netto et al., 2005; Pape et al., 2013b; Sebastian et al., 2007; Somerfield and Clarke, 1995; Vanreusel et al., 2010b). For investigating ecological concepts and the effect of environmental factors on nematode biodiversity, identification down to genus level seems to be sufficient, as most deep-sea nematode genera have low environmental specificity (Leduc et al., 2012a). Nevertheless, the lack of information up to species level can restrict comparisons between studies in terms of species distribution and biodiversity estimates. In general, the wide distribution, higher diversity, and higher abundances of nematodes in the deep sea, compared to other metazoan organisms (Brandt et al., 2014; Danovaro et al., 2010; Rex et al., 2006), support them as an ideal group to tackle paradigms of deep-sea biodiversity.

This study aimed to test whether the mentioned paradigms of deep-sea biodiversity can also be applied for nematode communities. The first paradigm tested in this study (1) refers to the deep sea (> 1000 m) as a highly diverse environment at a local scale (alpha diversity), while turnover (beta diversity) is limited (Lambshead and Boucher, 2003). Presently, few species-level comparisons support this statement (Gray, 2002, 1994, Hessler and Sanders, 1968, 1967; Rex et al., 1993; Sanders et al., 1965; Sanders and Hessler, 1969), and the subject has raised new discussions in recently published papers, where diversity varies according to different spatial scales (Bik et al., 2010; Levin et al.,

2001; McClain and Schlacher, 2015; Snelgrove and Smith, 2002). For deep-sea nematodes, for example, a high local alpha diversity is inferred, while regional beta diversity would change moderately (Lamshead, 2004; Lamshead and Boucher, 2003; Mokievskii et al., 2007). In this sense, it is important to consider at which spatial scale (alpha or beta) biodiversity is measured and compared. The second paradigm, (2) relies on how surface primary productivity regulates diversity at a local scale (Gooday, 2002; McClain and Schlacher, 2015; Moens et al., 2014; Snelgrove and Smith, 2002). Seasonal variation and geographical patterns in primary productivity are known to influence the flux of organic matter to the seafloor and consequently the organic matter uptake by the benthic biota (Gooday, 2002; Moodley et al., 2002). Moreover, regions under eutrophic conditions, mostly present at high latitude or in temperate environments, have shown to exhibit a stronger seasonal benthic-pelagic coupling in comparison with oligotrophic areas (Gooday, 2002; Smith et al., 2008; Wei et al., 2010). Usually, oligotrophic regions at lower latitudes exhibit weak seasonal signals, which are reflected in the small diatom cell production and slow sinking rates (Gooday, 2002). The resulting lower benthic standing stocks observed with increasing depth, e.g. in the abyss, where undisturbed muddy-sediment conditions predominate, might be a result of the low organic matter input in these areas (Lamshead et al., 2002; Woolley et al., 2016). For nematodes, higher local alpha diversity was observed under more productive regions in the abyss (Lamshead et al., 2002; Sebastian et al., 2007), but negative or no trends were also reported (Lamshead et al., 2000). Nevertheless, these observed positive or negative relationships might only be a reflection of part of a unimodal productivity-diversity distribution with maximum diversity at intermediate productivity (Leduc et al., 2012b). Therefore, organic matter input may be a limiting factor at its low and high extremes, where niche diversification and reduced species interactions can be favoured in one end, while species dominance can be enhanced in the other end (Leduc et al., 2012b; Snelgrove and Smith, 2002). A third deep-sea

paradigm is based on the (3) patch-mosaic hypothesis and the idea that patchiness has a positive effect on the structure of benthic assemblages (Grassle and Sanders, 1973). Patchiness, or microhabitats, can include for e.g. spatially localized or temporally pulsed food input. In addition, sediment heterogeneity could also be responsible for the concentration of organic matter in localised patches, as well as macrofaunal bioturbation activities (Dauwe et al., 1998; Levin et al., 2001). For nematodes, small-scale patchiness (i.e. patchiness at the level of site replicates) is considered imperative in determining their settling conditions more than large geographical distances (Ingels and Vanreusel, 2013). Together with food input, sediment particle-size diversity is considered to increase spatial-scale heterogeneity and consequently enhance nematode diversity through the increase in partitioning of food resources (Leduc et al., 2012c). In this case, one would expect that both food input and sediment heterogeneity would contribute to higher patchiness, and consequently to a positive effect on the nematode species beta diversity.

The genus *Acantholaimus* Allgén, 1933 is generally found in high diversity in different deep-sea environments worldwide (De Mesel et al., 2006; Muthumbi and Vincx, 1997; Vanreusel et al., 2010b). *Acantholaimus* is one of the most abundant nematode genera in abyssal plains (Lins et al., 2015; Miljutina et al., 2010; Sebastian et al., 2007; Singh et al., 2014), while it is only rare at coastal or shelf habitats (Vanreusel et al., 2010b). Represented by 51 described species at present, this diverse genus indeed increases in relative abundance with increasing water depth and possesses a large morphological variation, making it a highly suitable group for biodiversity comparison under different productivity regimes and at different spatial scales (Miljutin and Miljutina, 2016b). Although specific information on the trophic ecology of *Acantholaimus* is still lacking, other studied species from the same family, though from different genera, show a diatom-feeding behaviour (Jensen, 1987, 1982; Moens and Vincx, 1997). In this regard, since eutrophic regions are characterized by a higher fresh food input (e.g. increased sinking of

diatoms) to the benthos, they would consequently favour species establishment and diversity of this genus (De Mesel et al., 2006). Nevertheless, the success of *Acantholaimus* in the most food-depleted environments, such as the abyss, contrasts with this assumption.

The aim of this study was to investigate whether the paradigms of biodiversity stated above can be applied for nematodes in this study and elsewhere. Paradigm (1), the deep sea is diverse at a local scale but turnover is limited, was tested by comparing alpha (α) diversity (i.e. diversity at the scale of a core) of nematode genera with beta (β) diversity at increasing spatial scale through additive partitioning, where the contribution of each level (α and β) was brought to the same scale. Furthermore, data on species distribution of the nematode genus *Acantholaimus* collected in this study was combined with available literature data. Because the study areas comprised two comparable abyssal transects (Southern Ocean and southern North Atlantic) under different surface productivity regimes (seasonal eutrophic and oligotrophic areas, respectively), the second paradigm (2) on benthic-pelagic coupling, surface primary production and its role in regulating nematode alpha diversity, could be tested. Differences in genus and species diversity were correlated with differences in surface productivity between sites and regions. The third paradigm, (3) patch–mosaic dynamics structuring nematode communities, was supported by linking spatial changes in benthic environmental variables at a local scale (e.g. sediment particle size diversity and organic matter input within a station) to the observed nematode genus composition and *Acantholaimus* species diversity.

4.3 Material and methods

4.3.1 Sampling and study area

The studied areas comprised four sites (four replicates per site) in the Southern Ocean (SO) and six sites (three replicates per site except for one site (B1) with two replicates) in the North Atlantic (NA) (Fig. 4.1). Replicates within the SO sites were located between 11 m and 2 km apart within one site, while at the NA replicates were situated between 0 m and 3 km within sites. Sediment samples were collected on board of the RV Polarstern (ANT-XXVIII/3, 07.01.2012–11.03.2012) and RV Sonne (SO 237, 14.12.2014–26.01.2015), respectively. The SO transect was located at the Polar Front along an E-W gradient (between 10 °E and 39 °W), and covered depths from 3760.5 m to 4155.2 m (Table 4.1). The NA transect sampling sites were situated at the Vema fracture zone along an E-W gradient (between 25 °W and 50 °W), comprising depths from 4998.3 m to 5771.7 m (Table 4.1). The SO sites were less evenly spread compared to the NA sites. However, both covered more than 2700 km from one end to the other, while the distance between sites varied between 90 km and 1800 km. Both samplings were performed using a Multicorer (MUC) equipped with 12 plexiglass tubes yielding samples with a virtually undisturbed sediment-surface (cross-sectional area of 25.5 cm² for ANT-XXVIII/3 and of 69.4 cm² for SO 237).

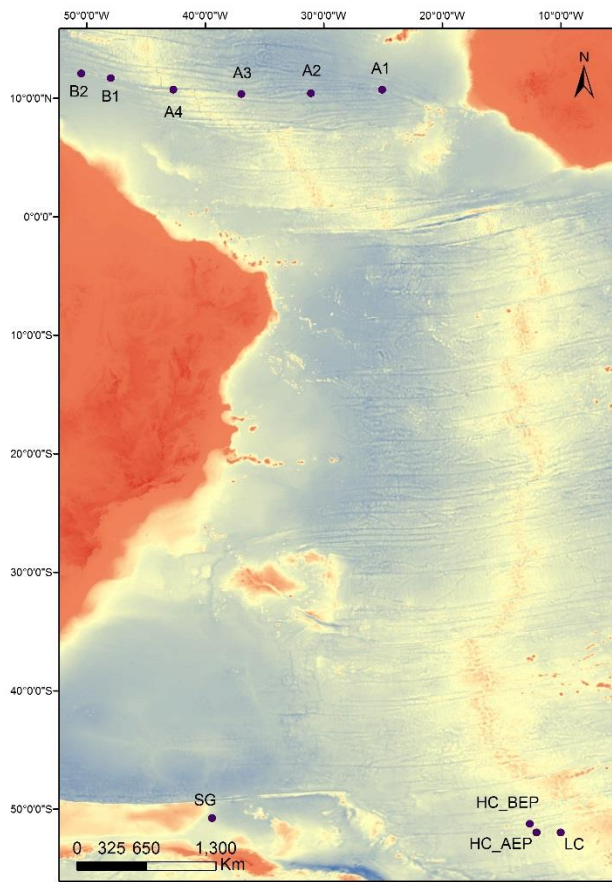


Figure 4.1. ANT-XXVIII/3 and SO 237 locations. Exact coordinates are given in Table 4.1. Bathymetry data was provided by GEBCO. Sampling sites are represented by symbols: SG (South Georgia), HC_BEP (High Chlorophyll_Before Eddy Pump), HC_AEP (High Chlorophyll_After Eddy Pump), LC (Low Chlorophyll); A1, A2, and A3 (East Mid-Atlantic Ridge), A4 (at the Mid-Atlantic Ridge), and B1, B2 (West of the Mid-Atlantic Ridge).

Along the transect in the SO (Wolf-Gladrow, 2012) there was a decrease in surface Chlorophyll *a* (Chla), with the most westward site South Georgia (SG), located northwest of South Georgia island, exhibiting higher surface Chla values (Lins et al., 2015).

South Georgia island and its surroundings are considered a highly productive region during austral summer, supporting high phytoplankton biomass (Atkinson et al., 2001). The second and third sites, HC_BEP (High Chlorophyll_Before Eddy Pump) and HC_AEP (High Chlorophyll_After Eddy Pump), are located at the same area (sites are situated ~90 km apart) which was resampled after 13 days of a phytoplankton bloom. Although a higher concentration of Chla was expected after the bloom, these differences could not be observed in the surface Chla maps.

Table 4.1. Sampling details for the ANT-XVIII/3 and SO 237 campaigns. PF (Polar Front), E MAR (East Mid-Atlantic Ridge), MAR (Mid-Atlantic Ridge), W MAR (West Mid-Atlantic Ridge). Replicate numbers represent the number of cores used for nematode community analyses and * represent the cores used for environmental analyses.

Sites	Deployment (Replicates)	Date (d/m/y)	Depth (m)	Latitude	Longitude	Remarks
SG	175-6*	4/03/2012	4155.2	50°46.59'S	39°25.33'W	South Georgia
SG	175-7*	4/03/2012	4154.2	50°46.60'S	39°25.38'W	South Georgia
SG	175-8	4/03/2012	4154	50°46.60'S	39°25.39'W	South Georgia
SG	175-9	4/03/2012	4152.1	50°46.57'S	39°25.33'W	South Georgia
HC_AEP	141-6*	18/02/2012	4113	51°15.98'S	12°37.04'W	PF(After Eddy Pump)
HC_AEP	141-9*	18/02/2012	4114	51°16.03'S	12°37.06'W	PF(After Eddy Pump)
HC_AEP	141-10	19/02/2012	4113	51°15.97'S	12°36.94'W	PF(After Eddy Pump)
HC_AEP	141-11	19/02/2012	4113.2	51°16.02'S	12°37.12'W	PF(After Eddy Pump)
HC_BEP	086-26*	1/02/2012	3966.2	51°58.87'S	12°3.76'W	PF(Before Eddy Pump)
HC_BEP	086-28*	1/02/2012	3968	51°58.74'S	12°2.11'W	PF(Before Eddy Pump)
HC_BEP	086-29	1/02/2012	3970.8	51°58.78'S	12°1.95'W	PF(Before Eddy Pump)
HC_BEP	086-30	2/02/2012	3965.4	51°58.91'S	12°2.16'W	PF(Before Eddy Pump)
LC	081-8*	19/01/2012	3760.5	51°59.99'S	9°59.99'E	PF(Low Chlorophyll)
LC	081-9*	19/01/2012	3760.7	52°0.01'S	10°0.05'E	PF(Low Chlorophyll)
LC	081-12*	19/01/2012	3757.5	51°59.93'S	10°0.06'E	PF(Low Chlorophyll)
LC	081-13	19/01/2012	3760.5	52°0.042'S	9°59.90'E	PF(Low Chlorophyll)
A1	3-3*	19/12/2014	5498	10°43.112'N	25°3.886' W	E MAR
A1	3-4*	19/12/2014	5507	10°43.108'N	25°3.888' W	E MAR
A1	3-5*	19/12/2014	5508	10°43.17'N	25°3.88' W	E MAR
A2	4-3*	25/12/2014	5771.7	10°25.11'N	31°4.61' W	E MAR
A2	4-4*	26/12/2014	5759.7	10°25.12'N	31°4.62' W	E MAR
A2	4-5*	26/12/2014	5767.7	10°25.12'N	31°4.62' W	E MAR
A3	6-2*	1/01/2015	5137	10°21.03'N	36°57.59'W	E MAR
A3	6-3*	2/01/2015	5137.4	10°21.03'N	36°57.61'W	E MAR
A3	6-4*	2/01/2015	5136.1	10°21.03'N	36°57.61'W	E MAR
A4	8-1*	6/01/2015	5182.2	10°43.562'N	42°41.593'W	MAR
A4	8-10*	8/01/2015	5117	10°42.58'N	42°40.99'W	MAR
A4	8-11*	8/01/2015	5121.9	10°42.59'N	42°40.99'W	MAR
B1	9-3*	11/01/2015	4999	11°41.37'N	47°57.36'W	W MAR
B1	9-4*	12/01/2015	4998.3	11°41.36'N	47°57.34'W	W MAR
B2	11-5*	14/01/2015	5090.7	12°5.40'N	50°26.98'W	W MAR
B2	11-6*	15/01/2015	5091.5	12°5.42'N	50°26.98'W	W MAR
B2	11-7*	15/01/2015	5091.4	12°5.40'N	50°26.97'W	W MAR

The site's names (before and after eddy pump) are derived from eddies (anomalies) observed after the first site (HC_BEP) was sampled. Additionally, the two last sites (HC_BEP and HC_AEP) are also characterized by a high surface annual productivity. The

easternmost site (LC; Low Chlorophyll), exhibited low surface Chla values throughout the whole year. The sampled sites were located in the Subantarctic Water Ring Province (SANT), and more specifically at the Polar Front Zone, where algal growth is enhanced and chlorophyll accumulates mainly during early austral fall (Longhurst, 1998).

The NA sampling comprised sites along the Vema fracture zone. The first three sites (A1, A2, and A3) were situated east of the Mid-Atlantic Ridge (MAR), one site was sampled at the central valley of the MAR (A4), and two other sites west of the MAR (B1 and B2). The sampled sites are located in the North Atlantic Tropical Gyral Province (NATR). This region lies below the North Atlantic trades and is separated from the westerlies by the Azores High (Longhurst, 1998). Moreover, the NATR exhibits low and uniform surface chlorophyll values, with weak winter convective mixing and no evidence of a spring bloom (Jochem and Zeitzschel, 1993).

4.3.2 Environmental variables

Samples for granulometric and geochemical analyses (1 g of sediment) were obtained from MUC deployments from the first sediment layer (0–1 cm) and were frozen at -80 °C. Replicates used for environmental analyses can be found in Table 4.1. Grain-size distribution was measured with a Malvern Mastersizer 2000 (0.02–2000 µm size range) and divided into five categories, from silt-clay to coarse sand fractions (Buchanan, 1984). Sediment particle-size diversity (SED) was calculated from the percent dry weight of the five size classes mentioned above using the Shannon-Wiener diversity index (Etter and Grassle, 1992; Leduc et al., 2012c). Total sedimentary organic carbon (% TOC) and nitrogen (% TN) were determined with a Carlo Erba elemental analyser on the freeze-dried and homogenized samples after acidification with 1 % HCl until carbonates are

removed (2–3 days). Total organic matter (% TOM) content was determined after combustion of the sediment samples at 550 °C.

Chla, chlorophyll degradation products, and carotenes in the sediment were measured with a Gibson fluorescence detector (Wright and Jeffrey, 1997) after lyophilisation, homogenization, and extraction in 90 % acetone. Separation of the samples occurred via reverse-phase HPLC (High-Performance Liquid Chromatography). Chloroplastic pigment equivalents (CPE: Chla + phaeopigments) were used as a proxy for surface-derived primary productivity at the seafloor.

Net primary productivity (NPP) values were extracted from the Vertically Generalized Production Model (VGPM; resolution 1°) described by Behrenfeld and Falkowski (1997) and explained in detail by Lins et al. (2014). The extracted NPP values corresponded to the average between the sampled month and the month before. This timeframe was chosen as a proxy for the time organic matter generally settles to the seafloor at approximately 4000 m depth. Monthly NPP were calculated in order to investigate seasonality of primary productivity within a year between the different sampled regions.

4.3.3 Nematode sampling processing

At each site two to four replicates (cores) from 0-1 cm sediment layer were used for nematode analyses (Table 4.1). They were fixed in sea-water buffered formalin 4 %, then washed using stacked sieves of 1000 µm and 32 µm, followed by three times centrifugation with Ludox HS40 Dupont (specific gravity 1.18). By using the 1000 µm sieve, the meiofauna could be separated from the macrofauna organisms. Subsequently, nematodes were counted under a stereomicroscope (50 x magnification) and 100 nematodes (five

replicates for the SO transect lacked enough individuals) were picked out. The individuals were transferred to glycerine (De Grisse, 1969), mounted on glass slides, and identified up to genus level and up to species level for the genus *Acantholaimus* (Guilini et al., 2016; Miljutin and Miljutina, 2016a). In addition, distribution maps of the *Acantholaimus* species found in this study and in previously published literature were created. Together with the geographical range, bathymetrical ranges, based on the new and previously published records, as well as line drawings of described and undescribed species of *Acantholaimus* from this study were also provided.

4.3.4 Data analyses

In order to investigate the first paradigm of biodiversity in our study (the deep sea is diverse at a local scale but turnover is limited), genus and species densities and diversity were estimated. Diversity was estimated based on Shannon-Wiener diversity (H'), and genus and species richness (S). Multispatial scale variability was measured at four different levels. Using the additive partitioning approach, total nematode diversity (gamma diversity) was calculated as the sum of alpha diversity within each core (α), beta diversity within a site (β_1), and beta diversity between sites from the same transect (β_2) using the software PARTITION 3.0 (Crist et al., 2003). Comparisons within each hierarchical level together with differences between transects (SO and NA) were also performed. For within-level comparison, alpha diversity was calculated based on S and H' , and beta diversity was obtained based on the dissimilarities within and between sites using SIMPER ((dis)similarity percentages) routines in PRIMER v6 software (Clarke and Gorley, 2006). Finally, SIMPER was also used to assess the average percent contribution of each genus/species to the total dissimilarity between sites (Anderson et al., 2008).

The nematode genus structure and *Acantholaimus* species multivariate matrix analyses were based on Bray-Curtis similarities (and Euclidean distances for the univariate data: density, S, and H'). Genus rarefaction curves were calculated based on the Chao1 estimator, which takes into account abundance values. Species matrices were used to investigate differences between regions and sites within the same regions. Non-parametric multivariate ANOVA (PERMANOVA) was used and analyses were performed using a 2-factor nested design: it included 'Region' (NA and SO) as a fixed factor and 'site' as a fixed factor nested in 'Region' (Anderson et al., 2008). Pair-wise comparisons were performed using pseudo-*t* tests obtained from the PERMANOVA permutations, and calculated as the square root of Pseudo-F. Furthermore, PERMDISP routines were used to test the homogeneity of multivariate dispersions between sites.

The data analyses for the second and third paradigm testing were interlinked through correlation and DistLM (distance-based linear model) analyses. Univariate correlations between nematode variables (density per 10 cm², S, and H') and trends in environmental variables (% TOC, % TN, % TOM, CPE, depth, NPP, and SED) were investigated using Spearman rank correlations and Draftsman plots (Anderson et al., 2008; R Core team, 2013).

The relationship between community/species diversity/density and environmental data were performed through DistLM routines in PRIMER (Anderson et al., 2008) and used variables with correlations lower than 0.9. The environmental data was first normalized (subtracted mean divided by standard deviation) and resemblance matrices were obtained using Euclidean distances. Then, PERMANOVA tests were conducted using the same design used for species analyses (see above). Highly correlated variables were first transformed to cosine to reduce the linearity of the correlation, and if correlations persisted they were excluded from the DistLM analyses. The DistLM procedure was built

using a step-wise selection and adjusted R^2 as selection criterion. Significant results for all analyses were considered when $p < 0.05$.

4.4 Results

4.4.1 The deep sea is diverse at a local scale, but turnover is limited

Total nematode densities were significantly higher at the SO transect in comparison with those along the NA transect (PERMANOVA $p < 0.05$). The highest values were observed at SG (235.4 ± 70 ind/ 10 cm²) and HC_AEP (172.8 ± 38 ind/10 cm²), which differed significantly from the other SO sites (Fig. 4.2a; Table S1). Along the NA transect, lowest densities were observed at A3 (23.3 ± 2 ind/10 cm²), although pairwise differences between NA sites were not statistically significant (Table S1).

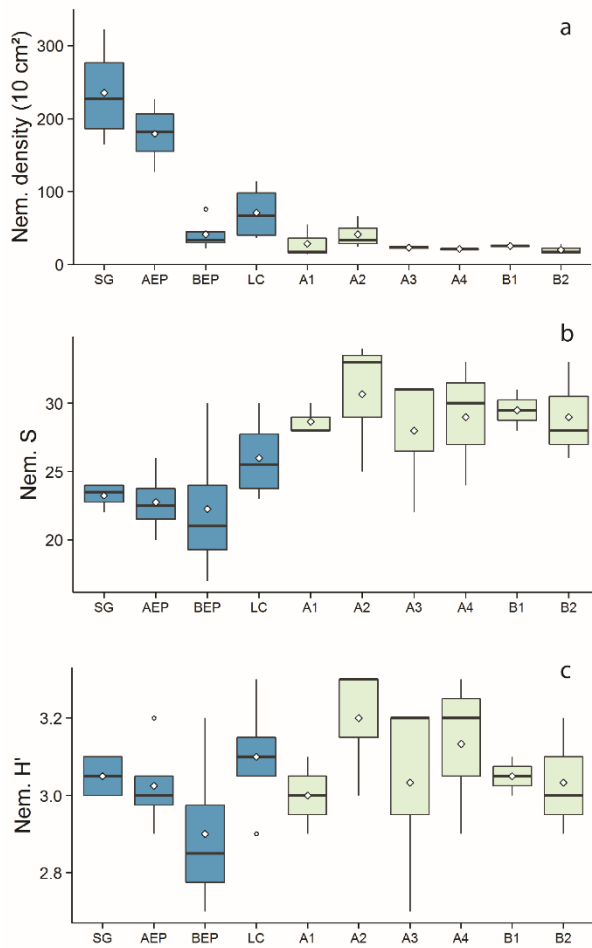


Figure 4.2. Nematode boxplots data for univariate data (a) total density (ind/10 cm²), (b) genus richness (S), and (c) Shannon-Wiener (H') diversity. Blue boxplots represent Southern Ocean sites and green boxplots represent North Atlantic sites. Thick black lines represent the median, empty circles represent the mean, lower box indicates the first quartile and upper box the third quartile. Upper line shows the maximum value and lower line the minimum value.

The total density of *Acantholaimus* was significantly higher at the SO sites when compared to the NA sites. SG possessed the highest densities (34.9 ± 19.6 ind/ 10 cm²), followed by HC_AEP (17.3 ± 7.7 ind/10 cm²), although pairwise comparison for this transect was only significant

between the pair [SG, HC_BEP] (Table S1). The NA transect did not show any significant pairwise difference. In addition, relative abundances of this genus revealed no significant differences, neither between regions nor between sites (Fig.4.3a).

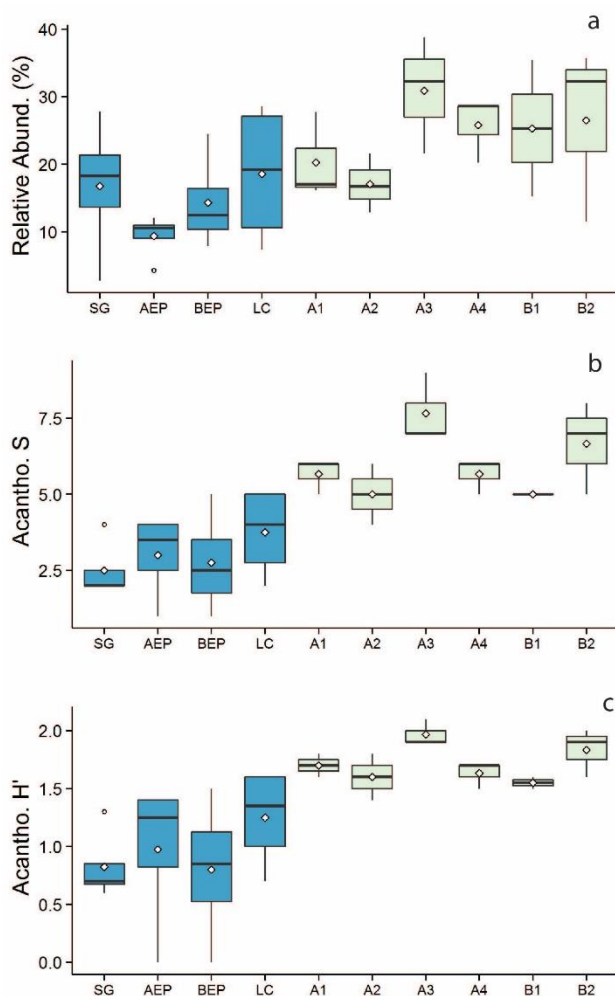


Figure 4.3. Univariate boxplots data for *Acantholaimus* (a) relative abundance (%), (b) species richness (S), and (c) Shannon-Wiener diversity (H'). Blue boxplots represent Southern Ocean sites and green boxplots represent North Atlantic sites. Thick black lines represent the median, empty circles represent the mean, lower box indicates the first quartile and upper box the third quartile. Upper line shows the maximum value and lower line the minimum value.

A total of 150 nematode genera were found for the two regions. At the SO, 62 genera occurred only at this region, while 47 genera were restricted to the NA transect. The genera restricted to only one transect were mostly rare genera ($< 2\%$) or singletons. Rare taxa ranged from 41 to 53 % in the SO

transect, while at the NA transect they composed from 26 to 33 % of the total nematode assemblage. Average genus richness per site was significantly higher at the NA transect when compared to the SO (Fig. 4.2b). Pair-wise comparisons revealed no significant differences between sites from the same transect (Table S1). The abundant genera per site, with percentages $\geq 2\%$, are represented in Table 4.2. Shannon-Wiener diversity (H') showed no significant differences between and within both transects (Fig. 4.2c; Table S1).

For both studied regions together, 23 species of *Acantholaimus* were identified. Five species were represented by only one individual and/or only by females and were excluded from the analyses due to taxonomic uncertainty. From the remaining 18 species, eight species occurred only in the NA and one species was restricted to the SO, leaving nine species shared between regions (Fig. 4.4). Species richness was significantly higher at the

NA transect when compared to the SO (Fig.4.3b). Within the NA transect, significant differences were only observed for the NA pair [A2, A3] (Table S1). Also species H' values were significantly higher at the NA sites and exhibited significantly higher values at A3 (1.97 ± 0.1) compared to the other sites of the same transect (Fig.4.3c). Pairwise comparisons revealed no significant differences within the sites from the SO transect (Table S1).

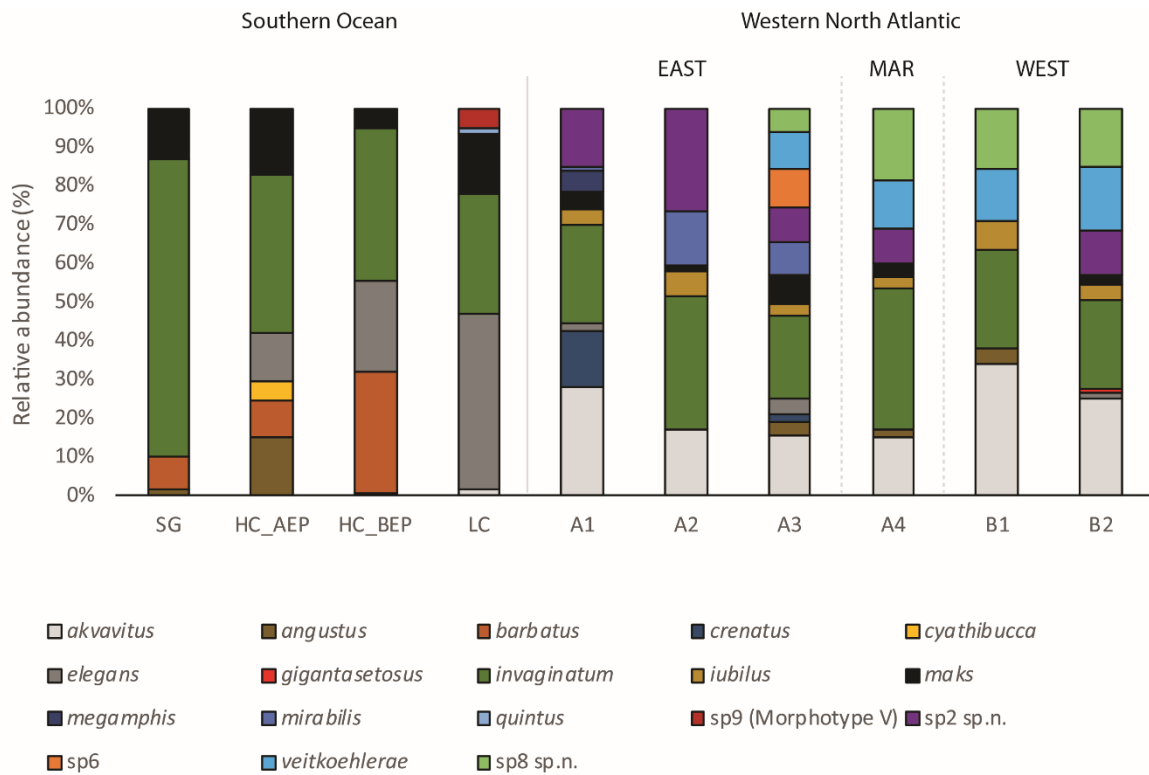


Figure 4.4. Relative abundances of *Acantholaimus* species per site for each transect. MAR= Mid-Atlantic Ridge.

The results for the nematode multivariate community analyses based on nematode genera relative abundances showed significant differences between regions and sites (Table S1). Pairwise comparisons for both transects revealed that for the SO, all sites were significantly different from each other, except for the pairs [HC_AEP, LC] and [HC_BEP,

LC]. Sites located at the NA did not exhibit any significant difference between pairs of sites. SIMPER routines revealed a dissimilarity of 59.8 % between regions. The genera *Microloaimus*, *Desmodora*, and *Tricoma*, found in higher abundances at the SO, and the genera *Acantholaimus* and *Thalassomonhystera*, showing higher abundances in the NA, contributed the most to the dissimilarity between regions (combined 35 %). Fig. 4.5a illustrates that dissimilarity increases with increasing geographical distance. When comparisons were performed within each transect, dissimilarities varied from 49-62 % for the SO transect, and from 38-53 % for the NA transect, revealing that NA sites differ less than SO sites (Fig. 4.5a). The genus rarefaction curve for each site from both transects only reached an asymptote for the sites SG, HC_AEP, and HC_BEP located at the SO transect. (Fig. S1).

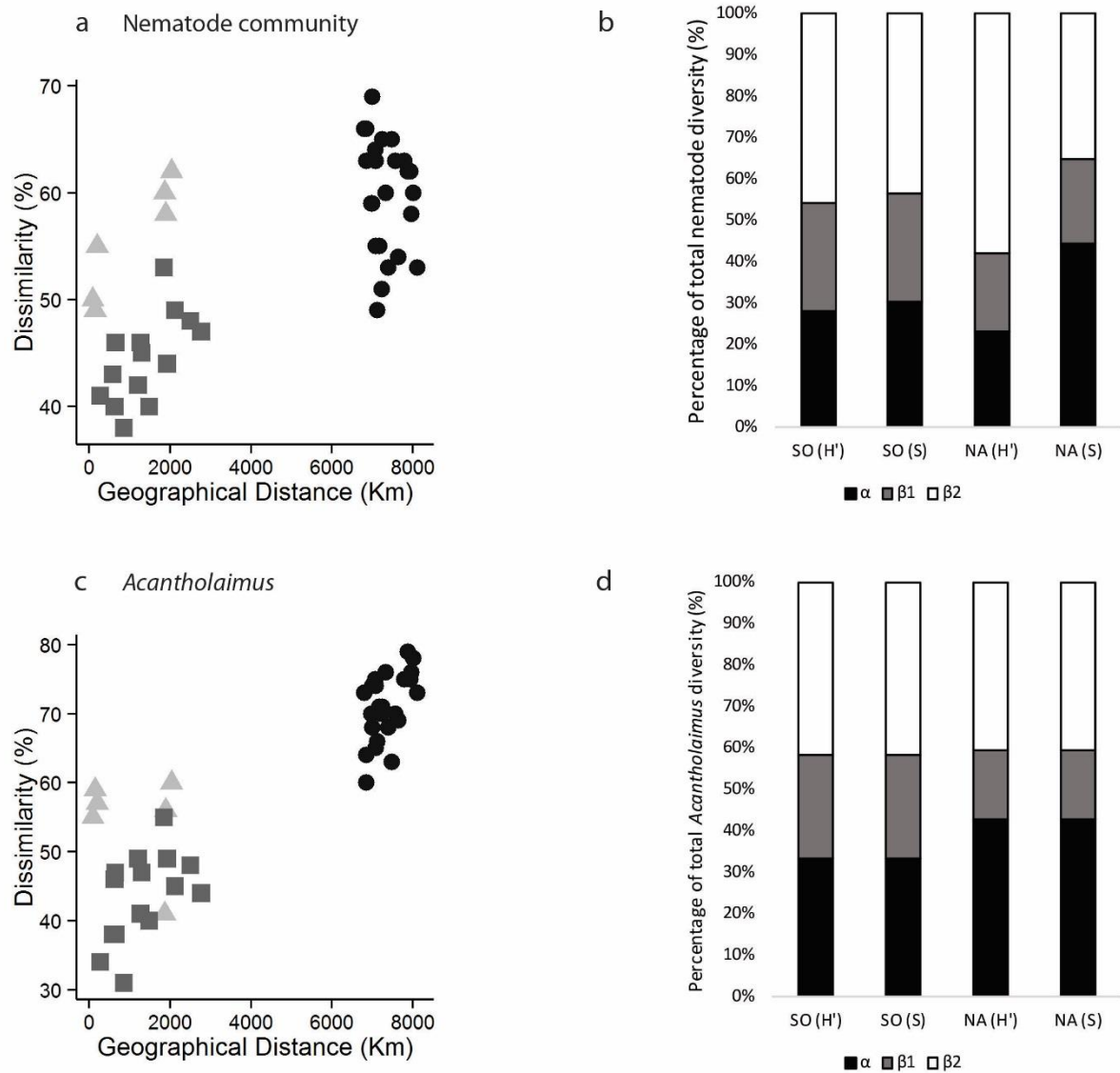


Figure 4.5. Dissimilarities between sites from different regions for nematode genus composition (a) and *Acantholaimus* species (c) in relation to geographical distance (Km). Black circles represent dissimilarities between regions, grey triangles stand for dissimilarities between SO sites, and dark grey squares exhibit dissimilarities between NA sites. Stacked columns (b and d) represent the additive partitioning per transect (Southern Ocean (SO) and North Atlantic (NA)) of species richness (S) and the Shannon index of diversity across three sampling scales: α = within each core, β_1 = within sites, and β_2 = between sites from the same transect.

Additive partitioning results for nematode assemblages showed the highest contribution of beta diversity between sites from the same transect (β_2) to the total diversity based on H' for SO and NA. (Fig. 4.5b). For genus richness, a different pattern was observed, where β_2 explained most of the community variability for SO, while α showed greatest

contribution to the total diversity for NA (Fig. 4.5b). The within-site diversity (H') was higher at the SO transect for both genus richness (26 %) and H' (26 %), when compared to the NA (19 and 20 %, respectively) sites.

Table 4.2. Most abundant nematode genera (> 2 %) per site (average \pm st.dev.).

SG	%	HC_AEP	%	HC_BEP	%
<i>Tricoma</i>	11.9 \pm 3.9	<i>Microlaimus</i>	17.4 \pm 6.3	<i>Thalassomonhystera</i>	12.4 \pm 3.2
<i>Desmodora</i>	11.2 \pm 9.1	<i>Thalassomonhystera</i>	11.5 \pm 1.2	<i>Daptonema</i>	7.3 \pm 2.5
<i>Acantholaimus</i>	8.4 \pm 5.2	<i>Southerniella</i>	5.1 \pm 4.6	<i>Acantholaimus</i>	7.2 \pm 3.5
<i>Microlaimus</i>	6.8 \pm 1.4	<i>Acantholaimus</i>	4.7 \pm 1.7	<i>Diplopeltula</i>	4.8 \pm 2.7
<i>Thalassomonhystera</i>	3.0 \pm 2.2	<i>Tricoma</i>	3.3 \pm 3.4	<i>Microlaimus</i>	4.6 \pm 2.2
<i>Actinonema</i>	2.8 \pm 1.7	<i>Diplopeltula</i>	2.8 \pm 2.4	<i>Theristus</i>	3.7 \pm 2.0
<i>Halalaimus</i>	2.0 \pm 1.8	<i>Molgolaimus</i>	2.3 \pm 1.1	<i>Tricoma</i>	2.8 \pm 3.3
		XYALIDAE sp2	2.1 \pm 3.0	<i>Desmodora</i>	2.8 \pm 2.0
				<i>Enchonema</i>	2.5 \pm 1.3
				<i>(Pareu)Desmoscolex</i>	2.5 \pm 2.3
				<i>Leptolaimus</i>	2.0 \pm 1.2

LC	%	A1	%	A2	%
<i>Thalassomonhystera</i>	14.0 \pm 5.2	<i>Thalassomonhystera</i>	25.5 \pm 0.6	<i>Acantholaimus</i>	18.3 \pm 4.4
<i>Acantholaimus</i>	9.3 \pm 5.3	<i>Acantholaimus</i>	19.0 \pm 6.4	<i>Thalassomonhystera</i>	14.0 \pm 0.56
<i>Halalaimus</i>	3.9 \pm 1.4	<i>Desmodora</i>	6.1 \pm 0.6	<i>Ceramonema</i>	6.0 \pm 3.7
<i>Molgolaimus</i>	3.5 \pm 3.2	<i>Halalaimus</i>	4.8 \pm 0	<i>Halalaimus</i>	5.8 \pm 0
<i>Microlaimus</i>	3.1 \pm 3.0	<i>Prochaetosoma</i>	3.8 \pm 0.9	<i>Daptonema</i>	5.1 \pm 0.1
<i>Desmoscolex</i>	2.7 \pm 2.4	<i>Tricoma</i>	3.5 \pm 0	<i>Theristus</i>	3.4 \pm 0.6
<i>Tricoma</i>	2.2 \pm 0.7	<i>Daptonema</i>	3.4 \pm 0.6	<i>Paramonhystera</i>	3.2 \pm 1.8
<i>Daptonema</i>	2.1 \pm 0.4	<i>Manganonema</i>	3.3 \pm 0.6	<i>Actinonema</i>	3.1 \pm 2.6
		<i>Ceramonema</i>	2.5 \pm 1.8	<i>Metasphaerolaimus</i>	3.0 \pm 1.2
		<i>Southerniella</i>	2.5 \pm 0	<i>Pselionema</i>	2.8 \pm 0
		<i>Desmoscolex</i>	2.3 \pm 1.0	<i>Amphimonhystrella</i>	2.1 \pm 1.2
				<i>Tricoma</i>	2.1 \pm 0.6

A3	%	A4	%	B1	%
<i>Acantholaimus</i>	30.4 \pm 8.6	<i>Acantholaimus</i>	25.9 \pm 4.8	<i>Acantholaimus</i>	25.4 \pm 14.3
<i>Thalassomonhystera</i>	16.8 \pm 0.6	<i>Thalassomonhystera</i>	12.4 \pm 0	<i>Thalassomonhystera</i>	14.3 \pm 0.7
<i>Syringolaimus</i>	3.8 \pm 1.6	<i>Halalaimus</i>	5.8 \pm 0	<i>Diplopeltoides</i>	11.1 \pm 0
<i>Tricoma</i>	3.5 \pm 0	<i>Pararaeolaimus</i>	4.7 \pm 1.2	<i>Syringolaimus</i>	7.2 \pm 2.2
<i>Daptonema</i>	3.5 \pm 0.6	<i>Desmoscolex</i>	3.7 \pm 1.2	<i>Manganonema</i>	3.6 \pm 0
<i>Desmoscolex</i>	3.4 \pm 1.0	<i>Manganonema</i>	3.4 \pm 0.6	<i>Halalaimus</i>	3.5 \pm 0.7
<i>Halalaimus</i>	3.4 \pm 0	<i>Tricoma</i>	3.2 \pm 0	<i>Cervonema</i>	3.0 \pm 1.4
<i>Cervonema</i>	3.1 \pm 0	<i>Chromadora</i>	2.4 \pm 0	<i>Pararaeolaimus</i>	2.6 \pm 1.4

<i>Manganonema</i>	3.0 ± 0.6	<i>Paramonohystera</i>	2.3 ± 1.0	<i>Tricoma</i>	2.6 ± 0
		<i>Prototricoma</i>	2.3 ± 0	<i>Chromadora</i>	2.0 ± 0
		<i>Ceramonema</i>	2.0 ± 0		

B2	%
<i>Acantholaimus</i>	28.5 ± 13.0
<i>Thalassomonhystera</i>	12.4 ± 0
<i>Halalaimus</i>	5.3 ± 0
<i>Cervonema</i>	4.5 ± 0.6
<i>Pararaeolaimus</i>	3.5 ± 1.6
<i>Syringolaimus</i>	3.3 ± 2.6
<i>Manganonema</i>	3.2 ± 0.6
<i>Diplopeltula</i>	3.1 ± 0
<i>Desmoscolex</i>	2.7 ± 0.6
<i>Daptonema</i>	2.3 ± 0.6
<i>Tricoma</i>	2.3 ± 0

PERMANOVA multivariate analysis on the *Acantholaimus* species structure matrix revealed significant differences between both regions and sites (Table S1). Pairwise comparisons for both transects showed significant differences between the SO pairs [SG, LC], and the NA pairs [A2, B1] and [A2, B2]. The most abundant species for both regions was *Acantholaimus invaginatum* (33 ± 11 ind/10 cm²), followed by *A. maks* (9.5 ± 7 ind/10 cm²). SIMPER exhibited 70.8 % dissimilarity between regions, with differences mainly attributed to higher relative abundances of *A. invaginatum* and *A. elegans* in the SO, and *A. akvavitus* in the NA. Dissimilarities in species structure of the genus *Acantholaimus* increased with increasing geographical distances (Fig. 4.5c). Higher dissimilarities (β_2) were observed between sites within the SO transect (41–60 %) than within the NA transect (31–55 %) (Fig. 4.5c). Additive partitioning results revealed highest contribution of beta diversity between sites (β_2) to the total diversity for both genus richness and H' diversity within the SO transect (Fig. 4.5d). For the NA transect, α diversity showed highest contribution to the total diversity for both H' and S (Fig. 4.5d). Within-site beta diversity

(61) accounted for 25 % of the total diversity at SO, while at NA a lower contribution of 16 % was observed.

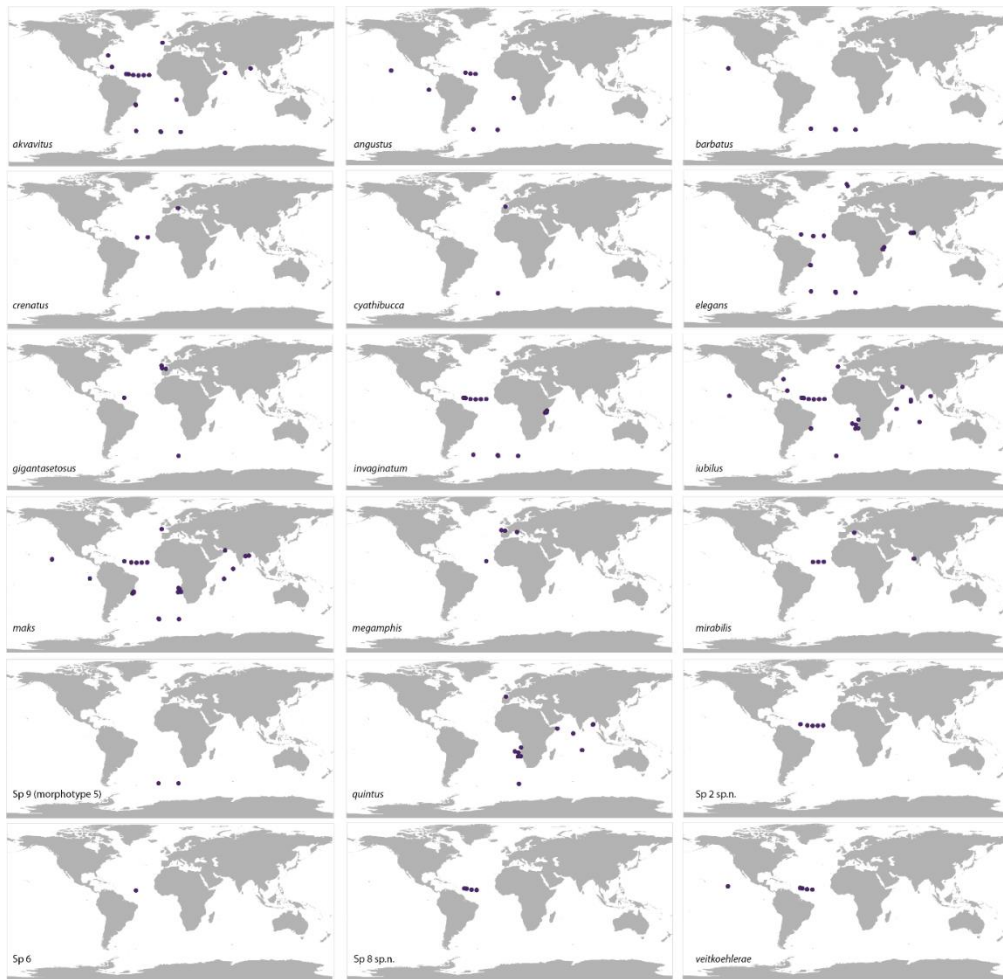


Figure 4.6. Species occurrences for *Acantholaimus* species found in this study combined with records from the literature (Table S2).

The global distribution of species found in this study is shown in Fig. 4.6. *A. iubilis* was the most widespread species, having been encountered in ten different ocean basins. It was followed by *A. maks*, found in eight different ocean basins, and *A. akvavitus*, distributed in six ocean basins. The depth distribution for each species can be found in Fig. 4.7. The most eurybathic species found was *A. maks* (400–6313 m), followed by *A. mirabilis* (34 – 5767 m), *A. megamphis* (160–5508 m), and *A. invaginatium* (511–5771 m).

Sp6 was the only species restricted to a single depth range. Nine species were only encountered in abyssal plains (Fig. 4.7).

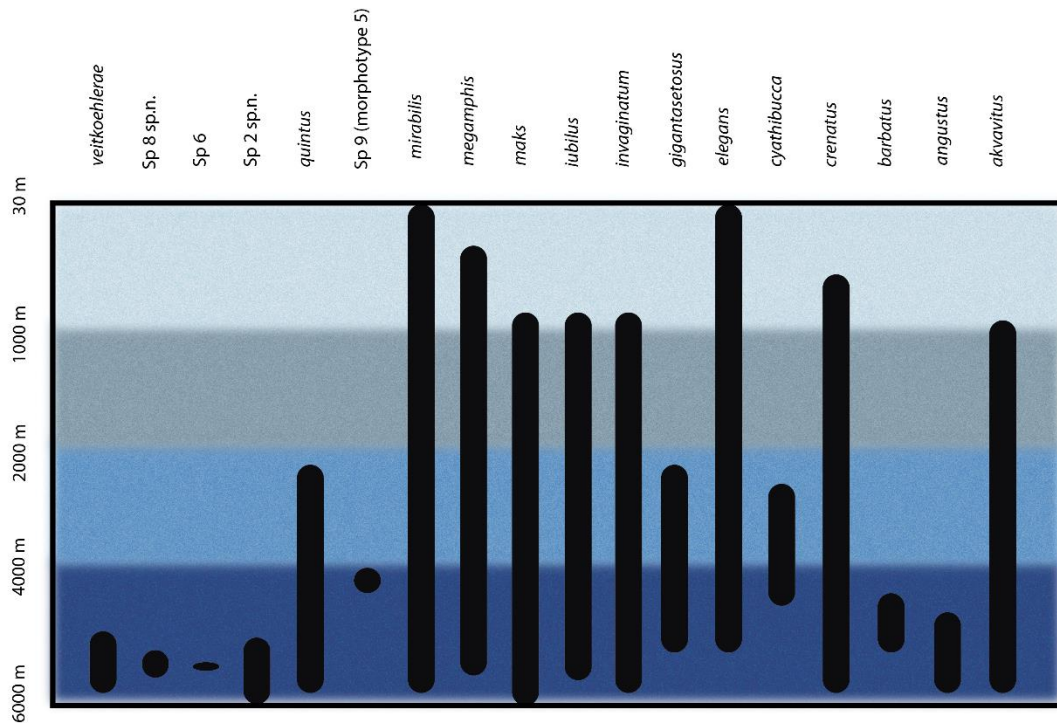


Figure 4.7. Depth distribution of the *Acantholaimus* species found in this study combined with previous records from the literature (Table S2). Sp 9 in this study is referred as morphotype 5 by Lins et al. (2015).

4.4.2 Benthic-pelagic coupling and patch-mosaic dynamics

4.4.2.1 Environmental variables

Mean values for abiotic variables are shown in Fig. 4.8. Sediment diversity (SED) revealed significant differences between regions (Table 4.3). SED significantly decreased eastwards for the SO sites due to the increase in silt-clay content, while for the NA sites a significant westward increase (except for site A1) was observed (Fig. 4.8a). Highest SED were observed at sites B1 and B2 (1.0 and 0.68, respectively). The main differences between sites were derived from the greater content of very fine sand, fine sand, and medium sand

at the sites with higher SED. Pairwise comparisons between sites for each region can be found in Table 4.3. In addition, total organic matter content (% TOM) showed significant differences between regions, and between sites within the same transects (Fig. 4.8b). Significant pairwise comparisons for SO and NA can be found in Table 4.3. Total organic carbon content (% TOC) was significantly higher at SO (from 0.77 to 1.14 %) (Fig. 4.8c), while pairwise comparisons within transects revealed significant differences only between NA sites (Table 4.3). Total nitrogen (% TN) (Fig. 4.8d) average values did not differ significantly, neither between regions nor between sites.

Table 4.3. PERMANOVA results for the environmental variables used in this study. SED (sediment grain size diversity), TOM (Total Organic Matter), TOC (Total Organic Carbon), TN (Total Nitrogen), CPE (Chloroplastic Pigment Equivalents), NPP (average Net Primary Productivity). Main *p* perm represents *p*-values for the 2-factor nested design test. Significantly different *p*-values are displayed in bold. Pairwise *t*-test results are only shown if values were significant. When all differences between sites pairs were not significant, pairwise *t*-tests were displayed as ND.

Abiotic variable	Main test <i>p</i> perm	pairwise <i>t</i> -tests for SO		pairwise <i>t</i> -tests for NA	
SED	Region = 0.0005 Site = 0.0001	SG, HC_AEP	0.032	A1, A2	0.0009
		SG, HC_BEP	0.0059	A1, A3	0.0092
		SG, LC	0.0001	A1, B2	0.0006
				A2, B1	0.0016
				A2, B2	0.0001
				A3, B1	0.0145
% TOM	Region = 0.0357 Site = 0.0001	SG, LC	0.0196	A2, A3	0.0278
				A2, A4	0.0226
				A2, B2	0.0043
% TOC	Region = 0.027 Site = 0.2067	ND		A1, B2	0.0117
				A2, B2	0.0089
% TN	Region = 0.7135 Site = 0.5817	ND		ND	
CPE	Region = 0.016 Site = 0.0263	ND		ND	
NPP	Region = 0.0001 Site = 0.0001	SG, HC_BEP	0.0002	ND	
		HC_AEP, HC_BEP	0.0094		
		HC_BEP, LC	0.0001		

Chloroplasic pigment equivalents (CPE) were significantly higher at the SO transect (Fig. 4.8e). Higher mean values were observed at the SG site ($22.5 \pm 16.5 \mu\text{g/g}$), although those were highly variable between replicates and not significantly different from other sites.

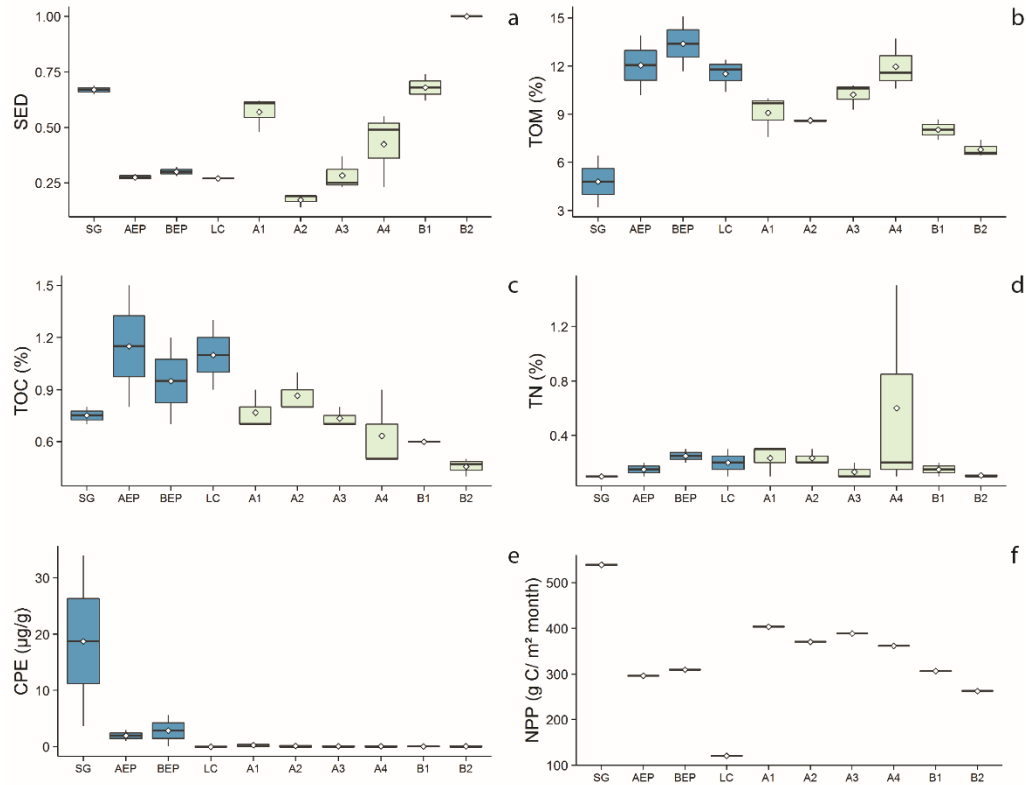


Figure 4.8. Environmental variables used in this study per site: (a) SED (sediment grain size diversity), (b) TOM (Total Organic Matter), (c) TOC (Total Organic Carbon), (d) TN (Total Nitrogen), (e) CPE (Chloroplasic Pigment Equivalents), (f) NPP (average Net Primary Productivity). Blue boxplots represent Southern Ocean sites and green boxplots represent North Atlantic sites. Black lines represent the median, empty circles represent the mean, lower box indicates the first quartile and upper box the third quartile. Upper line shows the maximum value and lower line the minimum value.

Low CPE content was observed for all other sites and, although significant differences were found between regions and sites ($p < 0.05$) in the PERMANOVA analyses, no significant differences were observed between pairs of sites within transects (Table 4.3). Net primary productivity values (NPP) revealed significant differences between regions and between sites located at the SO transect (Table 4.3). NPP were significantly higher at SG site ($539 \pm 0 \text{ g C/ m}^2 \text{ month}$) and decreased eastwards for the SO sites (Fig. 4.8f). For the NA sites, NPP slightly decreased westwards, but pairwise comparisons were not

significant. Yearly NPP trends showed a higher variation between months at the SO region than at the NA transect (Fig. 4.9), revealing a higher seasonality at the first transect.

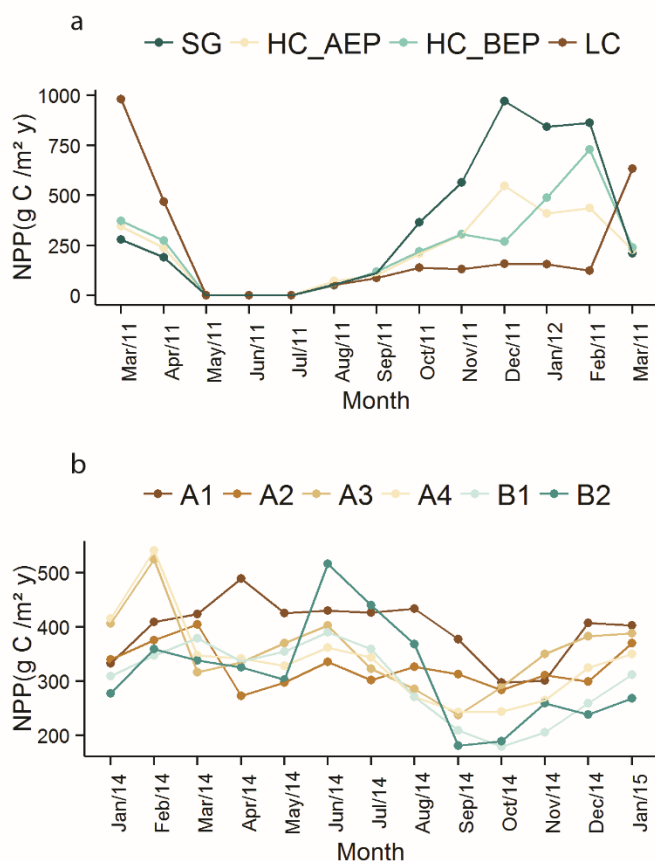


Figure 4.9. Values of net primary productivity (NPP) per month for the SO (a) and NA (b) sites during the years 2011/2012 and 2014/2015, respectively.

4.4.2.2 Correlation between environmental variables with nematode genera and *Acantholaimus* species relative abundance and biodiversity

Univariate correlations between nematode response variables (nematode total density, richness, H' , and *Acantholaimus* density, relative abundance, and richness) and environmental predictor variables (CPE, % TN, % TOC, % TOM, NPP, and SED) revealed no significant results.

DistLM routines based on the nematode community structure for seven environmental variables explained 24 % of the total community variation (Table S3). The values of % TOC and CPE displayed a significant impact on the nematode relative abundance, whereas the other variables did not contribute significantly to the model.

The DistLM analysis of the *Acantholaimus* species structure revealed a significant effect of % TOC, CPE, NPP, and % TOM on the differences between species, accounting together

for 40 % of the total variation (Table S3). The other environmental variables used for the model did not exhibit a significant correlation on the fitted model.

4.5 Discussion

4.5.1 The deep sea is diverse at a local scale, while turnover can be restricted

Nematode genus and *Acantholaimus* species alpha diversity (i.e. local species richness and Shannon-Wiener diversity of individual cores) was similar to other studies conducted in abyssal plains. However, caution should be exercised when comparing results, as different sampling equipment and sediment layers were used, hampering exact comparisons of diversity at a macro scale between different areas (Miljutina et al., 2010; Muthumbi and Vincx, 1997; Sebastian et al., 2007; Singh et al., 2014; Thistle et al., 1985; Vanreusel et al., 2010b). In this study, the North Atlantic (NA) transect showed higher alpha genus and *Acantholaimus* species diversity and richness per sample when compared to the local (i.e. alpha) diversity in the Southern Ocean (SO) transect. One has to take into account that the sampling cores used at NA sites sampled a larger surface (25.5 cm² for SO vs. 69.4 cm² for NA), which could result in the higher diversity and higher species pool found there. Nevertheless, the same number of nematodes was picked out randomly after sample homogenisation in order to allow between-sample comparisons, and rarefaction curves did reach an asymptote for the SO sites (except for LC), partially eliminating sampling biases related to sample size.

Despite the higher local diversity exhibited at the NA transect in comparison with the SO transect, it has already been observed that abyssal plains can be distinguished by a set of

taxa dominated by the nematode genera *Acantholaimus* and *Thalassomonhystera* (Vanreusel et al., 2010b). In this study, these two genera were also dominant at every site of the NA transect and at the LC site in the SO. Also the same *Acantholaimus* species were shared between both areas. These results confirm the homogeneous nature of abyssal sediments on a large scale and suggest that at least for these deep areas “everything is everywhere, but the environment selects” at least at the genus and even at *Acantholaimus* species levels, when environmental conditions are favourable (Baas-Becking, 1934; Fenchel and Finlay, 2004; Moens et al., 2014). Thus, although genus and *Acantholaimus* local diversity was higher at the NA transect when compared to the SO, overall the same abundant nematode taxa were found, revealing a low genus and *Acantholaimus* species turnover between NA sites. Nevertheless, the distribution of species in the deep sea could be better supported with further molecular analysis, since the species reported here could also represent cryptic species. A previous study has already suggested low endemism for nematodes in the deep sea (Bik et al., 2010), but whether this pattern is taxon specific is still not clear.

This observed high local diversity and dominance of specific nematode genera was already expected based on previous studies (Lamshead, 2004; Lamshead and Boucher, 2003), confirming thus, that the deep sea is diverse at a local scale. Nevertheless, the expected low beta diversity (i.e. low turnover) already reported for nematodes (Fenchel and Finlay, 2004; Lamshead, 2004; Leduc et al., 2012a) did not hold for both studied transects. When dissimilarities in nematode genus and *Acantholaimus* species structure were compared between sites from the same transect (β_2), beta diversity for genera and *Acantholaimus* species was higher for the SO transect than for the NA (Fig. 4.3a), indicating that turnover was greater along the first transect. In addition, the additive partitioning results revealed differences between both transects regarding the contribution of local and regional diversity to the total genus and species variability (Fig. 4.3b). For genus richness, alpha

diversity accounted for most of the total diversity at the NA transect, while beta diversity between sites (β_2) was proportionally much higher for H' . The higher importance of turnover (β_2) when genus diversity was considered is probably due to the dominance of *Acantholaimus* (up to 30 %) within the NA sites, since this index takes both abundance and evenness into consideration. The highest contribution of β_2 in comparison to alpha for both genus richness and H' was revealed in the SO, and this higher turnover might be explained by the higher aggregation of organisms and by the high number of rare genera (62 genera were restricted to this region) found in this transect (Gering and Crist, 2002), and not by the core size, since SO rarefaction curves reached an asymptote (except for LC). Nematode community structure in the SO was not only different between sites, but also diverged in terms of community structure from the usual communities found in other abyssal areas, which are generally dominated by *Thalassomonhystera* and *Acantholaimus* (Lamshead et al., 2003; Miljutina et al., 2010; Singh et al., 2014; Vanreusel et al., 2010b). However, the question remains if environmental differences rather than geographical distances are responsible for the high turnover between these sites (see below).

Additive partitioning results for the *Acantholaimus* species revealed contrasting patterns for the SO and NA transects (Fig. 4.3d). While turnover between stations (β_2) contributed most to total *Acantholaimus* (species richness and H') species diversity between stations along the SO transect, alpha diversity contributed the most for species divergences (species richness and H') in the NA. Therefore, the SO transect did not follow the expected high local, low regional diversity already reported for nematode distribution. These results do not support the second part of the paradigm about limited species turnover in the deep sea (Lamshead and Boucher, 2003).

Our results indicate more divergent communities at a regional scale (β_2) along the Polar Front than across the NA transect, where a more homogenous genus pool seems to be

present, since none of the sites differed significantly in genus structure. This may seem a remarkable observation for organisms lacking a pelagic life stage, as the NA transect was ~1500 km long and interrupted by the Mid-Atlantic Ridge, but similar wide distributions were already reported for deep-sea nematodes, suggesting low endemism of this group at genus level (Bik et al., 2010, Zeppilli et al., 2011).

At species level, a high degree of cosmopolitanism was also observed for many species of *Acantholaimus* (Fig.4.10). Two species, *A. invaginatium* and *A. maks* were encountered at all sites (except site B1 for *A. maks*) of this study, being also previously observed in different ocean basins (Table S2). Global literature-based distribution maps of *Acantholaimus* species showed that *A. invaginatium* and *A. maks* (together with *A. megamphis* and *A. mirabilis*) are also the ones covering a larger bathymetrical range, occurring from the continental shelf to the abyss (Fig. 4.7). These results are unexpected since bathymetry is considered an ecological barrier for many taxa, limiting species dispersal in the deep sea (Etter et al., 2005; Etter and Bower, 2015; Havermans et al., 2013; Wilson, 1983). However, molecular evidence would be required to identify haplotype distribution for these eurybathic morphospecies assisting in the inference of connectivity or divergence. The number of *Acantholaimus* species found in this study was similar to other studies (Muthumbi and Vincx, 1997; Thistle et al., 1985) except for the high number of morphotypes found by De Mesel et al. (2006) along the Antarctic continental shelf and slope. The success of *Acantholaimus* on the Antarctic shelf is not in accordance with its establishment in the oligotrophic abyss and requires further investigation.

The idea of the deep sea (> 1000 m) as a highly diverse environment (Hessler and Sanders, 1967), possessing greater richness at a local scale compared to shallower environments (Gage, 1996), should be interpreted with caution. We have observed in this study that the comparison of diversity can depend on the area studied, on the spatial scale used, and on the choice of the diversity index. The high diversity at local scale (alpha diversity)

accounted for the deep sea, thus, cannot be considered a general rule for all environments. For genus richness, for e.g., high beta diversity can be derived from the high number of rare taxa, but undersampling and limited taxonomic identification may be partly responsible for their high turnover. Therefore, macro-scale trends of benthic deep-sea diversity still remain largely unknown, being based on local and regional descriptions (Gooday et al., 2004; Woolley et al., 2016).

In general, our results corroborate the idea that deep-sea environments provide relatively few barriers to dispersal (Grassle, 1989; van der Heijden et al., 2012), enabling connectivity between extensive areas, and consequently low endemism, particularly for nematodes (Bik et al., 2010; Strugnell et al., 2008; van der Heijden et al., 2012). The wide distribution of many nematode genera and *Acantholaimus* species in this study suggests either that radiation of nematodes in abyssal environments occurred a long time ago, or that dispersal of nematodes is highly efficient, promoting a widespread distribution of individuals (Bik et al., 2010, Tietjen, 1989, Zeppilli et al., 2011). Concurrently, the different nematode community observed for SG, HC_AEP, and HC_BEP in this study, and the high levels of molecular-based endemism already reported for some shallow-water nematode taxa (Derycke et al., 2013; Van Campenhout et al., 2014) also suggest that habitat type and environmental conditions might play a role in shaping nematode assemblages and consequently nematode distribution (Heip et al., 1985; Moens et al., 2014; Vincx et al., 1994).

4.5.2 Deep-sea diversity does not increase with increasing organic matter input at a local scale

Although no correlation was observed between univariate data for the total nematode genus and *Acantholaimus* species assemblages (density and diversity) and organic matter input, DistLM results based on the multivariate community data reflected a significant effect of % TOC, CPE, and NPP on the nematode genus and *Acantholaimus* species structure. Highest densities of nematodes were observed at the SG site, characterized by the highest average net primary productivity (NPP). In general, marine nematode densities are highly correlated with food input in the sediments (Lambshead, 2004), and here highest total densities were observed at the SO transect. The increasing densities of benthic organisms with increasing food input in abyssal plains is already well documented for meiofaunal and macrofaunal groups (Danovaro et al., 2013; Gage et al., 2004; Glover et al., 2001; Gooday and Jorissen, 2012). In contrast, nematode genera and *Acantholaimus* species diversity differed for both studied transects. The highest contribution of alpha diversity was found at the NA transect, while turnover was more pronounced at the SO transect.

The low turnover observed for the NA, the high turnover reported for the SO, and the lowest genus and species diversity exhibited at the SG site are in accordance with the species-energy hypothesis, where the effect of organic matter input on the diversity is believed to be expressed as a parabolic curve (Leduc et al., 2012b; Whittaker et al., 2001). In this hypothesis, the amount of available energy, here understood as food availability, sets limits to the richness of the system, where both extremes (very low and high food availability) can diminish diversity at a local scale (Leduc et al., 2012b; Moens et al., 2014). In this regard, the general relative stability of the deep-sea abyssal plains under low food input, when compared to other environments, is believed to promote local diversity by reducing rates of interactions (e.g. competition and predation) between organisms and enhancing the evolution of specialized forms (Snelgrove and Smith, 2002). This could explain the higher nematode and *Acantholaimus* species alpha diversity found at the NA

transect, which is characterized by annual low and constant food input (Jochem and Zeitzschel, 1993; Longhurst, 1998). The genus *Acantholaimus* is typically abundant in abyssal plains and tends to increase in importance (relative abundance) and diversity with increasing water depth (Muthumbi and Vincx, 1997; Soetaert and Heip, 1995). In addition, this genus exhibits high inter-specific buccal parts variability, indicating food selectivity as a potential strategy for species coexistence in food-depleted environments (Fig.4.10).

Therefore, the high local diversity and low turnover observed at the NA can be explained by a potential stability of this transect, which is characterized by a constantly low food input. However, low organic matter input also seems to be responsible for the homogeneous pattern of nematode community structure that is generally found in abyssal plains, supporting the “everything is everywhere, but the environment selects” hypothesis (Baas-Becking, 1934). In contrast to this low turnover and common abyssal community found at the NA transect, we have observed in our study that the sites SG, HC_AEP, and HC_BEP possessed higher turnover rates and divergent nematode genera and *Acantholaimus* species structure when compared to other studies (Miljutina et al., 2010; Singh et al., 2014). In general, higher beta diversity can be observed in environments subjected to pulsed food input, which is responsible for increasing patchiness, and consequently diversity, which can be discordantly distributed (Lamshead, 2004). This idea of relating diversity to aggregation was proposed by Shorrocks and Sevenster (1995), and our results for the SO corroborate their idea of species coexistence in patches. They stated that, if communities are patch-dependent, then within-habitat variability would be lower and among-habitat diversity would be higher than expected (Shorrocks and Sevenster, 1995) (Fig. 4.3).

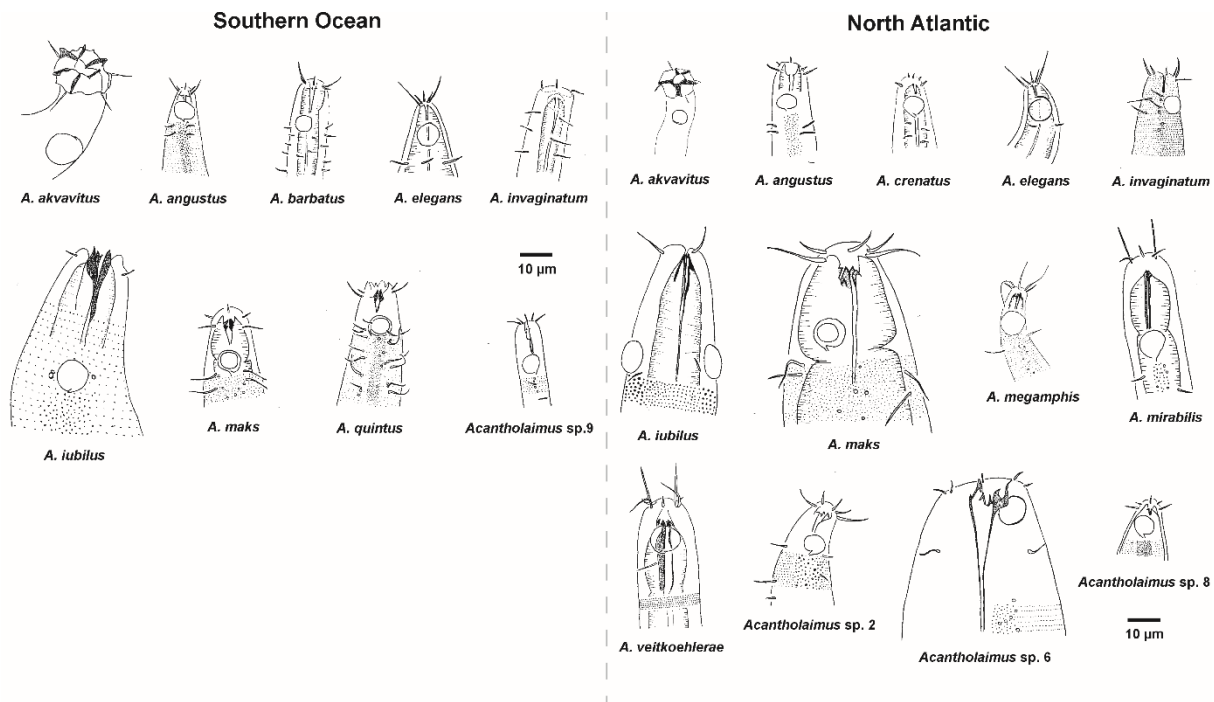


Figure 4.10. Line drawings of the *Acantholaimus* species found at the Southern Ocean and the North Atlantic transects. Only species for which male specimens were found are presented.

Furthermore, pulsed organic matter input regimes can promote the dominance of opportunistic species (Grassle, 1989; Levin et al., 2001; Whittaker et al., 2001). The genus *Microloaimus*, which occurred in high abundances at HC_AEP and HC_BEP, as well as at SG may indicate an opportunistic behaviour in response to food input at these sites respectively. This genus has been reported from other bathyal and abyssal areas of the Southern Ocean and elsewhere, and when present in high abundances, this has generally been correlated to either fresh food input or to disturbance events (Hauquier et al., 2016; Lee et al., 2001; Sebastian et al., 2007) suggesting an opportunistic character. Moreover, the highest surface productivity values at SG were correlated to the lowest alpha diversity values at this station for, both, nematode genera and *Acantholaimus* species. This could be a result of the increase in density of few competitive taxa, such as *Microloaimus* and *Desmodora*, at SG, in response to the high surface productivity (Gooday, 2002; Woolley et al., 2016). The genus *Desmodora* was represented by only one species, *D. profundum*,

which dominated the nematode community at SG (Lins et al., 2015). This genus is normally found in food-rich environments, such as seeps, vents, and seamounts, and has also been reported from adjacent areas, but *Desmodora* was not commonly observed in high abundances in abyssal plains (Ingels et al., 2006; Vanreusel et al., 2010). As a result, the low species diversity of *Acantholaimus* would be a consequence of a stronger competition rather than a lack of response to organic matter input. Therefore, the heterogeneity in food input for the SO transect lead to a higher turnover of nematode genera/species, and consequently to a more heterogeneous environment at a regional scale.

4.5.3 Increased patch dynamics (does not) increase local diversity

The influence of patch-dynamics on species coexistence at a small scale ($\beta 1$) can be shaped by at least three different factors: sediment composition and diversity, sediment topography, and partitioning of food resources related to particle size (Levin et al., 2001; Tyler, 1995). In addition, patchiness in the sediment can also be significantly influenced by biotic factors, such as the macrofauna. Macrofauna has been shown to interfere in sediment mixing in deep-sea sediments through bioturbation activities, causing surface deposition and biodiffusion (Dauwe et al., 1998). In order to investigate patchiness in sediment composition, variability at the $\beta 1$ level (i.e. between cores from the same site) was considered. In this study, within-site sediment diversity (SED) was in general higher for NA sites than for SO sites. Contrastingly, $\beta 1$ diversity exhibited similar within site variation for both transects (Fig. 4.3a). In fact, differences in nematode genus diversity and species diversity of *Acantholaimus*, and differences in SED between cores from the same sites were not concurrent, meaning that community divergences could not be explained by differences in SED. Nevertheless, sediment structuring is believed to be a

major factor shaping meiofaunal communities and explaining diversity in the deep sea (Grassle, 1989; Leduc et al., 2012c). Levin et al. (2001) stated that more species are able to coexist where sediment grain size is more heterogeneous. The lack of correlation between nematode diversity and SED might be due to the range which SED varied in this study. Here, SED ranged from 0.14–1.0, while in another study it showed much higher values (Leduc et al., 2012c). This indicates that, although sediment differences were present, these were not large enough to influence nematode genus and species coexistence.

However, the greater SED observed at NA is untypical for abyssal plains. Environments possessing a higher SED, specially for abyssal plains which are dominated by silt-clay sediments, are generally more dynamic (Gage, 1997). More dynamic environments can lead to an increase in roughness and habitat heterogeneity of the sea bottom, consequently increasing the presence of mounds and burrows which contribute to the accumulation and patchiness of organic matter (Gage, 1997). The Vema area has a strong influence from the eastward Antarctic Bottom Water (AABW) flux, which can exhibit bottom currents of 18–35 cm/s and increased turbidity, enabling passive dispersal of organisms through the transform (Eittrheim et al., 1983; Ludwig and Rabinowitz, 1980; Morozov et al., 2015). Small organisms, such as nematodes, are likely easily resuspended and transported through the water column (da Fonseca-Genevois et al., 2006; Gallucci et al., 2008). Therefore, the high bottom dynamics at the NA transect might have influenced the sediment topography, and increased species distribution ranges. At the same time, if nematodes can be passively resuspended into the water column, this might also have favoured the low beta diversity (β_1 and β_2) observed for this transect, together with the low and constant surface primary productivity already discussed in the previous section.

4.6 Conclusions

Our results are partially in agreement with Paradigm 1. Although for the North Atlantic a high alpha diversity and low turnover (i.e. beta diversity) was observed, turnover might not be necessarily low in the deep sea and can be related to the environmental conditions prevailing at different areas studied. The high local alpha diversity at the North Atlantic transect, associated with a low turnover rate between stations (β_2), both at genus and *Acantholaimus* species level, are probably related to the stability of this environment due to the constant and low food input usually found at abyssal plains. Nevertheless, despite the high local diversity observed at the North Atlantic transect, all of its stations were dominated by the same nematode genera (*Acantholaimus* and *Thalassomonhystera*), corroborating the hypothesis that “everything is everywhere, but the environment selects”. The different nematode communities found in the Southern Ocean in relation to other deep-sea abyssal areas, and the higher turnover of genera and species of *Acantholaimus*, indicate that turnover might be dependent on the surface productivity and seasonal input of organic matter. Increased organic matter input at some Southern Ocean stations might have resulted in a lower alpha diversity but a higher beta diversity due to a shift in dominant genera and species between stations. Thus, these results corroborate Paradigm 2, surface productivity regulates diversity. Finally, sediment heterogeneity did not significantly influence genus or species coexistence in this study possibly due to the low sediment variability compared to other deep-sea environments. Although the NA transect possessed higher SED and higher alpha diversity, sediment variability was not related to community differences at a small (β_1) scale. Therefore, based on the results of this study, Paradigm 3 could not be validated, as patchiness did not show any association with nematode community structure at a small scale.

4.7 Supplementary data

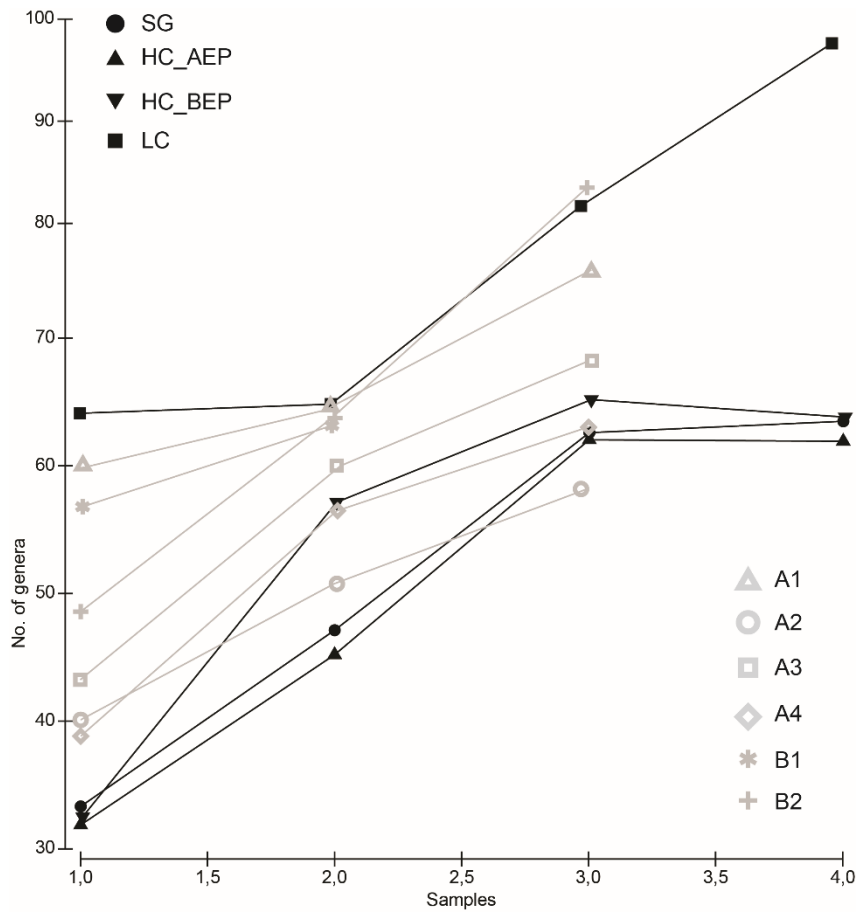


Figure S1. Rarefaction curve calculated per site using the chao1 estimator. Symbols and line in black represent the sites located at the Southern Ocean, while grey symbols and lines belong to sites at the North Atlantic.

Table S1. PERMANOVA results for the response variables used in this study: Nematode total density, nematode genus richness (S), nematode Shannon-Wiener diversity (H'), nematode community relative abundance, *Acantholaimus* total density, *Acantholaimus* species richness (*Acantholaimus* S), *Acantholaimus* Shannon-Wiener diversity (H'), and *Acantholaimus* species relative abundance. Main *p* perm represents *p*-values for the 2-factor nested design test. Significant values are represented in bold. Pairwise *t*-tests are shown for each transect. Only the significantly different pairs are shown. When all differences between sites pairs were not significant, pairwise *t*-tests were displayed as NS.

Response variable	Main test <i>p</i> perm	pairwise <i>t</i> -tests for SO	pairwise <i>t</i> -tests for NA
Nematode total density (10 cm ²)	Region = 0.0001 Site = 0.0001	SG, HC_BEP 0.0022 SG, LC 0.0084 HC_AEP, HC_BEP 0.0011 HC_AEP, LC 0.0173	NS
Nematode S	Region = 0.0008 Site = 0.9043	NS	NS
Nematode H'	Region = 0.2107 Site = 0.6303	NS	NS
Nematode community relative abundance (%)	Region = 0.0001 Site = 0.0001	SG, HC_AEP 0.0134 SG, HC_BEP 0.0051 SG, LC 0.0167 HC_AEP, HC_BEP 0.0143	NS
<i>Acantholaimus</i> total density (10 cm ²)	Region = 0.002 Site = 0.0348	SG, HC_BEP 0.0396	NS
<i>Acantholaimus</i> S	Region = 0.0001 Site = 0.2052	NS	A2, A3 0.0384
<i>Acantholaimus</i> H'	Region = 0.0002 Site = 0.7621	NS	A1, A3 0.0287 A3, A4 0.0157 A2, A3 0.0367 A3, B1 0.0113
<i>Acantholaimus</i> species relative abundance (%)	Region = 0.0001 Site = 0.0174	SG, LC 0.0136	A2, B1 0.0403 A2, B2 0.0125

Table S2. *Acantholaimus* species occurrence list for the species reported in this study. Region stands for where the species occurred, and site shows the original name of the site where the species were found in the provided source.

Region	Site	Latitude	Longitude	Species	depth (m)	Source
Southern Ocean	SG	-50.7782	-39.4225	akvavitus	4154.2	Lins et al., 2015
Southern Ocean	HC_AE P	-51.2663	-12.6173	akvavitus	4113	Lins et al., 2015
Southern Ocean	HC_BE P	-51.9812	-12.0627	akvavitus	3966	Lins et al., 2015
Southern Ocean	LC	-51.9998	9.9998	akvavitus	3760	Lins et al., 2015
SE Pacific, Peru Basin	59	18	87.266667	akvavitus	4526	Gerlach et al., 1979
SE Pacific, Peru Basin	179	13.2	58.966667	akvavitus	4823	Gerlach et al., 1979
NE Atlantic, Bay of Biscay	KR66	46.528333	-10.456667	akvavitus	4700	Vivier, 1985
Central Western Atlantic, Haterras plain	HP	32.493333	-70.35	akvavitus	5411	Tietjen, 1989
Puerto Rico Trench	PR3	19.708333	-66.203333	akvavitus	8380	Tietjen, 1989
SE Atlantic, Angola Basin	346	-16.28333	5.45	akvavitus	5389	Miljutina et al., 2013
SW Atlantic, Campos Basin	CANG 9	-21.9126	-39.8429	akvavitus	1300	da Silva, 2012
SW Atlantic, Campos Basin	G8	-22.1227	-39.8732	akvavitus	1000	da Silva, 2012
SW Atlantic, Campos Basin	G9	-22.1222	-39.7404	akvavitus	1300	da Silva, 2012
SW Atlantic, Campos Basin	CANAC 6	-21.8344	-40.1042	akvavitus	600	da Silva, 2012
SW Atlantic, Campos Basin	CANAC 7	-21.7912	-40.0374	akvavitus	700	da Silva, 2012
SW Atlantic, Campos Basin	CANAC 8	-21.97657	-39.9914	akvavitus	1000	da Silva, 2012
SW Atlantic, Campos Basin	H7	-21.6872	-40.0393	akvavitus	700	da Silva, 2012
NW Atlantic	A1 3-3	10.718533	-25.064767	akvavitus	5498	Lins et al., this study
NW Atlantic	A1 3-4	10.718467	-25.0648	akvavitus	5507	Lins et al., this study
NW Atlantic	A1 3-5	10.7195	-25.064667	akvavitus	5508	Lins et al., this study
NW Atlantic	A2 4-3	10.4185	-31.076833	akvavitus	5771	Lins et al., this study
NW Atlantic	A2 4-4	10.418667	-31.077	akvavitus	5759	Lins et al., this study
NW Atlantic	A2 4-5	10.418667	-31.077	akvavitus	5767	Lins et al., this study
NW Atlantic	A3 6-2	10.3505	-36.959833	akvavitus	5137	Lins et al., this study
NW Atlantic	A3 6-3	10.3505	-36.960167	akvavitus	5137	Lins et al., this study
NW Atlantic	A3 6-4	10.3505	-36.960167	akvavitus	5136	Lins et al., this study
NW Atlantic	A4 8-1	10.726033	-42.693217	akvavitus	5182	Lins et al., this study
NW Atlantic	A4 8-10	10.709667	-42.683167	akvavitus	5117	Lins et al., this study
NW Atlantic	A4 8-11	10.709833	-42.683167	akvavitus	5121	Lins et al., this study
NW Atlantic	B1 9-3	11.6895	-47.956	akvavitus	4999	Lins et al., this study
NW Atlantic	B1 9-4	11.689333	-47.955667	akvavitus	4998	Lins et al., this study
NW Atlantic	B2 11-5	12.09	-50.449667	akvavitus	5090	Lins et al., this study

Benthic-pelagic coupling and spatial variability in the deep-sea meiofauna

NW Atlantic	B2 11-6	12.090333	-50.449667	akvavitus	5091	Lins et al., this study
NW Atlantic	B2 11-7	12.09	-50.4495	akvavitus	5091	Lins et al., this study
Southern Ocean	SG	-50.7782	-39.4225	angustus	4154.2	Lins et al., 2015
Southern Ocean	HC_AE P	-51.2663	-12.6173	angustus	4113	Lins et al., 2015
SE Atlantic, Angola Basin	346	-16.28333	5.45	angustus	5389	Miljutina et al., 2013
NE Tropical Pacific, CCZ	MTB-1	14.066333	-130.116	angustus	4983	Miljutina and Miljutin, 2012
NE Tropical Pacific, CCZ	MTB-7	14.048	-130.08283	angustus	5042	Miljutina and Miljutin, 2012
NE Tropical Pacific, CCZ	MTB-17	14.036667	-130.11	angustus	5000	Miljutina and Miljutin, 2012
SE Pacific, Peru Basin	MC196	-7.064444	-88.463333	angustus	4159	Bussau, 1993
NW Atlantic	A3 6-3	10.3505	-36.960167	angustus	5137	Lins et al., this study
NW Atlantic	A4 8-10	10.709667	-42.683167	angustus	5117	Lins et al., this study
NW Atlantic	B1 9-4	11.689333	-47.955667	angustus	4998	Lins et al., this study
Southern Ocean	SG	-50.7782	-39.4225	barbatus	4154.2	Lins et al., 2015
Southern Ocean	HC_AE P	-51.2663	-12.6173	barbatus	4113	Lins et al., 2015
Southern Ocean	HC_BE P	-51.9812	-12.0627	barbatus	3966	Lins et al., 2015
Southern Ocean	LC	-51.9998	9.9998	barbatus	3760	Lins et al., 2015
NE Tropical Pacific, CCZ	MTB-10	14.046667	-130.08333	barbatus	5035	Miljutina and Miljutin, 2012
NE Tropical Pacific, CCZ	MTB-16	14.045	-130.12883	barbatus	4950	Miljutina and Miljutin, 2012
NE Tropical Pacific, CCZ	MTB-18	14.042	-130.133	barbatus	4950	Miljutina and Miljutin, 2012
Western Mediterranean, Ligurian Sea	2	42.633333	8.666667	crenatus	280	Soetaert, 1988
Western Mediterranean, Ligurian Sea	3	42.641667	8.66	crenatus	530	Soetaert, 1988
Western Mediterranean, Ligurian Sea	4	42.656667	8.656667	crenatus	820	Soetaert, 1988
Western Mediterranean, Ligurian Sea	5	42.665	8.653333	crenatus	990	Soetaert, 1988
Western Mediterranean, Ligurian Sea	6	42.685	8.641667	crenatus	1220	Soetaert, 1988
NW Atlantic	A1 3-4	10.718467	-25.0648	crenatus	5507	Lins et al., this study
NW Atlantic	A1 3-5	10.7195	-25.064667	crenatus	5508	Lins et al., this study
NW Atlantic	A3 6-2	10.3505	-36.959833	crenatus	5137	Lins et al., this study
Southern Ocean	HC_AE P	-51.2663	-12.6173	cyathibucca	4113	Lins et al., 2015
NE Atlantic, Bay of Biscay	KR26	44.178333	-4.25	cyathibucca	2480	Vivier, 1985
Southern Ocean	SG	-50.7782	-39.4225	elegans	4154.2	Lins et al., 2015
Southern Ocean	HC_AE P	-51.2663	-12.6173	elegans	4113	Lins et al., 2015
Southern Ocean	HC_BE P	-51.9812	-12.0627	elegans	3966	Lins et al., 2015
Southern Ocean	LC	-51.9998	9.9998	elegans	3760	Lins et al., 2015
Central Western Indian Ocean	133	-2.030278	41.782667	elegans	2015	Muthumbi and Vincx, 1997
Central Western Indian Ocean	506	-4.329167	40.363333	elegans	1020	Muthumbi and Vincx, 1997
Central Western Indian Ocean	552	-4.1285	39.911167	elegans	500	Muthumbi and Vincx, 1997

North Atlantic, Norway Sea	59	65.517778	1.221111	elegans	3062	Jensen, 1988
North Atlantic, Norway Sea	61	67.716667	0.098611	elegans	1245	Jensen, 1988
SW Atlantic, Campos Basin	CANG 7	-21.9371	-39.9662	elegans	700	da Silva, 2012
SW Atlantic, Campos Basin	CANG 8	-21.9191	-39.9091	elegans	1000	da Silva, 2012
SW Atlantic, Campos Basin	CANAC 6	-21.8344	-40.1042	elegans	600	da Silva, 2012
SW Atlantic, Campos Basin	CANAC 7	-21.7912	-40.0374	elegans	700	da Silva, 2012
SW Atlantic, Campos Basin	CANAC 8	-21.97657	-39.9914	elegans	1000	da Silva, 2012
Arabian Sea	34	13.904333	74.316167	elegans	34	Singh and Ingole, 2016
Arabian Sea	48	13.998	74.0005	elegans	48	Singh and Ingole, 2016
Arabian Sea	102	14.004833	73.499	elegans	102	Singh and Ingole, 2016
Arabian Sea	525	14.004	73.232833	elegans	525	Singh and Ingole, 2016
Arabian Sea	1001	14.004167	73.135167	elegans	1001	Singh and Ingole, 2016
Arabian Sea	1524	14.005	72.953667	elegans	1524	Singh and Ingole, 2016
Arabian Sea	2001	14.0015	71.220167	elegans	2001	Singh and Ingole, 2016
Arabian Sea	2546	13.9925	70.806667	elegans	2546	Singh and Ingole, 2016
NW Atlantic	A1 3-4	10.718467	-25.0648	elegans	5507	Lins et al., this study
NW Atlantic	A3 6-3	10.3505	-36.960167	elegans	5137	Lins et al., this study
NW Atlantic	A3 6-4	10.3505	-36.960167	elegans	5136	Lins et al., this study
NW Atlantic	B2 11-5	12.09	-50.449667	elegans	5090	Lins et al., this study
Southern Ocean	LC	-51.9998	9.9998	gigantasetosus	3760	Lins et al., 2015
NE Atlantic, Bay of Biscay	KR18	47.531667	-9.106667	gigantasetosus	2756	Vivier, 1985
NE Atlantic, Bay of Biscay	KR53	44.116667	-4.286667	gigantasetosus	1920	Vivier, 1985
NE Atlantic, Bay of Biscay	KR16	44.575	-8.683333	gigantasetosus	2157	Vivier, 1985
NW Atlantic	B2 11-5	12.09	-50.449667	gigantasetosus	5090	Lins et al., this study
Southern Ocean	SG	-50.7782	-39.4225	invaginatum	4154.2	Lins et al., 2015
Southern Ocean	HC_AE P	-51.2663	-12.6173	invaginatum	4113	Lins et al., 2015
Southern Ocean	HC_BE P	-51.9812	-12.0627	invaginatum	3966	Lins et al., 2015
Southern Ocean	LC	-51.9998	9.9998	invaginatum	3760	Lins et al., 2015
Central Western Indian Ocean	105	-4.401667	39.7665	invaginatum	511	Muthumbi and Vincx, 1997
Central Western Indian Ocean	107	-4.363833	41.221111	invaginatum	2053	Muthumbi and Vincx, 1997
Central Western Indian Ocean	133	-2.030278	41.782667	invaginatum	2015	Muthumbi and Vincx, 1997
Central Western Indian Ocean	505	-4.425833	39.755833	invaginatum	520	Muthumbi and Vincx, 1997
Central Western Indian Ocean	507	-4.358611	41.227333	invaginatum	2088	Muthumbi and Vincx, 1997
Central Western Indian Ocean	519	-3.157778	41.281389	invaginatum	2179	Muthumbi and Vincx, 1997
NW Atlantic	A1 3-3	10.718533	-25.064767	invaginatum	5498	Lins et al., this study
NW Atlantic	A1 3-4	10.718467	-25.0648	invaginatum	5507	Lins et al., this study

Benthic-pelagic coupling and spatial variability in the deep-sea meiofauna

NW Atlantic	A1 3-5	10.7195	- 25.064667	invaginatium	5508	Lins et al., this study
NW Atlantic	A2 4-3	10.4185	- 31.076833	invaginatium	5771	Lins et al., this study
NW Atlantic	A2 4-4	10.41866 7	-31.077	invaginatium	5759	Lins et al., this study
NW Atlantic	A2 4-5	10.41866 7	-31.077	invaginatium	5767	Lins et al., this study
NW Atlantic	A3 6-2	10.3505	- 36.959833	invaginatium	5137	Lins et al., this study
NW Atlantic	A3 6-3	10.3505	- 36.960167	invaginatium	5137	Lins et al., this study
NW Atlantic	A3 6-4	10.3505	- 36.960167	invaginatium	5136	Lins et al., this study
NW Atlantic	A4 8-1	10.72603 3	- 42.693217	invaginatium	5182	Lins et al., this study
NW Atlantic	A4 8-10	10.70966 7	- 42.683167	invaginatium	5117	Lins et al., this study
NW Atlantic	A4 8-11	10.70983 3	- 42.683167	invaginatium	5121	Lins et al., this study
NW Atlantic	B1 9-3	11.6895	-47.956	invaginatium	4999	Lins et al., this study
NW Atlantic	B1 9-4	11.68933 3	- 47.955667	invaginatium	4998	Lins et al., this study
NW Atlantic	B2 11-5	12.09	- 50.449667	invaginatium	5090	Lins et al., this study
NW Atlantic	B2 11-6	12.09033 3	- 50.449667	invaginatium	5091	Lins et al., this study
NW Atlantic	B2 11-7	12.09	-50.4495	invaginatium	5091	Lins et al., this study
NW Atlantic	A1 3-3	10.71853 3	- 25.064767	iubilus	5498	Lins et al., this study
NW Atlantic	A2 4-4	10.41866 7	-31.077	iubilus	5759	Lins et al., this study
NW Atlantic	A2 4-5	10.41866 7	-31.077	iubilus	5767	Lins et al., this study
NW Atlantic	A3 6-2	10.3505	- 36.959833	iubilus	5137	Lins et al., this study
NW Atlantic	A3 6-3	10.3505	- 36.960167	iubilus	5137	Lins et al., this study
NW Atlantic	A4 8-11	10.70983 3	- 42.683167	iubilus	5121	Lins et al., this study
NW Atlantic	B1 9-3	11.6895	-47.956	iubilus	4999	Lins et al., this study
NW Atlantic	B2 11-7	12.09	-50.4495	iubilus	5091	Lins et al., this study
Southern Ocean	HC_BE P	-51.9812	-12.0627	iubilus	3966	Lins et al., 2015
SE Pacific, Peru Basin	111	8.15	70.033333	iubilus	3086	Gerlach et al., 1979
SE Pacific, Peru Basin	166	-0.4	54.55	iubilus	3167	Gerlach et al., 1979
SE Pacific, Peru Basin	137	-14.73333	79.733333	iubilus	5648	Gerlach et al., 1979
SE Pacific, Peru Basin	110	9.766667	70.1	iubilus	5917	Gerlach et al., 1979
SE Pacific, Peru Basin	77	13.83333 3	92.283333	iubilus	6260	Gerlach et al., 1979
SE Pacific, Peru Basin	191	23.95	60.966667	iubilus	6313	Gerlach et al., 1979
NE Atlantic, Bay of Biscay	KR65	46.50333 3	- 10.361667	iubilus	4586	Vivier, 1985
SE Atlantic, Walvis Ridge	DS04	-21.985	9.025	iubilus	4180	Gourbault and Vincx, 1985
SE Atlantic, Walvis Ridge	DS05	-21.75	12.18	iubilus	2992	Gourbault and Vincx, 1985
SE Atlantic, Walvis Ridge	DS12	-17.54667	9.478333	iubilus	4308	Gourbault and Vincx, 1985
SE Atlantic, Walvis Ridge	KR16	-12.05	12.341667	iubilus	2063	Gourbault and Vincx, 1985
Central Western Atlantic, Haterras plain	HP	32.49333 3	-70.35	iubilus	5411	Tietjen, 1989
Puerto Rico Trench	PR3	19.70833 3	- 66.203333	iubilus	8380	Tietjen, 1989

NE Tropical Pacific, CCZ	MTB-17	14.03666 7	-130.11	iubilus	5000	Miljutina and Miljutin, 2012
NE Tropical Pacific, CCZ	MTB-10	14.04666 7	- 130.08333	iubilus	5035	Miljutina and Miljutin, 2012
SE Atlantic, Angola Basin	346	-16.28333	5.45	iubilus	5389	Miljutina et al., 2013
SW Atlantic, Campos Basin	CANG 7	-21.9371	-39.9662	iubilus	700	da Silva, 2012
SW Atlantic, Campos Basin	CANG 8	-21.9191	-39.9091	iubilus	1000	da Silva, 2012
SW Atlantic, Campos Basin	CANG 9	-21.9126	-39.8429	iubilus	1300	da Silva, 2012
SW Atlantic, Campos Basin	CANAC 7	-21.7912	-40.0374	iubilus	700	da Silva, 2012
SW Atlantic, Campos Basin	CANAC 8	-21.97657	-39.9914	iubilus	1000	da Silva, 2012
SW Atlantic, Campos Basin	CANAC 9	-21.7295	-39.9219	iubilus	1300	da Silva, 2012
Southern Ocean	SG	-51.9998	9.9998	maks	4154.2	Lins et al., 2015
Southern Ocean	HC_AE P	-51.2663	-12.6173	maks	4113	Lins et al., 2015
Southern Ocean	HC_BE P	-51.9812	-12.0627	maks	3966	Lins et al., 2015
Southern Ocean	LC	-51.9998	9.9998	maks	3760	Lins et al., 2015
SE Pacific, Peru Basin	152	-7.35	59.733333	maks	3498	Gerlach et al., 1979
SE Pacific, Peru Basin	59	18	87.266667	maks	4526	Gerlach et al., 1979
SE Pacific, Peru Basin	98	17.48333 3	83.45	maks	6052	Gerlach et al., 1979
SE Pacific, Peru Basin	113	3.55	69.9	maks	5986	Gerlach et al., 1979
SE Pacific, Peru Basin	191	23.95	60.966667	maks	6313	Gerlach et al., 1979
NE Atlantic, Bay of Biscay	KR18	47.53166 7	-9.106667	maks	2756	Vivier, 1985
SE Atlantic, Walvis Ridge	DS04	-21.985	9.025	maks	4180	Gourbault and Vincx, 1985
SE Atlantic, Walvis Ridge	DS05	-21.75	12.18	maks	2992	Gourbault and Vincx, 1985
SE Atlantic, Walvis Ridge	DS12	-17.54667	9.478333	maks	4308	Gourbault and Vincx, 1985
SE Atlantic, Walvis Ridge	KR11	-18.43333	10.463333	maks	3615	Gourbault and Vincx, 1986
SE Pacific, Peru Basin	KG1322	-7.064722	-88.46	maks	4150	Bussau, 1993
SE Pacific, Peru Basin	KG1314	-7.066	- 88.473889	maks	4142	Bussau, 1993
NE Tropical Pacific, CCZ	MTB-10	14.049	- 130.07883	maks	5035	Miljutina and Miljutin, 2012
NE Tropical Pacific, CCZ	PL- 1599/7	13.92716 7	- 130.20333	maks	4800	Miljutina and Miljutin, 2012
SW Atlantic, Campos Basin	CANAC 6	-21.8344	-40.1042	maks	600	da Silva, 2012
SW Atlantic, Campos Basin	CANAC 7	-21.7912	-40.0374	maks	700	da Silva, 2012
SW Atlantic, Campos Basin	CANAC 8	-21.97657	-39.9914	maks	1000	da Silva, 2012
SW Atlantic, Campos Basin	CANAC 9	-21.7295	-39.9219	maks	1300	da Silva, 2012
SW Atlantic, Campos Basin	CANG 7	-21.9371	-39.9662	maks	700	da Silva, 2012
SW Atlantic, Campos Basin	CANG 8	-21.9191	-39.9091	maks	1000	da Silva, 2012
SW Atlantic, Campos Basin	CANG 9	-21.9126	-39.8429	maks	1300	da Silva, 2012
SW Atlantic, Campos Basin	H6	-21.7012	-40.0887	maks	400	da Silva, 2012
SW Atlantic, Campos Basin	H7	-21.6872	-40.0393	maks	700	da Silva, 2012

Benthic-pelagic coupling and spatial variability in the deep-sea meiofauna

SW Atlantic, Campos Basin	H9	-23.686	-41.2684	maks	1000	da Silva, 2012
SW Atlantic, Campos Basin	H10	-237527	-41.1981	maks	1300	da Silva, 2012
SW Atlantic, Campos Basin	G8	-22.1227	-39.8732	maks	1000	da Silva, 2012
SW Atlantic, Campos Basin	G9	-22.1222	-39.7404	maks	1300	da Silva, 2012
NW Atlantic	A1 3-3	10.71853 3	- 25.064767	maks	5498	Lins et al., this study
NW Atlantic	A1 3-4	10.71846 7	-25.0648	maks	5507	Lins et al., this study
NW Atlantic	A2 4-5	10.41866 7	-31.077	maks	5767	Lins et al., this study
NW Atlantic	A3 6-3	10.3505	- 36.960167	maks	5137	Lins et al., this study
NW Atlantic	A3 6-4	10.3505	- 36.960167	maks	5136	Lins et al., this study
NW Atlantic	A4 8-1	10.72603 3	- 42.693217	maks	5182	Lins et al., this study
NW Atlantic	A4 8-11	10.70983 3	- 42.683167	maks	5121	Lins et al., this study
NW Atlantic	B2 11-5	12.09	- 50.449667	maks	5090	Lins et al., this study
NW Atlantic	B2 11-7	12.09	-50.4495	maks	5091	Lins et al., this study
NE Atlantic, Bay of Biscay	KR53	44.11666 7	-4.286667	megamphis	1920	Vivier, 1985
NE Atlantic, Bay of Biscay	KR16	44.575	-8.683333	megamphis	2157	Vivier, 1985
Western Mediterranean, Ligurian Sea	1	42.62166 7	8.671667	megamphis	160	Soetaert, 1988
Western Mediterranean, Ligurian Sea	2	42.63333 3	8.666667	megamphis	280	Soetaert, 1988
Western Mediterranean, Ligurian Sea	3	42.64166 7	8.66	megamphis	530	Soetaert, 1988
Western Mediterranean, Ligurian Sea	4	42.65666 7	8.656667	megamphis	820	Soetaert, 1988
Western Mediterranean, Ligurian Sea	5	42.665	8.653333	megamphis	990	Soetaert, 1988
NW Atlantic	A1 3-5	10.7195	- 25.064667	megamphis	5508	Lins et al., this study
Western Mediterranean, Ligurian Sea	5	42.665	8.653333	mirabilis	990	Soetaert, 1988
Western Mediterranean, Ligurian Sea	6	42.685	8.641667	mirabilis	1220	Soetaert, 1988
Arabian Sea	34	13.90433 3	74.316167	mirabilis	34	Singh and Ingole, 2016
Arabian Sea	48	13.998	74.0005	mirabilis	48	Singh and Ingole, 2016
NW Atlantic	A1 3-3	10.71853 3	- 25.064767	mirabilis	5498	Lins et al., this study
NW Atlantic	A2 4-3	10.4185	- 31.076833	mirabilis	5771	Lins et al., this study
NW Atlantic	A2 4-4	10.41866 7	-31.077	mirabilis	5759	Lins et al., this study
NW Atlantic	A2 4-5	10.41866 7	-31.077	mirabilis	5767	Lins et al., this study
NW Atlantic	A3 6-2	10.3505	- 36.959833	mirabilis	5137	Lins et al., this study
Southern Ocean	HC_BE P	-51.9812	-12.0627	Morphotype V	3966	Lins et al., 2015
Southern Ocean	LC	-51.9998	9.9998	Morphotype V	3760	Lins et al., 2015
Southern Ocean	LC	-51.9998	9.9998	quintus	3760	Lins et al., 2015
SE Pacific, Peru Basin	169	8.95	52.283333	quintus	3909	Gerlach et al., 1979
SE Pacific, Peru Basin	137	-14.73333	79.733333	quintus	5648	Gerlach et al., 1979
SE Pacific, Peru Basin	113	3.55	69.9	quintus	5986	Gerlach et al., 1979
SE Pacific, Peru Basin	77	13.83333 3	92.283333	quintus	6260	Gerlach et al., 1979

SE Pacific, Peru Basin	75	13.266667	91.566667	quintus	6220	Gerlach et al., 1979
NE Atlantic, Bay of Biscay	KR53	44.116667	-4.286667	quintus	1920	Vivier, 1985
SE Atlantic, Walvis Ridge	DS04	-21.985	9.025	quintus	4180	Gourbault and Vincx, 1985
SE Atlantic, Walvis Ridge	DS05	-21.75	12.18	quintus	2992	Gourbault and Vincx, 1985
SE Atlantic, Walvis Ridge	DS12	-17.54667	9.478333	quintus	4308	Gourbault and Vincx, 1985
SE Atlantic, Walvis Ridge	KR16	-12.05	12.341667	quintus	2063	Gourbault and Vincx, 1985
SE Atlantic, Walvis Ridge	DS08	-21.955	10.256667	quintus	3777	Gourbault and Vincx, 1985
SE Atlantic, Angola Basin	346	-16.28333	5.45	quintus	5389	Miljutina et al., 2013
NE Tropical Pacific, CCZ	MTB-1	14.066333	-130.116	veitkoehlerae	4983	Miljutina and Miljutin, 2012
NE Tropical Pacific, CCZ	MTB-7	14.048	-130.08283	veitkoehlerae	5042	Miljutina and Miljutin, 2012
NE Tropical Pacific, CCZ	MTB-16	14.045	-130.12883	veitkoehlerae	4950	Miljutina and Miljutin, 2012
NE Tropical Pacific, CCZ	PL-1599/7	13.927167	-130.20333	veitkoehlerae	4800	Miljutina and Miljutin, 2012
NE Tropical Pacific, CCZ	MTB-6	14.047667	-130.08917	veitkoehlerae	5040	Miljutina and Miljutin, 2013
NE Tropical Pacific, CCZ	MTB-15	14.044833	-130.13067	veitkoehlerae	4947	Miljutina and Miljutin, 2013
NE Tropical Pacific, CCZ	MTB-8	14.0425	-130.08917	veitkoehlerae	5035	Miljutina and Miljutin, 2013
NE Tropical Pacific, CCZ	MTB-11	14.049	-130.07883	veitkoehlerae	5035	Miljutina and Miljutin, 2013
NW Atlantic	A3 6-3	10.3505	-36.960167	veitkoehlerae	5137	Lins et al., this study
NW Atlantic	A3 6-4	10.3505	-36.960167	veitkoehlerae	5136	Lins et al., this study
NW Atlantic	A4 8-1	10.726033	-42.693217	veitkoehlerae	5182	Lins et al., this study
NW Atlantic	A4 8-10	10.709667	-42.683167	veitkoehlerae	5117	Lins et al., this study
NW Atlantic	B1 9-3	11.6895	-47.956	veitkoehlerae	4999	Lins et al., this study
NW Atlantic	B1 9-4	11.689333	-47.955667	veitkoehlerae	4998	Lins et al., this study
NW Atlantic	B2 11-5	12.09	-50.449667	veitkoehlerae	5090	Lins et al., this study
NW Atlantic	B2 11-6	12.090333	-50.449667	veitkoehlerae	5091	Lins et al., this study
NW Atlantic	B2 11-7	12.09	-50.4495	veitkoehlerae	5091	Lins et al., this study
NW Atlantic	A1 3-3	10.718533	-25.064767	sp2 sp.n.	5498	Lins et al., this study
NW Atlantic	A1 3-4	10.718467	-25.0648	sp2 sp.n.	5507	Lins et al., this study
NW Atlantic	A1 3-5	10.7195	-25.064667	sp2 sp.n.	5508	Lins et al., this study
NW Atlantic	A2 4-3	10.4185	-31.076833	sp2 sp.n.	5771	Lins et al., this study
NW Atlantic	A2 4-4	10.418667	-31.077	sp2 sp.n.	5759	Lins et al., this study
NW Atlantic	A2 4-5	10.418667	-31.077	sp2 sp.n.	5767	Lins et al., this study
NW Atlantic	A3 6-2	10.3505	-36.959833	sp2 sp.n.	5137	Lins et al., this study
NW Atlantic	A3 6-3	10.3505	-36.960167	sp2 sp.n.	5137	Lins et al., this study
NW Atlantic	A3 6-4	10.3505	-36.960167	sp2 sp.n.	5136	Lins et al., this study

Benthic-pelagic coupling and spatial variability in the deep-sea meiofauna

NW Atlantic	A4 8-10	10.70966 7	- 42.683167	sp2 sp.n.	5117	Lins et al., this study
NW Atlantic	A4 8-11	10.70983 3	- 42.683167	sp2 sp.n.	5121	Lins et al., this study
NW Atlantic	B2 11-5	12.09	- 50.449667	sp2 sp.n.	5090	Lins et al., this study
NW Atlantic	B2 11-6	12.09033 3	- 50.449667	sp2 sp.n.	5091	Lins et al., this study
NW Atlantic	B2 11-7	12.09	-50.4495	sp2 sp.n.	5091	Lins et al., this study
NW Atlantic	A3 6-2	10.3505	- 36.959833	sp6	5137	Lins et al., this study
NW Atlantic	A3 6-3	10.3505	- 36.960167	sp8 sp.n.	5137	Lins et al., this study
NW Atlantic	A3 6-4	10.3505	- 36.960167	sp8 sp.n.	5136	Lins et al., this study
NW Atlantic	A4 8-10	10.70966 7	- 42.683167	sp8 sp.n.	5117	Lins et al., this study
NW Atlantic	A4 8-11	10.70983 3	- 42.683167	sp8 sp.n.	5121	Lins et al., this study
NW Atlantic	B1 9-3	11.6895	-47.956	sp8 sp.n.	4999	Lins et al., this study
NW Atlantic	B1 9-4	11.68933 3	- 47.955667	sp8 sp.n.	4998	Lins et al., this study
NW Atlantic	B2 11-5	12.09	- 50.449667	sp8 sp.n.	5090	Lins et al., this study
NW Atlantic	B2 11-6	12.09033 3	- 50.449667	sp8 sp.n.	5091	Lins et al., this study
NW Atlantic	B2 11-7	12.09	-50.4495	sp8 sp.n.	5091	Lins et al., this study

Table S3. Marginal and sequential tests from DistLM (distance-based linear models) routines for nematode and *Acantholaimus* relative abundance (%). Environmental factors include: CPE (Chloroplastic Pigment Equivalents), %TN (total nitrogen), %TOC (total organic carbon), %TOM (total organic matter), avNPP (average net primary productivity), POC (particulate organic carbon), and SED (sediment diversity). Results of the marginal tests are related to the effect of each factor separately, while sequential tests show the effect of combined environmental variables on the nematode and *Acantholaimus* diversity. Significant p-values ($P < 0.05$), and the proportion of the total variation explained (Prop) and accumulative Prop (Cumul) are shown in bold for both marginal and sequential tests.

Marginal tests

Nematode community structure	SS(trace)	Pseudo-F	P	Prop.
CPE ($\mu\text{g/g}$)	2280.1	1.6530	0.009	6.44E-02
% TN	1181	0.8229	0.712	3.34E-02
% TOC	4458.8	34.6030	0.001	0.12601
%TOM	1000.8	0.6986	0.7949	2.83E-02
AvNPP	1874.6	13.4260	0.1544	5.30E-02
SED	2453.9	17.8840	0.0535	6.93E-02

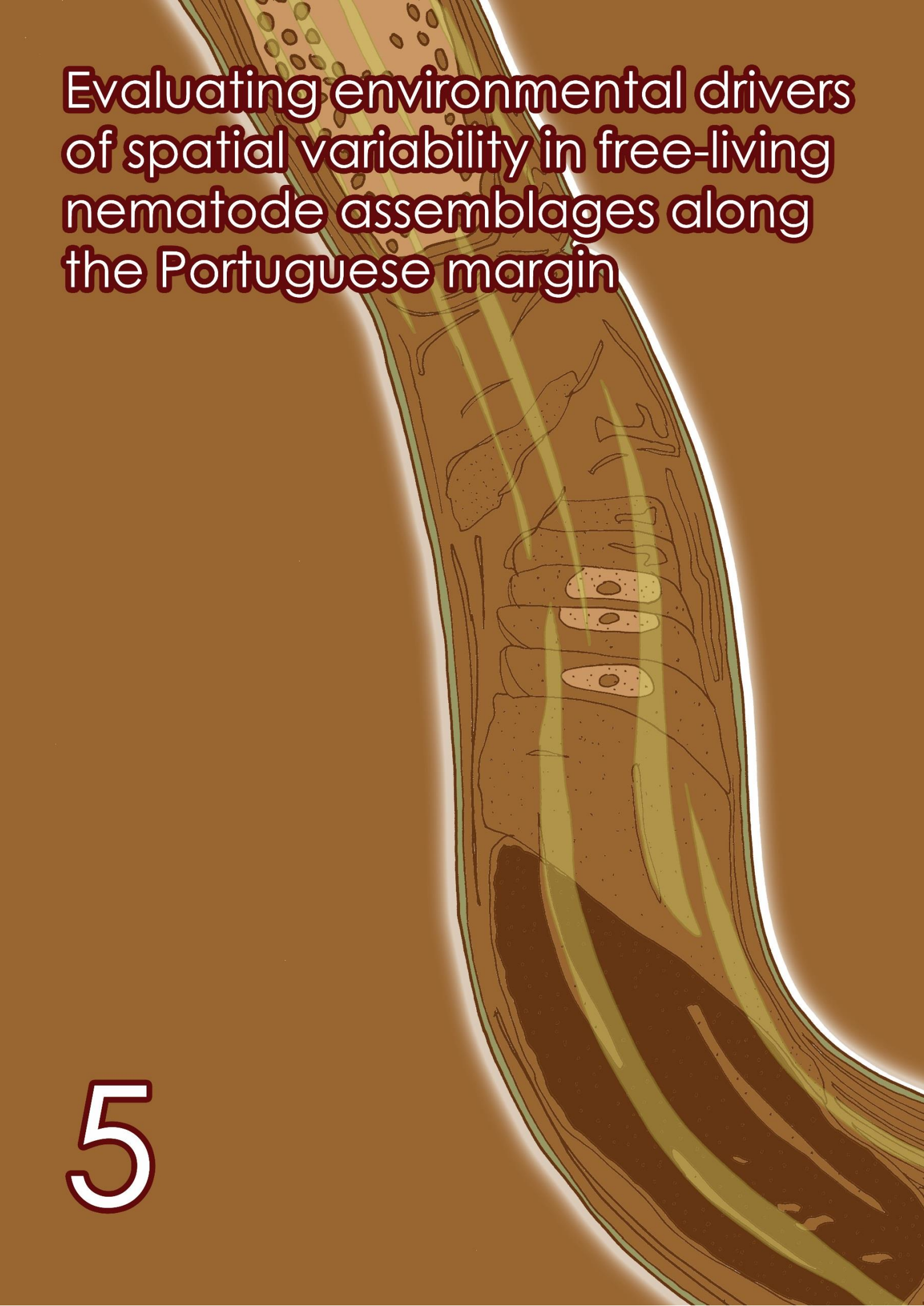
***Acantholaimus* species structure**

<i>Acantholaimus</i> species structure	SS(trace)	Pseudo-F	P	Prop.
CPE ($\mu\text{g/g}$)	4364.1	2.5188	0.0176	9.50E-02
% TN	1104.5	0.59115	0.7405	2.40E-02
% TOC	7929.9	5.0063	0.0003	0.17259
%TOM	1793.2	0.9747	0.4317	3.90E-02
AvNPP	4935.8	2.8886	0.0126	0.10743
SED	3372.5	1.9012	0.0827	7.34E-02

Sequential tests

Nematode community structure	Adj R²	SS(trace)	Pseudo-F	P	Prop.	Cumul.	res.df
+% TOC	8.96E-02	4458.8	34.6030	0.0009	0.12601	0.12601	24
+CPE ($\mu\text{g/g}$)	0.11777	2205.9	17.6650	0.0189	6.23E-01	0.18835	23
+NPP	0.13552	1801.4	14.7230	0.0779	5.09E-01	0.23926	22

<i>Acantholaimus</i> species structure	Adj R²	SS(trace)	Pseudo-F	P	Prop.	Cumul.	res.df
+% TOC	0.13812	7929.9	50.063	0.0006	0.17259	0.17259	24
+CPE ($\mu\text{g/g}$)	0.20221	4293.3	29.282	0.0011	9.34E-02	0.26603	23
+NPP	0.25157	3462	2.517	0.0126	7.54E-02	0.34139	22
+%TOM	0.28531	2677.3	20.384	0.0499	5.83E-02	0.39966	21
+SED	0.30174	1917.7	14.943	0.1585	4.17E-02	0.44139	20

A detailed illustration of a nematode, shown in a longitudinal section. The body is elongated and tapers slightly towards the right. The internal structure is visible, including the digestive tract, reproductive organs, and excretory system. The color palette is primarily brown and tan, with some yellow highlights. The nematode is set against a dark brown background.

Evaluating environmental drivers of spatial variability in free-living nematode assemblages along the Portuguese margin

5





Chapter 5: Evaluating environmental drivers of spatial variability in free-living nematode assemblages along the Portuguese margin

Manuscript currently under review as:

Lins L., Leliaert F., Riehl T., Ramalho S.P., Cordova E. A., Esteves A.M., Vanreusel A., 2016. "Species variability and connectivity in the deep sea: evaluating effects of spatial heterogeneity and hydrodynamics". **Biogeosciences Discussions**.

5.1 Abstract

Understanding processes responsible for shaping biodiversity patterns on continental margins is an important requirement for comprehending anthropogenic impacts in these environments and further management of biodiversity. Continental margins perform crucial functions linked to key ecological processes which are mainly structured by surface primary productivity and particulate organic matter flux to the seafloor, but also by heterogeneity in seafloor characteristics. However, to what extent these processes control local and regional biodiversity remains unclear. In this study, two isobathic parallel transects located at the shelf break (300–400 m) and upper slope (1000 m) of the Western Iberian margin were used to test how food input and sediment heterogeneity affect nematode diversity independently from spatial factors. We also examined the potential role of connectedness between both depth transects through molecular phylogenetic analyses. Regional generic diversity and turnover were investigated at three levels: within a station, between stations from the same depth transect, and between transects. High variability in food availability and high sediment heterogeneity at the shelf-break transect were directly linked to high diversity within stations, and higher variation in community

structure across stations compared to the upper slope transect. Contrastingly, environmental factors (food availability and sediment) did not vary significantly between stations located at the upper slope, and this lack of differences were also reflected in a low community turnover between these deeper stations. Finally, differences in nematode communities between both transects were more pronounced than differences within each of the isobathic transects, but these shifts were paralleled by the before-mentioned environmental shifts. These results suggest that changes in community structure are mainly dictated by environmental factors rather than spatial differences at the Western Iberian Margin. Furthermore, phylogenetic relationships revealed no evidence for depth-endemic lineages, indicating regular species interchanges across different depths.

5.2 Introduction

The link between biodiversity (i.e. species diversity) and ecological processes (e.g. carbon flow, surface productivity) has created a heightened interest in ecological research after large-scale human impacts were deemed responsible for declining species numbers and alterations of ecosystem properties (Loreau et al., 2001). Stretching between the coastal zone and the abyssal plains of the deep sea, continental margins (100–4000 m) encompass the largest habitat diversity in the marine environment (Levin and Dayton, 2009; Ramirez-Llodra et al., 2010). They harbour a high biodiversity, and are responsible for 90 % of the new biological productivity in oceans and seas, providing valuable food and energy resources for the marine fauna (Salgueiro et al., 2014).

It is generally accepted that principal biological oceanographic processes, such as carbon burial and nutrient cycling, remain concentrated within continental margins (Levin and Dayton, 2009). Yet, the biodiversity of continental margins is under severe threat by increasing commercial exploitation, ranging from fisheries, to gas, oil, and mineral

extraction (Levin and Dayton, 2009; Puig et al., 2012). The direct impact of these unabated commercial activities on the benthic environment and populations varies greatly, from pervasive sediment erosion, transportation and deposition, to the large-scale alteration of community composition (Puig et al., 2012). Therefore, continental margins comprise key locations to study the effects of environmental alterations on benthic biodiversity.

Understanding the processes that shape biodiversity patterns on continental margins is an important prerequisite for comprehending and managing anthropogenic impacts in these environments. Sea-surface processes have an important effect on the benthic fauna because part of the primary production is exported from overlying waters to the deep-sea floor, mostly in the form of phytodetritus, where it serves as food source to benthic communities (Billett et al., 1983; Lins et al., 2015; Serpetti et al., 2013; Wei et al., 2010). Particulate organic carbon input in the deep sea has been regarded as one of the main factors shaping benthic community structure and functioning (Rex, 1981). Phytodetritus creates patchiness, enhancing habitat heterogeneity, and consequently promotes species coexistence (Cardinale et al., 2000). In addition, water depth indirectly plays a role in structuring benthic communities, since organic matter flux is negatively related to depth, and deeper regions will consistently receive less input of labile organic matter compared to shallower regions (Danovaro et al., 2010; Garcia and Thomsen, 2008; Lutz et al., 2007; Ramalho et al., 2014). As a consequence of this decline in food availability, decreases in abundance and biomass associated with an increase in depth on the continental slopes have been observed for most benthic size classes (mega-, macro-, and meiofauna) (Flach et al., 2002; Muthumbi et al., 2011; Rex et al., 2005; Rowe et al., 2008; Thiel, 1978).

Food availability, as well as biological factors (predation, competition, facilitation, dispersal), are assumed to drive small-scale (1–10 m²) patterns of benthic communities (Gage, 1997) promoting local alpha diversity (Levin et al., 2001). Community differences

over large spatial scales (100–1000 m²; beta diversity) within continental margins have been observed both along bathymetric gradients as well as between different sites at similar depths. This indicates that beta diversity is not singularly depth-dependent (Danovaro et al., 2013; Easton and Thistle, 2016; Havermans et al., 2013; Leduc et al., 2012a). Physical factors, including near-bottom currents, sediment grain-size heterogeneity, boundary constraints, human activities, and topography are also considered of particular importance for beta diversity (Levin et al., 2001). They shape biodiversity as they may reduce the effect of a dominant species through the redistribution of resources among inferior and superior competitors (Stachowicz et al., 2007), and in this way increasing species diversity.

Moreover, population dynamics and dispersal (Derycke et al., 2013; Gage, 1997; Rex et al., 2005) have been shown to affect the structuring of benthic fauna at different spatial scales. Most benthic species have restricted active dispersal potential, although passive dispersal may be facilitated through ocean currents (Etter and Bower, 2015; Gallucci et al., 2008; Lins et al., 2014; Ullberg and Olafsson, 2003). The lack of a pelagic larval stage in free-living nematodes, the focus group of this study, could therefore be viewed as a disadvantage to dispersal. Nevertheless, this abundant and omnipresent group of benthic metazoans is found at all depths and in all deep-sea habitats (Giere, 2009; Vincx et al., 1994). Nematodes, which belong to the meiofauna (< 1 mm), exhibit high species richness and are one of the few taxa in which true cosmopolitan species may exist (Bik et al., 2010; Zeppilli et al., 2011). In shallow-water environments, some species were observed to have the ability to actively swim, following chemical cues, but more importantly, nematodes may be passively transported via water currents following resuspension from disturbance events (Jensen, 1981; Schratzberger et al., 2004). Molecular studies have indicated that different nematode taxa in diverse habitats exhibit population connectivity across a wide

geographical range, with some species showing subtle but significant genetic structuring at a small spatial scale, and other species exhibiting no differentiation along large distances (> 500 km). These findings confirm a high dispersal potential and low endemism for at least some species (Derycke et al., 2013, 2005). Nematodes therefore, hold ideal life history traits when seeking to understand dispersal, coexistence, and benthic-pelagic coupling in the deep sea.

Depth-related factors are thought to inhibit across-depth gene flow and thus to promote speciation in some taxa. This depth-range limitation provides another explanation for why the bathyal holds such a high biodiversity (Rex and Etter, 2010). However, while empirical data for macrofaunal molluscs, crustaceans, as well as octocorals has been found supporting this depth-differentiation hypothesis (France and Kocher, 1996; Jennings et al., 2013; Quattrini et al., 2015), it may not apply to nematodes, for which repeated and regular interchanges between depths have been observed (Bik et al., 2010).

Most previous research on nematode diversity has concentrated either on bathymetric differences (Danovaro et al., 2013; Muthumbi et al., 2011), or on geographical transects and macro-habitat heterogeneity (Baldrighi et al., 2014; Lambshead et al., 2000; Van Gaever et al., 2009). No studies so far has combined bathymetric with geographic analyses along an isobathic transect at a regional scale, which is crucial to understand patterns of biodiversity. Furthermore, the transition from the shelf to the slope remains a largely understudied area (Muthumbi et al., 2011; Vanaverbeke et al., 1997a, 1997b; Vanreusel et al., 1992), while major environmental shifts are observed here (Levin and Dayton, 2009). Through the analysis of two isobathic transects of about 20 km length, and separated by 30 km and 600 m water depth, we tested the effect of environmental (food availability and sediment heterogeneity) and spatial (depth and geographical distance) variables on nematode diversity. In this way, drivers for turnover in nematode taxonomic composition

were analysed at three spatial scales: within sites (i.e. beta diversity between cores from the same site), between sites from the same depth (i.e. beta diversity between sites belonging to the same depth transect), and between two depth transects. As food input and sediment heterogeneity are expected to vary more with depth than along regional isobathic transects, we expected a higher turnover in community composition between depths than within isobathic transects. To evaluate possible depth-mediated differentiation, genus turnover and phylogenetic relationships through DNA sequence clustering between the two isobathic transects was investigated based on 18S rDNA sequence data of selected nematode taxa. The following hypotheses were tested: (H1) Higher patchiness of food resources deposited at the seafloor results in a higher diversity at small spatial scales (i.e. beta diversity between cores from the same site); (H2) Increased sediment heterogeneity results in a higher beta diversity within sites; (H3) Beta diversity between different bathymetric transects is higher than beta diversity across similar depths; (H4) Clades/Taxa are shared between shelf break and slope areas.

5.3 Material and methods

5.3.1 Sampling and study area

The Western Iberian Margin (WIM) is characterized by a narrow shelf and steep slope (Garcia and Thomsen, 2008; Nolasco et al., 2013; Relvas et al., 2007). Primary production in this area increases in May–June and constitutes a significant proportion of the yearly production, reaching values higher than $90 \text{ g C m}^{-2} \text{ y}^{-1}$ (up to $171 \text{ g C m}^{-2} \text{ y}^{-1}$) (Salgueiro et al., 2014). The WIM exhibits seasonal upwelling with filaments that can penetrate more

than 200 km into the open ocean, influencing not only vertical transport but also horizontal particle transport from near shore towards the open ocean (Crespo et al., 2011; Figueiras et al., 2002; Relvas et al., 2007; Salgueiro et al., 2014, 2010). The high particle transport observed at the WIM occurs mainly due to the great bottom dynamics in the area. This region possesses an equatorward current flow generated by thermohaline structures of water masses and wind-forcing, eddy interactions with the alongshore circulation and buoyant plumes (Relvas et al., 2007). These features, together with shelf and coastal currents, upwelling filaments, and fronts, impact the subsurface circulation, internal waves, and consequently the transport of sinking particulate organic matter to the seabed (Alvarez-Salgado et al., 1997; Relvas et al., 2007).

During the RV Belgica B2013/17 (10.06.2013–18.06.2013) and B2014/15 (02.06.2014–10.06.2014) cruises to the WIM, sediment samples for nematode and environmental analyses were taken at the slope off the southwest coast of Portugal (Fig. 5.1). The study area comprised two main transects roughly parallel to the isobaths. The first transect was 23 km long, situated 294–445 m deep (further referred to as ‘shallow transect’), just beyond the shelf break; the second transect was located at the upper-slope, 19 km long, and at a water depth of 900–1006 m (named ‘deep transect’). The ‘shallow’ transect included six sites while the ‘deep’ transect comprised four sites (Table 5.1). Sampling was performed using a Multicorer (MUC) equipped with four Plexiglas tubes yielding samples with a virtually undisturbed sediment surface (inner core diameter 9.8 cm).

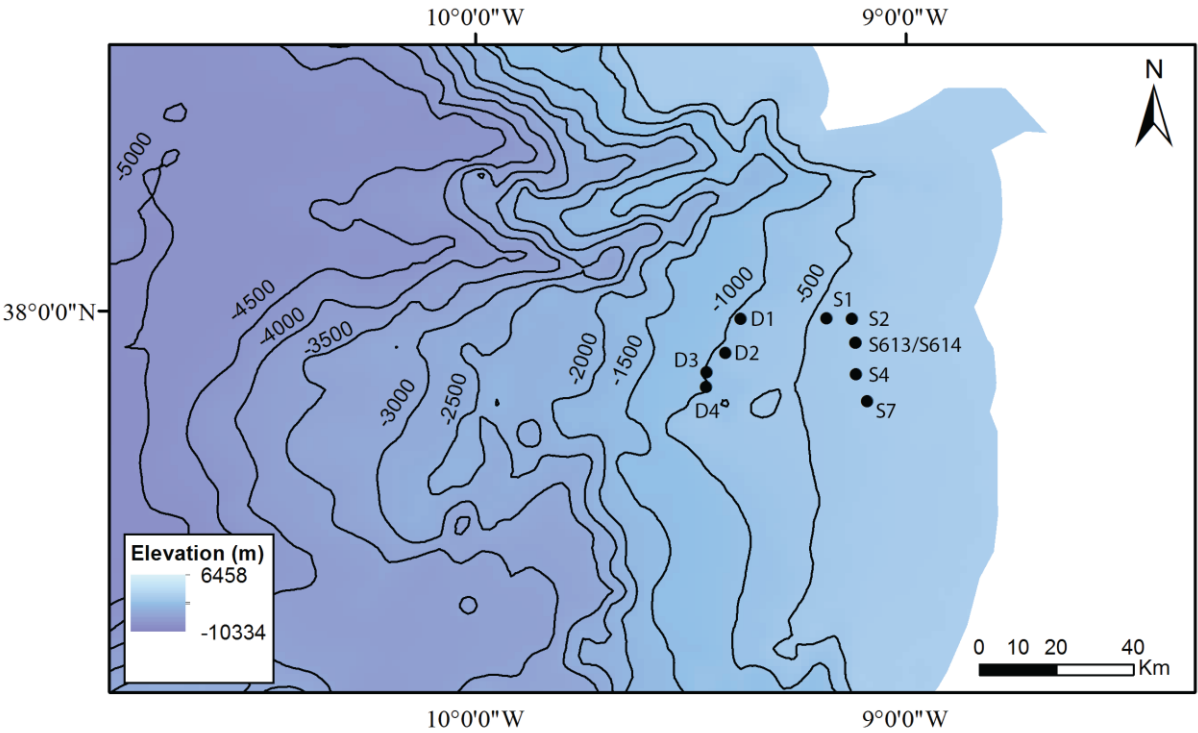


Figure 5.1. Location of B2013/17 and B2014/15 sites. Sampling sites are represented by black circles.

Table 5.1. Sampling details. St codes refer to sites sampled at the 'Shallow transect', while Deep codes refer to sites sampled at the 'Deep transect'. Each St site is characterized by three independent replicates obtained from three different deployments (three cores), while the Deep stations are characterized by four independent replicates obtained from four different deployments (four cores).

Site	Date	Depth (m)	Latitude	Longitude
St1	13/06/2013	445	37°58'959"N	09°11'050"W
St1	13/06/2013	445	37°58'953"N	09°11'094"W
St1	14/06/2013	445	37°58'967"N	09°11'090"W
St2	14/06/2013	335	37°58'904"N	09°07'525"W
St2	14/06/2013	335	37°58'913"N	09°07'528"W
St2	14/06/2013	335	37°58'888"N	09°07'513"W
St4	16/06/2013	325	37°51'171"N	09°06'944"W
St4	16/06/2013	325	37°51'188"N	09°06'974"W
St4	16/06/2013	325	37°51'174"N	09°06'950"W
St7	4/06/2014	295	37°47'448"N	09°05'430"W
St7	4/06/2014	294	37°47'494"N	09°05'442"W
St7	4/06/2014	290	37°47'490"N	09°05'380"W
St613	17/06/2013	296	37°55'597"N	09°06'998"W
St613	17/06/2013	298	37°55'594"N	09°07'001"W
St613	17/06/2013	298	37°55'594"N	09°07'002"W
St 614	3/06/2014	296	37°55'586"N	09°06'992"W
St 614	3/06/2014	294	37°55'455"N	09°06'934"W
St 614	3/06/2014	296	37°55'530"N	09°07'031"W
Deep1	5/06/2014	906	37°58'871"N	09°23'061"W
Deep1	5/06/2014	955	37°58'849"N	09°23'353"W
Deep1	5/06/2014	955	37°58'752"N	09°23'405"W
Deep1	6/06/2014	930	37°58'651"N	09°22'967"W
Deep2	5/06/2014	939	37°54'163"N	09°25'150"W
Deep2	5/06/2014	950	37°54'489"N	09°25'006"W
Deep2	5/06/2014	900	37°54'550"N	09°24'994"W
Deep2	5/06/2014	941	37°54'911"N	09°24'803"W
Deep3	5/06/2014	996	37°51'450"N	09°27'752"W
Deep3	5/06/2014	1001	37°51'650"N	09°27'615"W
Deep3	5/06/2014	998	37°51'567"N	09°27'606"W
Deep3	5/06/2014	950	37°51'595"N	09°27'324"W
Deep4	5/06/2014	900	37°49'375"N	09°27'839"W
Deep4	6/06/2014	957	37°49'661"N	09°28'042"W
Deep4	6/06/2014	1006	37°49'307"N	09°28'214"W
Deep4	6/06/2014	987	37°49'375"N	09°27'839"W

5.3.2 Sediment analyses

Three to four replicated samples for granulometric and geochemical analyses (1 g of sediment) from the first sediment layer (0–1 cm) were frozen at -80 °C. Grain-size distribution was measured with a Malvern Mastersizer 2000 (0.02–2000 µm size range) and divided into five categories, from silt-clay to coarse sand fractions (Buchanan, 1984). Sediment particle-size diversity (SED) was calculated as a measure for sediment heterogeneity from the percent dry weight of the five size classes mentioned above using the Shannon-Wiener diversity index (Etter and Grassle, 1992; Leduc et al., 2012b). Total sedimentary organic carbon (% TOC) and nitrogen (% TN) were determined with a Carlo Erba elemental analyser on freeze-dried and homogenized samples after acidification with 1 % HCl to eliminate carbonates. Total organic matter (% TOM) content was determined after combustion of the sediment samples at 550 °C.

Chlorophyll a (Chla), chlorophyll degradation products, and carotenes in the sediment were measured with a Gibson fluorescence detector (Wright and Jeffrey, 1997) after lyophilisation, homogenization, and extraction in 90 % acetone, and separation of the samples via reverse-phase HPLC (High-Performance Liquid Chromatography). Chloroplastic pigment equivalents (CPE: Chla + phaeopigments) were used as a proxy for surface-derived primary productivity at the seafloor.

5.3.3 Nematode sample processing for community analyses

At each site, three to four replicate samples of the 0–1 cm layer were used for nematode analysis. Samples were fixed on board with seawater buffered 4 % formalin. Sediment was washed over 1000 µm and 32 µm sieves. The fraction retained on the 32 µm sieve was centrifuged three times using LUDOX HS40 Dupont (specific gravity 1.19) as flotation

medium and then stained with Rose Bengal. In each sample, 140 nematode individuals (whenever enough present) were randomly picked out and gradually transferred to glycerine (De Grisse, 1969), mounted on glass slides and identified to genus level using relevant literature (Vanaverbeke et al., 2015; Warwick et al., 1998).

Functional diversity (based on the relative abundance of each trophic type) of nematodes was calculated using individuals trophic levels according to Wieser (1953): selective deposit feeders (1A), non-selective deposit feeders (1B), epistratum feeders (2A), and predators (2B), complementing the 2B group with the notion of ‘scavengers’ (Jensen, 1987). Trophic diversity (TD) was calculated using the index proposed by Heip et al. (1985):

$$TD = \frac{1}{\sum_{i=1}^4 q_i^2},$$

where q_i is the relative abundance of trophic type i . Taxonomic diversity was measured using Shannon-Wiener diversity (H'), expected nematode genus richness (EG (80)) and Pielou’s evenness (J). Each replicate (core) value was used as a measurement of alpha diversity, while differences in genus structure within sites (i.e. between cores from the same site), between sites from the same transect, and between transects were utilized to measure beta diversity.

5.3.4 Data analysis

Trends in environmental variables (% TOC, % TN, % TOM, Chla, CPE, carotenes, depth, sediment grain size, and SED) and univariate nematode variables (H' , J , EG (80), and TD) were investigated by means of Spearman rank correlations and Draftsman plots (Anderson et al., 2007) in R (R Core Team, 2013).

The untransformed nematode community data based on relative abundance of genera were analysed based on Bray-Curtis similarities (and Euclidean distances for the univariate data) by means of non-parametric multivariate ANOVA (PERMANOVA; Anderson et al., 2008) to assess differences between 'deep' (slope) and 'shallow' (shelf-break) areas (2-factor nested design). The 2-factor model included 'depth' as a fixed factor and 'site' as a fixed factor nested in 'depth'. Due to the use of an unbalanced design, the type I of sum of squares was chosen for the PERMANOVA analysis to make sure all possible re-arrangements of samples are equally likely (Anderson et al., 2008). A PERMANOVA analysis on the nematode community structure was conducted using the fixed factor 'year' to investigate whether samples collected in different years would influence the results, but differences between years were not significant. Subsequent pairwise pseudo *t*-tests were performed between all pairs of levels to determine where significant differences between each combination were found. Additionally, PERMDISP routines were used to test for homogeneity of multivariate dispersions between sites. PERMDISP results were not significant, indicating location differences through equally dispersed distances to centroids. SIMPER routines were executed based on Bray-Curtis similarity, with a cut-off of 90 % for low contributions. Dissimilarities within and between sites were compared with distances between geographical areas (km) and between depth differences (m).

The multivariate environmental data was first normalized (subtracted mean divided by standard deviation) and resemblance matrices were calculated based on Euclidean distances. Subsequently, PERMANOVA tests were performed using the same design as described for the multivariate nematode community data. PERMSDISP analyses were conducted on the multivariate environmental data to investigate variability in the environmental conditions between the two transects. Subsequently, SIMPER routines

were executed to identify which factors were responsible for between-transect differences. DistLM (distance-based linear model) routines were performed to analyse and model the relationship between nematode genus community and environmental variables with correlations lower than 0.9 (Chla, carotenes, CPE, % TN, silt-clay, very fine sand, medium sand, and coarse sand). Highly correlated variables (% TOC, % TOM, fine sand, and depth) were first transformed to cosine and if high correlations persisted they were excluded from the DistLM analysis. The DistLM model was built using a step-wise selection procedure and adjusted R^2 as a selection criterion. Euclidean distance was used as a resemblance measure for DistLM procedures and the results were displayed in dbRDA (distance-based redundancy analysis) plots.

5.3.5 Molecular phylogenetic analyses of nematodes

One sample (replicate) from each of the ‘shallow’ sites S4 and S2 and one from the ‘deep’ site D4 were preserved in DESS (Yoder et al., 2006) and used for molecular analyses. The first centimetre (0–1 cm) of each core was centrifuged with LUDOX HS40 Dupont, following the same protocol as for the community analysis (see above). One hundred nematodes were randomly picked out per sample under a stereomicroscope (50x magnification). Each individual was rinsed in sterile water, transferred to a microscope slide containing sterile water, and digitally photographed as morphological reference with a compound microscope Leica DMR and Leica LAS 3.3 imaging software. DNA extraction followed Derycke et al. (2005) using the entire specimens.

PCR amplification of the nuclear small subunit (SSU or 18S) rDNA was conducted using the primers G18S4 (5'-GCTTGTCTCAAAGATTAAGCC-3') and 22R (5'-GCCTGCTGCCTTCCTTGGA-3') (Blaxter et al., 1998). All PCR reactions were conducted

using an EXT PCR Kit, with a final reaction volume of 25 µl. Each reaction contained 2 µl of template solution containing nematode genomic DNA, 15.125 µl PCR grade water, 0.125 µl of each primer (25 mM), 2.5 µl 10x of PCR buffer, 2 µl of MgCl₂, 2.5 µl Loading dye, 0.5 µl dNTP 10mM and 0.125 µl DNA TopTaq polymerase. PCR amplifications were conducted for 39 cycles, each consisting of a 30s denaturation at 94 °C, 30 s annealing at 56 °C, and 30 s extension at 72 °C, with an initial denaturation step of 5 min at 94 °C and a final extension step of 10 min at 72 °C.

Successful PCR reactions were identified using agarose gels stained with ethidium bromide and were sequenced with both forward and reverse primers by Macrogen Europe (The Netherlands) with the fluorescent dye terminator Sanger sequencing method. The resulting reads were assembled using Mega 6.0 (Tamura et al., 2013). Sequences were checked for contamination using the BLAST algorithm on GenBank (Benson et al., 2008). The sequences that showed contamination or were of low quality (high amount of ambiguous nucleotides) were removed from the alignment. Nematode contig sequences (consensus of forward and reverse sequences) generated during this study were aligned using the MAFFT multiple sequence alignment algorithm (Katoh et al., 2009) as implemented in Geneious 9.0 (Kearse et al., 2012) at default settings (the alignment algorithm was automatically determined; scoring matrix was 200PAM / k=2; gap-opening penalty was 1.53 and the offset value was 0.123).

GenBank sequences for the most representative genera in the samples (all of the nematodes belonging to the class Chromadorea) were included from GenBank (Benson et al., 2008) (whenever available) to compare differences in genetic/phylogenetic diversity between different depths and locations. Sequences from Meldal et al. (2007) and from Bik et al. (2010) were used to compare genus diversity and diversity within the genus *Halalaimus*, respectively, between different habitats.

For both datasets, Modeltest 2.1 (Posada and Crandall, 1998) and jModeltest (Posada, 2008) were used to determine that the best suitable model for maximum likelihood analyses of the nuclear data was according to the Akaike Information Criterion (AIC) (Akaike, 1981) GTR+I+G.

Reconstruction of 18S relationships was conducted using Maximum Likelihood. The analyses were performed by means of Randomized Axelerated Maximum Likelihood (RAxML) (Stamatakis, 2006) in raxmlGUI (Silvestro and Michalak, 2012) using the fast Likelihood search with 1000 replicates to calculate Bootstrap support values.

For the *Halalaimus* dataset, Bayesian inference was additionally applied in MrBayes (Ronquist and Huelsenbeck, 2003) to supplement topological inferences. Analyses were run for 5 000 000 generations using 6 MCMC chains. From all runs the first 25 % of sampled trees were discarded as burn-in. Consensus trees were used for illustration here and were ordered and annotated in FigTree and Geneious tree viewer and colorized in Adobe Illustrator. In the supplement tree, line thickness indicates strength of bootstrap support.

5.4 Results

5.4.1 Environmental variables

Biogeochemical and granulometric properties of the sediment are shown in Figure 5.2. Nested PERMANOVA results for sediment particle-size diversity (SED) revealed significantly lower values ($p < 0.05$) at the ‘deep’ transect compared to the ‘shallow’ transect (Fig. 5.2D). Pairwise comparisons for SED showed significant differences for the

pairs [D2, D3] at the ‘deep’ transect and for all the pairs at the ‘shallow’ transect, except for [S1, S4], [S2, S614], and [S2, S613]. Sediment composition at the ‘deep’ sites was mainly composed of silt-clay fractions (81–89 %), while at the ‘shallow’ sites sediment was more heterogeneous. At the shelf-break, fine sand (25–42 %) dominated, except for S7, where medium sand showed a higher proportion (30 %). Nested PERMANOVA results showed significant differences in sediment composition between depth transects and among sites within the same transect ($p < 0.05$) (Table S1). Pairwise comparisons between sites showed higher variability in sediment composition for the ‘shallow’ sites, where the pairs of sites [S7, S2], [S2, S614], [S2, S613], and [S614, S613] showed similar sediment characteristics (Table S1). Pairwise comparison for ‘deep’ sites only showed differences between D2 and D3. Within-site comparison showed low variability (< 25 % deviation from the mean values) in silt-clay (Fig. 5.2E) and very fine sand (Fig. 5.2F) for most sites both shallow and deep (Fig. 5.2). Fine, medium, and coarse sand variability within each site was higher when compared to silt-clay and very fine sand (Fig. 5.2). Significantly higher values (nested PERMANOVA, $p < 0.05$) of % TOM (Table S2), % TOC (Table S3), and % TN (Table S4) were observed at the deeper transect. Additionally, ‘deep’ sites were not significantly different from each other ($p > 0.05$) for % TOM, % TOC and % TN, while ‘shallow’ sites exhibited significant differences between pairs of sites for % TOM (significantly different pairs: [S1, S4], [S1, S7], [S4, S7], [S4, S2], [S4, S614], and [S4, S613]), % TOC (significantly different pairs: [S1, S4], [S4, S2], [S4, S613], and [S614, S613]), and % TN (significantly different pairs: [S1, S4], [S4, S7], and [S4, S2]). No strong variability (< 25 % deviation from the mean values) was observed within sites for these three variables (Fig. 5.2). Chla ($0\text{--}0.17\ \mu\text{g g}^{-1}$), carotenes ($0\text{--}0.72\ \mu\text{g g}^{-1}$) and CPE ($0.01\text{--}1.79\ \mu\text{g g}^{-1}$) values were generally low. Chla showed no significant differences between depth transects ($p > 0.05$) and only the pairs [S1, S7] and [S1, S614] were significantly different from each other (Table S5).

In addition, Chla showed high variability ($> 25\%$ deviation from the mean values) at the ‘shallow’ sites, especially at S4 (Fig. 5.2). Carotenes and CPE also possessed high variability ($> 25\%$ deviation from the mean values) at the shelf-break sites, and revealed significant differences between depths and among pairs of sites ($p < 0.05$). For carotenes, the pairs of sites [S1, S4], [S1, S7], and [S1, S614] were significantly different from each other (Table S6), while for CPE only the pair [S1, S613] was significantly different (Table S7). Moreover, carotenes were completely absent at the ‘deep’ sites (Fig. 5. 2).

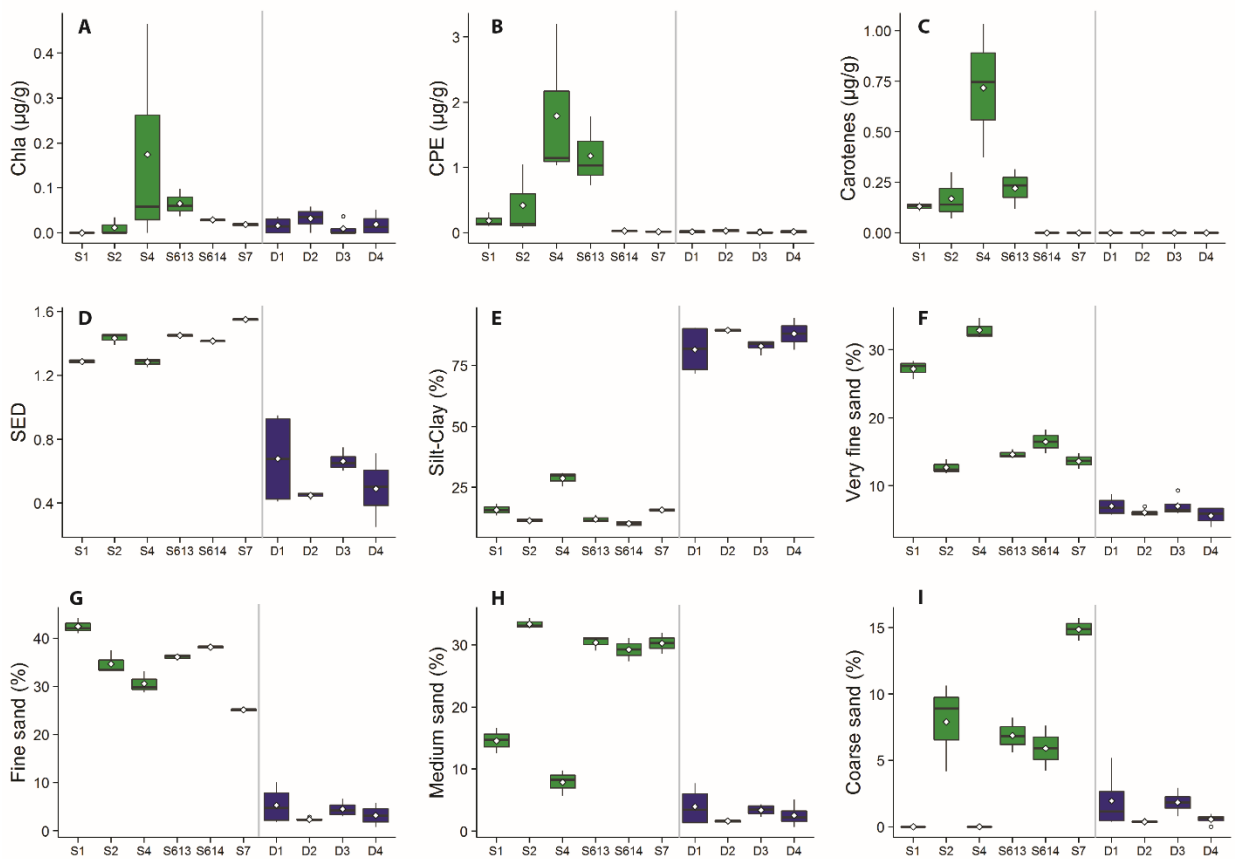


Figure 5.2. Environmental variables used in this study per site: Chla (Chlorophyll a), CPE (Chloroplasic Pigment Equivalent), Carotenes, SED (sediment diversity), Silt-Clay, Very fine sand, Fine sand, Medium sand, and Coarse sand. Green boxplots represent shallow sites and blue boxplots represent deep sites. Black lines represent the median, empty circles represent the mean, lower box indicates the first quartile and upper box the third quartile. Upper line of the boxes shows the maximum value and lower line the minimum value.

5.4.2 Nematode community structure

The most abundant nematode genera ($\geq 4\%$) per site are shown in Fig. 5.3. Total nematode density was significantly higher at the ‘shallow’ sites when compared to the ‘deep’ sites ($p < 0.05$), but pairwise comparisons revealed no significant differences between pairs of sites (Fig. 5.4). The genera *Acantholaimus* and *Halalaimus* dominated at all ‘deep’ sites (7.6–11.3 % and 7.2–11.7 %, respectively), whereas the ‘shallow’ sites showed high variability in the most abundant genera. Among the 155 identified genera, 62 were restricted to the ‘shallow’ areas, and 19 genera were only found in the ‘deep’ sites. Most of the genera showed low occurrence, with 87 genera found at relative abundances $< 1\%$. Evenness (J') was not different between the two transects and only revealed pairwise differences between D2 and D4 (Table S8). Shannon-Wiener (H') diversity at genus level varied from 3.18 (S1) to 3.74 (S613) at the ‘shallow’ sites and from 3.17 (D3) to 3.43 (D1) at the ‘deep’ transect (Fig. 5.4). In this sense, Shannon-Wiener (H') diversity was significantly higher at ‘shallow’ sites (nested PERMANOVA, $p < 0.05$), and the highest diversity was observed at S613 (Fig. 5.4, Table S9). Pairwise comparisons revealed significant differences between the pairs [S1, S7], [S7, S2], and [S2, S614]. Besides having the highest diversity, S613 also revealed the highest replicate variability (3.52 ± 0.19). Expected number of genera (EG(80)) varied from 27 (S2) to 34 (S4) at the ‘shallow’ sites and from 25 (D2) to 31 (D1) at the ‘deep’ sites (Fig 5.4). Nested PERMANOVA results revealed significant higher values at the ‘shallow’ sites when compared to the ‘deep’ sites ($p < 0.05$) for EG (80) (Table S10). Pairwise comparisons showed significant differences between the pairs [S1, S7], [S1, S614], [S7, S2], and [S2, S614].

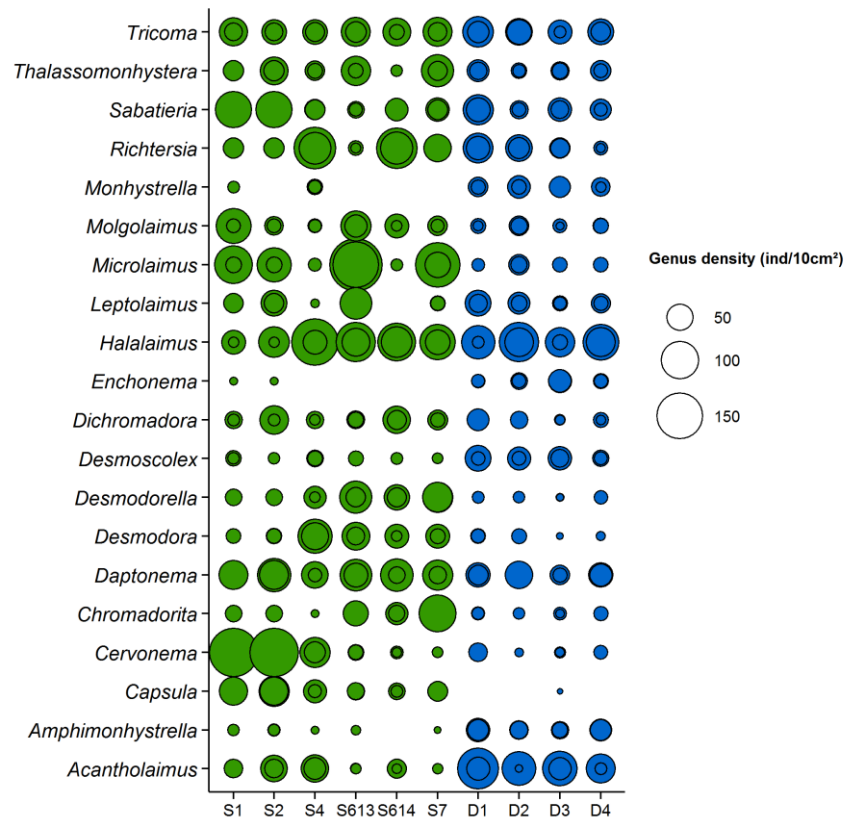


Figure 5.3. Most abundant nematode genera (> 4 %) per site. Inner circles indicate average genus density (ind/10 cm²) and outer circles genus standard deviation. Green circles represent shallow sites and blue circles deep sites.

Dissimilarities in nematode community structure between deployments within sites varied from 53–60 % (S1), 38–57 % (S2), 45–57 % (S4), 45–57 % (S613), 41–53 % (S614), and 42–58 % (S7) for the shallow sites, and 39–60 % (D1), 39–51 % (D2), 36–47 % (D3), and 44–64 % (D4) for the deep sites, thus revealing similar within-site variation for both transects. Moreover, dissimilarity values between sites increased with increasing geographical distance and sediment dissimilarity (Fig 5.5). SIMPER analysis revealed that the genera *Acantholaimus*, *Microlaimus*, *Richtersia*, and *Halalaimus* were mainly responsible for the average dissimilarity (63.99 %) between the two depth transects. The first genus was mainly found at ‘deep’ areas, whereas *Microlaimus* and *Richtersia* had higher densities at the ‘shallow’ sites. The genus *Halalaimus* showed similar average densities in both transects, but higher density fluctuations at the ‘shallow’ sites. Nested

PERMANOVA results showed significant differences between transects and among sites ($p < 0.05$) (Table S11). Pairwise comparisons revealed no significant differences between ‘deep’ sites, while the pairs of ‘shallow’ sites [S1, S7], [S4, S7], [S7, S2], and [S7, S613] possessed significant differences ($p < 0.05$) in nematode genera composition.

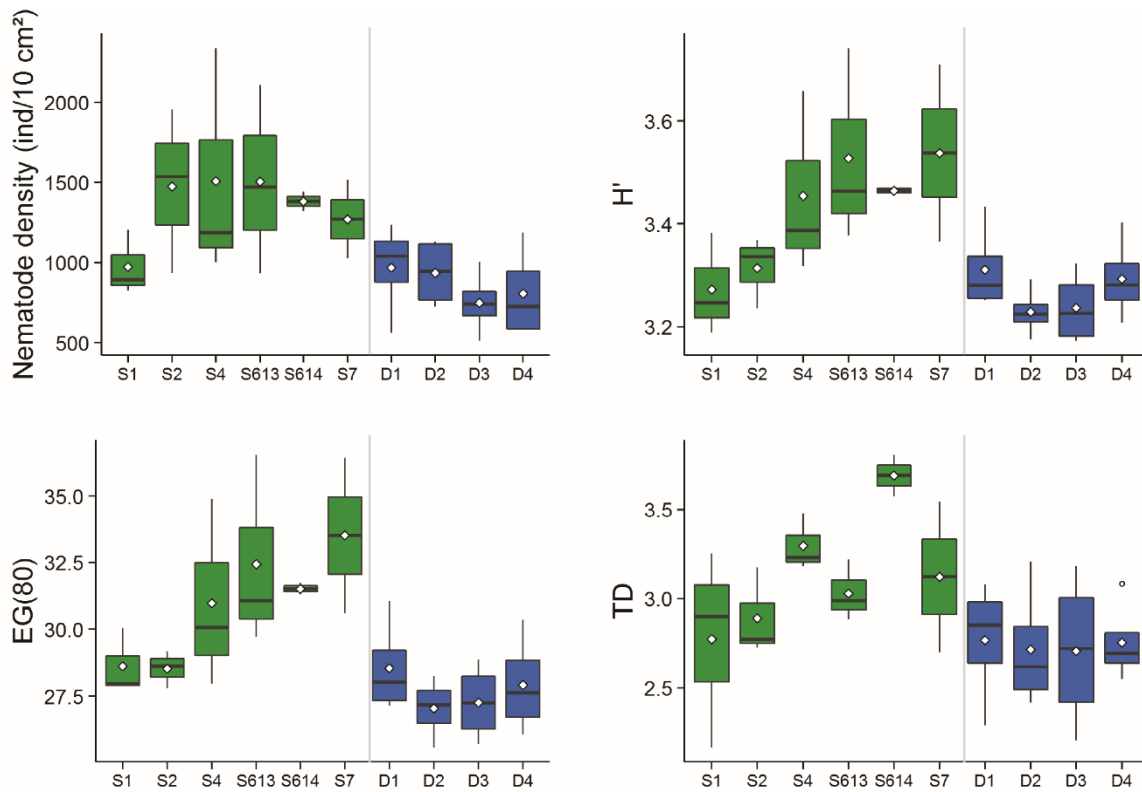


Figure 5.4. Nematode Shannon-Wiener (H') diversity, nematode density (individuals/10 cm^2), Expected number of genera (EG(80)) and trophic diversity (TD) per site. Green boxplots represent shallow sites and blue boxplots represent deep sites. Black lines represent the median, empty circles represent the mean, lower box indicates the first quartile and upper box the third quartile. Upper line of the boxes shows the maximum value and lower line the minimum value.

Trophic diversity revealed significantly higher values at the shallow sites ($p < 0.05$) but no significant pairwise difference was observed for the ‘shallow’ or ‘deep’ transects ($p > 0.05$) (Fig. 5.4). Nested PERMANOVA results for relative abundance of trophic groups displayed significant differences between the two transects, but not among sites from the same depth ($p > 0.05$) (Table S12). Average similarity between ‘deep’ and ‘shallow’ areas was 80 %. SIMPER analyses revealed that differences between depths were mainly due to the higher relative abundance of selective deposit feeders (1A) at deeper sites. The shallow

sites exhibited higher abundance of epistratum feeders (2A) and predators/scavengers (2B).

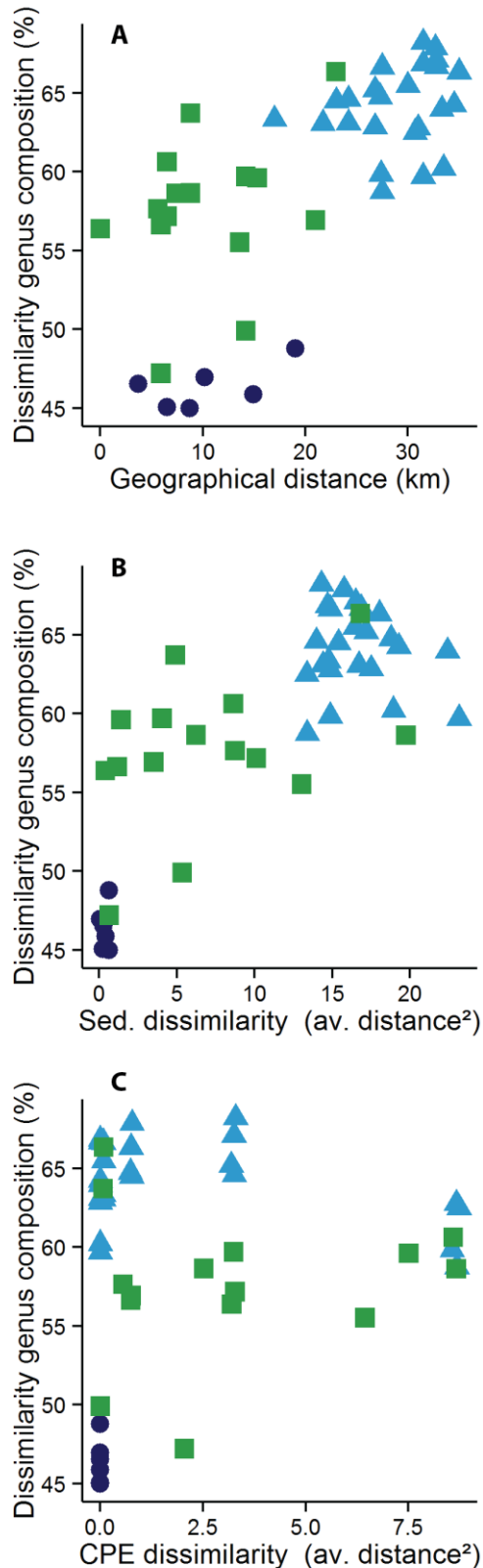


Figure 5.5. Dissimilarity values in nematode genus composition among geographical distance (A), sediment composition (B), and chloroplastic pigment equivalents (CPE). Green squares represent dissimilarities between shallow sites, dark blue circles between deep sites and light blue triangles show dissimilarities between shallow and deep.

5.4.3 Correlation between nematode community structure and environmental variables

The correlation between univariate diversity values (H' , J , EG (80), and TD) and environmental variables (% TN , % TOC , $Chla$, carotenes, CPE , sediment grain size, and SED) are shown in Table S13. Evenness (J') was not correlated to any environmental factor. Shannon-Wiener diversity (H') was negatively correlated to silt-clay, but positively correlated to very fine-medium sand, SED , and total carbon (% TOC) and nitrogen (% TN). EG (80) was negatively correlated with % TN , % TOC , and silt-clay, and positively correlated to CPE (Fig. 5.6), very fine sand, fine sand, medium sand, and SED (Fig. 5.6). Trophic diversity (TD) was negatively correlated with % TN and silt-clay, and positively correlated to $Chla$, CPE (Fig. 5.6), very fine sand, fine sand, and SED (Fig. 5.6).

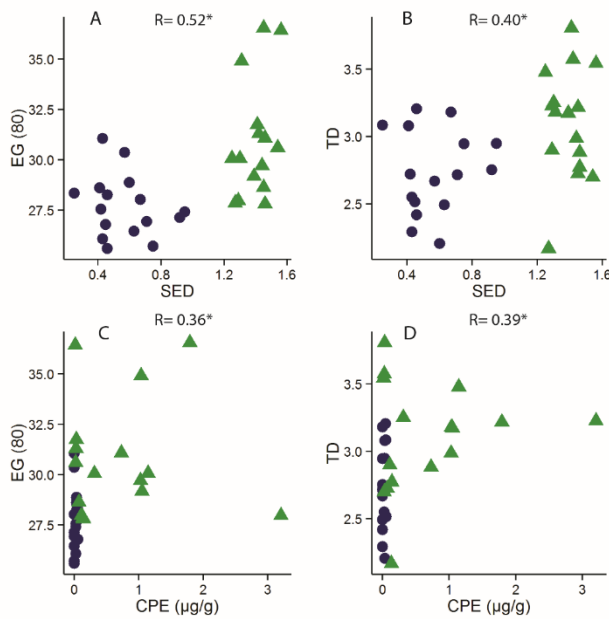


Figure 5.6. Scatterplot between (A) Sediment particle-size diversity (SED) and Expected genus diversity (EG (80)), (B) between SED and Trophic diversity (TD), (C) between EG (80) and Chloroplastic Pigment Equivalents (CPE) and (D) between TD and CPE. Green triangles represent correlations for shelf-break sites and dark blue circles between slope sites. R indicate correlation values of Spearman. * shows significant correlations.

PERMDISP results revealed a higher variability (2.4 ± 0.35 vs. 0.75 ± 0.087

after normalization of the data) in environmental conditions for the ‘shallow’ transect when compared with the ‘deep’ transect. According to the SIMPER results, these differences were mainly derived by higher average values of silt-clay and %TN in the ‘deep’ transect, and by the higher coarse sand content in the shallow transect, which together accounted for 45 % of the total dissimilarity. DistLM analyses based on twelve environmental variables explained 33 % of the total nematode diversity. Silt-clay accounted for 23 % of the total variation, being responsible for most differences found between ‘shallow’ and ‘deep’ sites (Fig. 5.7A). The other variables did not contribute significantly to the model and/or added < 5 % in explaining the total variation. When only ‘shallow’ sites were included in the model, the significant environmental variables explained 23 % of the total variation (Fig. 5.7B). Coarse sand was the main factor accounting for variation between ‘shallow’ sites (13 %). This sediment fraction showed highly fluctuating values (0.02–14.88 %) between sites of the ‘shallow’ areas.

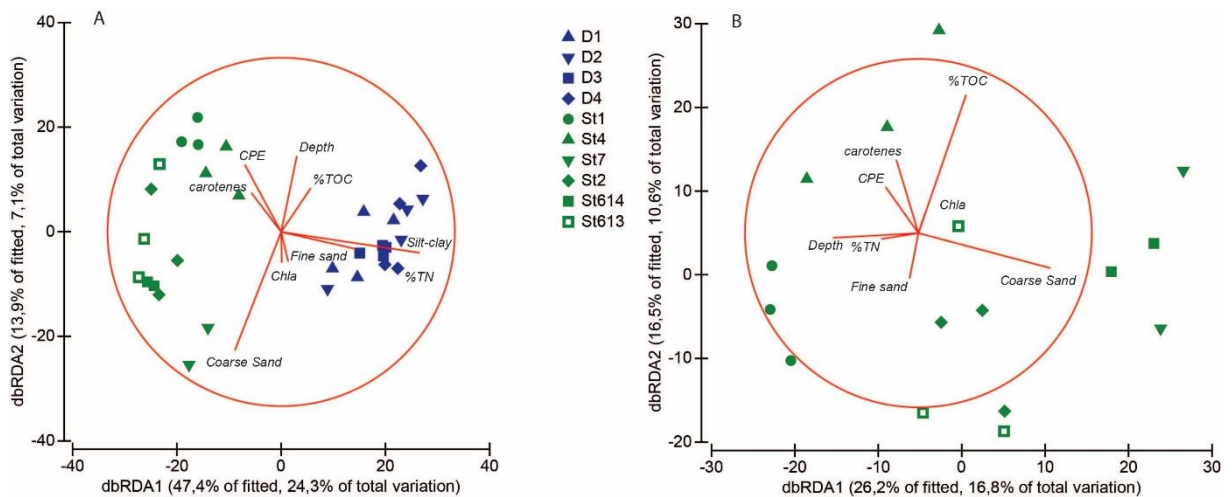


Figure 5.7. Distance-based redundancy analysis (dbRDA) illustrating the DistLM model based on the genera assemblage data for slope (blue) and shelf-break (green) sites (A) and only between shelf-break sites (B). Fitted environmental variables are shown with their vectors (strength and direction of effect of the variable on the ordination plot).

5.4.4 Nematode molecular phylogenetic analyses

From the 300 vouchered nematodes, the success rate of sequencing was only 30 %. For 199 specimens no PCR product was detected or sequences were of low quality. Phylogenetic analyses showed that the 101 sequenced nematodes belong to seven different orders of free-living marine nematodes (Table S14). The highest diversity derived from the successfully sequenced genera was reported for the order Enoplida, with 25 different 18S sequences, followed by the order Plectida (19 different 18S sequences) and Desmodorida (18 different 18S sequences). The Maximum Likelihood (ML) phylogeny inferred from 18S sequences is shown in Fig. S1.

In general, the backbone of the Chromadorea phylogeny was poorly supported, leading to several paraphyletic or polyphyletic orders and some families, such as Plectida, Desmodorida, and Oxystominidae. Well supported were the orders Tylenchida (bootstrap support (bs) = 99), Monhysterida (bs = 100), Dorylaimida (bs = 100), Monochida (bs = 100), and Tribolnchida (bs = 82). Desmodorida is polyphyletic in our analysis with the family

Microtrematidae forming a well-supported clade (bs = 100). The orders Chromadorida and Enoplida represent monophyletic but extremely weakly supported groups (bs = 5 and 41 respectively), while the orders Trefusiida and Triplonchida appeared nested within Enoplida. However, resolving the phylogenetic ties within Chromadorea was not within the scope of this article. What the consensus shows is that the 18S phylogeny supported the broad taxonomic representation of nematodes in the samples and furthermore indicated neither geographic nor depth clustering between ‘deep’ and ‘shallow’ taxa at any level of the tree topology (Fig. S1). This was moreover demonstrated within the best-represented and monophyletic (Fig. S1) genus in the dataset, *Halalaimus* (15 individuals, complemented with 42 GenBank sequences from different depths and locations globally distributed). Here, the new sequences showed no clustering related to depth or geography was observed but instead they seem randomly scattered between samples from different depths and regions (Fig. 5.8).

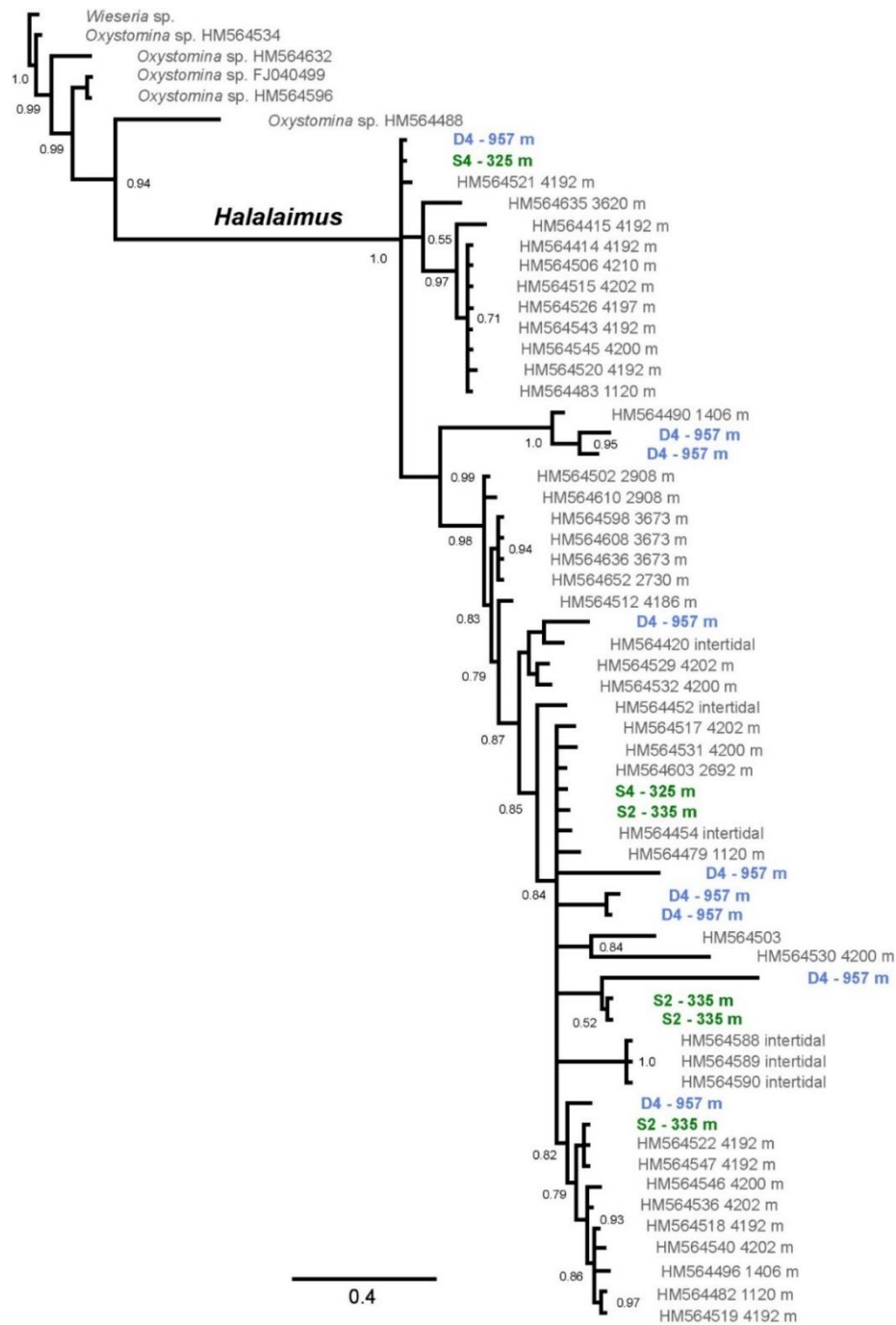


Figure 5.8. Consensus of Bayesian inference of phylogeny of the genus *Halalaimus* based on 18S rDNA sequence fragments generated in this study and from Bik et al. (2010); node support is given as posterior probabilities (PP); nodes with PP smaller than 0.50 were collapsed. The outgroup was set to *Wieseria*. The tree shows multiple instances of close relationships between individuals collected at different depth zones.

5.5 Discussion

Beta diversity within and between sites from the same transect along the Western Iberian Margin (WIM) were higher at the shelf break ('shallow' sites) when compared with the upper slope ('deep' sites). The lower within and between-site turnover observed at the upper slope occurred because nematode communities were in general dominated by the same genera (*Halalaimus* and *Acantholaimus*), while at the shelf break not only a higher beta diversity was present within site, but also the genus composition clearly differed between sites, resulting in a higher turnover. This higher within and between-site diversity and along transect turnover at the shallower sites coincided with a higher amount and patchiness in food supply, as well as a higher sediment heterogeneity within and between sites from the 'shallow' transect. However, the largest beta diversity community differences and therefore highest taxonomic turnover in nematode genera was present between transects, supported by the higher dissimilarities values observed between transects compared with within-transect variability. Nevertheless, the high number of shared genera between transects and the intermingled pattern of genetic clustering observed for *Halalaimus* suggested that depth differences did not restrict the distribution of nematodes.

5.5.1 Sediment heterogeneity in combination with increased amount and patchiness of food resources contributes to a higher beta diversity

In this study, nematode beta diversity within and between sites was significantly correlated with food availability. Moreover, the higher amount and variability (i.e. dissimilarities within and between sites from the same transect) of 'labile' food resources (Chla, CPE, and carotenes) within the 'shallow' sites when compared to the 'deep' sites (Fig. 5.2), was associated with a higher structural and trophic diversity. The interactions

between coastline features and wind forcing already reported for the WIM, certainly affect the export flux, and consequently the resource distribution on the seabed. For this region, the strong surface dynamics may explain the high variability of environmental variables, such as patchiness of food input and habitat heterogeneity, observed here, and consequently the high nematode beta diversity within and between sites exhibited at the 'shallow' sites (Cardinale et al., 2000; Crespo et al., 2011; Tokeshi, 1999). Concurrently, a different pattern was observed for the deeper transect, where the general lower amount and within and between-site variability of food resources were associated with a lower nematode beta diversity. A similar relationship between decreasing availability of 'labile' organic matter associated with a decrease in diversity was also observed at similar depths in other slope environments (Danovaro et al., 2013; Leduc et al., 2012a; Netto et al., 2005), and may thus represent a general pattern at continental margins.

Nevertheless, the relationship between food and beta diversity in the deep sea is still not well understood and seems to vary according to the different habitats studied. It appears that typical deep-sea communities dominated by similar genus composition can coexist in a food-depleted environment, while seemingly contrasting biodiversity at both local and regional scale increases with increasing food input. In this sense, when food input reaches a certain threshold, more competitive/opportunistic species are going to proliferate and dominate the community, setting a limit to the diversity of the system (Lins et al., 2015; Whittaker et al., 2001). This process may possibly explain why diversity in the deep sea is in general higher (at the slope) compared to coastal sediments (Gray, 2002; Moens et al., 2014), despite the higher food input in shallow waters.

However, the lower within and between-site beta diversity at the slope sites compared to the shelf break is not only explained by the lower and less patchy food input. In this study, beta diversity within and between site increased with increasing sediment dissimilarity

and sediment heterogeneity (SED), with SED also revealing positively correlated values with the expected number of genera and the trophic diversity within and between sites, exhibiting even stronger correlation results than the one between nematode diversity and CPE (Fig 5.6). In addition, distance-based linear models (DistLM) and SIMPER results based on the environmental data revealed a major significant effect of the silt-clay proportion on community beta diversity when compared between the two depth transects (Fig. 5.7). The high silt-clay contribution, together with the low variation in sediment composition within and between sites of the ‘deep’ transect, was associated with a lower beta diversity within and between sites in this area (Fig. 5.5). In addition, the lower trophic diversity (TD) and higher contribution of deposit feeders in the deep sites, were potentially caused by a combination between low food input and comparatively higher sediment stability for this transect, reflected by the finer sediment composition in relation to the ‘shallow’ sites (Fig. 5.2). The stability of the ‘deep’ transect seems to reduce the generic diversity, and favours the dominance of the genera *Acantholaimus* and *Halalaimus*, commonly abundant in deep-sea soft sediments (Vanreusel et al., 2010). This decline in TD with depth, positively associated with a decline in SED, was not observed in other studies along the slope, although the SED and TD values observed here were much higher than already reported before for other areas, and might reflect different environmental conditions at the WIM (Danovaro et al., 2013; Leduc et al., 2012b; Pape et al., 2013).

In this regard, the homogeneous silty sediments and the persistent low food availability along the ‘deep’ transect might reduce environmental variability, and may consequently limit the genus turnover within and between sites there. Contrastingly, the higher within and between-site trophic diversity at the ‘shallow’ sites suggests a higher niche differentiation within this transect and the possible transient stage of this habitat.

Moreover, higher prominence of opportunistic species and fast colonizers, such as *Microloaimus*, was observed at the shallower WIM sites (Fig. 5.3). The high abundance of opportunists has been reported for several bathyal areas in association with disturbance events (Muthumbi et al., 2011; Pape et al., 2013; Raes et al., 2010), pointing to potentially ongoing recolonization processes following the disturbances (Lee et al., 2001). The observed high densities of *Microloaimus*, which is considered both tolerant to disturbance and an early colonizer (Lee et al., 2001; Moreno et al., 2008; Raes et al., 2010), are in accordance with the assumed hydrodynamic regimes at the shallower sites and possible anthropogenic disturbance effects, for instance from fisheries, which further influence the bottom dynamics there (ICES, 2008; Quaresma et al., 2007; Relvas et al., 2007). Disturbance effects via either bedload movement or erosion and sedimentation of suspended load alters not only particle size, but also organic content. Thus, sediment heterogeneity in combination with increased patchiness of food resources deposited at the seafloor observed here were associated with a higher within and between-site beta diversity and trophic diversity at the shelf break compared to deeper areas. Disturbance has been suggested before as a strong driver for diversity in the deep sea, with disturbances ranging from small-scale bioturbation traces, to intermediate-scale phytodetritus falls, or large scale currents (Levin and Dayton, 2009). In our study, similar disturbances resulting in higher sediment heterogeneity and food patchiness at the sites located at the shelf break, are used to explain the higher within and between-site diversity compared to the 600 m deeper transect. Actually, the higher within and between-site beta diversity at the shelf break compared to the upper slope seems to contrast with the regular observed bathymetric diversity gradients for the deep sea, with mid-slope diversity maxima recorded for multiple taxa (Levin and Dayton, 2009; Rex, 1981). However, the higher diversity at genus level for nematodes at the shelf-break sites does not necessarily imply a higher species diversity for this environment, as some of the dominant deeper

water genera such as *Acantholaimus* and *Halalaimus* are known as highly diverse genera (De Mesel et al., 2006; Muthumbi and Vincx, 1997). Still, generic diversity may better represent the actual functional diversity for nematodes, as different genera are assumed to differ more in function than species within the same genus (Pape et al., 2013).

5.5.2 Beta diversity between different bathymetric transects is higher than beta diversity across similar depths

In general, dissimilarity in nematode genus structure increased with increasing geographical distance and DistLM results showed no significant effect of water depth on the nematode community structure. One has to take into account that geographical distances and depth distances were positively correlated as expected, as stations located far apart tend to belong to different depth transects. However, genus turnover between the ‘shallow’ sites was greater than between the ‘deep’ sites. If geographical distance was an important factor, one would also expect a similar high turnover for the ‘deep’ transect as observed for the ‘shallow’ transect as they are equally long. Concerning water depth, other studies on various taxa have shown that even small bathymetrical changes can be more important for promoting taxonomic differentiation than large geographical distances within the same depth (Havermans et al., 2013; Quattro et al., 2001). Nevertheless, water depth did not have a significant effect on the differences observed for the nematode community structure in this study, and explained only 3 % of the total nematode community variation between transects, appointing environmental differences as the main responsible factors for the higher beta diversity between transects rather than spatial differences. These findings suggest that diversity changes can be associated with both large and small-scale features driven by environmental alterations.

In general, beta diversity in the deep sea appears to be regulated by mechanisms of energy availability, biological interactions, disturbance, and habitat heterogeneity (Levin et al., 2001). In a large study comparing various water depths, Gray (2002) suggested that regional-scale species richness and turnover in the benthos are mainly affected by surface productivity, temperature and grain-size diversity. Changes in these features at the slope, like the WIM studied area, occur much faster with increasing depth than with increasing isobathic distances (Rex, 1981), even for short distances. However here, still a considerable percentage of shared genera occurred at both transects and some genera exhibited similar abundances for both shelf break and upper slope, such as *Tricoma*, *Daptonema*, and *Halalaimus* (Fig. 5.3). In this respect, our results do not support the idea of isolation by depth between the shelf break and slope at the WIM area (Bik et al., 2010; Riehl and Kaiser, 2012). To conclude, heterogeneity in sediment and possibly food availability to a lesser extent explain the main depth turnover patterns in this study, while depth and geographical distance are probably not the main cause for variations in community composition.

5.5.3 Absence of depth-specific clades

Although we observed differences in community structure between the shallow and deep sites, the large proportion of genera shared between the two depth transects may indicate that bathymetrical isolation between the respective populations does not exist (Fig. 5.3). Yet, such depth-differentiation could occur on the intra-specific and species level. In our study, phylogenetic relationships within and between the genera sampled at both shallow and deep sites revealed shared clades (Fig. S1), potentially representing eurybathic species and thus at least some degree of connectivity across depths, although we can make

no conclusions about spatial or time scales. The precise understanding of spatial variability and the processes which drive species diversity and connectivity in the deep sea are still poorly understood (Danovaro et al., 2013; Etter and Bower, 2015). Deep basins are confluent at extensive depths and connected by thermohaline circulation, suggesting they do not represent completely isolated systems (Levin et al., 2001). Processes such as deep-water formation and upwelling, potentially represent means of (passive) across-depths dispersal (Brandt, 1992; Brandt et al., 2007; Kussakin, 1973; Strugnell et al., 2008). Contrastingly, for some deep-sea taxa, such as protobranch bivalves, gastropods, and some crustaceans, depth-related diversification have been observed, indicating possible depth-related barriers to dispersal (Etter et al., 2011, 2005; Etter and Bower, 2015; Havermans et al., 2013; Wilson, 1983). The depth-related population differentiation observed in these studies, however, covered larger bathymetric ranges than the ones studied here, and were mostly situated at the lower bathyal and abyss (Etter et al., 2011; Etter and Bower, 2015). Just a few studies have assessed shallow-deep connectivity using a combined morphological and molecular approach (Bik et al., 2010; Riehl and Kaiser, 2012; Van Campenhout et al., 2014; Van Gaever et al., 2009). In contrast to the molluscs and crustaceans mentioned above, selected nematodes and isopods show high degrees of genetic similarity across depth, suggesting taxon-specific barriers (Bik et al., 2010; Riehl and Kaiser, 2012).

Except for *Halalaimus*, all deep-sea nematode genera sequences obtained in this study were sequenced for the first time. Although the relatively conserved 18S rDNA used here may not be the most suitable marker to assess dispersal, evolutionary rates of this gene are unknown for the nematode genera studied. Nevertheless, the presence of identical sequences between individuals from shallow and deep habitats (Fig. 5.8) provides hints towards dispersal between depths at relatively recent evolutionary time-scales. Our

results for *Halalaimus* are in accordance with Bik et al. (2010), revealing multiple historic interchanges between habitats of different depth for multiple species. Likewise, no clear geographical structuring was observed in our phylogenetic tree, although this result could be biased due to limited taxon and geographic sampling. Whether nematode dispersal occurs passively through hydrodynamics or is active employing chemical cues and active swimming, exchange among marine nematode assemblages can be maintained both over large (> 500 km) and small (50–100 km) geographical distances. This explains the success of these benthic organisms as colonizers (Boeckner et al., 2009; Derycke et al., 2013; Gallucci et al., 2008).

Even though our results indicate a link between shallow and deep habitats, other studies have suggested endemism in deep-sea habitats for nematodes (De Mesel et al., 2006; Van Campenhout et al., 2014). For example, *Halomonhystera disjuncta* was previously believed to occur in both shallow and deep habitats (Van Gaever et al., 2009), but a recent study based on 18S, COI, and ITS sequences showed that this species in fact constitutes two different lineages occupying deep and shallow environments, respectively (Van Campenhout et al., 2014). The bathymetric and geographic range was however broader than here.

Our phylogenetic results moreover highlight the scarcity of publically available DNA sequence data for deep-sea nematodes. For example, we present here the first sequence of the genus *Microtalamus* (no records in the GenBank, searched on 3 Dec 2015). Other genera are poorly represented in public sequence depositories (e.g. *Gammanema*: two 18S sequences, *Leptotalamus*: three 18S sequences, and *Richtersia*: two 28S sequences). The use of more specific and variable markers, such as the mitochondrial COI or the rDNA internal transcribed spacer, was not possible within this study due to low success rate of DNA amplification. Low success rates in PCR amplification are a known issue in deep-sea nematodes, but the causes are not well understood (Bik et al., 2010). Degradation of DNA

may have occurred during sample processing and could be caused by increases in temperature.

Genetic structuring of shallow-water nematode populations was shown by Derycke et al. (2013) based on more variable markers (COI, ITS). They showed that despite being capable of long distance dispersal, nematodes may also show clear genetic differentiation at small spatial scales. In this study, we demonstrated the high dispersal capabilities and connectivity for nematodes, but those were not high enough to counteract community differentiation observed in the genus composition. Moreover, it is likely that only a small number of species show relatively high dispersal (gene flow), while other species may have limited dispersal abilities.

5.6 Conclusions

Sediment heterogeneity seemed to be the most important factor responsible for the greater variation in nematode community structure within and between sites from the same transect, as well as between transects. ‘Deep’ sites were uniformly dominated by silt-clay and exhibited low nematode turnover and less variable nematode communities typically found in deep-sea soft sediments, dominated by the genera *Acantholaimus* and *Halalaimus*. Fig. 5.9 summarizes the main patterns (a) and processes (b) by illustrating the increase in generic turnover from beta 1 (beta diversity within and between sites from the ‘deep’ transect) to beta 2 (beta diversity within and between sites from the ‘shallow’ transect), and finally beta 3 (beta diversity between both transects). High sediment variability at the ‘shallow’ sites was associated with a more diverse and variable nematode community between sites, where high turnover was characterized by the dominance of different genera at each site. This high sediment heterogeneity at the shelf break suggests

that strong near-bottom current pulses might be an indirect factor promoting diversity at the scale of transect through the creation of patches and redistribution of resources. Moreover, the high beta diversity observed between transects surpassed the turnover within the shelf break and upper slope transects. These differences were attributed to the even higher differences in sediment variability observed between these two transects. This effect of sediment variability on the nematode community suggests that environmental factors were the main responsible for differences observed between sites and transects, rather than geographical distance or depth. Nevertheless, despite the larger differences observed between transects, still a considerable percentage of shared genera was observed between the shelf break and the upper slope. Finally, phylogenetic clusters suggested that depth may not be a factor isolating populations of the nematode genus *Halalaimus*.

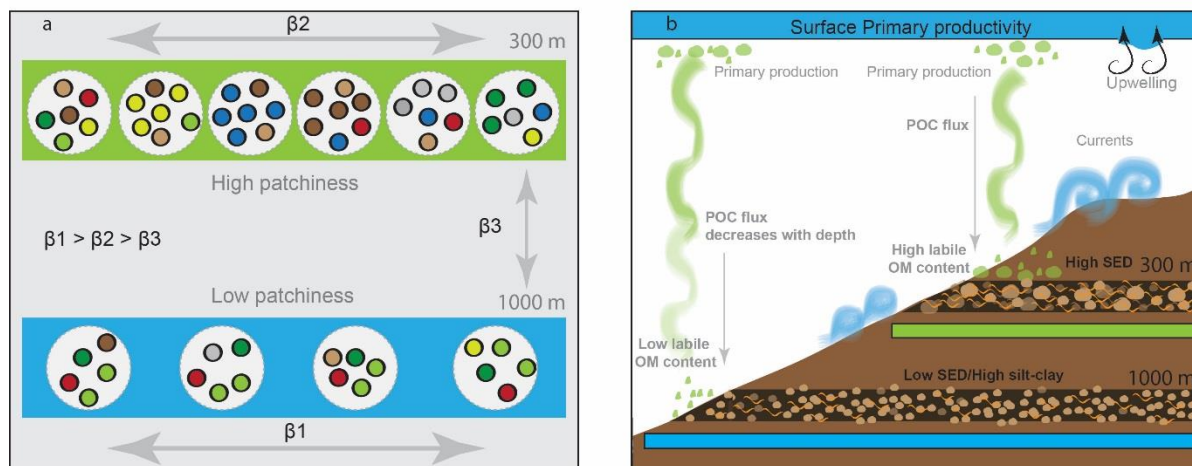


Figure 5.9. Scheme showing (a) how beta diversity varied across sites and between bathymetrical transects. The green bar represents the 'shallow' transect and the light blue bar the 'deep' transect. Grey circles inside the bars represent the sites sampled at each transect. Coloured circles inside grey circles refer to the variability in nematode genus composition within site and across sites. It illustrates the higher densities and patchiness found at the 'shallow' sites and the lower turnover found at the 'deep' sites. The (b) figure reveals the main environmental factors responsible for beta diversity between both depth transects. Upwelling effects, primary production, currents, and decrease of POC (particulate organic carbon) with increasing depth are considered to be correlated with both local and regional diversity. The fate of organic matter produced at the surface varies with depth, where deeper areas will receive lower labile organic matter (OM) when compared to shallower areas. This figure also illustrates the higher variability in sediment at the 'shallow' transect when compared to the deeper transect. The green bar represents the 'shallow' transect and the light blue bar the 'deep' transect.

5.7 Supplementary data

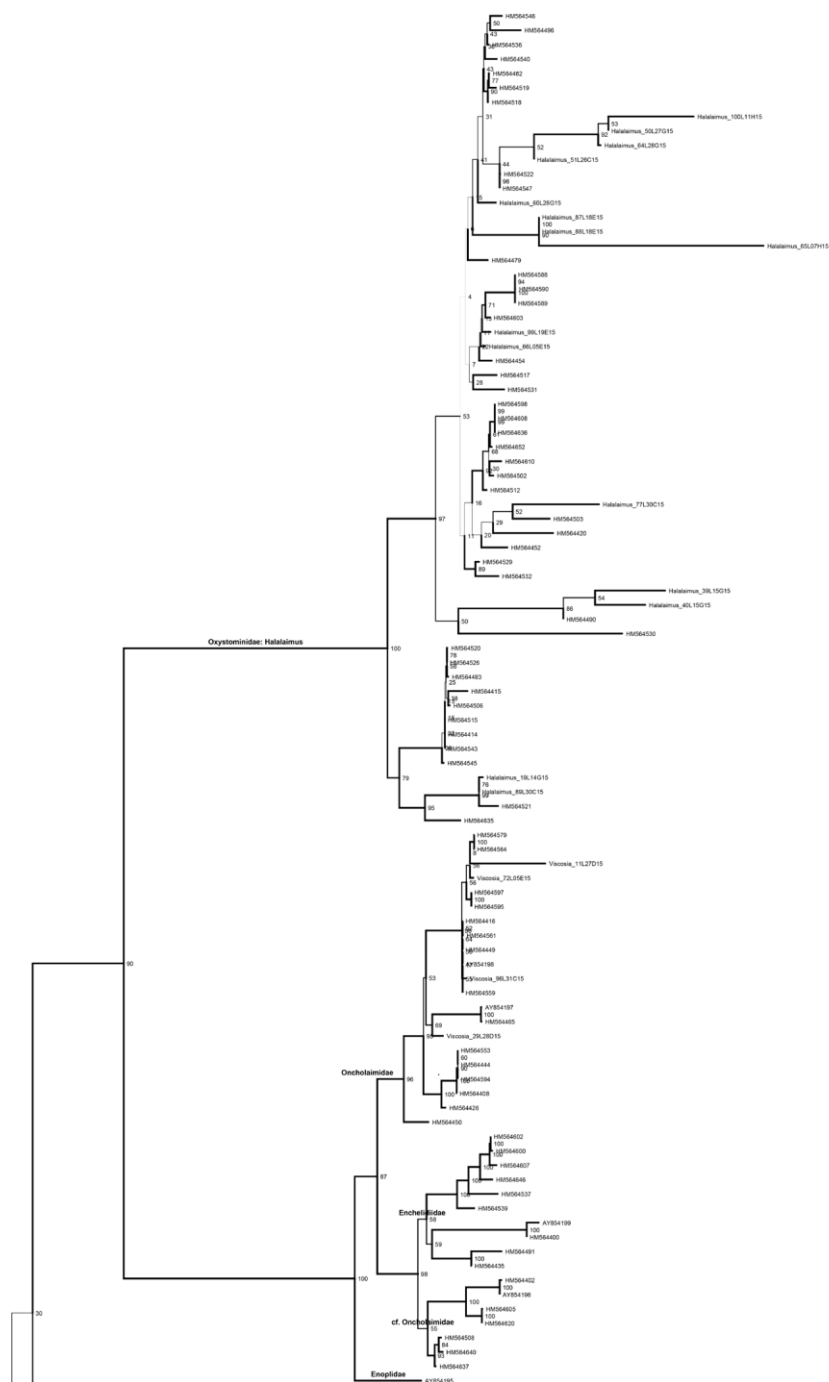


Figure S1 part 1. Partial-18S rDNA phylogeny of Nematoda: Chromadorea. The inferred relationships support a broad taxonomic representation of nematodes in samples from lower shelf and upper slope at the West-Iberian Margin and furthermore indicate neither geographic nor depth clustering between ‘deep’ and ‘shallow’ taxa at any level of the tree topology. Reconstruction of nematode 18S relationships was conducted using Maximum Likelihood. Bootstrap support values were generated using 1000 replicates and are presented as node support. The analyses were performed by means of Randomized Axelerated Maximum Likelihood (RAxML). Branch (line) width represents statistical support. Sequences retrieved from Genbank are represented by their Genbank Accession numbers. Orders and Families are annotated as branch labels. Continued next page.



Figure S1 part 2. Continuation from previous page. Partial-18S rDNA phylogeny of Nematoda: Chromadorea. The inferred relationships support a broad taxonomic representation of nematodes in samples from lower shelf and upper slope at the West-Iberian Margin and furthermore indicate neither geographic nor depth clustering between 'deep' and 'shallow' taxa at any level of the tree topology. Reconstruction of nematode 18S relationships was conducted using Maximum Likelihood. Bootstrap support values were generated using 1000 replicates and are presented as node support. The analyses were performed by means of Randomized Accelerated Maximum Likelihood (RAxML). Branch (line) width represents statistical support. Sequences retrieved from Genbank are represented by their Genbank Accession numbers. Orders and Families are annotated as branch labels. Continued next page.

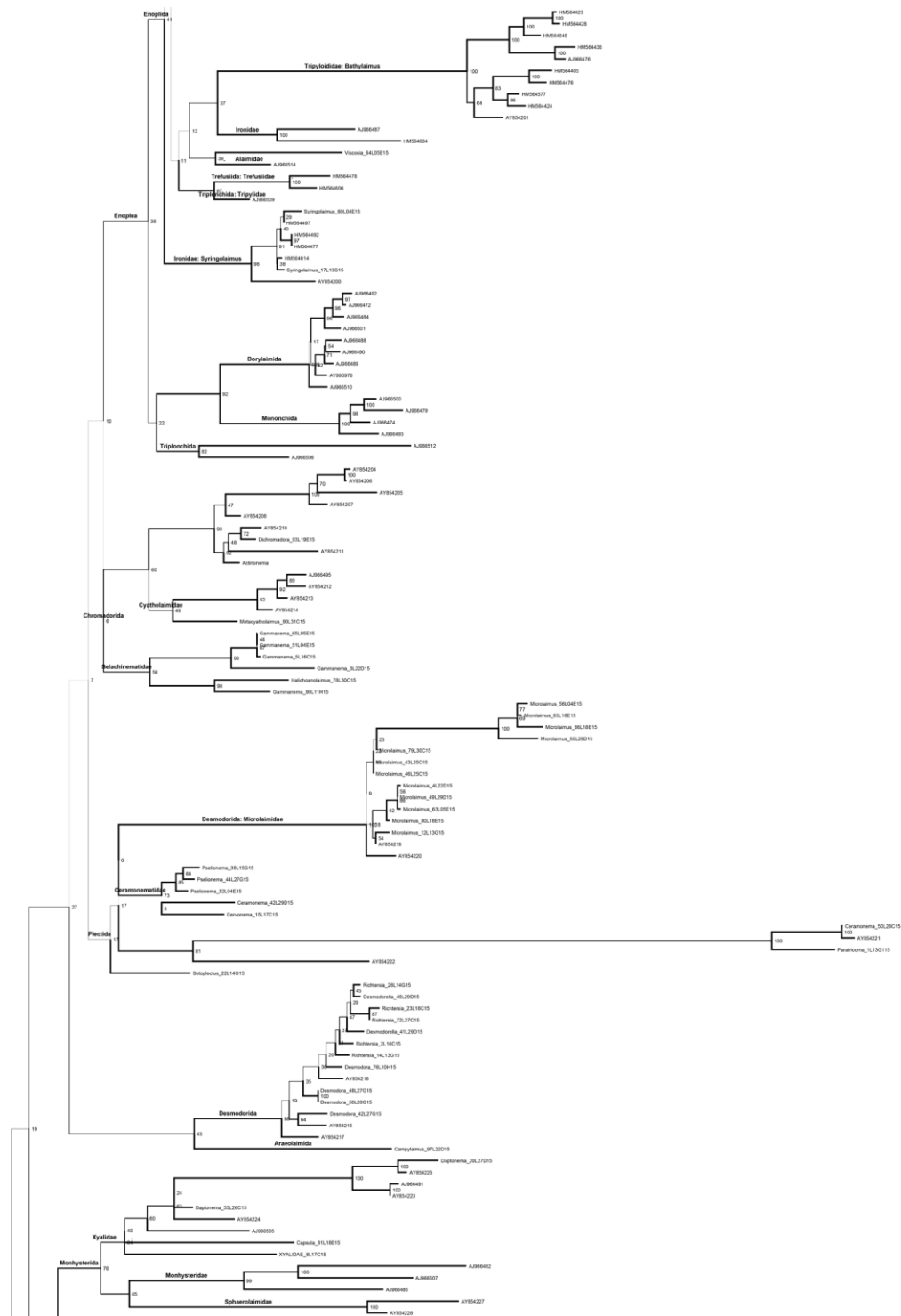


Figure S1 part 3. Continuation from previous page. Partial-18S rDNA phylogeny of Nematoda: Chromadorea. The inferred relationships support a broad taxonomic representation of nematodes in samples from lower shelf and upper slope at the West-Iberian Margin and furthermore indicate neither geographic nor depth clustering between 'deep' and 'shallow' taxa at any level of the tree topology. Reconstruction of nematode 18S relationships was conducted using Maximum Likelihood. Bootstrap support values were generated using 1000 replicates and are presented as node support. The analyses were performed by means of Randomized Accelerated Maximum Likelihood (RAXML). Branch (line) width represents statistical support. Sequences retrieved from Genbank are represented by their Genbank Accession numbers. Orders and Families are annotated as branch labels. Continued next page.

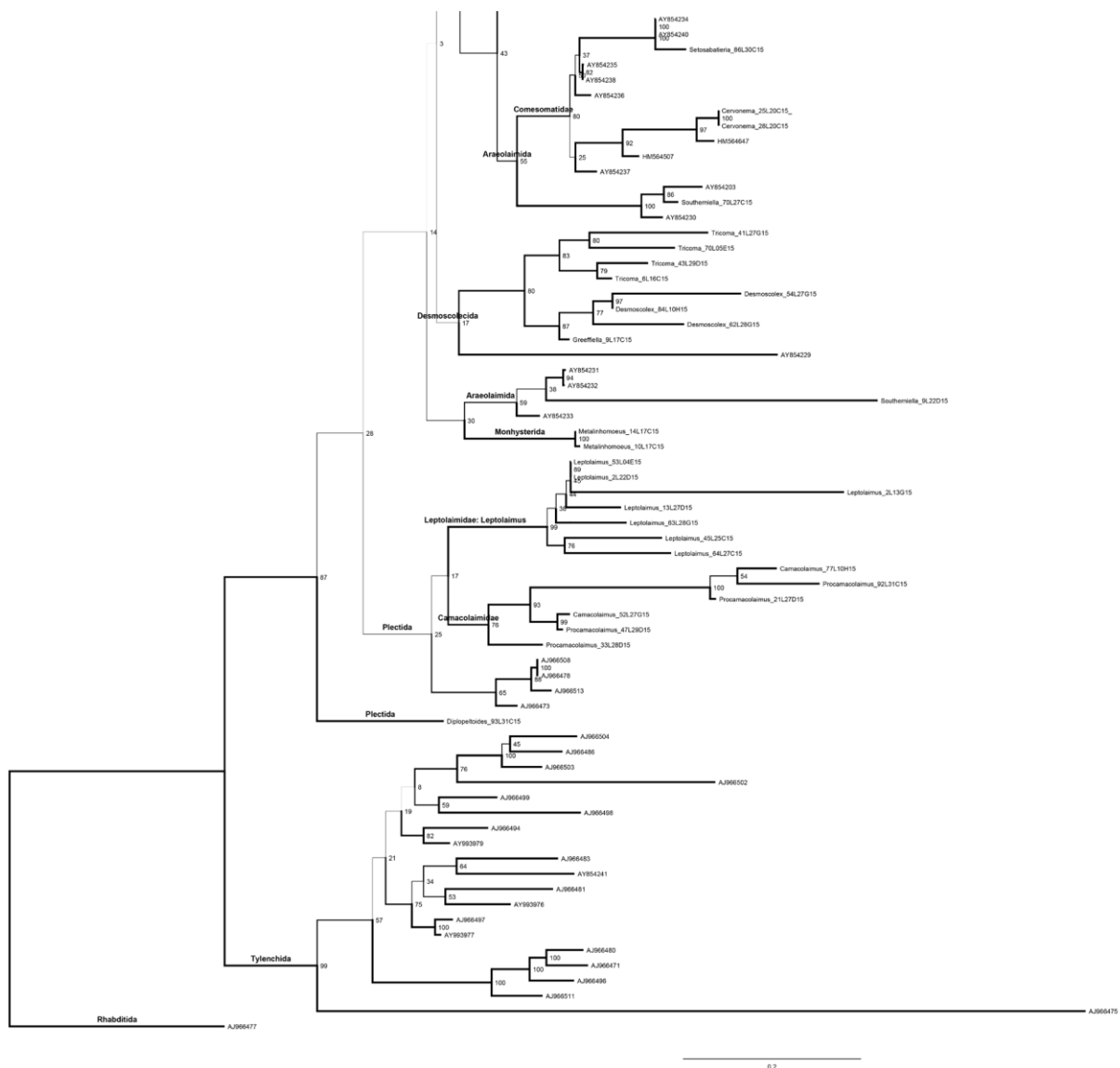


Figure S1 part 4 Continuation from previous page. Partial-18S rDNA phylogeny of Nematoda: Chromadorea. The inferred relationships support a broad taxonomic representation of nematodes in samples from lower shelf and upper slope at the West-Iberian Margin and furthermore indicate neither geographic nor depth clustering between 'deep' and 'shallow' taxa at any level of the tree topology. Reconstruction of nematode 18S relationships was conducted using Maximum Likelihood. Bootstrap support values were generated using 1000 replicates and are presented as node support. The analyses were performed by means of Randomized Axelerated Maximum Likelihood (RAXML). Branch (line) width represents statistical support. Sequences retrieved from Genbank are represented by their Genbank Accession numbers. Orders and Families are annotated as branch labels.

Table S1: Table of results from the multivariate PERMANOVA two-way nested design test and pairwise t-tests for sediment composition. Values in bold represent significant values.

PERMANOVA table of results

(2-factor design)

Source	df	SS	MS	Pseudo-F	P(perm)	Unique perms
Depth	1	105.29	105.29	18.037	0.0001	3014
Site(Depth)	8	45.042	56.302	28.113	0.0001	9929
Res	22	4.406	0.20027			
Total	31	155				

PAIR-WISE TESTS

Term 'Site(Depth)'

Within level 'DEEP' of factor 'Depth'

Groups	t	Unique perms	P(MC)
D1, D2	14.453	35	0.1792
D1, D3	0.21922	35	0.9647
D1, D4	11.404	35	0.2958
D2, D3	28.189	35	0.0069
D2, D4	0.74526	35	0.5381
D3, D4	17.462	35	0.0761

Within level 'SHALLOW' of factor 'Depth'

Groups	t	Unique perms	P(MC)
S1, S4	52.363	10	0.003
S1, S7	14.786	10	0.0009
S1, S2	59.548	10	0.0019
S1, S614	54.457	10	0.0091
S1, S613	10.274	10	0.0004
S4, S7	15.104	10	0.0006
S4, S2	72.374	10	0.0012
S4, S614	7.09	10	0.0039
S4, S613	12.505	10	0.0002
S7, S2	27.661	10	0.0538
S7, S614	41.579	3	0.0384
S7, S613	61.604	10	0.0052
S2, S614	10.659	10	0.3633
S2, S613	0.80935	10	0.4824
S614, S613	0.81016	10	0.4827

Table S2: Table of results from the multivariate PERMANOVA two-way nested design test and pairwise t-tests for Total Organic Matter (%). Values in bold represent significant values.

PERMANOVA table of results (2-factor design)						
Source	df	SS	MS	Pseudo-F	P(perm)	Unique perms
Depth	1	28.266	28.266	290.31	0.0001	3009
Site(Depth)	8	0.75128	9.39E - 01	13.912	0.2521	9951
Res	22	14.851	6.75E - 02			
Total	31	31				

PAIR-WISE TESTS			
Within level 'DEEP' of factor 'Depth'			
Groups	t	Unique perms	P(MC)
D1, D2	0.87706	35	0.4217
D1, D3	21.165	35	0.0754
D1, D4	15.794	35	0.1691
D2, D3	12.268	35	0.2658
D2, D4	0.4402	35	0.6675
D3, D4	0.94545	35	0.3833

Within level 'SHALLOW' of factor 'Depth'			
Groups	t	Unique perms	P(MC)
S1, S4	11.198	10	0.0007
S1, S7	38.705	10	0.0266
S1, S2	11.958	10	0.2997
S1, S614	0.69613	10	0.5438
S1, S613	10.709	10	0.3382
S4, S7	12.439	10	0.0012
S4, S2	59.381	10	0.0036
S4, S614	36.069	10	0.0344
S4, S613	81.676	10	0.0014
S7, S2	12.966	10	0.2882
S7, S614	0.7778	3	0.5241
S7, S613	21.078	10	0.1253
S2, S614	4.62E+02	10	0.966
S2, S613	0.2926	10	0.7816
S614, S613	0.13656	10	0.8993

Table S3: Table of results from the multivariate PERMANOVA two-way nested design test and pairwise t-tests for Total Organic Carbon (%). Values in bold represent significant values.

PERMANOVA table of results (2-factor design)						
Source	df	SS	MS	Pseudo-F	P(perm)	Unique perms
Depth	1	26.291	26.291	117.4	0.0001	2982
Site(Depth)	8	1.728	0.216	2.1723	0.069	9948
Res	22	2.1876	9.94E - 02			
Total	31	31				

PAIR-WISE TESTS			
Term 'Site(Depth)'			
Within level 'DEEP' of factor 'Depth'			
Groups	t	Unique perms	P(MC)
D1, D2	6.24E - 02	35	0.9529
D1, D3	14.616	35	0.1873
D1, D4	16.115	35	0.1564
D2, D3	14.857	35	0.1758
D2, D4	16.355	35	0.1542
D3, D4	0.52802	35	0.6053

Within level 'SHALLOW' of factor 'Depth'			
Groups	t	Unique perms	P(MC)
S1, S4	43.932	10	0.0122
S1, S7	4.85E - 02	10	0.9652
S1, S2	13.419	10	0.2483
S1, S614	2.617	10	0.0817
S1, S613	25.712	10	0.0576
S4, S7	21.765	10	0.1246
S4, S2	42.708	10	0.0146
S4, S614	20.996	10	0.1278
S4, S613	65.162	10	0.0028
S7, S2	0.85525	10	0.4525
S7, S614	0.97067	3	0.4335
S7, S613	13.943	10	0.2571
S2, S614	25.694	10	0.0849
S2, S613	0.49958	10	0.6475
S614, S613	47.643	10	0.0182

Table S4: Table of results from the multivariate PERMANOVA two-way nested design test and pairwise t-tests for Total Nitrogen (%). Values in bold represent significant values.

PERMANOVA table of results (2-factor design)						
Source	df	SS	MS	Pseudo-F	P(perm)	Unique perms
Depth	1	24.328	24.328	68.19	0.0001	2975
Site(Depth)	8	27.534	0.34417	1.7061	0.1601	9942
Res	22	4.4381	0.20173			
Total	31	31				

PAIR-WISE TESTS			
Term 'Site(Depth)'			
Within level 'DEEP' of factor 'Depth'			
Groups	t	Unique perms	P(MC)
D1, D2	0.23752	35	0.8175
D1, D3	25.534	35	0.0437
D1, D4	0.91472	35	0.3957
D2, D3	11.073	35	0.307
D2, D4	0.34137	35	0.7421
D3, D4	11.913	35	0.2883

Within level 'SHALLOW' of factor 'Depth'			
Groups	t	Unique perms	P(MC)
S1, S4	69.773	10	0.0025
S1, S7	0.721	10	0.5261
S1, S2	0.64104	10	0.5611
S1, S614	0.31006	10	0.7793
S1, S613	2.198	10	0.0956
S4, S7	59.241	10	0.0086
S4, S2	29.036	10	0.0439
S4, S614	24.086	10	0.0967
S4, S613	1.21	10	0.3018
S7, S2	0.91122	10	0.432
S7, S614	0.53866	3	0.6416
S7, S613	20.931	10	0.127
S2, S614	0.14015	10	0.8971
S2, S613	12.206	10	0.2886
S614, S613	10.775	10	0.3599

Table S5: Table of results from the multivariate PERMANOVA two-way nested design test and pairwise t-tests for Chlorophyll a ($\mu\text{g/g}$). Values in bold represent significant values.

PERMANOVA table of results (2-factor design)						
Source	df	SS	MS	Pseudo-F	P(perm)	Unique perms
Depth	1	13.669	13.669	1.149	0.3356	3010
Site(Depth)	8	93.176	11.647	12.613	0.2532	9929
Res	22	20.316	0.92343			
Total	31	31				

PAIR-WISE TESTS			
Term 'Site(Depth)'			
Within level 'DEEP' of factor 'Depth'			
Groups	t	Unique perms	P(MC)
D1, D2	10.171	15	0.3488
D1, D3	0.51803	4	0.6242
D1, D4	0.1894	8	0.8539
D2, D3	14.632	8	0.1959
D2, D4	0.74632	15	0.4786
D3, D4	0.63864	4	0.5448

Within level 'SHALLOW' of factor 'Depth'			
Groups	t	Unique perms	P(MC)
S1, S4	11.913	2	0.2975
S1, S7	51.545	4	0.014
S1, S2	1	1	0.3721
S1, S614	12.399	4	0.0009
S1, S613	36.177	4	0.0219
S4, S7	0.82471	10	0.4729
S4, S2	11.092	4	0.3256
S4, S614	0.77009	10	0.4918
S4, S613	0.74004	10	0.5107
S7, S2	0.45648	7	0.6853
S7, S614	1.801	3	0.2137
S7, S613	19.838	10	0.1435
S2, S614	11.506	7	0.3399
S2, S613	2.51	7	0.0636
S614, S613	15.554	10	0.2178

Table S6: Table of results from the multivariate PERMANOVA two-way nested design test and pairwise t-tests for Carotenenes ($\mu\text{g/g}$). Values in bold represent significant values.

PERMANOVA table of results (2-factor design)							
Source	df	SS	MS	Pseudo-F	P(perm)	Unique perms	P(MC)
Depth	1	80.288	80.288	33.462	0.0001	72	0.1063
Site(Depth)	8	17.986	22.482	99.215	0.0025	9931	
Res	22	49.853	0.2266				
Total	31	31					
PAIR-WISE TESTS							
Within level 'DEEP' of factor 'Depth'							
Groups	t						
D1, D2	Denominator is 0						
D1, D3	Denominator is 0						
D1, D4	Denominator is 0						
D2, D3	Denominator is 0						
D2, D4	Denominator is 0						
D3, D4	Denominator is 0						
Within level 'SHALLOW' of factor 'Depth'							
Groups	t	Unique perms	P(MC)				
S1, S4	3.064	10	0.0366				
S1, S7	82.415	7	0.0034				
S1, S2	0.56826	10	0.6052				
S1, S614	82.415	7	0.0031				
S1, S613	15.569	10	0.1943				
S4, S7	2.905	7	0.0644				
S4, S2	27.014	10	0.0501				
S4, S614	2.905	7	0.0624				
S4, S613	24.855	10	0.0662				
S7, S2	1.935	7	0.1469				
S7, S614	Denominator is 0						
S7, S613	29.953	7	0.0568				
S2, S614	1.935	7	0.1478				
S2, S613	0.58587	10	0.5934				
S614, S613	29.953	7	0.0579				

Table S7: Table of results from the multivariate PERMANOVA two-way nested design test and pairwise t-tests for Chloroplastic Pigment Equivalents (Chla + phaeopigments) in µg/g. Values in bold represent significant values.

PERMANOVA table of results (2-factor design)						
Source	df	SS	MS	Pseudo-F	P(perm)	Unique perms
Depth	1	72.472	72.472	3,644	0.0011	2997
Site(Depth)	8	14.936	1.867	46,588	0.0044	9952
Res	22	88.166	0.40075			
Total	31	31				

PAIR-WISE TESTS			
Term 'Site(Depth)'			
Within level 'DEEP' of factor 'Depth'			
Groups	t	Unique perms	P(MC)
D1, D2	10.171	15	0.3463
D1, D3	0.51803	4	0.6203
D1, D4	0.1894	8	0.8579
D2, D3	14.632	8	0.2005
D2, D4	0.74632	15	0.4802
D3, D4	0.63864	4	0.5548

Within level 'SHALLOW' of factor 'Depth'			
Groups	t	Unique perms	P(MC)
S1, S4	2.271	10	0.0893
S1, S7	19.895	10	0.1383
S1, S2	0.72924	10	0.5012
S1, S614	18.669	10	0.1548
S1, S613	30.912	10	0.0344
S4, S7	19.487	10	0.149
S4, S2	17.777	10	0.1472
S4, S614	19.374	10	0.1456
S4, S613	0.79021	10	0.4686
S7, S2	0.98405	10	0.4022
S7, S614	1.801	3	0.2116
S7, S613	28.504	10	0.0623
S2, S614	0.95874	10	0.4094
S2, S613	17.076	10	0.1721
S614, S613	28.251	10	0.0688

Table S8: Table of results from the multivariate PERMANOVA two-way nested design test and pairwise t-tests for Pielou's Evenness (J). Values in bold represent significant values.

PERMANOVA table of results (2-factor design)						
Source	df	SS	MS	Pseudo-F	P(perm)	Unique perms
Depth	1	1.7584	1.7584	0.88153	0.1758	1247
Site(Depth)	8	15.683	1.9604	2,188	0.0594	9944
Res	25	22.399	0.89596			
Total	34	39.745				

PAIR-WISE TESTS			
Term 'Site(Depth)'			
Within level 'DEEP' of factor 'Depth'			
Groups	t	Unique perms	P(MC)
D1, D2	19.931	35	0.0958
D1, D3	11.297	35	0.3015
D1, D4	11.256	35	0.3011
D2, D3	0.32117	35	0.7567
D2, D4	29.688	35	0.0243
D3, D4	1.803	35	0.1204

Within level 'SHALLOW' of factor 'Depth'			
Groups	t	Unique perms	P(MC)
S1, S4	21.911	10	0.0943
S1, S7	20.528	35	0.0978
S1, S2	15.427	10	0.2033
S1, S614	21.028	10	0.1003
S1, S613	25.457	10	0.0622
S4, S7	0.55518	35	0.6002
S4, S2	0.59708	10	0.594
S4, S614	0.87619	10	0.4363
S4, S613	0.39437	10	0.7203
S7, S2	0.16946	35	0.8749
S7, S614	0.25975	35	0.8047
S7, S613	0.30146	35	0.7719
S2, S614	2.61E+02	10	0.9849
S2, S613	0.43361	10	0.6828
S614, S613	16.224	10	0.1798

Table S9: Table of results from the multivariate PERMANOVA two-way nested design test and pairwise t-tests for Shanon-Wiener diversity (H'). Values in bold represent significant values.

PERMANOVA table of results (2-factor design)						
Source	df	SS	MS	Pseudo-F	P(perm)	Unique perms
Depth	1	51.09	51.09	7.9858	0.0002	1256
Site(Depth)	8	49.471	6.1838	2.5175	0.0373	9950
Res	25	61.407	2.4563			
Total	34	166.19				

PAIR-WISE TESTS			
Term 'Site(Depth)'			
Within level 'DEEP' of factor 'Depth'			
Groups	t	Unique perms	P(MC)
D1, D2	17.005	35	0.1381
D1, D3	13.561	35	0.2245
D1, D4	0.30917	35	0.7694
D2, D3	0.17259	35	0.866
D2, D4	13.559	35	0.2259
D3, D4	10.458	35	0.3463

Within level 'SHALLOW' of factor 'Depth'			
Groups	t	Unique perms	P(MC)
S1, S4	15.485	10	0.196
S1, S7	29.366	35	0.0328
S1, S2	0.60365	10	0.581
S1, S614	34.028	10	0.0261
S1, S613	20.977	10	0.1072
S4, S7	0.83038	35	0.4459
S4, S2	12.653	10	0.2845
S4, S614	0.24289	10	0.8228
S4, S613	0.48703	10	0.657
S7, S2	26.766	35	0.0477
S7, S614	0.89408	35	0.4069
S7, S613	0.22099	35	0.8393
S2, S614	37.889	10	0.0211
S2, S613	18.584	10	0.141
S614, S613	0.4437	10	0.6826

Table S10: Table of results from the multivariate PERMANOVA two-way nested design test and pairwise t-tests for Expected genera (EG(80)). Values in bold represent significant values.

PERMANOVA table of results 2-Factor design						
Source	df	SS	MS	Pseudo-F	P(perm)	Unique perms
Depth	1	94.88	94.88	91.429	0.0002	1256
Site(Depth)	8	80.234	10.029	24.215	0.0431	9941
Res	25	103.55	41.419			
Total	34	287.97				

PAIR-WISE TESTS			
Term 'Site(Depth)'			
Within level 'DEEP' of factor 'Depth'			
Groups	t	Unique perms	P(MC)
D1, D2	14.246	35	0.2109
D1, D3	11.205	35	0.3101
D1, D4	0.48756	35	0.6461
D2, D3	0.24395	35	0.8191
D2, D4	0.80301	35	0.4529
D3, D4	0.55524	35	0.6

Within level 'SHALLOW' of factor 'Depth'			
Groups	t	Unique perms	P(MC)
St1, St4	10.783	10	0.3402
St1, St7	33.664	35	0.0202
St1, St2	0.1162	10	0.9148
St1, St614	40.957	10	0.0132
St1, St613	17.301	10	0.1543
St4, St7	12.852	35	0.2603
St4, St2	11.654	10	0.3065
St4, St614	0.31719	10	0.7634
St4, St613	0.50139	10	0.6393
St7, St2	36.149	35	0.0141
St7, St614	15.434	35	0.1759
St7, St613	0.62355	35	0.5594
St2, St614	71.147	10	0.0018
St2, St613	18.401	10	0.139
St614, St613	0.38887	10	0.7209

Table S11: Table of results from the multivariate PERMANOVA two-way nested design test and pairwise t-tests for nematode community structure. Values in bold represent significant values.

PERMANOVA table of results (2-factor design)						
Source	df	SS	MS	Pseudo-F	P(perm)	Unique perms
Depth	1	13517	13517	6.7478	0.0001	1259
Site(Depth)	8	15514	1939.2	1.5908	0.0002	9745
Res	25	30475	1219			
Total	34	59461				

PAIR-WISE TESTS			
Term 'Site(Depth)'			
Within level 'DEEP' of factor 'Depth'			
Groups	t	Unique perms	P(MC)
D1, D2	0.76301	35	0.6748
D1, D3	0.9061	35	0.5955
D1, D4	0.84413	35	0.5596
D2, D3	10.155	35	0.5461
D2, D4	0.86606	35	0.6436
D3, D4	0.88881	35	0.5671

Within level 'SHALLOW' of factor 'Depth'			
Groups	t	Unique perms	P(MC)
S1, S4	1.248	10	0.1862
S1, S7	19.035	35	0.0271
S1, S2	12.887	10	0.163
S1, S614	15.582	10	0.0634
S1, S613	11.945	10	0.2147
S4, S7	16.065	35	0.0475
S4, S2	12.669	10	0.1312
S4, S614	15.113	10	0.0645
S4, S613	12.013	10	0.1635
S7, S2	1.67	35	0.0263
S7, S614	12.541	35	0.1685
S7, S613	16.441	35	0.0321
S2, S614	14.735	10	0.0795
S2, S613	0.77248	10	0.5591
S614, S613	12.894	10	0.1084

Table S12: Table of results from the multivariate PERMANOVA two-way nested design test and pairwise t-tests for nematode trophic composition. Values in bold represent significant values.

PERMANOVA table of results (2-factor design)						
Source	df	SS	MS	Pseudo-F	P(perm)	Unique perms
Depth	1	1974.6	1974.6	14,297	0.0001	1257
Site(Depth)	8	1068.2	133.53	1.2756	0.252	9929
Res	25	2617	104.68			
Total	34	5606				
PAIR-WISE TESTS						
Term 'Site(Depth)'						
Within level 'DEEP' of factor 'Depth'						
Groups	t	Unique perms	P(MC)			
D1, D2	0.51763	35	0.7986			
D1, D3	0.37384	35	0.8148			
D1, D4	0.71546	35	0.6113			
D2, D3	0.38009	35	0.8575			
D2, D4	0.51489	35	0.7931			
D3, D4	0.38968	35	0.8603			
Within level 'SHALLOW' of factor 'Depth'						
Groups	t	Unique perms	P(MC)			
S1, S4	0.58178	10	0.6978			
S1, S7	10.792	35	0.3488			
S1, S2	10.727	10	0.3562			
S1, S614	0.88803	10	0.4812			
S1, S613	0.88786	10	0.4752			
S4, S7	0.97944	35	0.4185			
S4, S2	22.706	10	0.0502			
S4, S614	0.5012	10	0.7587			
S4, S613	19.218	10	0.1004			
S7, S2	20.569	35	0.0378			
S7, S614	0.44003	35	0.8302			
S7, S613	15.491	35	0.1273			
S2, S614	23.118	10	0.0606			
S2, S613	0.83393	10	0.5432			
S614, S613	20.307	10	0.1041			

Table S13: Spearman correlations between the nematode univariate variables Shanon-Wiener diversity (H'), Pielou's Evenness (J'), Expected genera (EG (80)) and Trophic Diversity (TD) with sediment environmental variables. %TN= Total Nitrogen (%), %TOC=Total Organic Carbon (%), Chla= Chlorophyll a, Carotenes, CPE= Chloroplastic Pigment Equivalents, Silt-Clay, Very Fine Sand, Fine Sand, Medium Sand, Coarse Sand and SED=Sediment Diversity. Significant correlations are shown in bold.

	%TN	%TOC	Chla	Carotenes	CPE	Silt-Clay	Very Fine Sand	Fine Sand	Medium Sand	Coarse Sand	SED
H'	-0.38	-0.44	0.26	0.32	0.32	-0.46	0.43	0.41	0.42	0.3	0.51
J	0.26	0.12	-0.11	-0.09	-0.28	0.19	-0.22	-0.26	-0.2	0.04	-0.17
EG (80)	-0.43	-0.46	0.25	0.31	0.36	-0.47	0.45	0.45	0.44	0.28	0.52
TD	-0.4	-0.28	0.37	0.3	0.39	-0.37	0.48	0.41	0.34	0.05	0.4

Table S14. Sequenced nematode genera by ID (Identification number), taxonomic position, location and GenBank Accession numbers.


Field ID	Order	Family	Genus	Latitude	Longitude	Depth (m)	GenBank Accession numbers
77L10H15	Plectida	Camacolaimidae	<i>Camacolaimus</i>		09°28'042"W	1006	N/A - to be provided upon acceptance
52L27G15	Plectida	Camacolaimidae	<i>Camacolaimus</i>	37°49'661"N	09°28'042"W	1006	N/A - to be provided upon acceptance
97L22D15	Araeolaimida	Diplopeltidae	<i>Campylaimus</i>	37°58.904"N	09°07.525"W	335	N/A - to be provided upon acceptance
81L18E15	Monhysterida	Xyalidae	<i>Capsula</i>	37°58.904"N	09°07.525"W	335	N/A - to be provided upon acceptance
42L29D15	Plectida	Ceramonematidae	<i>Ceramonema</i>	37°58.904"N	09°07.525"W	335	N/A - to be provided upon acceptance
50L26C15	Plectida	Ceramonematidae	<i>Ceramonema</i>	37°51.171"N	09°06.944"W	325	N/A - to be provided upon acceptance
15L17C15	Araeolaimida	Comesomatidae	<i>Cervonema</i>	37°51.171"N	09°06.944"W	325	N/A - to be provided upon acceptance
25L20C15	Araeolaimida	Comesomatidae	<i>Cervonema</i>	37°51.171"N	09°06.944"W	325	N/A - to be provided upon acceptance
28L20C15	Araeolaimida	Comesomatidae	<i>Cervonema</i>	37°51.171"N	09°06.944"W	325	N/A - to be provided upon acceptance
20L27D15	Monhysterida	Xyalidae	<i>Daptonema</i>	37°58.904"N	09°07.525"W	335	N/A - to be provided upon acceptance
55L26C15	Monhysterida	Xyalidae	<i>Daptonema</i>	37°51.171"N	09°06.944"W	325	N/A - to be provided upon acceptance
48L27G15	Desmodorida	Desmodoridae	<i>Desmodora</i>	37°49'661"N	09°28'042"W	1006	N/A - to be provided upon acceptance
56L28G15	Desmodorida	Desmodoridae	<i>Desmodora</i>	37°49'661"N	09°28'042"W	1006	N/A - to be provided upon acceptance
76L10H15	Desmodorida	Desmodoridae	<i>Desmodora</i>	37°49'661"N	09°28'042"W	1006	N/A - to be provided upon acceptance
42L27G15	Desmodorida	Desmodoridae	<i>Desmodora</i>	37°49'661"N	09°28'042"W	1006	N/A - to be provided upon acceptance

41L29D15	Desmodorida	Desmodoridae	<i>Desmodorella</i>	37°58.904'N	09°07.525'W	335	N/A - to be provided upon acceptance
46L29D15	Desmodorida	Desmodoridae	<i>Desmodorella</i>	37°58.904'N	09°07.525'W	335	N/A - to be provided upon acceptance
54L27G15	Desmoscolecida	Desmoscolecidae	<i>Desmoscolex</i>	37°49'661'N	09°28'042'W	1006	N/A - to be provided upon acceptance
84L10H15	Desmoscolecida	Desmoscolecidae	<i>Desmoscolex</i>	37°49'661'N	09°28'042'W	1006	N/A - to be provided upon acceptance
62L28G15	Desmoscolecida	Desmoscolecidae	<i>Desmoscolex</i>	37°49'661'N	09°28'042'W	1006	N/A - to be provided upon acceptance
93L19E15	Chromadorida	Chromadoridae	<i>Dichromadora</i>	37°58.904'N	09°07.525'W	335	N/A - to be provided upon acceptance
93L31C15	Plectida	Diplopeltoidea	<i>Diplopeltoidea</i>	37°51.171'N	09°06.944'W	325	N/A - to be provided upon acceptance
90L11H15	Chromadorida	Selachinematidae	<i>Gammanema</i>	37°49'661'N	09°28'042'W	1006	N/A - to be provided upon acceptance
3L22D15	Chromadorida	Selachinematidae	<i>Gammanema</i>	37°58.904'N	09°07.525'W	335	N/A - to be provided upon acceptance
51L04E15	Chromadorida	Selachinematidae	<i>Gammanema</i>	37°58.904'N	09°07.525'W	335	N/A - to be provided upon acceptance
5L16C15	Chromadorida	Selachinematidae	<i>Gammanema</i>	37°51.171'N	09°06.944'W	325	N/A - to be provided upon acceptance
65L05E15	Chromadorida	Selachinematidae	<i>Gammanema</i>	37°58.904'N	09°07.525'W	335	N/A - to be provided upon acceptance
9L17C15	Desmoscolecida	Desmoscolecidae	<i>Greeffiella</i>	37°51.171'N	09°06.944'W	325	N/A - to be provided upon acceptance
89L30C15	Enoplida	Oxystominidae	<i>Halalaimus</i>	37°51.171'N	09°06.944'W	325	N/A - to be provided upon acceptance
19L14G15	Enoplida	Oxystominidae	<i>Halalaimus</i>	37°49'661'N	09°28'042'W	1006	N/A - to be provided upon acceptance
60L28G15	Enoplida	Oxystominidae	<i>Halalaimus</i>	37°49'661'N	09°28'042'W	1006	N/A - to be provided upon acceptance
51L26C15	Enoplida	Oxystominidae	<i>Halalaimus</i>	37°51.171'N	09°06.944'W	325	N/A - to be provided upon acceptance
88L18E15	Enoplida	Oxystominidae	<i>Halalaimus</i>	37°58.904'N	09°07.525'W	335	N/A - to be provided upon acceptance
87L18E15	Enoplida	Oxystominidae	<i>Halalaimus</i>	37°58.904'N	09°07.525'W	335	N/A - to be provided upon acceptance
66L05E15	Enoplida	Oxystominidae	<i>Halalaimus</i>	37°58.904'N	09°07.525'W	335	N/A - to be provided upon acceptance
100L11H15	Enoplida	Oxystominidae	<i>Halalaimus</i>	37°49'661'N	09°28'042'W	1006	N/A - to be provided upon acceptance
64L28G15	Enoplida	Oxystominidae	<i>Halalaimus</i>	37°49'661'N	09°28'042'W	1006	N/A - to be provided upon acceptance
50L27G15	Enoplida	Oxystominidae	<i>Halalaimus</i>	37°49'661'N	09°28'042'W	1006	N/A - to be provided upon acceptance
99L19E15	Enoplida	Oxystominidae	<i>Halalaimus</i>	37°58.904'N	09°07.525'W	335	N/A - to be provided upon acceptance

77L30C15	Enoplida	Oxystominidae	<i>Halalaimus</i>	37°51.171'N	09°06.944'W	325	N/A - to be provided upon acceptance
65L07H15	Enoplida	Oxystominidae	<i>Halalaimus</i>	37°49'661"N	09°28'042"W	1006	N/A - to be provided upon acceptance
40L15G15	Enoplida	Oxystominidae	<i>Halalaimus</i>	37°49'661"N	09°28'042"W	1006	N/A - to be provided upon acceptance
39L15G15	Enoplida	Oxystominidae	<i>Halalaimus</i>	37°49'661"N	09°28'042"W	1006	N/A - to be provided upon acceptance
78L30C15	Chromadorida	Selachinematidae	<i>Halichoanolaimus</i>	37°51.171'N	09°06.944'W	325	N/A - to be provided upon acceptance
7L13G15	Enoplida	Enchelidiidae	<i>Ledovitia</i>	37°49'661"N	09°28'042"W	1006	N/A - to be provided upon acceptance
64L27C15	Plectida	Leptolaimidae	<i>Leptolaimus</i>	37°51.171'N	09°06.944'W	325	N/A - to be provided upon acceptance
45L25C15	Plectida	Leptolaimidae	<i>Leptolaimus</i>	37°51.171'N	09°06.944'W	325	N/A - to be provided upon acceptance
13L27D15	Plectida	Leptolaimidae	<i>Leptolaimus</i>	37°58.904'N	09°07.525'W	335	N/A - to be provided upon acceptance
2L13G15	Plectida	Leptolaimidae	<i>Leptolaimus</i>	37°49'661"N	09°28'042"W	1006	N/A - to be provided upon acceptance
53L04E15	Plectida	Leptolaimidae	<i>Leptolaimus</i>	37°58.904'N	09°07.525'W	335	N/A - to be provided upon acceptance
2L22D15	Plectida	Leptolaimidae	<i>Leptolaimus</i>	37°58.904'N	09°07.525'W	335	N/A - to be provided upon acceptance
63L28G15	Plectida	Leptolaimidae	<i>Leptolaimus</i>	37°49'661"N	09°28'042"W	1006	N/A - to be provided upon acceptance
24L18C15	Enoplida	Thoracostomopsidae	<i>Mesacanthion</i>	37°51.171'N	09°06.944'W	325	N/A - to be provided upon acceptance
90L31C15	Chromadorida	Cyatholaimidae	<i>Metacyatholaimus</i>	37°51.171'N	09°06.944'W	325	N/A - to be provided upon acceptance
14L17C15	Monhysterida	Linhomoeidae	<i>Metalinhomoeus</i>	37°51.171'N	09°06.944'W	325	N/A - to be provided upon acceptance
10L17C15	Monhysterida	Linhomoeidae	<i>Metalinhomoeus</i>	37°51.171'N	09°06.944'W	325	N/A - to be provided upon acceptance
12L13G15	Desmodorida	Microlaimidae	<i>Microlaimus</i>	37°49'661"N	09°28'042"W	1006	N/A - to be provided upon acceptance
50L29D15	Desmodorida	Microlaimidae	<i>Microlaimus</i>	37°58.904'N	09°07.525'W	335	N/A - to be provided upon acceptance
56L04E15	Desmodorida	Microlaimidae	<i>Microlaimus</i>	37°58.904'N	09°07.525'W	335	N/A - to be provided upon acceptance
83L18E15	Desmodorida	Microlaimidae	<i>Microlaimus</i>	37°58.904'N	09°07.525'W	335	N/A - to be provided upon acceptance
86L18E15	Desmodorida	Microlaimidae	<i>Microlaimus</i>	37°58.904'N	09°07.525'W	335	N/A - to be provided upon acceptance
80L18E15	Desmodorida	Microlaimidae	<i>Microlaimus</i>	37°58.904'N	09°07.525'W	335	N/A - to be provided upon acceptance
63L05E15	Desmodorida	Microlaimidae	<i>Microlaimus</i>	37°58.904'N	09°07.525'W	335	N/A - to be provided upon acceptance

49L29D15	Desmodorida	Microlaimidae	<i>Microlaimus</i>	37°58.904'N	09°07.525'W	335	N/A - to be provided upon acceptance
4L22D15	Desmodorida	Microlaimidae	<i>Microlaimus</i>	37°58.904'N	09°07.525'W	335	N/A - to be provided upon acceptance
79L30C15	Desmodorida	Microlaimidae	<i>Microlaimus</i>	37°51.171'N	09°06.944'W	325	N/A - to be provided upon acceptance
43L25C15	Desmodorida	Microlaimidae	<i>Microlaimus</i>	37°51.171'N	09°06.944'W	325	N/A - to be provided upon acceptance
46L25C15	Desmodorida	Microlaimidae	<i>Microlaimus</i>	37°51.171'N	09°06.944'W	325	N/A - to be provided upon acceptance
1L13G115	Desmoscolecida	Meyliidae	<i>Paratricoma</i>	37°49'661'N	09°28'042'W	1006	N/A - to be provided upon acceptance
33L28D15	Plectida	Camacolaimidae	<i>Procamacolaimus</i>	37°58.904'N	09°07.525'W	335	N/A - to be provided upon acceptance
92L31C15	Plectida	Camacolaimidae	<i>Procamacolaimus</i>	37°51.171'N	09°06.944'W	325	N/A - to be provided upon acceptance
21L27D15	Plectida	Camacolaimidae	<i>Procamacolaimus</i>	37°58.904'N	09°07.525'W	335	N/A - to be provided upon acceptance
47L29D15	Plectida	Camacolaimidae	<i>Procamacolaimus</i>	37°58.904'N	09°07.525'W	335	N/A - to be provided upon acceptance
52L04E15	Plectida	Ceramonematidae	<i>Pselionema</i>	37°58.904'N	09°07.525'W	335	N/A - to be provided upon acceptance
44L27G15	Plectida	Ceramonematidae	<i>Pselionema</i>	37°49'661'N	09°28'042'W	1006	N/A - to be provided upon acceptance
38L15G15	Plectida	Ceramonematidae	<i>Pselionema</i>	37°49'661'N	09°28'042'W	1006	N/A - to be provided upon acceptance
14L13G15	Chromadorida	Selachinematidae	<i>Richtersia</i>	37°49'661'N	09°28'042'W	1006	N/A - to be provided upon acceptance
2L16C15	Chromadorida	Selachinematidae	<i>Richtersia</i>	37°51.171'N	09°06.944'W	325	N/A - to be provided upon acceptance
23L18C15	Chromadorida	Selachinematidae	<i>Richtersia</i>	37°51.171'N	09°06.944'W	325	N/A - to be provided upon acceptance
72L27C15	Chromadorida	Selachinematidae	<i>Richtersia</i>	37°51.171'N	09°06.944'W	325	N/A - to be provided upon acceptance
26L14G15	Chromadorida	Selachinematidae	<i>Richtersia</i>	37°49'661'N	09°28'042'W	1006	N/A - to be provided upon acceptance
22L14G15	Plectida	Haliplectidae	<i>Setoplectus</i>	37°49'661'N	09°28'042'W	1006	N/A - to be provided upon acceptance
86L30C15	Araeolaimida	Comesomatidae	<i>Setosabatieria</i>	37°51.171'N	09°06.944'W	325	N/A - to be provided upon acceptance
70L27C15	Araeolaimida	Diplopeltidae	<i>Southerniella</i>	37°51.171'N	09°06.944'W	325	N/A - to be provided upon acceptance
9L22D15	Araeolaimida	Diplopeltidae	<i>Southerniella</i>	37°58.904'N	09°07.525'W	335	N/A - to be provided upon acceptance
17L13G15	Enoplida	Ironidae	<i>Syringolaimus</i>	37°49'661'N	09°28'042'W	1006	N/A - to be provided upon acceptance
60L04E15	Enoplida	Ironidae	<i>Syringolaimus</i>	37°58.904'N	09°07.525'W	335	N/A - to be provided upon acceptance

6L16C15	Desmoscolecida	Desmoscolecidae	<i>Tricoma</i>	37°51.171'N	09°06.944'W	325	N/A - to be provided upon acceptance
43L29D15	Desmoscolecida	Desmoscolecidae	<i>Tricoma</i>	37°58.904'N	09°07.525'W	335	N/A - to be provided upon acceptance
41L27G15	Desmoscolecida	Desmoscolecidae	<i>Tricoma</i>	37°49'661'N	09°28'042'W	1006	N/A - to be provided upon acceptance
70L05E15	Desmoscolecida	Desmoscolecidae	<i>Tricoma</i>	37°58.904'N	09°07.525'W	335	N/A - to be provided upon acceptance
11L27D15	Enoplida	Oncholaimidae	<i>Viscosia</i>	37°58.904'N	09°07.525'W	335	N/A - to be provided upon acceptance
96L31C15	Enoplida	Oncholaimidae	<i>Viscosia</i>	37°51.171'N	09°06.944'W	325	N/A - to be provided upon acceptance
72L05E15	Enoplida	Oncholaimidae	<i>Viscosia</i>	37°58.904'N	09°07.525'W	335	N/A - to be provided upon acceptance
29L28D15	Enoplida	Oncholaimidae	<i>Viscosia</i>	37°58.904'N	09°07.525'W	335	N/A - to be provided upon acceptance
64L05E15	Enoplida	Oncholaimidae	<i>Viscosia</i>	37°58.904'N	09°07.525'W	335	N/A - to be provided upon acceptance
32L15G15	Enoplida	Oxystominidae	<i>Wieseria</i>	37°49'661'N	09°28'042'W	1006	N/A - to be provided upon acceptance
8L17C15	Monhysterida	Xyalidae	not defined	37°51.171'N	09°06.944'W	325	N/A - to be provided upon acceptance

A stylized illustration of a nematode, a small worm-like creature, shown in profile. The nematode has a segmented body with a red head and tail, and a brownish-orange body. It is positioned diagonally across the frame, appearing to be on or near a plant root. The background is a light blue color with dark blue, curved lines representing plant roots or soil structure. The text 'General discussion on patterns and processes elucidating nematode assemblage structure' is written in a red, outlined font in the upper right corner.

General discussion on patterns and processes elucidating nematode assemblage structure





Chapter 6: General discussion on patterns and processes elucidating nematode assemblage structure

6.1 Patterns of nematode diversity, density and biomass in the deep sea

6.1.1 Local and regional diversity, density, and biomass

With the increasing anthropogenic impacts in various deep-sea environments (Van Cauwenberghe et al., 2013; Vanreusel et al., 2016), the assessment of how much biodiversity a habitat holds and approximations of how much of this biodiversity a habitat can be lost without collapsing is essential for management decisions (Davies et al., 2007). The measure of diversity in a system is perceived as a proxy for ecosystem health and considered of substantial importance for ecosystem stability and productivity (Davies et al., 2007). Our knowledge concerning diversity in the deep sea is mostly derived from regional-scale sampling studies which were focussed either on geographical or bathymetrical transects (Lambshead and Boucher, 2003; Levin et al., 2001; Muthumbi et al., 2011). Determining how standing stocks (i.e. density and biomass) and diversity change according to the different spatial scales studied and which factors affect species turnover and coexistence has been a challenge, because this large and hard to sample environment covers a wide range of habitats and environmental conditions (Levin et al., 2001; Ramirez-Llodra et al., 2010).

In this thesis, it was investigated how meiofauna, and in particular nematode standing stocks as well as nematode genus and species diversity, from dissimilar environments and areas varied according to different spatial scales. While the focus was mainly on abyssal depths from the Southern Ocean (SO) and the North Atlantic (NA), also the upper slope and shelf break at the Western Iberian Margin (WIM) were studied here comparing diversity across scales. The use of different spatial scales can be important, especially in the deep sea, as species are believed to be aggregated in patches or habitats, altering within- and between habitat diversity (Danovaro et al., 2013; Kaiser et al., 2007). Four levels of hierarchy have been defined in this thesis (Fig. 6.1): alpha diversity (α), as the diversity at core level (individual sample of a Multiple Corer); beta diversity within a site (between cores of the same deployment, β_1); beta diversity between sites of the same transect (β_2); and beta diversity between regions or transects (β_3).

Core and site density and biomass, as well as core and site diversity, were higher at the sites located at the WIM when compared with other areas in this study (Figs 6.2 and 6.3). All studied regions and depths showed a similar pattern in terms of importance of rare genera within core samples, in that they were roughly characterised by 50 % of rare genera and 50 % of common genera (genera with abundances > 2 %) (Fig. 6.2D). For the shelf-break sites, not only a higher Shannon-Wiener genus diversity was observed within and between sites, but also a lower relative abundance of the most common genera, indicating that dominance (i.e. relative abundance > 2 %) was shared between many different genera. At the same time, the dominant genera were different between cores and sites (**Chapter 5**). Thus, at the shelf-break sites, a higher alpha diversity and genera coexistence was observed, while also a larger turnover in dominant genera occurred between sites. For the WIM upper slope sites, however, a different pattern was observed, where the most dominant genera were responsible for a higher proportion of the community and were found consistently among cores and sites. At the slope, the most commonly found genera

were *Acantholaimus*, *Halalaimus*, *Daptonema*, *Desmoscolex*, *Leptolaimus*, *Monhystrella*, *Sabatieria*, and *Tricoma*. Therefore, for this area, alpha diversity was high, but turnover within and between stations was lower compared with the shelf break.

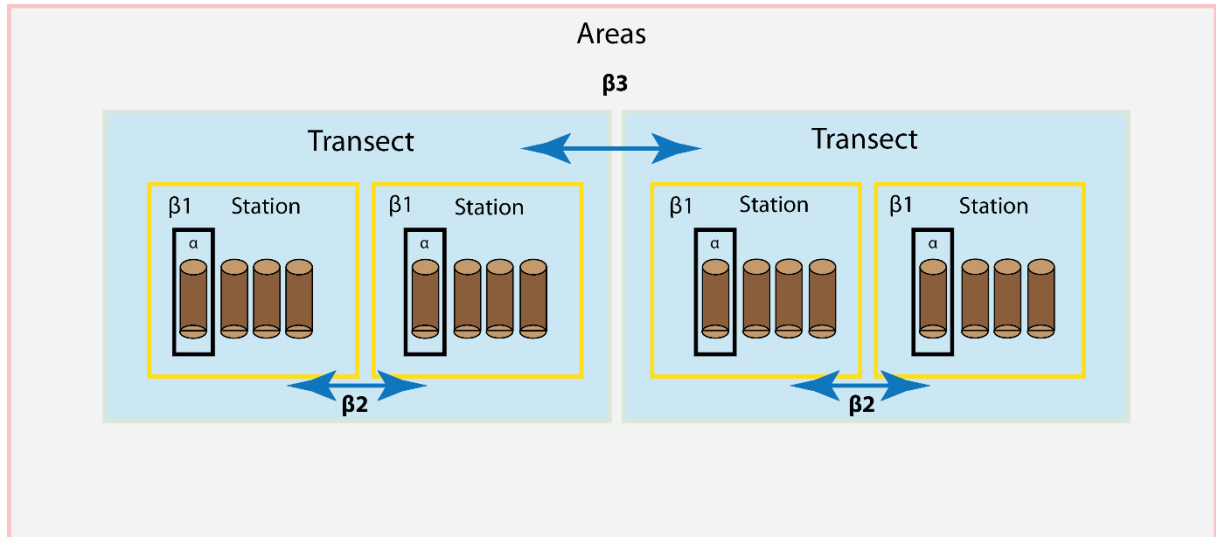


Figure 6.1. Levels of biodiversity used in this thesis: (α), alpha diversity at core level; (β_1) turnover between cores and within a site; (β_2) turnover between sites in the same transect; (β_3) turnover between areas.

Density, biomass, and α and β_1 diversity were lower for the abyssal cores and sites, except for the South Georgia (SG) site in the SO, which showed ten times higher nematode densities when compared to the other abyssal sites and for all cores, and biomass values similar to the slope sites at the WIM (Figs. 6.2A and B). The SG site was also different in comparison with the other abyssal sites in terms of nematode community structure and Shannon-Wiener genus diversity (α and β_1). It was characterized by a very high dominance of the genus *Desmodora* (relative abundances up to 42 % in SG_175-8), which is usually not found in such high abundances, except in chemosynthetic deep-sea environments (Chapter 3; Vanreusel et al., 2010b). The other abyssal sites located in the SO and NA were represented by a common deep-sea soft-bottom nematode community, with the genera *Acantholaimus*, *Thalassomonhystera*, being found in high abundances in all cores with the exception of the SO abyssal site HC_AEP and the NA site B1.

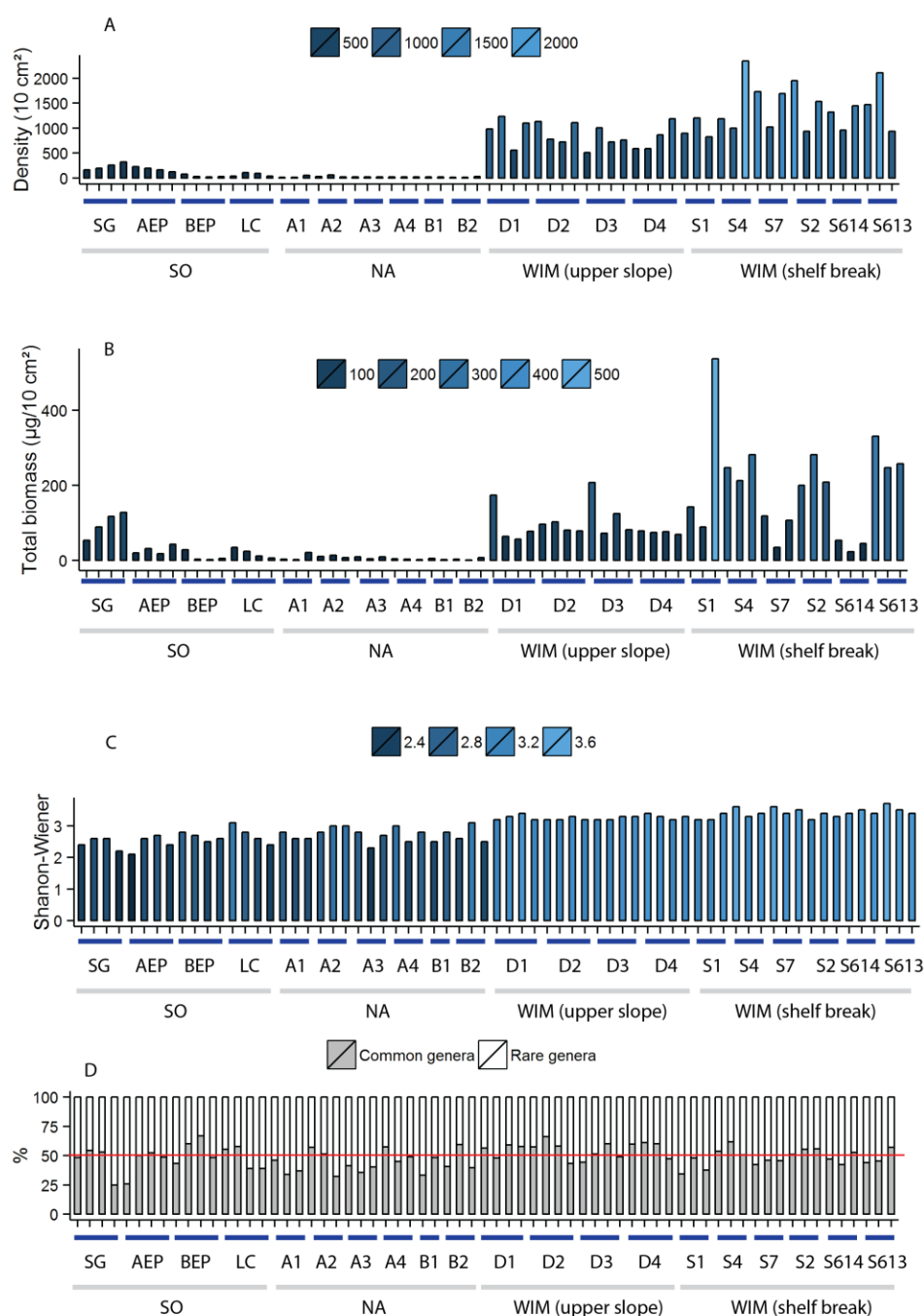


Figure 6. 2. Total nematode density per 10 cm² (A), total nematode biomass (B), and Shannon-Wiener diversity (C) of nematode genera per core found in all studied regions in this thesis. (D) shows the percentage of the common (abundances > 2 %) versus the rare genera found per core. Red line indicate threshold of 50 %. The sites SG (South Georgia), HC_AEP (high chlorophyll after eddy pump), HC_BEP (high chlorophyll before eddy pump), and LC (low chlorophyll) were part of the Southern Ocean (SO) transect; sites A1, A2, A3, A4, B1, and B2 were the sites sampled in the North Atlantic (NA), along the Vema fracture zone. Sites D1, D2, D3, and D4 were part of the slope at the Western Iberian Margin (WIM), while sites S1, S4, S7, S2, and S6 represent sites sampled at the shelf break of the WIM.

Nevertheless, the most surprising results in this study come from the comparisons of geographical and bathymetric diversity patterns here presented by the genus turnover

between sites (β2) and between areas (β3). High nematode community turnover was observed between sites from the WIM shelf break and SO abyss. Furthermore, for the WIM area, the higher turnover between the shelf break and the slope sites was unexpected, because these two transects are located only roughly 30 km apart (**Chapter 5**). However, considering that the WIM is characterized by a steep slope, strong gradients in environmental factors can probably affect the two depth zones differently, thus shaping the differences encountered in the multivariate community turnover between transects, as well as the lower abundances and densities found at the slope transect (Fig. 6.4A and B). Similarly, sites along the longitudinal transect in the SO were characterized by a high genus turnover between stations, contrasting with the high alpha diversity but low turnover within and between stations found at the NA sites (Fig. 6.4D) (**Chapter 4**). The trend of high alpha genus diversity associated with low genus turnover versus low alpha genus diversity with high genus turnover found when comparing these two abyssal areas (SO and NA) was also observed at species level for the genus *Acantholaimus* (**Chapter 4**). Nevertheless, although differing in diversity (β2 and β3) trends, these two abyssal areas exhibited the same dominant genera for most of the sites studied (i.e. *Acantholaimus*, *Thalassomonhystera*, and *Halalaimus*), except for the high abundances of *Desmodora* found in SG, and *Microtalamus* in HC_AEP and HC_BEP.

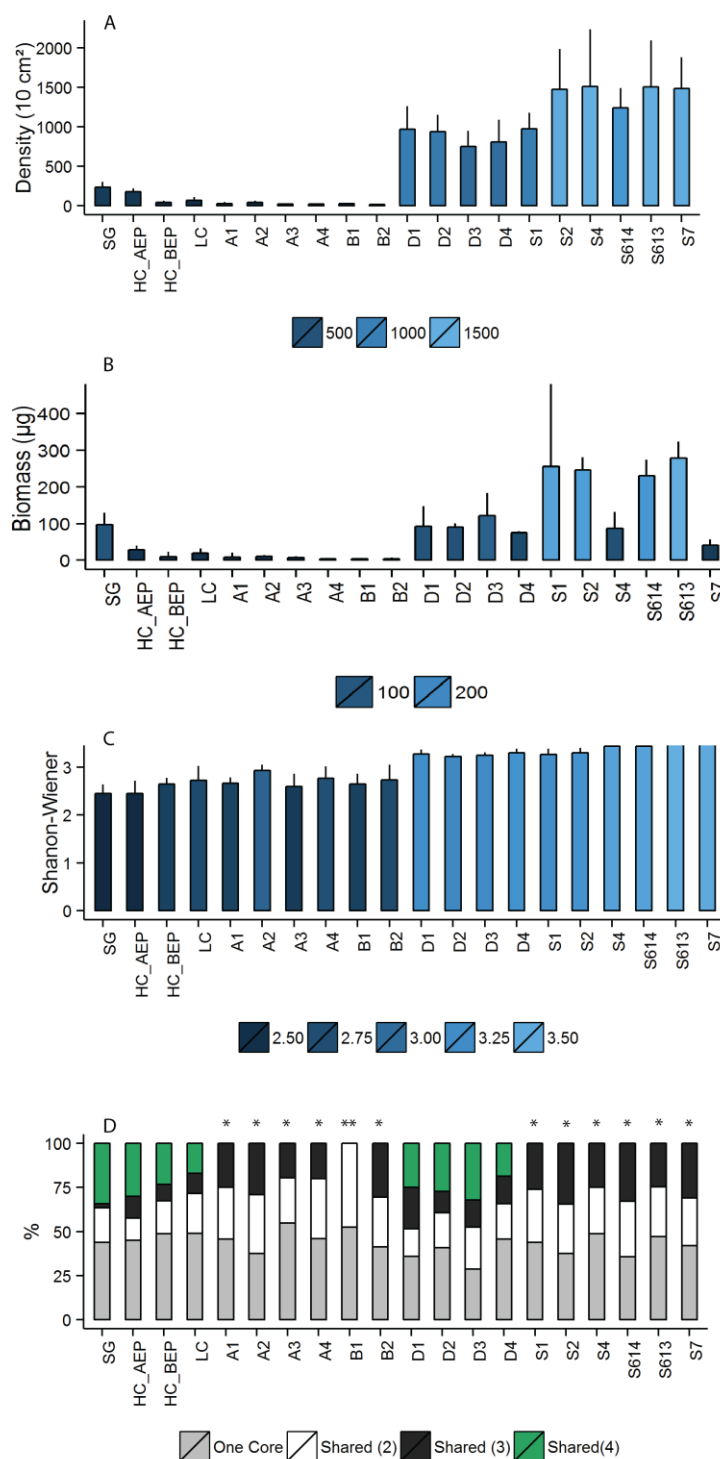


Figure 6.3. Total nematode density (A), biomass (B), and Shannon-Wiener diversity (C) of nematode genera per site for all studied areas. (D) shows the contribution of genera shared per site. “One core” represents the genera found only in one core, “Shared (2)” through “Shared (4)” signifies genera present in two–four cores respectively. The * symbol indicates sites where only three cores were sampled and ** sites with only two cores. The sites SG (South Georgia), HC_AEP (high chlorophyll after eddy pump), HC_BEP (high chlorophyll before eddy pump), and LC (low chlorophyll) were part of the Southern Ocean transect; sites A1, A2, A3, A4, B1, and B2 were the sites sampled in the North Atlantic, along the Vema Fracture Zone. Sites D1, D2, D3, and D4 were part of the slope at the Western Iberian Margin, while sites S1, S4, S7, S2, and S6 represent sites sampled at the shelf break of the Western Iberian Margin.

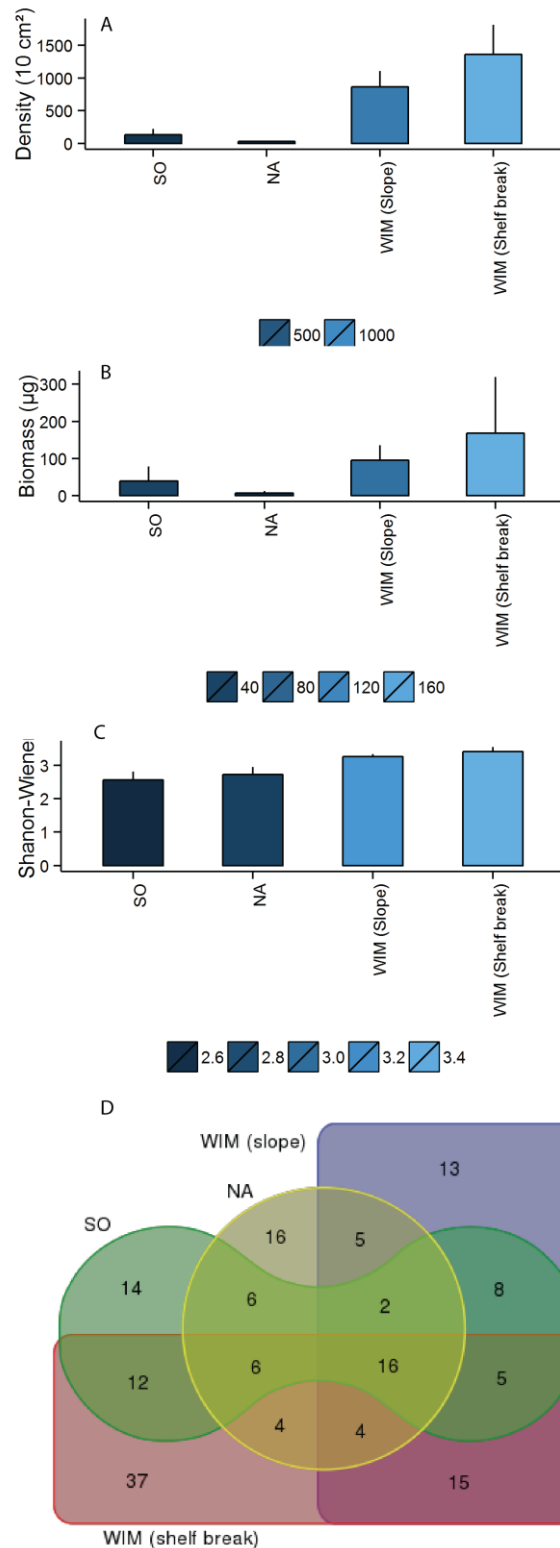


Figure 6.4. Total nematode density (A), total biomass (B), and Shannon-Wiener diversity (C) of nematode genera per region studied in this thesis. (D) represents a Venn diagram based on genus richness, where the overlap shows the number of shared genera between the different regions for all studied areas. SO= Southern Ocean, NA= North Atlantic, WIM= Western Iberian Margin.

Being typically found in the deep sea, *Acantholaimus*, *Thalassomonhystera*, and *Halalaimus*, are common inhabitants of soft-bottom sediments and exhibit a wide distribution (Soetaert and Heip, 1995; Vanreusel et al., 2010b). While dominant in all sites in the SO and NA, as well as at the slope sites from the WIM, relative abundances of *Acantholaimus* did not exceed 3 % at the low continental shelf-break sites of the WIM. This genus is rarely found in shallow water (< 200 m), with only one species description for intertidal habitats (Platt and Zhang, 1982). This absence of *Acantholaimus* in shallow waters has been attributed to a secondary displacement of *Acantholaimus* species in these habitats, following speciation in the deep sea (Bik et al., 2010). Hence, it may be possible that *Acantholaimus* has its phylogenetic origin at great depths and has colonized shallow waters secondarily. This assumption may be supported by the biogeography of this genus, which shows increases in diversity with increasing depth globally, except for the continental shelf and slope in Antarctica, where it exhibits high species diversity at all depths (De Mesel et al., 2006).

While *Acantholaimus* seems to be a typical deep-sea genus, *Halalaimus* appears to be eurybathic and very successful at both abyssal plains and continental margins (Lampadariou and Tselepides, 2006; Netto et al., 2005; Vanreusel et al., 2010b), but also occurring in high numbers in several shallow-water habitats (Fonseca et al., 2014; Mirto et al., 2014; Patrício et al., 2012). This genus was one of the most abundant genera at all sites studied in this thesis, and a high relative abundance of *Halalaimus* has been found in various other deep-sea habitats as well, such as canyons, seamounts, cold seeps, trenches, as well as around corals and nodules (Vanreusel et al., 2010b). *Thalassomonhystera* occurred in high abundances (9.0–29.3 %) in the SO and NA, while for the WIM the highest relative abundance of this genus was < 5 %. *Thalassomonhystera* is commonly found in high relative abundances at abyssal plains and in trenches, while it can be also encountered in lower abundances in highly productive areas, such as

hydrothermal vents (Vanreusel et al., 2010b). The relative contribution of *Thalassomonhystera* to the nematode community at the slope (WIM) was surprisingly low compared to the literature, but it was still one of the most abundant genera at sites dominated by fine sand, thus suggesting preference of this genus of certain sediment types.

6.2 What drives alpha and beta diversity in the deep sea?

6.2.1 Environmental factors

In the deep sea, **surface primary productivity and food supply to the seafloor**, together with **habitat heterogeneity**, are believed to play a major role in structuring benthic communities. Especially in the meiofauna, species coexistence is influenced by these factors (Gooday, 2002; Leduc et al., 2012b; Levin et al., 2001; Snelgrove and Butman, 1994; Wei et al., 2010).

According to Woolley et al. (2016), bathyal and abyssal habitats are affected differently in terms of energy availability, where bathyal habitats are greatly subjected to the influence of temperature and energy derived from surface primary productivity, while abyssal environments are under the influence of energy input only. Temperature is known to affect species survival in shallow-water habitats (Birchenough et al., 2015; Werbrouck et al., 2016), but how it affects deep-sea benthic communities is so far poorly understood (Belley et al., 2016; Tyler, 1995). Energy input through surface primary productivity, however, is believed to greatly affect species diversity and standing stocks in the deep sea (Gooday,

2002; Lambshead et al., 2002; Levin et al., 2001; McClain and Schlacher, 2015; Vanreusel et al., 1995).

The link between surface primary production and benthic community structure was one of the main topics treated in this thesis. It was studied in three target areas, which were, the WIM in the North Atlantic, characterized by high productivity (Nolasco et al., 2013), the Atlantic sector of the SO, exhibiting high seasonal productivity, and also high spatial (longitudinal) productivity differences (Abelmann et al., 2006; Demidov et al., 2012), and finally the NA along the Vema Fracture Zone, possessing a low surface productivity regime (Jochem and Zeitzschel, 1993). Beside its annual and seasonal variation, the general distribution of primary production in the oceans is patchy in space. This patchiness is mainly a result of interactions between coastline features and wind forcing (Crespo et al., 2011). Both of these factors appear to be more important at the WIM than in the SO and NA, because the former study region is located near a land mass and at the continental slope. At the WIM, the influence from the coast is generally high compared to the open ocean (Crespo et al., 2011). While the WIM possesses similar upwelling characteristics to other continental margins (Salgueiro et al., 2010), surface primary productivity in the SO and NA was greatly determined by its unique regional features (Jochem and Zeitzschel, 1993; Knox, 1994). The SO and NA receive low terrestrial input (except for the SG site) and their dominant energy flow is determined by seasonal phytoplankton surface production, followed by sinking and breakdown in both pelagic and benthic microbial loops (Griffiths, 2010; Rowe et al., 2008).

The studied transects at the WIM covered approximately 400 km² and were thus subjected to the same surface productivity regime (Salgueiro et al., 2014). For the NA, although the total transect covered a distance of ~ 5000 km, productivity (net primary production, NPP) was constant between the sites (**Chapter 4**). The SO transect also encompassed a large distance (~ 2000 km), and here significant differences in NPP were observed between sites.

For the sites situated at the Polar Front (PF), NPP increased westwards and the SG site showed the highest NPP values (**Chapters 2 and 3**). The higher NPP at SG was already expected, as this region exhibits constant local nutrient supply throughout the year through hydrodynamics, supporting high plankton productivity (Brandon et al., 2000; Orsi et al., 1995; Whitehouse et al., 1996). Moreover, from the sites located at the PF, SG is part of the so-called ‘diatom ooze belt’ and is the only studied site featuring a high surface abundance of the nutrient-rich diatom *Chaetoceros* spp., which is responsible for high organic matter (OM) accumulation at the sea bottom (Sachs et al., 2009).

Sites located south of the PF studied in this thesis showed lower annual NPP values when compared to those at the PF. However, these results could be an underestimation caused by the longer ice-coverage period in winter around these sites, and consequently the lack of satellite-based chlorophyll a (chl_a) information (**Chapter 2**). Although undetectable with satellites, these sea ice-covered areas located south of the PF are potentially regions of strong sea-ice algal production in winter and subsequent decay in the summer, which creates a shallow mixed layer of melted sea-ice algae and sea-surface water, and consequently enhances primary production (Beckmann et al., 2001; Flores et al., 2011). In general, sea-ice algal productivity can account for up to 25 % of total primary production in the SO (Arrigo and Thomas, 2004).

In **Chapter 2**, the particulate organic carbon flux was estimated for the SO sites to assess how much OM reaches the seabed (Lutz et al., 2002, 2007). The estimated particulate organic carbon flux at the sites south of the PF was clearly exceeding that estimated for the PF sites (**Chapter 2**). Nevertheless, the algorithm used to estimate carbon flux is depth-dependent and takes neither sea-ice algae production into account nor biological-pump interrelated processes, such as (dis)aggregation of organic particles (De La Rocha and Passow, 2007). This means that the contrast between the PF sites and those south of

the PF could in reality be even higher. Nevertheless, the depth-dependence of this algorithm illustrates the crucial role of water depth in the transfer efficiency of particulate organic carbon (De La Rocha and Passow, 2007; Lutz et al., 2007).

After being transferred through the water column, OM undergoes mineralization processes and finally acts as food source for benthic organisms. Depth differences result in differences in OM amount arriving at the seabed (e.g. measured as chl_a, chloroplastic pigment equivalents (CPE), total organic carbon (% TOC), total nitrogen (%TN), and total organic matter (%TOM)) between areas under similar surface primary productivity, such transects at the WIM that differed in their depths (**Chapter 5**). Moreover, also the comparison between the bathyal and the abyssal sites revealed lower OM input and, consequently, lower density and biomass of nematodes with increasing water depth (Fig. 6.4B). This confirms previous assumptions that density and biomass have negative correlations with depth as a consequence of the lower OM input with increasing depth (Danovaro et al., 2010; Rex et al., 2006).

Nonetheless, sites located at similar depths but under different productivity regimes also showed different responses. Areas of high surface productivity in the SO showed higher benthic meiofaunal standing stocks (**Chapters 2 and 4**) than the NA sites situated in an oligotrophic area (**Chapter 4**). South of the PF, meiofauna densities were highest. Moreover, at the Maud Rise (MR) and Lazarev Sea (LS) sites located south of the PF, high meiofauna densities were associated with extended seasonal ice coverage and elevated primary production at the seasonal ice edge (Froneman et al., 2004; Hunt et al., 2011). Concurrently, enriched carbon isotope values of the meiofauna from Antarctica (including the same sites studied here) indicated feeding activity on sea-ice algae at deep-sea sites that were located beneath the ice cover (Moens et al., 2007; Veit-Köhler et al., 2013). Similar associations with productivity patterns in the same area could be shown for microbial communities (Ruff et al., 2014), echinoderms (Würzberg et al., 2014), as well as

ostracods (Brandão et al., 2014). Although the SO represents a unique environment under the influence of complex current regimes and high seasonality (Griffiths, 2010; Knox, 1994), the same positive correlation between surface productivity and benthic standing stocks has also been observed in different regions displaying contrasting surface productivity (Danovaro et al., 1999; Pape et al., 2013; Smith et al., 2008; Vanreusel et al., 1995). It can hence be concluded that these data support earlier studies and may represent a global pattern applying to all different benthic size classes (Etter et al., 2005; Wei et al., 2010).

Genus diversity patterns for all studied regions showed different outcomes than those observed for standing stocks. The increase in OM input was positively correlated to nematode alpha and beta diversity, but only to a certain extent. While for the WIM sites a decrease in OM with depth resulted in a clear decrease of beta diversity within and between stations, for the abyssal transects this trend did not hold. While the SO represented an eutrophic environment, and the NA an oligotrophic environment, the latter exhibited higher genus and species alpha diversity than the SO (**Chapter 4**). Due to the high OM input observed especially for HC_AEP, HC_BEP, and SG, nematode alpha diversity was depressed due to a high dominance of certain genera, such as *Desmodora* in SG and *Microlaimus* in HC_AEP and HC_BEP. The presence of the genera *Microlaimus* and *Desmodora* indicates a certain degree of disturbance, as these genera are characterized as opportunistic and typical colonizers, showing a rapid response to enhanced OM input fluxes (Vanreusel et al., 2010b). For both the SO and WIM (shelf) sites, *Microlaimus* was the most or one of the most abundant genera (> 5 %) (**Chapters 4 and 5**). Moreover, at the SO, also vertical migration to the sediment surface was observed for *Microlaimus* when one site was sampled before and after the phytoplankton bloom. This indicates that vertical migration is a response to seasonal phytodetritus input to the seafloor (**Chapter 2**).

In the SO, fatty acid analyses revealed that nematodes may selectively take up high quality fatty acids, named polyunsaturated fatty acids, or PUFAs (Guilini et al., 2013; **Chapter 3**). PUFAs are considered plankton-based and their high relative concentration in nematodes indicated a diet based on fresh phytodetritus derived from surface waters. The high concentration of 'labile' plankton-derived PUFAs in nematodes was mainly observed for nematodes at the SG site. Contrastingly, the other sites located at the PF exhibited high levels of the fatty acid DHA, which potentially represents food sources with high refractory material content (Dalsgaard et al., 2003). In the deep sea, the generally low food input might favour organisms which are adapted to a deposit feeding behaviour, as well as a possible food resource partitioning. Therefore, we can assume that whenever high quality food is available, nematodes feed selectively, whereas when high-quality food is limited they will show a more opportunistic feeding behaviour, ingesting mainly refractory material or developing a food resource partitioning strategy (**Chapter 5**).

In conclusion, variation in OM input could explain most of the regional differences observed. While NA showed a higher alpha diversity in comparison with the SO sites, low regional diversity was observed within and across sites. The constancy of low OM input was probably the responsible factor for the low turnover observed in this area. In contrast, a higher range of food input probably enhanced patchiness and aggregation of benthic communities in the SO, resulting in a higher community turnover (Shorrocks and Sevenster, 1995). High between-core variability in food availability at the WIM (shelf break) sites, however, indicates that other productivity-related processes played a role in determining small-scale patchiness as well as habitat heterogeneity and alpha diversity in this habitat (Danovaro et al., 2013; **Chapter 5**; and see below).

Sediment heterogeneity and composition are considered to indirectly affect nematode communities through biochemical processes prevailing in different sediment types, and the interaction with hydrodynamics (Vanaverbeke et al., 2011; Vincx et al., 1994).

However, trends in sediment composition and nematode assemblages are still controversial (Fonseca et al., 2014). While elevated alpha diversity and reduced dominance was observed for areas with coarser sediment, (Leduc et al., 2012a; Vanaverbeke et al., 2011), the opposite effect or no effect has also been reported, but at genus level (Fonseca et al., 2014). Our results also showed a positive correlation between relative abundance of sediment grain size classes and nematode Shannon-Wiener diversity (Fig. 6.5). Higher variation in sediment composition both at the WIM (shelf break) and NA sites were associated with higher nematode alpha and within-station beta diversity. The coarser sediment at the SG site formed an exception, not resulting in a higher alpha diversity. Moreover, the increase in sediment particle size diversity (i.e. the proportion of each sediment fraction) also contributed to the even higher alpha diversity exhibited at the WIM (shelf break) in relation to the NA. In general, the high sediment heterogeneity observed at NA and WIM (shelf break) in comparison with SO and WIM (slope), strongly indicates an effect of hydrodynamics in both areas. In this regard, it can be assumed that if sediment can be resuspended, so can small organisms, especially those dwelling in the surface layers (0–2 cm). At the WIM, hydrodynamics at the shelf-break sites was possibly the main driver responsible for among-site variation, supporting high habitat heterogeneity and subsequently not only high alpha, but also high beta diversity between sites. Concurrently, at the NA transect nematode communities also seem to be under the influence of strong bottom dynamics through the eastward Antarctic bottom water (AABW) flux, which exhibits currents of 18–35 cm/s (Eitrem et al., 1983; Ludwig and Rabinowitz, 1980; Morozov et al., 2015). These findings depict a complex interaction of water-column features, such as surface primary productivity, as well as current regimes, on the benthic communities. While here this connection could be inferred for nematodes, other studies indicate similar patterns for other taxonomic groups and size classes as well, thus suggesting generality of these findings (Havermans et al., 2013; Rex et al., 2006).

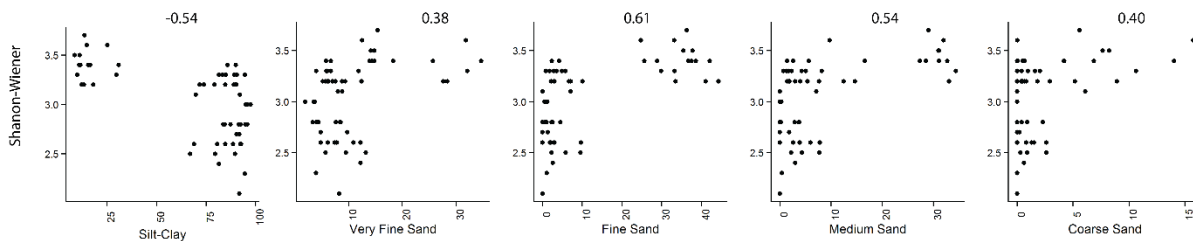


Figure 6.5. Nematode Shannon-Wiener diversity in relation to sediment grain size for five different sediment fractions: silt-clay, very fine sand, fine sand, medium sand, and coarse sand. Values on top of each graph refer to the Spearman rank correlation values for each correlation coefficient. All correlations are statistically significantly ($p < 0.05$).

The effect of hydrodynamics can result in the increase in passive dispersal through the water column. Nematodes, despite lacking a larval stage, can disperse throughout their whole life either passively by drifting in the water column or through bedload movement, or actively using chemical cues (Boeckner et al., 2009; Gallucci et al., 2008). Moreover, dispersal capabilities could be species-specific, since some nematode species have morphological adaptations, such as a long tail, to avoid erosion into the water column (da Fonseca-Genevois et al., 2006; Lins et al., 2013). This way, the higher beta diversity observed in the NA and WIM (shelf break) transects could have not only exhibited higher diversity due to OM input and sediment heterogeneity, but also as a result of dispersal events.

6.2.2 Spatial variation in nematode composition (bathymetrical and geographical patterns)

In general, faunal dispersal over large geographical distances (1000s of km) appears to be favoured by the physical uniformity of the deep sea at extensive depths (France and Kocher, 1996). Therefore, deep-sea basins seem not to represent completely isolated

systems (Levin et al., 2001). Depth or depth-related factors on the contrary seem to impose dispersal limitations on selected taxa, such as some crustaceans and molluscs (France and Kocher, 1996; Havermans et al., 2013; Jennings et al., 2013). For other taxa, such as nematodes from the order Enoplida however, regular interchanges between shallow and deep waters could be detected genetically (Bik et al., 2010). In this thesis, nematodes collected at different depths from the WIM (**Chapter 5**) revealed no evidence for depth-endemic lineages or isolation for the genus *Halalaimus*. Instead, species collected at different bathymetrical transects (300 m vs. 1000 m) were intermingled in the phylogenetic reconstruction, indicating exchange between shelf break and upper-slope habitats (**Chapter 3**).

In this general discussion, in order to identify the potential depth and spatial variation influence we have conducted a DistLM (Distance-based Lineal Model) analysis on all study areas together to identify which factors (environmental versus spatial) would explain most of the variability found in the nematode community structure between areas. SIMPER (Similarity percentages) analyses were performed to investigate which factors contributed the most for the variability between bathyal and abyssal areas. As environmental factors we have included **OM input** (CPE, %TN, %TOC, %TOM, NPP, and estimated POC flux) and **sediment granulometry characteristics** (silt-clay, very fine sand, fine sand, medium sand, and coarse sand), while as spatial factors **water depth** and **geographical distances** (latitude, longitude, latitude², longitude², latitude³, and longitude³)⁶ were included. Food availability and sediment characteristics had a strong effect on the nematode community between areas rather than spatial variation (Table 6.1.).

⁶ Quadratic and cubic components were used in order to take gaps and patches into account. This design followed Leduc et al. (2012a).

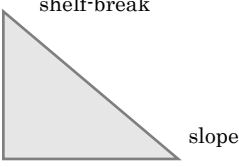

Table 6.1. DistLM (Distance-based Linear Model) results for marginal tests and sequential tests showing the influence of environmental (food availability and sediment characteristics) and spatial (depth and spatial structure) factors on the nematode multivariate community beta diversity. Food availability refers to the following variables: chloroplastic pigment equivalents (CPE), total nitrogen (% TN), total carbon (% TOC), total organic matter (% TOM), net primary productivity (NPP), and estimated particulated organic carbon flux (POC). Sediment characteristics include: silt-clay, very fine sand, fine sand, medium sand, and coarse sand. Geographical distances include: latitude, longitude, latitude², longitude², latitude³, and longitude³. Prop. = proportion of total variation explained; Prop. (cumul) = proportion of total accumulative variation. Only variables with $p < 0.05$ were added.

	Prop.	Prop. (cumul)
Marginal		
Depth	0.12	
Spatial structure	0.79	-
Sediment characteristics	0.64	-
Food availability	0.59	-
Sequential (Env. Factors)		
Food availability + Sediment characteristics	0.39	0.39
+ Spatial structure	0.18	0.57
+ Water Depth	0.01	0.58
Sequential (Spatial)		
Spatial structure + Water Depth	0.19	0.19
+ Sediment characteristics	0.07	0.26
+ Food availability	0.32	0.58

In the studies presented here it could be shown that a complex interaction of factors, such as sediment heterogeneity (possibly due to hydrodynamic conditions), OM input, water depth, and spatial variability, are reflected in diversity patterns between areas. According to our results, water depth had a low impact on nematode distribution between areas, together with spatial geographical differences. Nematode communities between areas, thus, seem to be regulated mainly by environmental factors, which is summarized in Table 6.2. According to the SIMPER results, it seems that for bathyal habitats, both sediment characteristics and OM input have an additive effect, enhancing nematode density and biomass, as well as alpha and beta diversity. At abyssal plains, however, high alpha

diversity is related to high sediment diversity and silt-clay content, while regional diversity seem to be determined mostly by food availability.

Table 6.2. Main environmental factors and diversity scales studied in this thesis. The grey triangle illustrates the continental margin (bathymetrical difference), and the grey square the abyssal plain (geographical difference). WIM = Western Iberian Margin; NA = North Atlantic, VEMA transect; SO= Southern Ocean transect. OM = organic matter.

	Variable	WIM (shelf break) vs. WIM (slope)	
	Diversity (local)	High diversity	Low diversity
	Diversity (regional)	High diversity	Low diversity
	Density	High	Low
	Biomass	High	Low
	OM input	High	Low
	Sediment diversity	High	Low
	Silt-clay content	Low	High
		NA vs. SO	
	Diversity (local)	High diversity	Low diversity
	Diversity (regional)	Low diversity	High diversity
	Density	Low	High
	Biomass	Low	High
	OM input	Low	High
	Sediment diversity	High	Low (except for SG)
	Silt-clay content	Low	High

Changes in diversity patterns between deep-sea and shallow-water environments can vary greatly. In a large overview comparing different habitats, Moens et al. (2014) suggested that variability between these two environments is mostly dictated by physical disturbance and food availability (including quality and quantity). Patterns in food availability would explain, for instance, why estuaries possess a high dominance of few species (Heip et al., 1985), while upper slopes and abyssal plains are highly diverse (Vanaverbeke et al., 1997; Vanreusel et al., 2010b). When food is available in higher amounts, dominance of few species or genera occurs by these species outcompeting other species, and thus reducing the diversity of an area. In contrast, if food is scarce, then likewise a decrease in diversity can be observed due to the low food availability (Leduc et

al., 2012b). In this regard, it seems that productivity regulates both shallow-water and deep-sea environments in similar ways.

Physical disturbance, when at intermediate levels, can enhance diversity in both deep sea and shallow water. While abyssal environments are believed to be relatively stable, mid-intertidal peaks of nematode diversity are consistent with the intermediate disturbance hypothesis (Schratzberger et al., 2009). Moens et al. (2014) suggest that a decrease in disturbance occurs with increasing water depth, as well as a bathymetrical trend of decrease in productivity (for non-chemosynthetic environments).

In general, it seems that similar factors are responsible for determining diversity patterns in both deep sea and shallow water, but that their spectra vary differently in these two environments. Shallow-water environments seem to exhibit a wider range of disturbance effects and productivity, as well as of other environmental factors, such as sediment heterogeneity, temperature, salinity, currents, and oxygen concentrations. In contrast, the deep sea exhibits relatively stable environmental conditions.

6.2.3 Non-ecological drivers of nematode diversity

The distribution of macrobenthic species in the deep sea has shown a general pattern of increasing species richness with increasing latitude (maximum richness between 20 and 30° N), for the northern hemisphere, while the southern hemisphere showed no trend (Gray, 2002). For nematode species diversity on a global scale, Lambshead et al. (2000) suggested an increase in nematode species richness for the northern hemisphere, while Ramirez-Llodra et al. (2010) indicated that nematode species richness is very similar at all latitudes, with slightly higher values at mid-high latitudes. In this sense, a gradient in

nematode species distribution should be interpreted with caution since sampling strategies should be comparable both quantitatively and qualitatively.

Thus, what drives species distribution and speciation in the deep sea and what might be the effect of evolutionary history on local and regional diversity? Until present, two opposing hypotheses have been suggested for the origin of the deep-sea fauna: the first states that evolution occurred within the deep sea, while the second suggest that the deep-sea diversity is a result of migration events from shallow water (Gage and Tyler, 1991). Some recent studies have indicated that both ideas are valid, as some shallow-water groups seem to have colonized the deep sea, while other groups have originated and diversified at great depths (Wilson, 1999). Studies concerning the evolutionary history of deep-sea meiofauna suggest genetic continuity across large geographic distances and multiple exchanges between shallow and deep waters on an evolutionary scale (Bik et al., 2010; Easton and Thistle, 2016). This large dispersibility and capability for large-distance migration make the reconstruction of colonization patterns difficult to conduct for nematodes.

Jennings and Etter (2014) have observed that colonisation of the North Atlantic by protobranch bivalves was paralleled with patterns observed in shallow water. They suggest that pan-Atlantic species distributions of these organisms could have resulted from various colonization pathways which connected different regions of the Atlantic. Generally, one might think that the reduced or absence of planktonic larvae typically found in deep-sea organisms would restrict gene flow in the deep sea (Wilson and Hessler, 1987). However, the presence of widespread or cosmopolitan species together with the low genetic variability already observed for some groups of crustaceans and bivalves could be explained by the homogeneity of this habitat (Easton and Thistle, 2016; Havermans et al., 2013).

For nematodes, the presence of cosmopolitan species (Zeppilli et al., 2011) indicates very high dispersibility of this group. This makes allopatric speciation caused by dispersal barriers less likely to offer an explanation for the high diversity of these organisms (Lins et al., unpublished). On the other hand, the high local diversity of nematodes found in the deep sea could be the result of sympatric speciation due to partitioning of food resources over evolutionary time scales. Sympatric speciation, together with the slow rate of ecological interactions, potential low predation, and low extinction rates, might explain the coexistence of a high number of species belonging to the same genus, as it occurs for the genera *Acantholaimus* and *Halalaimus*.

6.3 Research constraints and future perspectives

The deep sea is a rather unexplored environment, still offering many possibilities for research and new discoveries (Ramirez-Llodra et al., 2010). In the last years, some mysterious and amazing species and even higher taxa, associated with different environments have been discovered at a high rate (Bezerra et al., 2013; Osborn et al., 2011; Ramirez-Llodra et al., 2010; Riehl et al., 2014). However, at the same time the deep sea is a difficult environment to study due to its vastness and difficult accessibility due to technical constraints.

One could start with the sampling constraints researchers face due to limited ship time and lack of depth-proof technologies. Research campaigns are very costly and, hence, most of the ecological studies are restricted to 3–4 replicates and few sites. In this sense, macro-ecological scales (1000s of km) are highly favoured instead of smaller sampling scales (10s of m). Nevertheless, with the advent of new technology, small-scale and *in situ*

experimental research have made great progress. As an example, during a recent research cruise onboard of the RV Sonne, refined *in situ* experiments have been conducted in the Peru Basin, Pacific Ocean with the use of small-scale nutrient and oxygen profilers, crawlers, as well as sedimentation and respiration experiments with the aid of an arm-equipped ROV (Boetius, 2015). This research allowed the sampling of meiofaunal cores at centimeter scale and the close monitoring of environment conditions that are normally difficult to measure, such as oxygen, which could be important to explain patterns of meiofauna diversity at a local scale.

A second important future aspect of deep-sea research is the study of the importance of biodiversity in this environment, and how and why it varies across different spatial and temporal scales. In this context, taxonomic expertise is critical. For nematodes, due to time constraints, in most studies the identifications are restricted to genus level. However, it is still not clear how reliable this generic information is in comparison with species-level data (Leduc et al., 2012a). The addition of molecular techniques has been successful for some taxa (e.g. *Halalaimus*, *Desmodora*, *Sabatieria*), though the lack of robust information for other taxa (e.g. the family Phanodermatidae) is still a challenge and a bottleneck in meiofauna research, especially considering the poor quality of many species descriptions (Lins et al., unpublished results). For example, we have attempted to use Sanger sequencing on the macrofauna-sized nematodes from the NA along the Vema fracture zone in order to test whether species belonging to the family Phanodermatidae could be found at both sides of the Mid-Atlantic Ridge (MAR) or if the MAR would represent a physical barrier. The preliminary phylogenetic results (Fig. 6.6) are difficult to interpret due to the lack of node support (low bootstrap values) at deep and intermediate nodes as well as the lack of clear groupings based on morphology. Nevertheless, in the COI phylogeny (Fig. 6.6) the close relationships and clustering of specimens from either east or west revealed that there seems to be geographic structuring in these nematodes at species level. However,

due to the lack of node support, the presence of region-specific lower clades could not be inferred. Here, the low bootstrap values observed for COI were also reported for 18S and ITS, suggesting that the deeper nodes within the family Phanodermatidae is not resolved. In this regard, the use of new techniques, such as DNA barcoding, is promising. Still, because DNA barcoding relies upon a well-established reference library, at this point rather a combination of morphological and molecular (phylogenetic and species-delimitation) methods (i.e., integrative taxonomy) seems to be the best solution for unravelling taxonomic and biodiversity patterns in the deep sea at species level.

Beyond we illustrate in Fig. 6.7. preliminary metabarcoding results obtained for the WIM and NA. Although we can have an idea about diversity when comparing different areas, these results illustrate that taxonomic refinement (i.e. correct matches at either genus or species level) is still a challenge if no extensive species library has been developed.

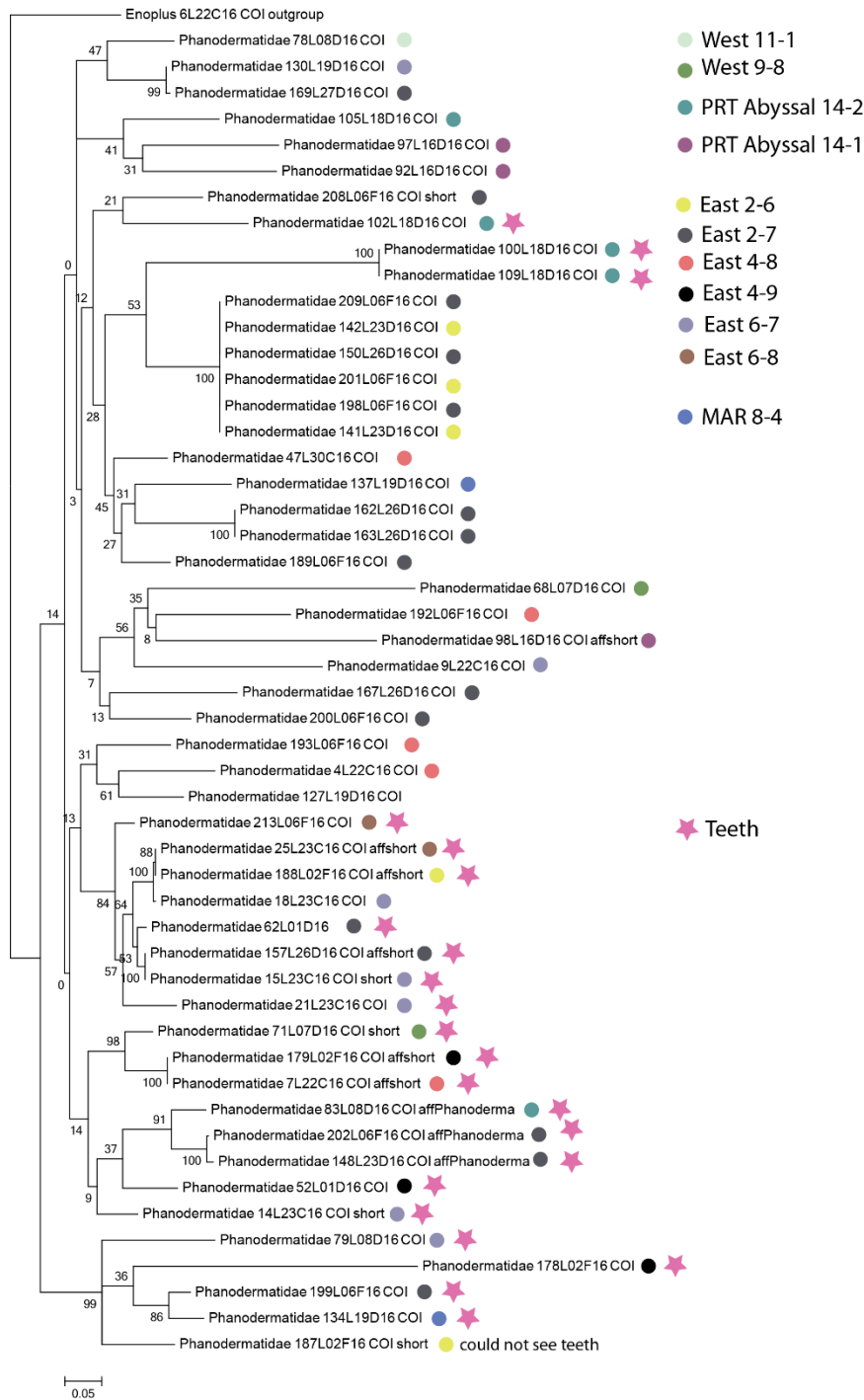


Figure 6.6. Preliminary results from the partial COI phylogeny of the nematode family Phanodermatidae. The inferred relationships support no clear separation of clades into groups restricted to east or west of the Mid-Atlantic Ridge (MAR). Generally, clades are intermingled between sites and regions. However, on species level (i.e., sequences with separation < 0.05) a clear geographic clustering was found. Nodes deep within the family have no statistical support. Reconstruction of Phanodermatidae COI relationships was conducted using Maximum Likelihood. Bootstrap support values were generated using 1000 replicates. The analyses were performed by means of Randomized Axelerated Maximum likelihood (RAxML). Due to the poor description of the genera from this family, an attempt was made to separate groups by the presence of teeth (pink star). This morphological character is distributed over several major clades in the tree. Due to the unsupported deeper nodes, inference of origins of teeth were not always possible, however, this character appears to be generally conservative as it is present in all specimens of several well-supported clades, while it is completely absent in

others. West represents sites west of the MAR, East sites east of the MAR, and PRT Abyssal, sites from the same depth collected at the adjacent Porto Rico Trench.

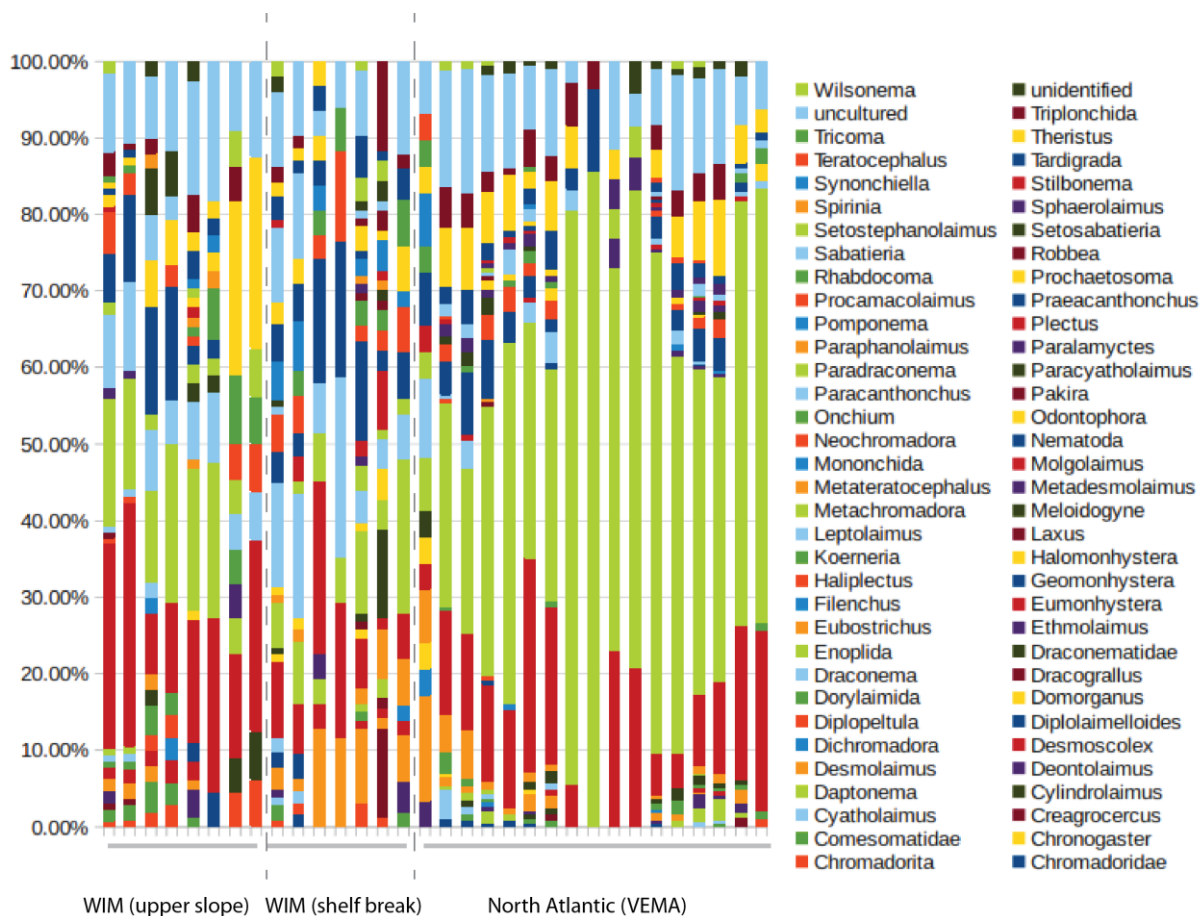


Figure 6.7. Preliminary results from the metabarcoding analysis for the Western Iberian Margin (WIM) and North Atlantic along the Vema Fracture Zone. This figure shows that for some groups low refinement (e.g. Enoplida is only kept at order level) and wrong BLAST results due to the low amount of sequences available in the database (e.g. *Wilsonema*, a soil nematode) can still hamper the broad use of this technique. Some groups are identified with the same colour, this means that the BLAST did not exhibit clear results, i.e. that matches could be one group or the other. The y axis shows the relative abundance of each group.

Understanding biodiversity can subsequently help in clarifying how ecosystem functioning in the deep sea is influenced by biodiversity patterns and how changes in diversity may alter functioning or vice-versa. During this PhD, we have tried to understand how deep-sea functioning differs from shallow water by conducting a respiration experiment at the WIM area (Fig. 6.8). Unfortunately, the use of this data was not possible due to the low amount of replicates performed, but nevertheless a hint could be provided indicating that deep-sea environments may be different from shallow-water systems (see shallow-water

nematode respiration rates in Braeckman et al., 2013). Oxygen consumption due to respiration seems to be much slower for deep-sea organisms than for shallow-water individuals, possibly resulting from a lower metabolism in the first. These results indicate that caution should be taken when transposing concepts accepted for one environment to another. Recently, the development of new respiration chambers have already allowed *in situ* respiration experiments at abyssal depths (Boetius, 2015). This progress will bring understanding ecosystem functioning aspects into reach in the near future.

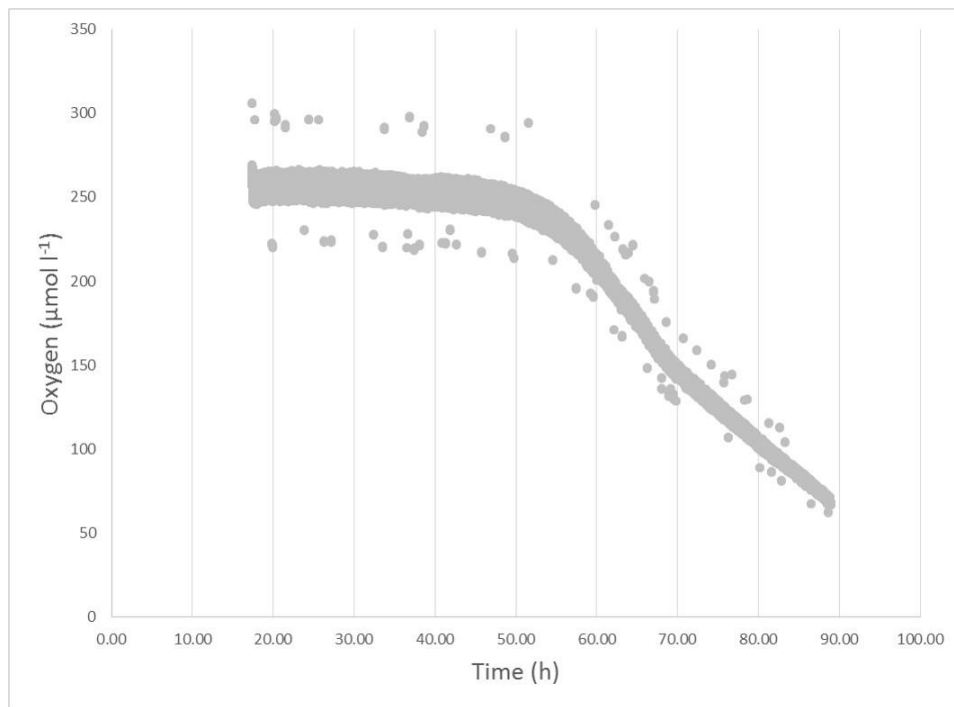


Figure 6.8. Nematode oxygen consumption in function of time for nematodes collected at the 1000 m upper slope sites at the Western Iberian Margin campaign (B2014/15).

The last constraint found in this thesis was mostly related to the small size of meiofauna. Due to the small size of nematodes, the use of some molecular tools, such as barcoding, food-web analyses based on fatty acids, compound specific stable isotopes, and simple stable isotopes, was restricted to “bulk” analysis. Our barcoding results had a success rate

of 30 % for meiofauna-sized nematodes (**Chapter 5**), while for macrofauna-sized nematodes success rate was almost 100 % (Lins et al. unpublished results). Our fatty acid analyses could only be possible for specific groups due to the unusually high abundance of some groups (**Chapter 3**). Moreover, we also have tried to conduct specific compound stable isotope analyses using amino acids on bulk nematodes to investigate the role of nematode in food-webs without the need of a primary producer, since some amino acids vary with increasing trophic level while others remain constant. However, few milligrams of nitrogen are needed for this analyses and even 500 individuals were not enough to obtain clear peaks, possibly because deep-sea nematodes are not only smaller, but also more slender than shallow-water ones (Soetaert et al., 2002). Although we have faced limitations due to our low sample size here, increase in the sensitivity of fatty acid and stable isotope analyses with a lower number of individuals was already possible in a recent study by Leduc et al. (2014).

Overall, considering past research and future perspectives, current deep-sea research has faced great breakthroughs, especially technology-wise. This thesis contributed with new information regarding the ecology of deep-sea meiofauna in terms of benthic-pelagic coupling and food selectivity, as well as to how and why nematode communities change across different spatial scales and environmental gradients. The increasing knowledge about the different habitats and organisms dwelling in the deep ocean is growing at a fast pace, helping to understand the big amazing puzzle that the deep sea represents. To conclude, with the increasing amount of collaborations between different research groups and consequently the amount of shared knowledge, the future of deep-sea research seems very auspicious and exciting regarding what next discoveries will bring.



20,0 μm

Cited literature

- Abdulkadir, S., Tsuchiya, M., 2008. One-step method for quantitative and qualitative analysis of fatty acids in marine animal samples. *J. Exp. Mar. Bio. Ecol.* 354, 1–8. doi:10.1016/j.jembe.2007.08.024
- Abelmann, A., Gersonde, R., Cortese, G., Kuhn, G., Smetacek, V., 2006. Extensive phytoplankton blooms in the Atlantic sector of the glacial Southern Ocean. *Paleoceanography* 21. doi:Pa101310.1029/2005pa001199
- Akaike, H., 1981. A new look at the statistical-model identification. *Curr. Contents/Engineering Technol. Appl. Sci.* 22.
- Alvarez-Salgado, X.A., Castro, C.G., Perez, F.F., Fraga, F., 1997. Nutrient mineralization patterns in shelf waters of the Western Iberian upwelling. *Cont. Shelf Res.* 17, 1247–1270. doi:10.1016/s0278-4343(97)00014-9
- Amante, C., Eakins, B.W., 2009. ETOPO1 1 Arc-Minute Global Relief Model: Procedures, Data Sources and Analysis. NOAA Tech. Memo. NESDIS NGDC-24 19. doi:10.1594/PANGAEA.769615
- Amaro, T., Witte, H., Herndl, G.J., Cunha, M.R., Billett, D.S.M., 2009. Deep-sea bacterial communities in sediments and guts of deposit-feeding holothurians in Portuguese canyons (NE Atlantic). *Deep. Res. I.*
- Anderson, M.J., Gorley, R.N., Clarke, K.R., 2008. PERMANOVA+ for PRIMER: Guide to software and statistical methods.
- Arrigo, K.R., Thomas, D.N., 2004. Large scale importance of sea ice biology in the Southern Ocean. *Antarct. Sci.* 16, 471–486. doi:10.1017/s0954102004002263
- Atkinson, A., Whitehouse, M.J., Priddle, J., Cripps, G.C., Ward, P., Brandon, M.A., 2001. South Georgia, Antarctica: a productive, cold water, pelagic ecosystem. *Mar. Ecol. Prog. Ser.* 216, 279–308. doi:10.3354/meps216279
- Baas-Becking, L.G.M., 1934. *Geobiologie of inleiding tot de milieukunde*, The Hague, Neth.: van Stockum and Zoon.
- Baldrighi, E., Lavaleye, M., Aliani, S., Conversi, A., Manini, E., 2014. Large Spatial Scale Variability in Bathyal Macrobenthos Abundance, Biomass, alpha- and beta-Diversity along the Mediterranean Continental Margin. *PLoS One* 9, 1–16. doi:http://dx.doi.org/10.1371/journal.pone.0107261
- Bathmann, U., 2010. The expedition of the research vessel “Polarstern” to the Antarctic in 2007/2008 (ANT-XXIV/2), *Berichte zur Polar- und Meeresforschung* (Reports on Polar and Marine Research). Bremerhaven.
- Bathmann, U., Herrmann, S., 2010. Plankton parameters: Chlorophyll a, particulate organic carbon, biological silica (Report), The Expedition of the Research Vessel “Polarstern” to the Antarctic in 2007/2008 (ANT-XXIV/2). *Berichte zur Polar- und Meeresforschung*.
- Beckmann, A., Timmermann, R., Pereira, A.F., Mohn, C., 2001. The effect of flow at Maud Rise on the sea-ice cover - numerical experiments. *Ocean Dyn.* 52, 11–25.
- Behrenfeld, M.J., Falkowski, P.G., 1997. Photosynthetic rates derived from satellite-based chlorophyll concentration. *Limnol. Oceanogr.* 42, 1–20.

- Belley, R., Snelgrove, P.V.R., Archambault, P., Juniper, S.K., 2016. Environmental Drivers of Benthic Flux Variation and Ecosystem Functioning in Salish Sea and Northeast Pacific Sediments. *PLoS One* 11. doi:10.1371/journal.pone.0151110
- Benson, D.A., Karsch-Mizrachi, I., Lipman, D.J., Ostell, J., Wheeler, D.L., 2008. GenBank. Nucleic Acids Research [WWW Document]. URL <http://www.ncbi.nlm.nih.gov/genbank/>
- Bezerra, T.N., Pape, E., Hauquier, F., Vanreusel, A., Ingels, J., 2013. New genus and two new species of the family Ethmolaimidae (Nematoda: Chromadorida), found in two different cold-seep environments. *Zootaxa* 3692, 7–27. doi:10.11646/zootaxa.3692.1.4
- Bik, H.M., Thomas, W.K., Lunt, D.H., Lambshead, P.J.D., 2010. Low endemism, continued deep-shallow interchanges, and evidence for cosmopolitan distributions in free-living marine nematodes (order Enoplida). *Bmc Evol. Biol.* 10. doi:38910.1186/1471-2148-10-389
- Billett, D.S.M., Bett, B.J., Evans, R., Cross, I., Tyler, P.A., Wolff, G.A., 2013. The reproductive ecology of deep-sea ophiuroids around the Crozet plateau, Southern Indian ocean, under contrasting productivity regimes. *Deep. Res. Part II-Topical Stud. Oceanogr.* 92, 18–26. doi:10.1016/j.dsr2.2013.03.002
- Billett, D.S.M., Lampitt, R.S., Rice, A.L., Mantoura, R.F.C., 1983. Seasonal sedimentation of phytoplankton to the deep-sea benthos. *Nature* 302, 520–522. doi:10.1038/302520a0
- Birchenough, S.N.R., Reiss, H., Degraer, S., Craeymeersch, J.A.M., Mesel, de I.G., 2015. Climate change and marine benthos: a review of existing research and future directions in the North Atlantic. *Wiley Interdiscip. Rev. Clim. Chang.* 6, 203–223.
- Blaxter, M., Floyd, R., 2003. Molecular taxonomics for biodiversity surveys: already a reality. *Trends Ecol. Evol.* 18, 268–269. doi:10.1016/s0169-5347(03)00102-2
- Blaxter, M.L., De Ley, P., Garey, J.R., Liu, L.X., Scheldeman, P., Vierstraete, A., Vanfleteren, J.R., Mackey, L.Y., Dorris, M., Frisse, L.M., Vida, J.T., Thomas, W.K., 1998. A molecular evolutionary framework for the phylum Nematoda. *Nature* 392, 71–75. doi:10.1038/32160
- Boeckner, M.J., Sharma, J., Proctor, H.C., 2009. Revisiting the meiofauna paradox: dispersal and colonization of nematodes and other meiofaunal organisms in low- and high-energy environments. *Hydrobiologia* 624, 91–106. doi:10.1007/s10750-008-9669-5
- Boetius, A., 2015. Short Cruise Report RV SONNE – SO242 / 2 Guayaquil – Guayaquil.
- Boon, A.R., Duineveld, G.C.A., 1996. Phytopigments and fatty acids as molecular markers for the quality of near-bottom particulate organic matter in the North Sea. *J. Sea Res.* 35, 279–291. doi:10.1016/s1385-1101(96)90755-8
- Braeckman, U., Vanaverbeke, J., Vincx, M., van Oevelen, D., Soetaert, K., 2013. Meiofauna Metabolism in Suboxic Sediments: Currently Overestimated. *PLoS One* 8. doi:e5928910.1371/journal.pone.0059289
- Brandão, S.N., Vital, H., Brandt, A., 2014. Southern Polar Front macroecological and biogeographical insights gained from benthic Ostracoda. *Deep. Res. II* 108, 33–50. doi:http://dx.doi.org/10.1016/j.dsr2.2014.06.004

- Brandon, M.A., Murphy, E.J., Trathan, P.N., Bone, D.G., 2000. Physical oceanographic conditions to the northwest of the sub-Antarctic Island of South Georgia. *J. Geophys. Res.* 105, 23983–23996. doi:10.1029/2000jc900098
- Brandt, A., Bathmann, U., Brix, S., Cisewski, B., Flores, H., Goecke, C., Janussen, D., Kraegefsky, S., Kruse, S., Leach, H., Linse, K., Pakhomov, E., Peeken, I., Riehl, T., Sauter, E., Sachs, O., Schueller, M., Schroedl, M., Schwabe, E., Strass, V., van Franeker, J.A., Wilmsen, E., 2011a. Maud Rise - a snapshot through the water column. *Deep. Res. Part II-Topical Stud. Oceanogr.* 58, 1962–1982. doi:10.1016/j.dsr2.2011.01.008
- Brandt, A., Ebbe, B., 2009. Southern Ocean deep-sea biodiversity-From patterns to processes. *Deep. Res. Part II-Topical Stud. Oceanogr.* 56, 1732–1738. doi:10.1016/j.dsr2.2009.05.017
- Brandt, A., Ebbe, B., Bathmann, U., 2011b. Southern Ocean biodiversity-From pelagic processes to deep-sea response. *Deep. Res. Part II-Topical Stud. Oceanogr.* 58, 1945–1947. doi:10.1016/j.dsr2.2011.05.003
- Brandt, A., Gooday, A.J., Brandao, S.N., Brix, S., Broekeland, W., Cedhagen, T., Choudhury, M., Cornelius, N., Danis, B., De Mesel, I., Diaz, R.J., Gillan, D.C., Ebbe, B., Howe, J.A., Janussen, D., Kaiser, S., Linse, K., Malyutina, M., Pawlowski, J., Raupach, M., Vanreusel, A., 2007. First insights into the biodiversity and biogeography of the Southern Ocean deep sea. *Nature* 447, 307–311. doi:10.1038/nature05827
- Brandt, A., Vanreusel, A., Bracher, A., Hoppe, C.J.M., Lins, L., Meyer-Löbbecke, A., Soppa, M.A., Würzberg, L., 2014. Are boundary conditions in surface productivity at the Southern Polar Front reflected in benthic activity? *Deep. Res. Part II-Topical Stud. Oceanogr.* 108, 51–59.
- Buchanan, J.B., 1984. Sediment analysis, in: Holme, N.A., McIntyre, A.D. (Eds.), *Methods for the Study of Marine Benthos*. Blackwell Scientific Publications, Oxford, pp. 41–65.
- Calabrese, J.M., Fagan, W.F., 2004. A comparison-shopper's guide to connectivity metrics. *Front. Ecol. Environ.* doi:10.1890/1540-9295(2004)002[0529:ACGTCM]2.0.CO;2
- Cannat, M., Mamaloukas-Frangoulis, V., Auzende, J.-M., Bideau, D., Bonatti, E., Honnorez, J., Lagabrielle, Y., Malavieille, J., Mevel, C., 1991. A geological cross-section of the VEMA fracture zone transverse ridge, Atlantic ocean. *J. Geodyn.* 13, 97–117.
- Cardinale, B.J., Gross, K., Fritschie, K., Flombaum, P., Fox, J.W., Rixen, C., van Ruijven, J., Reich, P.B., Scherer-Lorenzen, M., Wilsey, B.J., 2013. Biodiversity simultaneously enhances the production and stability of community biomass, but the effects are independent. *Ecology* 94, 1697–1707. doi:10.1890/12-1334.1
- Cardinale, B.J., Nelson, K., Palmer, M.A., 2000. Linking species diversity to the functioning of ecosystems: on the importance of environmental context. *Oikos* 91, 175–183. doi:10.1034/j.1600-0706.2000.910117.x
- Clarke, K.R., Gorley, R.N., 2006. *PRIMERv6:UserManual/Tutorial*.
- Closset, I., Cardinal, D., Bray, S.G., Thil, F., Djoureaev, I., Rigual-Hernández, A.S., Trull, T.W., 1992. Global biogeochemical cycles. *Global Biogeochem. Cycles* 1495–1510. doi:10.1002/2015GB005129.Received

- Company, J.B., Puig, P., Sarda, F., Palanques, A., Latasa, M., Scharek, R., 2008. Climate Influence on Deep Sea Populations. *PLoS One* 3. doi:10.1371/journal.pone.0001431
- Condie, S.A., Sherwood, C.R., 2006. Sediment distribution and transport across the continental shelf and slope under idealized wind forcing. *Prog. Oceanogr.* 70, 255–270. doi:10.1016/j.pocean.2005.07.003
- Crespo, B.G., Espinoza-Gonzalez, O., Teixeira, I.G., Castro, C.G., Figueiras, F.G., 2011. Possible mixotrophy of pigmented nanoflagellates: Microbial plankton biomass, primary production and phytoplankton growth in the NW Iberian upwelling in spring. *Estuar. Coast. Shelf Sci.* 94, 172–181. doi:10.1016/j.ecss.2011.06.008
- Crist, T.O., Veech, J.A., Gering, J.C., Summerville, K.S., 2003. Partitioning species diversity across landscapes and regions: A hierarchical analysis of alpha, beta, and gamma diversity. *Am. Nat.* 162, 734–743. doi:10.1086/378901
- da Fonseca-Genevois, V., Somerfield, P.J., Neves, M.H.B., Coutinho, R., Moens, T., 2006. Colonization and early succession on artificial hard substrata by meiofauna. *Mar. Biol.* 148, 1039–1050. doi:10.1007/s00227-005-0145-8
- Dalsgaard, J., St. John, M., Kattner, G., Müller-Navarra, D., Hagen, W., 2003. Fatty acid trophic markers in the pelagic marine environment. *Adv. Mar. Biol.* 46, 225–340.
- Danovaro, R., Carugati, L., Corinaldesi, C., Gambi, C., Guilini, K., Pusceddu, A., Vanreusel, A., 2013. Multiple spatial scale analyses provide new clues on patterns and drivers of deep-sea nematode diversity. *Deep. Res. Part II-Topical Stud. Oceanogr.* 92, 97–106. doi:10.1016/j.dsr2.2013.03.035
- Danovaro, R., Company, J.B., Corinaldesi, C., D'Onghia, G., Galil, B., Gambi, C., Gooday, A.J., Lampadariou, N., Luna, G.M., Morigi, C., Olu, K., Polymenakou, P., Ramirez-Llodra, E., Sabbatini, A., Sarda, F., Sibuet, M., Tselepidis, A., 2010. Deep-Sea Biodiversity in the Mediterranean Sea: The Known, the Unknown, and the Unknowable. *PLoS One* 5. doi:10.1371/journal.pone.0011832
- Danovaro, R., Dell'Anno, A., Martorano, D., Parodi, P., Marrale, N.D., Fabiano, M., 1999. Seasonal variation in the biochemical composition of deep-sea nematodes: bioenergetic and methodological considerations. *Mar. Ecol. Prog. Ser.* 179, 273–283. doi:10.3354/meps179273
- Danovaro, R., Gambi, C., Dell'Anno, A., Corinaldesi, C., Frascchetti, S., Vanreusel, A., Vincx, M., Gooday, A.J., 2008. Exponential decline of deep-sea ecosystem functioning linked to benthic biodiversity loss. *Curr. Biol.* 18, 1–8. doi:10.1016/j.cub.2007.11.056
- Dauwe, B., Herman, P.M.J., Heip, C.H.R., 1998. Community structure and bioturbation potential of macrofauna at four North Sea sites with contrasting food supply. *Mar. Ecol. Prog. Ser.* 173, 67–83. doi:10.3354/meps173067
- Davies, A.J., Roberts, J.M., Hall-Spencer, J., 2007. Preserving deep-sea natural heritage: Emerging issues in offshore conservation and management. *Biol. Conserv.* doi:10.1016/j.biocon.2007.05.011
- de Bovée, F., Labat, P.H., 1993. A simulation model of a deep meiobenthic compartment: A preliminary approach. *Mar. Ecol. Prog. Ser.* 14, 159–173.
- De Grisse, A., 1969. Redescription ou modification de quelques techniques utilisés dans l'étude des nématodes phytoparasitaires. *Meded. Rijksfakulteit Landbouwwet. Gent* 34, 251–369.

- De La Rocha, C.L., Passow, U., 2007. Factors influencing the sinking of POC and the efficiency of the biological carbon pump. *Deep. Res. Part II-Topical Stud. Oceanogr.* 54, 639–658. doi:10.1016/j.dsr2.2007.01.004
- de Meester, N., Derycke, S., Moens, T., 2012. Differences in time until dispersal between cryptic species of a marine nematode species complex. *PLoS One* 7, 1–8. doi:10.1371/journal.pone.0042674
- De Mesel, I., Lee, H.J., Vanhove, S., Vincx, M., Vanreusel, A., 2006. Species diversity and distribution within the deep-sea nematode genus *Acantholaimus* on the continental shelf and slope in Antarctica. *Polar Biol.* 29, 860–871. doi:10.1007/s00300-006-0124-7
- De Troch, M., Boeckx, P., Cnudde, C., Van Gansbeke, D., Vanreusel, A., Vincx, M., Caramujo, M.J., 2012. Bioconversion of fatty acids at the basis of marine food webs: insights from a compound-specific stable isotope analysis. *Mar. Ecol. Prog. Ser.* 465, 53–67. doi:10.3354/meps09920
- Decraemer, W., Gourbault, N., Helléouet, M.N., 2001. Cosmopolitanism among nematodes: examples from epsilonematidae. *vie milieu* 51, 11–19.
- Demidov, A.B., Mosharov, S.A., Gagarin, V.I., 2012. Meridional asymmetric distribution of the primary production in the Atlantic Sector of the Southern Ocean in the austral spring and summer. *Oceanology* 52, 623–634. doi:10.1134/s0001437012050050
- Derycke, S., Backeljau, T., Moens, T., 2013. Dispersal and gene flow in free-living marine nematodes. *Front. Zool.* 10. doi:10.1186/1742-9994-10-1
- Derycke, S., Remerie, T., Vierstraete, A., Backeljau, T., Vanfleteren, J., Vincx, M., Moens, T., 2005. Mitochondrial DNA variation and cryptic speciation within the free-living marine nematode *Pelioditis marina*. *Mar. Ecol. Prog. Ser.* 300, 91–103. doi:10.3354/meps300091
- Devey, C., Arndt, H., Augustin, N., Bober, S., Borges, V., Brandt, A., Brenke, N., Brix, S., Elsner, N., Frutos, I., Guggolz, T., Heitland, N., Jeuck, A., Klischies, M., Köhler, J., Lejzerowicz, F., Lins, L., Linse, K., Malyutina, M., Metz, D., Minzlaff, U., Prausse, D., Palgan, D., Riehl, T., Rothenbeck, M., Schimdt, C., Schmidt, C., Schoenle, A., Schultze, G., Schwabe, E., Springer, T., Steinführer, A., Triebe, L., Voltski, I., Walter, T., Wenzlaff, E., Yeo, I., Zinnkann, A.-C., Zoeller, K., 2015. SONNE-Berichte, Cruise No. SO-237, VEMA-Transit.
- Drago, T., Oliveira, A., Magalhaes, F., Cascalho, J., Jouanneau, J.M., Vitorino, J., 1998. Some evidences of northward fine sediment transport in the northern Portuguese continental shelf. *Oceanol. Acta* 21, 223–231. doi:10.1016/s0399-1784(98)80010-8
- Duros, P., Fontanier, C., Metzger, E., Pusceddu, A., Cesbron, F., de Stigter, H.C., Bianchelli, S., Danovaro, R., Jorissen, F.J., 2011. Live (stained) benthic foraminifera in the Whittard Canyon, Celtic margin (NE Atlantic). *Deep. Res. Part I-Oceanographic Res. Pap.* 58, 128–146. doi:10.1016/j.dsr.2010.11.008
- Easton, E.E., Thistle, D., 2016. Do some deep-sea, sediment-dwelling species of harpacticoid copepods have 1000-km-scale range sizes? *Mol. Ecol.* doi:10.1111/mec.13744
- Eittem, S.L., Biscaye, P.E., Jacobs, S.S., 1983. Bottom-water observations in the Vema fracture zone. *J. Geophys. Res.* 88, 2609–2614.

- Ercilla, G., Juan, C., Hernández-Molina, F.J., Bruno, M., Estrada, F., Alonso, B., Casas, D., Farran, M. I., Llave, E., García, M., Vázquez, J.T., D'Acremont, E., Gorini, C., Palomino, D., Valencia, J., El Mounni, B., Ammar, A., 2016. Significance of bottom currents in deep-sea morphodynamics: An example from the Alboran Sea. *Mar. Geol.* 378, 157–170. doi:10.1016/j.margeo.2015.09.007
- Etter, R.J., Bower, A.S., 2015. Dispersal and population connectivity in the deep North Atlantic estimated from physical transport processes. *Deep. Res. Part I-Oceanographic Res. Pap.* 104, 159–172. doi:10.1016/j.dsr.2015.06.009
- Etter, R.J., Boyle, E.E., Glazier, A., Jennings, R.M., Dutra, E., Chase, M.R., 2011. Phylogeography of a pan-Atlantic abyssal protobranch bivalve: implications for evolution in the Deep Atlantic. *Mol. Ecol.* 20, 829–843. doi:10.1111/j.1365-294X.2010.04978.x
- Etter, R.J., Grassle, J.F., 1992. Patterns of species-diversity in the deep sea as a function of sediment particle-size diversity. *Nature* 360, 576–578. doi:10.1038/360576a0
- Etter, R.J., Rex, M.A., Chase, M.R., Quattro, J.M., 2005. Population differentiation decreases with depth in deep-sea bivalves. *Evolution (N. Y.)* 59, 1479–1491. doi:10.1111/j.0014-3820.2005.tb01797.x
- Fabiano, M., Danovaro, R., 1999. Meiofauna distribution and mesoscale variability in two sites of the Ross Sea (Antarctica) with contrasting food supply. *Polar Biol.* 22, 115–123. doi:10.1007/s003000050398
- Fenchel, T., Finlay, B.J., 2004. The Ubiquity of Small Species: Patterns of Local and Global Diversity. *Bioscience* 54, 777. doi:10.1641/0006-3568(2004)054[0777:TUOSSP]2.0.CO;2
- Figueiras, F.G., Labarta, U., Reiriz, M.J.F., 2002. Coastal upwelling, primary production and mussel growth in the Rias Baixas of Galicia. *Hydrobiologia* 484, 121–131. doi:10.1023/a:1021309222459
- Fischer, G., Ratmeyer, V., Wefer, G., 2000. Organic carbon fluxes in the Atlantic and the Southern Ocean: Relationship to primary production compiled from satellite radiometer data. *Deep. Res. Part II Top. Stud. Oceanogr.* 47, 1961–1997. doi:10.1016/S0967-0645(00)00013-8
- Flach, E., Muthumbi, A., Heip, C., 2002. Meiofauna and macrofauna community structure in relation to sediment composition at the Iberian margin compared to the Goban Spur (NE Atlantic). *Prog. Oceanogr.* 52, 433–457. doi:10.1016/S0079-6611(02)00018-6
- Flores, H., van Franeker, J.-A., Cisewski, B., Leach, H., Van de Putte, A.P., Meesters, E., Bathmann, U., Wolff, W.J., 2011. Macrofauna under sea ice and in the open surface layer of the Lazarev Sea, Southern Ocean. *Deep. Res. Part II-Topical Stud. Oceanogr.* 58, 1948–1961. doi:10.1016/j.dsr2.2011.01.010
- Fonseca, G., Maria, T.F., Kandratavicius, N., Venekey, V., Gheller, P.F., Gallucci, F., 2014. Testing for nematode-granulometry relationships. *Mar. Biodivers.* 44, 435–443. doi:10.1007/s12526-014-0241-4
- Fonseca, G., Soltwedel, T., 2009. Regional patterns of nematode assemblages in the Arctic deep seas. *Polar Biol.* 32, 1345–1357. doi:10.1007/s00300-009-0631-4

- Forbes, E., 1844. Report on the Mollusca and Radiata of the Aegean Sea: And on Their Distribution, Considered as Bearing on Geology. Rep. Br. Assoc. Adv. Sci. 1843 129–193.
- France, S.C., Kocher, T.D., 1996. Geographic and bathymetric patterns of mitochondrial 16S rRNA sequence divergence among deep-sea amphipods, *Eurythenes gryllus*. Mar. Biol. 126, 633–643. doi:10.1007/bf00351330
- Franco, M. de A., Vanaverbeke, J., van Oevelen, D., Soetaert, K., Costa, M.J., Vincx, M., Moens, T., 2010. Respiration partitioning in contrasting subtidal sediments: seasonality and response to a spring phytoplankton deposition. Mar. Ecol. 31, 276–290. doi:10.1111/j.1439-0485.2009.00319.x
- Frid, C.L.J., Caswell, B.A., 2016. Does ecological redundancy maintain functioning of marine benthos on centennial to millennial time scales? Mar. Ecol. Evol. Perspect. 37, 392–410. doi:10.1111/maec.12297
- Froneman, P.W., Pakhomov, E.A., Balarin, M.G., 2004. Size-fractionated phytoplankton biomass, production and biogenic carbon flux in the eastern Atlantic sector of the Southern Ocean in late austral summer 1997-1998. Deep. Res. Part II-Topical Stud. Oceanogr. 51, 2715–2729. doi:10.1016/j.dsr2.2002.09.001
- Gage, J.D., 1997. High benthic species diversity in deep-sea sediments: The importance of hydrodynamics, Marine Biodiversity: patterns and processes. Cambridge University Press, Cambridge.
- Gage, J.D., 1996. Why are there so many species in deep-sea sediments? J. Exp. Mar. Bio. Ecol. 200, 257–286. doi:10.1016/s0022-0981(96)02638-x
- Gage, J.D., Lamshead, P.J.D., Bishop, J.D.D., Stuart, C.T., Jones, N.S., 2004. Large-scale biodiversity pattern of Cumacea (Peracarida: Crustacea) in the deep Atlantic. Mar. Ecol. Prog. Ser. 277, 181–196. doi:10.3354/meps277181
- Gage, J.D., Tyler, P.A., 1991. Deep-sea biology: a natural history of organisms at the deep-sea floor. Cambridge University Press, Cambridge.
- Gallucci, F., Moens, T., Vanreusel, A., Fonseca, G., 2008. Active colonisation of disturbed sediments by deep-sea nematodes: evidence for the patch mosaic model. Mar. Ecol. Ser. 367, 173–183. doi:10.3354/meps07537
- Gambi, C., Pusceddu, A., Benedetti-Cecchi, L., Danovaro, R., 2014. Species richness, species turnover and functional diversity in nematodes of the deep Mediterranean Sea: Searching for drivers at different spatial scales. Glob. Ecol. Biogeogr. 23, 24–39. doi:10.1111/geb.12094
- Garcia, R., Thomsen, L., 2008. Bioavailable organic matter in surface sediments of the Nazare canyon and adjacent slope (Western Iberian Margin). J. Mar. Syst. 74, 44–59. doi:10.1016/j.jmarsys.2007.11.004
- Gering, J.C., Crist, T.O., 2002. The alpha-beta-regional relationship: providing new insights into local-regional patterns of species richness and scale dependence of diversity components. Ecol. Lett. 5, 433–444. doi:10.1046/j.1461-0248.2002.00335.x
- Gerlach, S.A., Schrage, M., 1972. Life cycles at low temperatures in some free-living marine Nematodes. Veröff. Inst. Meeresforsch. Bremen 14, 5–11.
- Giere, O., 2009. Meiobenthology: the microscopic motile fauna of aquatic sediments.

- Ginger, M.L., Billett, D.S.M., Mackenzie, K.L., Kiriakoulakis, K., Neto, R.R., Boardman, D.K., Santos, V., Horsfall, I.M., Wolff, G.A., 2001. Organic matter assimilation and selective feeding by holothurians in the deep sea: some observations and comments. *Prog. Oceanogr.* 50, 407–421. doi:10.1016/s0079-6611(01)00063-5
- Glover, A., Paterson, G., Bett, B., Gage, J., Sibuet, M., Shearer, M., Hawkins, L., 2001. Patterns in polychaete abundance and diversity from the Madeira Abyssal Plain, northeast Atlantic. *Deep. Res. I* 48, 217–236.
- Glud, R.N., 2008. Oxygen dynamics of marine sediments. *Mar. Biol. Res.* 4, 243–289. doi:10.1080/17451000801888726
- Gontikaki, E., van Oevelen, D., Soetaert, K., Witte, U., 2011. Food web flows through a sub-arctic deep-sea benthic community. *Prog. Oceanogr.* 91, 245–259. doi:10.1016/j.pocean.2010.12.014
- Gooday, A.J., 2002. Biological responses to seasonally varying fluxes of organic matter to the ocean floor: A review. *J. Oceanogr.* 58, 305–332.
- Gooday, A.J., Hori, S., Todo, Y., Okamoto, T., Kitazato, H., Sabbatini, A., 2004. Soft-walled, monothalamous benthic foraminiferans in the Pacific, Indian and Atlantic Oceans: aspects of biodiversity and biogeography. *Deep. Res. Part I-Oceanographic Res. Pap.* 51, 33–53. doi:10.1016/j.dsr.2003.07.002
- Gooday, A.J., Jorissen, F.J., 2012. Benthic foraminiferal biogeography: controls on global distribution patterns in deep-water settings. *Ann. Rev. Mar. Sci.* 4, 237–62. doi:10.1146/annurev-marine-120709-142737
- Graeve, M., Kattner, G., Piepenburg, D., 1997. Lipids in Arctic benthos: does the fatty acid and alcohol composition reflect feeding and trophic interactions? *Polar Biol.* 18.
- Grassle, J.F., 1989. Species diversity in deep-sea communities. *Trends Ecol. Evol.* 4, 12–15. doi:10.1016/0169-5347(89)90007-4
- Grassle, J.F., Sanders, H.L., 1973. Life stories and the role of disturbance. *Deep. Res.* 20, 643–659.
- Gray, J.S., 2002. Species richness of marine soft sediments. *Mar. Ecol. Prog. Ser.* 244, 285–297. doi:10.3354/meps244285
- Gray, J.S., 1994. Is deep-sea species diversity really so high? Species diversity of the Norwegian continental shelf. *Mar. Ecol. Prog. Ser.* 112, 205. doi:10.3354/meps112205
- Griffiths, H.J., 2010. Antarctic Marine Biodiversity - What Do We Know About the Distribution of Life in the Southern Ocean? *PLoS One* 5. doi:e1168310.1371/journal.pone.0011683
- Guilini, K., Bezerra, T.N., Deprez, T., Fonseca, G., Holovachov, O., Leduc, D., Miljutin, D., Moens, T., Sharma, J., Smol, N., Tchesunov, A., Mokievsky, V., Vanaverbeke, J., Vanreusel, A., Vincx, M., 2016. NeMys: World Database of Free-Living Marine Nematodes [WWW Document]. URL <http://nemys.ugent.be> (accessed 8.29.16).
- Guilini, K., Veit-Köhler, G., De Troch, M., Van Gansbeke, D., Vanreusel, A., 2013. Latitudinal and temporal variability in the community structure and fatty acid composition of deep-sea nematodes in the Southern Ocean. *Prog. Oceanogr.* doi:http://dx.doi.org/10.1016/j.pocean.2013.01.002

- Gutzmann, E., Martínez Arbizu, P., Rose, A., Veit-Köhler, G., 2004. Meiofauna communities along an abyssal depth gradient in the Drake Passage. *Deep. Res. Part II-Topical Stud. Oceanogr.* 51, 1617–1628. doi:10.1016/j.dsr2.2004.06.026
- Hauquier, F., Ballesteros-Redondo, L., Gutt, J., Vanreusel, A., 2016. Community dynamics of nematodes after Larsen ice-shelf collapse in the eastern Antarctic Peninsula. *Ecol. Evol.* 6, 305–317. doi:10.1002/ece3.1869
- Havermans, C., Sonet, G., D'Acoz, C. d'Udekem, Nagy, Z.T., Martin, P., Brix, S., Riehl, T., Agrawal, S., Held, C., 2013. Genetic and Morphological Divergences in the Cosmopolitan Deep-Sea Amphipod *Eurythenes gryllus* Reveal a Diverse Abyss and a Bipolar Species. *PLoS One* 8. doi:UNSP e74218 10.1371/journal.pone.0074218
- Heip, C., Vincx, M., Vranken, G., 1985. The ecology of marine nematodes. *Oceanogr. Mar. Biol.* 23, 399–489.
- Hessler, R.R., Sanders, H.L., 1968. Faunal diversity in the deep sea. *Deep. Res. Oceanogr. Abstr.* 14, 65–70.
- Hessler, R.R., Sanders, H.L., 1967. Faunal diversity in the deep sea. *Deep. Res.* 14, 65–78.
- Hessler, R.R., Thistle, D., 1975. On the Place of Origin of Deep-Sea Isopods. *Mar. Biol.* 32, 155–165.
- Higgins, R.P., Thiel, H., 1988. Introduction to the study of meiofauna.
- Honnens, H., Assheuer, T., Ehlers, R.-U., 2014. Enrichment of the nematode *Panagrolaimus* sp., a potential live food for marine aquaculture, with essential n-3 fatty acids. *Aquac. Int.* 22, 399–409. doi:10.1007/s10499-013-9648-3
- Hughes, D.J., Gage, J.D., 2004. Benthic metazoan biomass, community structure and bioturbation at three contrasting deep-water sites on the northwest European continental margin. *Prog. Oceanogr.* 63, 29–55. doi:10.1016/j.pocean.2004.09.002
- Hunt, B.P. V, Pakhomov, E.A., Siegel, V., Strass, V., Cisewski, B., Bathmann, U., 2011. The seasonal cycle of the Lazarev Sea macrozooplankton community and a potential shift to top-down trophic control in winter. *Deep. Res. Part II-Topical Stud. Oceanogr.* 58, 1662–1676. doi:10.1016/j.dsr2.2010.11.016
- ICES, 2008. Report of the ICES Advisory Committee (Report). ICES Advice.
- Ingels, J., Tchesunov, A. V, Vanreusel, A., 2011. Meiofauna in the Gollum Channels and the Whittard Canyon, Celtic Margin-How Local Environmental Conditions Shape Nematode Structure and Function. *PLoS One* 6. doi:e2009410.1371/journal.pone.0020094
- Ingels, J., Van den Driessche, P., De Mesel, I., Vanhove, S., Moens, T., Vanreusel, A., 2010. Preferred use of bacteria over phytoplankton by deep-sea nematodes in polar regions. *Mar. Ecol. Ser.* 406, 121–133. doi:10.3354/meps08535
- Ingels, J., Vanhove, S., De Mesel, I., Vanreusel, A., 2006. The biodiversity and biogeography of the free-living nematode genera *Desmodora* and *Desmodorella* (family *Desmodoridae*) at both sides of the Scotia Arc. *Polar Biol.* 29, 936–949. doi:10.1007/s00300-006-0135-4
- Ingels, J., Vanreusel, A., 2013. The importance of different spatial scales in determining structural and functional characteristics of deep-sea infauna communities. *Biogeosciences* 10, 4547–4563. doi:10.5194/bg-10-4547-2013

- Iversen, M.H., Ploug, H., 2013. Temperature effects on carbon-specific respiration rate and sinking velocity of diatom aggregates - potential implications for deep ocean export processes. *Biogeosciences* 10, 4073–4085. doi:10.5194/bg-10-4073-2013
- Jamieson, R.E., Heywood, J.L., Rogers, A.D., Billett, D.S.M., Pearce, D.A., 2013. Bacterial biodiversity in deep-sea sediments from two regions of contrasting surface water productivity near the Crozet Islands, Southern Ocean. *Deep. Res. Part I-Oceanographic Res. Pap.* 75, 67–77. doi:10.1016/j.dsr.2012.12.012
- Janssen, A., Kaiser, S., Meissner, K., Brenke, N., Menot, L., Arbizu, P.M., 2015. A reverse taxonomic approach to assess macrofaunal distribution patterns in abyssal Pacific polymetallic nodule fields. *PLoS One* 10. doi:e011779010.1371/journal.pone.0117790
- Jeffreys, R.M., Burke, C., Jamieson, A.J., Narayanaswamy, B.E., Ruhl, H.A., Smith Jr., K.L., Witte, U., 2013. Feeding Preferences of Abyssal Macrofauna Inferred from In Situ Pulse Chase Experiments. *PLoS One* 8. doi:e8051010.1371/journal.pone.0080510
- Jennings, R.M., Etter, R.J., 2014. Phylogeographic estimates of colonization of the deep Atlantic by the protobranch bivalve *Nucula atacellana*. *Polish Polar Res.* 35, 261–278
- Jennings, R.M., Etter, R.J., Ficarra, L., 2013. Population Differentiation and Species Formation in the Deep Sea: The Potential Role of Environmental Gradients and Depth. *PLoS One* 8. doi:UNSP e7759410.1371/journal.pone.0077594
- Jensen, P., 1987. Feeding ecology of free-living aquatic nematodes. *Mar. Ecol. Ser.* 35, 187–196.
- Jensen, P., 1986. Nematode fauna in the sulphide-rich brine seep and adjacent bottoms of the East Flower Garden, NW Gulf of Mexico. *Mar. Biol.* 92, 489–503.
- Jensen, P., 1981. Phyto-chemical sensitivity and swimming behavior of the free-living marine nematode *Chromadorita tenuis*. *Mar. Ecol. Ser.* 4, 203–206. doi:10.3354/meps004203
- Jochem, F.J., Pollehne, F., Zeitzschel, B., 1993. Productivity regime and phytoplankton size structure in the Arabian Sea. *Deep. Res. Part II-Topical Stud. Oceanogr.* 40, 711–735. doi:10.1016/0967-0645(93)90054-q
- Jochem, F.J., Zeitzschel, B., 1993. Productivity regime and phytoplankton size structure in the tropical and subtropical North-Atlantic in Spring 1989. *Deep. Res. Part II-Topical Stud. Oceanogr.* 40, 495–519. doi:10.1016/0967-0645(93)90029-m
- Kaiser, S., Barnes, D.K.A., Brandt, A., 2007. Slope and deep-sea abundance across scales: Southern Ocean isopods show how complex the deep sea can be. *Deep. Res. Part II-Topical Stud. Oceanogr.* 54, 1776–1789. doi:10.1016/j.dsr2.2007.07.006
- Karakas, G., Nowald, N., Schäfer-Neth, C., Iversen, M., Barkmann, W., Fischer, G., Marchesiello, P., Schlitzer, R., 2009. Impact of particle aggregation on vertical fluxes of organic matter. *Prog. Oceanogr.* 83, 331–341. doi:10.1016/j.pocean.2009.07.047
- Katoh, K., Asimenos, G., Toh, H., 2009. Multiple Alignment of DNA Sequences with MAFFT (D Posada, Ed.). *Bioinforma. DNA Seq. Anal.* 537: 39–64.
- Kearse, M., Moir, R., Wilson, A., Stones-Havas, S., Cheung, M., Sturrock, S., Buxton, S., Cooper, A., Markowitz, S., Duran, C., Thierer, T., Ashton, B., Meintjes, P., Drummond, A., 2012. Geneious Basic: An integrated and extendable desktop

- software platform for the organization and analysis of sequence data. *Bioinformatics* 28, 1647–1649. doi:10.1093/bioinformatics/bts199
- Kelly, J.R., Scheibling, R.E., 2012. Fatty acids as dietary tracers in benthic food webs. *Mar. Ecol. Prog. Ser.* 446, 1–22. doi:10.3354/meps09559
- Killops, S., Killops, V., 2005. *Introduction to organic geochemistry*. Blackwell publishing, Oxford.
- Kim, S., 2013. Partial and Semi-partial (Part) correlation.
- Knox, G.A., 1994. *The biology of the Southern Ocean, The Southern Ocean*. Cambridge University Press, Cambridge.
- Kussakin, O.G., 1973. Peculiarities of geographical and vertical distribution of marine Isopods and problem of deep-sea fauna origin. *Mar. Biol.* 23, 19–34. doi:10.1007/bf00394108
- Lamshead, P.J.D., 2004. *Marine nematode biodiversity, Nematology: Advances and Perspectives*. CABI Publishing, Cambridge.
- Lamshead, P.J.D., Boucher, G., 2003. Marine nematode deep-sea biodiversity - hyperdiverse or hype? *J. Biogeogr.* 30, 475–485.
- Lamshead, P.J.D., Brown, C.J., Ferrero, T.J., Mitchell, N.J., Smith, C.R., Hawkins, L.E., Tietjen, J., 2002. Latitudinal diversity patterns of deep-sea marine nematodes and organic fluxes: a test from the central equatorial Pacific. *Mar. Ecol. Prog. Ser.* 236, 129–135. doi:10.3354/meps236129
- Lamshead, P.J.D., Tietjen, J., Ferrero, T., Jensen, P., 2000. Latitudinal diversity gradients in the deep sea with special reference to North Atlantic nematodes. *Mar. Ecol. Prog. Ser.* 194, 159–167. doi:10.3354/meps194159
- Lampadariou, N., Tselepides, A., 2006. Spatial variability of meiofaunal communities at areas of contrasting depth and productivity in the Aegean Sea (NE Mediterranean). *Prog. Oceanogr.* 69, 19–36. doi:10.1016/j.pocean.2006.02.013
- Lampitt, R.S., 1985. Evidence of the seasonal deposition of detritus to the deep-sea floor and its subsequent resuspension. *Deep. Res. Part a-Oceanographic Res. Pap.* 32, 885–897. doi:10.1016/0198-0149(85)90034-2
- Lampitt, R.S., Antia, A.N., 1997. Particle flux in deep seas: regional characteristics and temporal variability. *Deep. Res. Part I-Oceanographic Res. Pap.* 44, 1377–1403. doi:10.1016/s0967-0637(97)00020-4
- Lampitt, R.S., Salter, I., de Cuevas, B.A., Hartman, S., Larkin, K.E., Pebody, C.A., 2010. Long-term variability of downward particle flux in the deep northeast Atlantic: Causes and trends. *Deep. Res. Part II Top. Stud. Oceanogr.* 57, 1346–1361. doi:10.1016/j.dsr2.2010.01.011
- Lande, R., 1996. Statistics and Partitioning of Species Diversity, and Similarity among Multiple Communities. *Oikos* 76, 5–13. doi:10.2307/3545743
- Leduc, D., 2009. Description of *Oncholaimus moanae* sp nov (Nematoda: Oncholaimidae), with notes on feeding ecology based on isotopic and fatty acid composition. *J. Mar. Biol. Assoc. United Kingdom* 89, 337–344. doi:10.1017/s0025315408002464

- Leduc, D., Brown, C.J., Bury, S.J., Lörz, A.-N., 2014. High intraspecific variability in the diet of a deep-sea nematode: stable isotope and fatty acid analyses of *Deontostoma tridentum* on Chatham Rise, Southwest Pacific. *Deep. Res. I*.
- Leduc, D., Probert, P.K., 2009. The effect of bacterivorous nematodes on detritus incorporation by macrofaunal detritivores: A study using stable isotope and fatty acid analyses. *J. Exp. Mar. Bio. Ecol.* 371, 130–139. doi:10.1016/j.jembe.2009.01.011
- Leduc, D., Rowden, A.A., Bowden, D.A., Nodder, S.D.S., Probert, P.K., Pilditch, C.C.A., Duineveld, G.G.C.A., Witbaard, R., 2012a. Nematode beta diversity on the continental slope of New Zealand: spatial patterns and environmental drivers. *Mar. Ecol. Prog. Ser.* 454, 37–52. doi:10.3354/meps09690
- Leduc, D., Rowden, A.A., Bowden, D.A., Probert, P.K., Pilditch, C.A., Nodder, S.D., 2012b. Unimodal relationship between biomass and species richness of deep-sea nematodes: Implications for the link between productivity and diversity. *Mar. Ecol. Prog. Ser.* 454, 53–64. doi:10.3354/meps09609
- Leduc, D., Rowden, A.A., Probert, P.K., Pilditch, C.A., Nodder, S.D., Vanreusel, A., Duineveld, G.C.A., Witbaard, R., 2012c. Further evidence for the effect of particle-size diversity on deep-sea benthic biodiversity. *Deep. Res. Part I-Oceanographic Res. Pap.* 63, 164–169. doi:10.1016/j.dsr.2011.10.009
- Lee, H.J., Vanhove, S., Peck, L.S., Vincx, M., 2001. Recolonisation of meiofauna after catastrophic iceberg scouring in shallow Antarctic sediments. *Polar Biol.* 24, 918–925. doi:10.1007/s003000100300
- Lejzerowicz, F., Esling, P., Pawlowski, J., 2014. Patchiness of deep-sea benthic Foraminifera across the Southern Ocean: Insights from high-throughput DNA sequencing. *Deep. Res. II* 108, 17–26.
- Levin, L.A., 2003. Oxygen minimum zone benthos: Adaptation and community response to hypoxia. *Oceanogr. Mar. Biol. Vol 41* 41, 1–45.
- Levin, L.A., Dayton, P.K., 2009. Ecological theory and continental margins: where shallow meets deep. *Trends Ecol. Evol.* 24, 606–617. doi:10.1016/j.tree.2009.04.012
- Levin, L.A., Etter, R.J., Rex, M.A., Gooday, A.J., Smith, C.R., Pineda, J., Stuart, C.T., Hessler, R.R., Pawson, D., 2001. Environmental influences on regional deep-sea species diversity. *Annu. Rev. Ecol. Syst.* 32, 51–93.
- Levin, L.A., Sibuet, M., 2012. Understanding Continental Margin Biodiversity: A New Imperative, in: Carlson, C.A., Giovannoni, S.J. (Eds.), *Annual Review of Marine Science*, Vol 4. p. 79–+. doi:10.1146/annurev-marine-120709-142714
- Levin, L., Blair, N., DeMaster, D., Plaia, G., Fornes, W., Martin, C., Thomas, C., 1997. Rapid subduction of organic matter by maldanid polychaetes on the North Carolina slope. *J. Mar. Res.* 55, 595–611. doi:10.1357/0022240973224337
- Levin, S., 1992. The Problem of Pattern and Scale in Ecology. *Ecology* 73, 1943–1967. doi:doi:10.2307/1941447
- Lins, L., da Silva, M.C., Hauquier, F., Esteves, A.M., Vanreusel, A., 2015. Nematode community composition and feeding shaped by contrasting productivity regimes in the Southern Ocean. *Prog. Oceanogr.* 134, 356–369. doi:10.1016/j.pocean.2015.03.006

- Lins, L., Guilini, K., Veit-Köhler, G., Hauquier, F., Alves, R.M.S., Esteves, A.M., vanreusel, A., 2014. The link between meiofauna and surface productivity in the Southern Ocean. *Deep. Res. II* 108, 60–68. doi:http://dx.doi.org/10.1016/j.dsr2.2014.05.003
- Lins, L., Vanreusel, A., van Campenhout, J., Ingels, J., 2013. Selective settlement of deep-sea canyon nematodes after resuspension — an experimental approach. *J. Exp. Mar. Bio. Ecol.* 441, 110–116. doi:http://dx.doi.org/10.1016/j.jembe.2013.01.021
- Longhurst, A., 1998. *Ecological geography of the sea*. Academic Press, San Diego, California.
- Loreau, M., Naeem, S., Inchausti, P., Bengtsson, J., Grime, J.P., Hector, A., Hooper, D.U., Huston, M.A., Raffaelli, D., Schmid, B., Tilman, D., Wardle, D.A., 2001. Ecology - Biodiversity and ecosystem functioning: Current knowledge and future challenges. *Science* (80-.). 294, 804–808. doi:10.1126/science.1064088
- Louden, K.E., White, R.S., Potts, C.G., Forsyth, D.W., 1986. Structure and Seismotectonics of the Vema Fracture-Zone, Atlantic-Ocean. *J. Geol. Soc. London.* 143, 795–805.
- Ludwig, W.J., Rabinowitz, P.D., 1980. Structure of VEMA fracture zone. *Mar. Geol.* 35, 99–110.
- Lutz, M., Dunbar, R., Caldeira, K., 2002. Regional variability in the vertical flux of particulate organic carbon in the ocean interior. *Global Biogeochem. Cycles* 16. doi:10.1029/2000gb001383
- Lutz, M.J., Caldeira, K., Dunbar, R.B., Behrenfeld, M.J., 2007. Seasonal rhythms of net primary production and particulate organic carbon flux to depth describe the efficiency of biological pump in the global ocean. *J. Geophys. Res.* 112. doi:C1001110.1029/2006jc003706
- Mare, M.F., 1942. A study of a marine benthic community with special reference to the micro-organisms. *J. Mar. Biol. Assoc. United Kingdom* 25, 517–554. doi:10.1017/S0025315400055132
- McClain, C.R., Hardy, S.M., 2010. The dynamics of biogeographic ranges in the deep sea. *Proc. R. Soc. B Biol. Sci.* 277, 3533–3546. doi:10.1098/rspb.2010.1057
- McClain, C.R., Rex, M.A., 2015. Toward a Conceptual Understanding of beta-Diversity, in: Futuyma, D.J. (Ed.), *Annual Review of Ecology, Evolution, and Systematics*, Vol 46. pp. 623–642. doi:10.1146/annurev-ecolsys-120213-091640
- McClain, C.R., Schlacher, T.A., 2015. On some hypotheses of diversity of animal life at great depths on the sea floor. *Mar. Ecol.* 1–24. doi:10.1111/maec.12288
- Meldal, B.H.M., Debenham, N.J., De Ley, P., De Ley, I.T., Vanfleteren, J.R., Vierstraete, A.R., Bert, W., Borgonie, G., Moens, T., Tyler, P.A., Austen, M.C., Blaxter, M.L., Rogers, A.D., Lamshead, P.J.D., 2007. An improved molecular phylogeny of the Nematoda with special emphasis on marine taxa. *Mol. Phylogenet. Evol.* 42, 622–636. doi:10.1016/j.ympev.2006.08.025
- Menard, H.W., 1967. Sea Floor Spreading, Topography, and Second Layer. *Science* (80-.). 157, 923–924. doi:10.1126/science.157.3791.923
- Menzel, L., George, K.H., Martínez-Arbizu, P., 2011. Submarine ridges do not prevent large-scale dispersal of abyssal fauna: A case study of Mesocletodes (Crustacea,

- Copepoda, Harpacticoida). *Deep. Res. Part I Oceanogr. Res. Pap.* 58, 839–864. doi:10.1016/j.dsr.2011.05.008
- Menzies, R.J., 1965. Conditions for the existence of life on the abyssal sea floor. *Ocean. Mar. Biol. Annu. Rev.* 3, 195–210.
- Middelburg, J.J., Soetaert, K., Herman, P.M.J., 1997. Empirical relationships for use in global diagenetic models. *Deep. Res. Part I-Oceanographic Res. Pap.* 44, 327–344. doi:10.1016/s0967-0637(96)00101-x
- Miljutin, D.M., Miljutina, M.A., 2016a. Review of *Acantholaimus* Allgén, 1933 (Nematoda: Chromadoridae), a genus of marine free-living nematodes, with a tabular key to species. *Nematology* 0, 1–22. doi:10.1163/15685411-00002976
- Miljutin, D.M., Miljutina, M.A., 2016b. Intraspecific variability of morphological characters in the species-rich deep-sea genus *Acantholaimus* Allgen, 1933 (Nematoda: Chromadoridae). *Nematology* 18, 455–473. doi:10.1163/15685411-00002970
- Miljutina, M.A., Miljutin, D.M., Mahatma, R., Gal'eron, J., 2010. Deep-sea nematode assemblages of the Clarion-Clipperton Nodule Province (Tropical North-Eastern Pacific). *Mar. Biodivers.* 40, 1–15. doi:10.1007/s12526-009-0029-0
- Mirto, S., Arigò, C., Genovese, L., Pusceddu, A., Gambi, C., Danovaro, R., 2014. Nematode assemblage response to fish-farm impact in vegetated (*Posidonia oceanica*) and non-vegetated habitats. *Aquac. Environ. Interact.* 5, 17–28. doi:10.3354/aei00091
- Moens, T., Braeckman, U., Derycke, S., Fonseca, G., Gallucci, F., Gingold, R., Guilini, K., Ingels, J., Leduc, D., Vanaverbeke, J., Van Colen, C., Vanreusel, A., Vincx, M., 2014. Ecology of free-living marine nematodes, in: Schmidt-Rhaesa, A. (Ed.), *Handbook of Zoology: Gastrotricha, Cycloneuralia and Gnathifera*. Volume 2: Nematoda. pp. 109–152.
- Moens, T., Vanhove, S., De Mesel, I., Kelemen, B., Janssens, T., Dewicke, A., Vanreusel, A., 2007. Carbon sources of Antarctic nematodes as revealed by natural carbon isotope ratios and a pulse-chase experiment. *Polar Biol.* 31, 1–13. doi:10.1007/s00300-007-0323-x
- Moens, T., Vincx, M., 1997. Observations on the feeding ecology of estuarine nematodes. *J. Mar. Biol. Assoc. United Kingdom* 77, 211–227.
- Mokievskii, V.O., Udalov, A.A., Azovskii, A.I., 2007. Quantitative distribution of meiobenthos in deep-water zones of the World Ocean. *Oceanology* 47, 797–813. doi:10.1134/s0001437007060057
- Moodley, L., Middelburg, J.J., Boschker, H.T.S., Duineveld, G.C.A., Pel, R., Herman, P.M.J., Heip, C.H.R., 2002. Bacteria and Foraminifera: key players in a short-term deep-sea benthic response to phytodetritus. *Mar. Ecol. Prog. Ser.* 236, 23–29. doi:10.3354/meps236023
- Moodley, L., Steyaert, M., Epping, E., Middelburg, J.J., Vincx, M., van Avesaath, P., Moens, T., Soetaert, K., 2008. Biomass-specific respiration rates of benthic meiofauna: Demonstrating a novel oxygen micro-respiration system. *J. Exp. Mar. Bio. Ecol.* 357, 41–47. doi:10.1016/j.jembe.2007.12.025
- Moreno, M., Ferrero, T.J., Gallizia, I., Vezzulli, L., Albertelli, G., Fabiano, M., 2008. An assessment of the spatial heterogeneity of environmental disturbance within an

- enclosed harbour through the analysis of meiofauna and nematode assemblages. *Estuar. Coast. Shelf Sci.* 77, 565–576. doi:10.1016/j.ecss.2007.10.016
- Morozov, E.G., Demidov, A.N., Tarakanov, R.Y., Zenk, W., 2010. Abyssal channels in the Atlantic Ocean: Water structure and flows, Statewide Agricultural Land Use Baseline 2015. doi:10.1017/CBO9781107415324.004
- Morozov, E.G., Tarakanov, R.Y., Makarenko, N.I., 2015. Flows of Antarctic bottom water through fractures in the southern part of the North Mid-Atlantic Ridge. *Oceanology* 55, 796–800. doi:10.1134/S0001437015060120
- Moura, C.J., Cunha, M.R., Porteiro, F.M., Yesson, C., Rogers, A.D., 2012. Evolution of Nemertesia hydroids (Cnidaria: Hydrozoa, Plumulariidae) from the shallow and deep waters of the NE Atlantic and western Mediterranean. *Zool. Scr.* 41, 79–96. doi:10.1111/j.1463-6409.2011.00503.x
- Moura, J. da R., Silva, M.C. da, Esteves, A.M., 2014. Four new species of Desmodora (Nematoda) from the deep south-east Atlantic, and a case of intersexuality in Desmodoridae. *J. Mar. Biol. Assoc. United Kingdom* 94, 85–104. doi:10.1017/S0025315413001458
- Muthumbi, A.W., Vincx, M., 1997. Acantholaimus (Chromadoridae: Nematoda) from the Indian Ocean: description of seven species. *Hydrobiologia* 346, 59–76. doi:10.1023/a:1002937226161
- Muthumbi, W.N.A., Vanreusel, A., Vincx, M., 2011. Taxon-related diversity patterns from the continental shelf to the slope: a case study on nematodes from the Western Indian Ocean. *Mar. Ecol.* 32, 453–467. doi:10.1111/j.1439-0485.2011.00449.x
- Nascimento, F.J.A., Näslund, J., Elmgren, R., 2012. Meiofauna enhances organic matter mineralization in soft sediment ecosystems. *Limnol. Oceanogr.* 57, 338–346. doi:10.4319/lo.2012.57.1.0338
- Netto, S.A., Gallucci, F., Fonseca, G.F.C., 2005. Meiofauna communities of continental slope and deep-sea sites off SE Brazil. *Deep. Res. Part I-Oceanographic Res. Pap.* 52, 845–859. doi:10.1016/j.dsr.2004.11.009
- Nolasco, R., Pires, A.C., Cordeiro, N., Le Cann, B., Dubert, J., 2013. A high-resolution modeling study of the Western Iberian Margin mean and seasonal upper ocean circulation. *Ocean Dyn.* 63, 1041–1062. doi:10.1007/s10236-013-0647-8
- Nygren, A., Eklöf, J., Pleijel, F., 2010. Cryptic species of Notophyllum (Polychaeta: Phyllodocidae) in Scandinavian waters. *Org. Divers. Evol.* 10, 193–204. doi:10.1007/s13127-010-0014-2
- Orsi, A.H., Harris, U., 2001. Locations of the various fronts in the Southern Ocean [WWW Document].
- Orsi, A.H., Whitworth, T., Nowlin, W.D., 1995. On the meridional extent and fronts of the antarctic circumpolar current. *Deep. Res. Part I-Oceanographic Res. Pap.* 42, 641–673. doi:10.1016/0967-0637(95)00021-w
- Osborn, K.J., Madin, L.P., Rouse, G.W., 2011. The remarkable squidworm is an example of discoveries that await in deep-pelagic habitats. *Biol. Lett.* 7, 449–453. doi:10.1098/rsbl.2010.0923

- Palmer, M.A., 1988. Dispersal of marine meiofauna - A review and conceptual-model explaining passive transport and active emergence with implications for recruitment. *Mar. Ecol. Ser.* 48, 81–91.
- Pape, E., Bezerra, T.N., Jones, D.O.B., Vanreusel, A., 2013a. Unravelling the environmental drivers of deep-sea nematode biodiversity and its relation with carbon mineralisation along a longitudinal primary productivity gradient. *Biogeosciences* 10, 3127–3143. doi:10.5194/bg-10-3127-2013
- Pape, E., Jones, D.O.B., Manini, E., Bezerra, T.N., Vanreusel, A., 2013b. Benthic-Pelagic Coupling: Effects on Nematode Communities along Southern European Continental Margins. *PLoS One* 8. doi:e5995410.1371/journal.pone.0059954
- Patrício, J., Adão, H., Neto, J.M., Alves, A.S., Traunspurger, W., Marques, J.C., 2012. Do nematode and macrofauna assemblages provide similar ecological assessment information? *Ecol. Indic.* 14, 124–137. doi:10.1016/j.ecolind.2011.06.027
- Pawlowski, J., Bowser, S.S., Gooday, A.J., 2007. A note on the genetic similarity between shallow- and deep-water *Epistominella vitrea* (Foraminifera) in the Antarctic. *Deep. Res. Part II Top. Stud. Oceanogr.* 54, 1720–1726. doi:10.1016/j.dsr2.2007.07.016
- Peck, L.S., Convey, P., Barnes, D.K.A., 2006. Environmental constraints on life histories in Antarctic ecosystems: tempos, timings and predictability. *Biol. Rev.* 81, 75–109. doi:10.1017/s1464793105006871
- Peterson, R.G., Stramma, L., 1991. Upper-level circulation in the south-atlantic ocean. *Prog. Oceanogr.* 26, 1–73. doi:10.1016/0079-6611(91)90006-8
- Pfannkuche, O., Lochte, K., 1993. Open ocean pelago-benthic coupling: cyanobacteria as tracers of sedimenting salp faeces . *Deep. Res. I* 40, 727–737.
- Pinheiro, L.M., Wilson, R.C.L., Reis, R.P. Dos, Whitmarsh, R.B., Ribeiro, A., 1996. The Western Iberia Margin: a Geophysical and Geological Overview. *Proc. Ocean Drill. Program, Sci. Results* 149, 3–23. doi:10.2973/odp.proc.sr.149.246.1996
- Platt, H.M., Zhang, Z.N., 1982. New species of marine nematodes from Loch Ewe, Scotland. *Bull. Br. Mus. Nat. Hist* 42, 227–246.
- Posada, D., 2008. jModelTest: Phylogenetic model averaging. *Mol. Biol. Evol.* 25, 1253–1256. doi:10.1093/molbev/msn083
- Posada, D., Crandall, K.A., 1998. MODELTEST: testing the model of DNA substitution. *Bioinformatics* 14, 817–818. doi:10.1093/bioinformatics/14.9.817
- Puig, P., Canals, M., Company, J.B., Martin, J., Amblas, D., Lastras, G., Palanques, A., Calafat, A.M., 2012. Ploughing the deep sea floor. *Nature* 489, 286–+. doi:10.1038/nature11410
- Pusceddu, A., Bianchelli, S., Martin, J., Puig, P., Palanques, A., Masque, P., Danovaro, R., 2014. Chronic and intensive bottom trawling impairs deep-sea biodiversity and ecosystem functioning. *Proc. Natl. Acad. Sci. U. S. A.* 111, 8861–8866. doi:10.1073/pnas.1405454111
- Quaresma, L.S., Vitorino, J., Oliveira, A., da Silva, J.C.B., 2007. Evidence of sediment resuspension by nonlinear internal waves on the western Portuguese mid-shelf. *Mar. Geol.* 246, 123–143. doi:10.1016/j.margeo.2007.04.019

- Quattrini, A.M., Baums, I.B., Shank, T.M., Morrison, C.L., Cordes, E.E., 2015. Testing the depth-differentiation hypothesis in a deepwater octocoral. *Proc. R. Soc. B-Biological Sci.* 282. doi:Unsp 2015000810.1098/rspb.2015.0008
- Quattro, J.M., Chase, M.R., Rex, M.A., Greig, T.W., Etter, R.J., 2001. Extreme mitochondrial DNA divergence within populations of the deep-sea gastropod *Frigidoalvania brychia*. *Mar. Biol.* 139, 1107–1113.
- R Core Team, 2013. R: A language and environment for statistical computing. R Found. for Stat. Comput.
- Raes, M., Rose, A., Vanreusel, A., 2010. Response of nematode communities after large-scale ice-shelf collapse events in the Antarctic Larsen area. *Glob. Chang. Biol.* 16, 1618–1631. doi:10.1111/j.1365-2486.2009.02137.x
- Ramalho, S.P., Adao, H., Kiriakoulakis, K., Wolff, G.A., Vanreusel, A., Ingels, J., 2014. Temporal and spatial variation in the Nazare Canyon (Western Iberian margin): Inter-annual and canyon heterogeneity effects on meiofauna biomass and diversity. *Deep. Res. Part I-Oceanographic Res. Pap.* 83, 102–114. doi:10.1016/j.dsr.2013.09.010
- Ramirez-Llodra, E., Brandt, A., Danovaro, R., De Mol, B., Escobar, E., German, C.R., Levin, L.A., Martinez Arbizu, P., Menot, L., Buhl-Mortensen, P., Narayanaswamy, B.E., Smith, C.R., Tittensor, D.P., Tyler, P.A., Vanreusel, A., Vecchione, M., 2010. Deep, diverse and definitely different: unique attributes of the world's largest ecosystem. *Biogeosciences* 7, 2851–2899. doi:10.5194/bg-7-2851-2010
- Reemtsma, T., Haake, B., Ittekkot, V., Nair, R.R., W., B.U., 1990. Downward Flux of Particulate Fatty Acids in the Central Arabian Sea. *Mar. Chem.* 29, 183–202.
- Relvas, P., Barton, E.D., Dubert, J., Oliveira, P.B., Peliz, A., da Silva, J.C.B., Santos, A.M.P., 2007. Physical oceanography of the western Iberia ecosystem: Latest views and challenges. *Prog. Oceanogr.* 74, 149–173. doi:10.1016/j.pocean.2007.04.021
- Rex, M.A., 1981. Community structure in the deep-sea benthos. *Annu. Rev. Ecol. Syst.* 12, 331–353.
- Rex, M.A., Etter, R.J., 2010. Deep-sea biodiversity: pattern and scale, Setting the stage: patterns of benthic standing stock. Harvard University Press.
- Rex, M.A., Etter, R.J., Morris, J.S., Crouse, J., McClain, C.R., Johnson, N.A., Stuart, C.T., Deming, J.W., Thies, R., Avery, R., 2006. Global bathymetric patterns of standing stock and body size in the deep-sea benthos. *Mar. Ecol. Prog. Ser.* 317, 1–8. doi:10.3354/meps317001
- Rex, M.A., McClain, C.R., Johnson, N.A., Etter, R.J., Allen, J.A., Bouchet, P., Waren, A., 2005. A source-sink hypothesis for abyssal biodiversity. *Am. Nat.* 165, 163–178.
- Rex, M.A., Stuart, C.T., Hessler, R.R., Allen, J.A., Sanders, H.L., Wilson, G.D.F., 1993. Global-scale latitudinal patterns of species-diversity in the deep-sea benthos. *Nature* 365, 636–639. doi:10.1038/365636a0
- Riehl, T., Kaiser, S., 2012. Conquered from the Deep Sea? A New Deep-Sea Isopod Species from the Antarctic Shelf Shows Pattern of Recent Colonization. *PLoS One* 7. doi:e4935410.1371/journal.pone.0049354

- Riehl, T., Wilson, G.D.F., Malyutina, M. V., 2014. Urstylidae - a new family of abyssal isopods (Crustacea: Asellota) and its phylogenetic implications. *Zool. J. Linn. Soc.* 170, 245–296. doi:10.1111/zoj.12104
- Ronce, O., 2007. How does it feel to be like a rolling stone? Ten questions about dispersal evolution, in: *Annual Review of Ecology Evolution and Systematics*. pp. 231–253. doi:10.1146/annurev.ecolsys.38.091206.095611
- Ronquist, F., Huelsenbeck, J.P., 2003. MrBayes 3: Bayesian phylogenetic inference under mixed models. *Bioinformatics* 19, 1572–1574. doi:10.1093/bioinformatics/btg180
- Rowe, G.T., Wei, C., Nunnally, C., Haedrich, R., Montagna, P., Baguley, J.G., Bernhard, J.M., Wicksten, M., Ammons, A., Escobar Briones, E., Soliman, Y., Deming, J.W., 2008. Comparative biomass structure and estimated carbon flow in food webs in the deep Gulf of Mexico. *Deep. Res. Part II-Topical Stud. Oceanogr.* 55, 2699–2711. doi:10.1016/j.dsr2.2008.07.020
- Ruff, E.S., Probandt, D., Zinkann, A.-C., Iversen, M., Klaas, C., Würzberg, L., Krombholz, N., Wolf-Gladrow, D., Amann, R., Knittel, K., 2014. Indications for algae-degrading benthic microbial communities in deep-sea sediments along the Antarctic Polar Front. *Deep. Res. II* 108, 6–16. doi:http://dx.doi.org/10.1016/j.dsr2.2014.05.011
- Ruhl, H.A., Ellena, J.A., Smith Jr., K.L., 2008. Connections between climate, food limitation, and carbon cycling in abyssal sediment communities. *Proc. Natl. Acad. Sci. U. S. A.* 105, 17006–17011. doi:10.1073/pnas.0803898105
- Sachs, O., Sauter, E.J., Schlueter, M., van der Loeff, M.M.R., Jerosch, K., Holby, O., 2009. Benthic organic carbon flux and oxygen penetration reflect different plankton provinces in the Southern Ocean. *Deep. Res. Part I-Oceanographic Res. Pap.* 56, 1319–1335. doi:10.1016/j.dsr.2009.02.003
- Salgueiro, E., Naughton, F., Voelker, A.H.L., de Abreu, L., Alberto, A., Rossignol, L., Duprat, J., Magalhaes, V.H., Vaqueiro, S., Turon, J.L., Abrantes, F., 2014. Past circulation along the western Iberian margin: a time slice vision from the Last Glacial to the Holocene. *Quat. Sci. Rev.* 106, 316–329. doi:10.1016/j.quascirev.2014.09.001
- Sanders, H.L., Hessler, R.R., 1969. Ecology of deep-sea benthos. *Science* (80-). 163, 1419–1424.
- Sanders, H.L., Hessler, R.R., Hampson, G.R., 1965. An introduction to the study of deep-sea benthic faunal assemblages along the Gay Head-Bermuda transect. *Deep. Res. Oceanogr. Abstr.* 12, 845–867.
- Schoener, T.W., 1974. Resource partitioning in ecological communities. *Science* 185, 27–39. doi:10.1126/science.185.4145.27
- Schratzberger, M., Lampadariou, N., Somerfield, P.J., Vandepitte, L., Vanden Berghe, E., 2009. The impact of seabed disturbance on nematode communities: Linking field and laboratory observations. *Mar. Biol.* 156, 709–724.
- Schratzberger, M., Whomersley, P., Warr, K., Bolam, S.G., Rees, H.L., 2004. Colonisation of various types of sediment by estuarine nematodes via lateral infaunal migration: a laboratory study. *Mar. Biol.* 145, 69–78. doi:10.1007/s00227-004-1302-1
- Sebastian, S., Raes, M., De Mesel, I., Vanreusel, A., 2007. Comparison of the nematode fauna from the Weddell Sea abyssal plain with two North Atlantic abyssal sites.

- Deep. Res. Part II-Topical Stud. Oceanogr. 54, 1727–1736. doi:10.1016/j.dsr2.2007.07.004
- Serpetti, N., Gontikaki, E., Narayanaswamy, B.E., Witte, U., 2013. Macrofaunal community inside and outside of the Darwin Mounds Special Area of Conservation, NE Atlantic. *Biogeosciences* 10, 3705–3714. doi:10.5194/bg-10-3705-2013
- Shirayama, Y., 1992. Respiration rates of bathyal meiobenthos collected using a deep-sea submersible SHINKAI 2000. *Deep. Res.* 39, 781–788.
- Shorrocks, B., Sevenster, J.G., 1995. Explaining local species diversity. *Proc. R. Soc. B-Biological Sci.* 260, 305–309. doi:10.1098/rspb.1995.0096
- Silvestro, D., Michalak, I., 2012. raxmlGUI: a graphical front-end for RAxML. *Org. Divers. Evol.* 12, 335–337. doi:10.1007/s13127-011-0056-0
- Singh, R., Miljutin, D.M., Miljutina, M.A., Martinez Arbizu, P., Ingole, B.S., 2014. Deep-sea nematode assemblages from a commercially important polymetallic nodule area in the Central Indian Ocean Basin. *Mar. Biol. Res.* 10, 906–916. doi:10.1080/17451000.2013.866251
- Smith, C.R., De Leo, F.C., Bernardino, A.F., Sweetman, A.K., Arbizu, P.M., 2008. Abyssal food limitation, ecosystem structure and climate change. *Trends Ecol. Evol.* 23, 518–528.
- Snelgrove, P.V.R., Butman, C.A., 1994. Animal Sediment Relationships Revisited - Cause Versus Effect. *Oceanogr. Mar. Biol.* 32, 111–177.
- Snelgrove, P.V.R., Smith, C.R., 2002. A riot of species in an environmental calm: The paradox of the species-rich deep-sea floor, in: Gibson, R.N., Barnes, M., Atkinson, R.J.A. (Eds.), *Oceanography and Marine Biology*, Vol 40. pp. 311–342.
- Soetaert, K., Heip, C., 1995. Nematode assemblages of deep-sea and shelf break sites in the North Atlantic and Mediterranean Sea. *Mar. Ecol. Ser.* 125, 171–183. doi:10.3354/meps125171
- Soetaert, K., Heip, C., 1989. The size structure of nematode assemblages along a Mediterranean deep-sea transect. *Deep. Res. Part a-Oceanographic Res. Pap.* 36, 93–102.
- Soetaert, K., Muthumbi, A., Heip, C., 2002. Size and shape of ocean margin nematodes: morphological diversity and depth-related patterns. *Mar. Ecol. Ser.* 242, 179–193.
- Soetaert, K., Vanaverbeke, J., Heip, C., Herman, P.M.J., Middelburg, J.J., Sandee, A., Duineveld, G., 1997. Nematode distribution in ocean margin sediments of the Goban Spur (northeast Atlantic) in relation to sediment geochemistry. *Deep. Res. Part I-Oceanographic Res. Pap.* 44, 1671–1683. doi:10.1016/s0967-0637(97)00043-5
- Somerfield, P.J., Clarke, K.R., 1995. Taxonomic levels, in marine studies, revisited. *Mar. Ecol. Prog. Ser.* 127, 113–119. doi:10.3354/meps127113
- Soreide, J.E., Leu, E., Berge, J., Graeve, M., Falk-Petersen, S., 2010. Timing of blooms, algal food quality and *Calanus glacialis* reproduction and growth in a changing Arctic. *Glob. Chang. Biol.* 16, 3154–3163. doi:10.1111/j.1365-2486.2010.02175.x
- Stachowicz, J.J., Bruno, J.F., Duffy, J.E., 2007. Understanding the effects of marine biodiversity on communities and ecosystems, in: *Annual Review of Ecology Evolution and Systematics*. pp. 739–766. doi:10.1146/annurev.ecolsys.38.091206.095659

- Stamatakis, A., 2006. RAxML-VI-HPC: Maximum likelihood-based phylogenetic analyses with thousands of taxa and mixed models. *Bioinformatics* 22, 2688–2690. doi:10.1093/bioinformatics/btl446
- Steyaert, M., Moodley, L., Vanaverbeke, J., Vandewiele, S., Vincx, M., 2005. Laboratory experiments on the infaunal activity of intertidal nematodes. *Hydrobiologia* 540, 217–223. doi:10.1007/s10750-004-7145-4
- Strugnell, J.M., Rogers, A.D., Prodohl, P.A., Collins, M.A., Allcock, A.L., 2008. The thermohaline expressway: the Southern Ocean as a centre of origin for deep-sea octopuses. *Cladistics* 24, 853–860. doi:10.1111/j.1096-0031.2008.00234.x
- Suhr, S.B., Pond, D.W., Gooday, A.J., Smith, C.R., 2003. Selective feeding by benthic foraminifera on phytodetritus on the western Antarctic Peninsula shelf: evidence from fatty acid biomarker analysis. *Mar. Ecol. Prog. Ser.* 262, 153–162. doi:10.3354/meps262153
- Tamura, K., Stecher, G., Peterson, D., Filipowski, A., Kumar, S., 2013. MEGA6: molecular evolutionary genetics analysis version 6.0. *Mol. Biol. Evol.* 30, 2725–2729.
- Thiel, H., 1978. Benthos in Upwelling Regions, Upwelling Ecosystems. Springer Berlin Heidelberg, Berlin. doi:10.1007/978-3-642-66985-9_11
- Thiel, H., 1975. The size structure of deep-sea benthos. *Int. Rev. Der Gesamten Hydrobiol.* 60, 575–606.
- Thistle, D., 2003. Harpacticoid copepod emergence at a shelf site in summer and winter: implications for hydrodynamic and mating hypotheses. *Mar. Ecol. Prog. Ser.* 248, 177–185. doi:10.3354/meps248177
- Thistle, D., Ertman, S.C., Fauchald, K., 1991. The fauna of the HEBBLE site: patterns in standing stock and sediment-dynamic effects. *Mar. Geol.* 99, 413–422. doi:10.1016/0025-3227(91)90053-7
- Thistle, D., Yingst, J.Y., Fauchald, K., 1985. A deep-sea benthic community exposed to strong near-bottom currents on the Scotian Rise (Western Atlantic). *Mar. Geol.* 66, 91–112. doi:10.1016/0025-3227(85)90024-6
- Thullner, M., Dale, A.W., Regnier, P., 2009. Global-scale quantification of mineralization pathways in marine sediments: A reaction-transport modeling approach. *Geochemistry Geophys. Geosystems* 10. doi:10.1029/2009gc002484
- Thurber, A.R., Sweetman, A.K., Narayanaswamy, B.E., Jones, D.O.B., Ingels, J., Hansman, R.L., 2014. Ecosystem function and services provided by the deep sea. *Biogeosciences* 11, 3941–3963. doi:10.5194/bg-11-3941-2014
- Tietjen, J.H., 1989. Ecology of deep-sea nematodes from the Puerto Rico Trench and Hatteras abyssal plain. *Deep. Res. Part a-Oceanographic Res. Pap.* 36, 1579–1594. doi:10.1016/0198-0149(89)90059-9
- Tokeshi, M., 1999. Species Coexistence: Ecological and evolutionary perspectives. Cambridge.
- Tyler, P.A., 1995. Conditions for the existence of life at the deep sea floor: An update. *Oceanogr. Mar. Biol. An Annu. Rev.* 33, 221–244.
- Ullberg, J., Olafsson, E., 2003. Free-living marine nematodes actively choose habitat when descending from the water column. *Mar. Ecol. Ser.* 260, 141–149.

- Van Campenhout, J., Derycke, S., Tchesunov, A., Portnova, D., Vanreusel, A., 2014. The *Halomonhystera disjuncta* population is homogeneous across the Hakon Mosby mud volcano (Barents Sea) but is genetically differentiated from its shallow-water relatives. *J. Zool. Syst. Evol. Res.* 52, 203–216. doi:10.1111/jzs.12054
- Van Cauwenberghe, L., Vanreusel, A., Mees, J., Janssen, C.R., 2013. Microplastic pollution in deep-sea sediments. *Environ. Pollut.* doi:10.1016/j.envpol.2013.08.013
- van der Heijden, K., Petersen, J.M., Dubilier, N., Borowski, C., 2012. Genetic Connectivity between North and South Mid- Atlantic Ridge Chemosynthetic Bivalves and Their Symbionts. *PLoS One* 7. doi:10.1371/journal.pone.0039994
- Van Gaever, S., Olu, K., Derycke, S., Vanreusel, A., 2009. Metazoan meiofaunal communities at cold seeps along the Norwegian margin: Influence of habitat heterogeneity and evidence for connection with shallow-water habitats. *Deep. Res. Part I-Oceanographic Res. Pap.* 56, 772–785. doi:10.1016/j.dsr.2008.12.015
- Vanaverbeke, J., Arbizu, P.M., Dahms, H.U., Schminke, H.K., 1997a. The metazoan meiobenthos along a depth gradient in the Arctic Laptev Sea with special attention to nematode communities. *Polar Biol.* 18, 391–401. doi:10.1007/s003000050205
- Vanaverbeke, J., Bezerra, T.N., Braeckman, U., De Groote, A., de Meester, N., Deprez, T., Derycke, S., Gilarte, P., Guilini, K., Hauquier, F., Lins, L., Maria, T., Moens, T., Pape, E., Smol, N., Taheri, M., Van Campenhout, J., Vanreusel, A., Wu, X., Vincx, M., 2015. Nemys: World Database of Free-living Marine Nematodes [WWW Document]. URL <http://nemys.ugent.be>
- Vanaverbeke, J., Merckx, B., Degraer, S., Vincx, M., 2011. Sediment-related distribution patterns of nematodes and macrofauna: Two sides of the benthic coin? *Mar. Environ. Res.* 71, 31–40. doi:10.1016/j.marenvres.2010.09.006
- Vanaverbeke, J., Soetaert, K., Heip, C., Vanreusel, A., 1997b. The metazoan meiobenthos along the continental slope of the Goban Spur (NE Atlantic). *J. Sea Res.* 38, 93–107. doi:10.1016/S1385-1101(97)00038-5
- Vancoppenolle, M., Meiners, K.M., Michel, C., Bopp, L., Brabant, F., Carnat, G., Delille, B., Lannuzel, D., Madec, G., Moreau, S., Tison, J.-L., van der Merwe, P., 2013. Role of sea ice in global biogeochemical cycles: emerging views and challenges. *Quat. Sci. Rev.* 79, 207–230. doi:10.1016/j.quascirev.2013.04.011
- Vanreusel, A., De Groote, A., Gollner, S., Bright, M., 2010a. Ecology and Biogeography of Free-Living Nematodes Associated with Chemosynthetic Environments in the Deep Sea: A Review. *PLoS One* 5. doi:10.1371/journal.pone.0012449
- Vanreusel, A., Fonseca, G., Danovaro, R., da Silva, M.C., Esteves, A.M., Ferrero, T., Gad, G., Galtsova, V., Gambi, C., Genevois, V.D., Ingels, J., Ingole, B., Lampadariou, N., Merckx, B., Miljutin, D., Miljutina, M., Muthumbi, A., Netto, S., Portnova, D., Radziejewska, T., Raes, M., Tchesunov, A., Vanaverbeke, J., Van Gaever, S., Venekey, V., Bezerra, T.N., Flint, H., Copley, J., Pape, E., Zeppilli, D., Martinez, P.A., Galeron, J., 2010b. The contribution of deep-sea macrohabitat heterogeneity to global nematode diversity. *Mar. Ecol. Evol. Perspect.* 31, 6–20. doi:10.1111/j.1439-0485.2009.00352.x
- Vanreusel, A., Hilario, A., Ribeiro, P.A., Menot, L., Arbizu, P.M., 2016. Threatened by mining, polymetallic nodules are required to preserve abyssal epifauna. *Sci. Rep.* 6, 26808. doi:10.1038/srep26808

- Vanreusel, A., Vincx, M., Bett, B.J., Rice, A.L., 1995. Nematode biomass spectra at two abyssal sites in the NE Atlantic with a contrasting food-supply. *Int. Rev. Der Gesamten Hydrobiol.* 80, 287–296. doi:10.1002/iroh.19950800215
- Vanreusel, A., Vincx, M., Van Gansbeke, D., Gijssels, W., 1992. Structural Analysis of the meiobenthos communities of the shelf break area in two sites of the Gulf of Biscay. *Belgian J. Zool.* 122, 185–202.
- Veit-Köhler, G., Guilini, K., Peeken, I., Quillfeldt, P., Mayr, C., 2013. Carbon and nitrogen stable isotope signatures of deep-sea meiofauna follow oceanographical gradients across the Southern Ocean. *Prog. Oceanogr.* doi:http://dx.doi.org/10.1016/j.pocean.2013.01.001
- Veit-Köhler, G., Guilini, K., Peeken, I., Sachs, O., Sauter, E.J., Würzberg, L., 2011. Antarctic deep-sea meiofauna and bacteria react to the deposition of particulate organic matter after a phytoplankton bloom. *Deep. Res. Part II-Topical Stud. Oceanogr.* 58, 1983–1995. doi:10.1016/j.dsr2.2011.05.008
- Vincx, M., Bett, B.J., Dinert, A., Ferrero, T., Gooday, A.J., Lamshead, P.J.D., Pfannkuche, O., Soltwedel, T., Vanreusel, A., 1994. Meiobenthos of the deep Northeast Atlantic. *Adv. Mar. Biol.* Vol 30 30, 1–88.
- Warwick, H.M., Somerfield, P.J., Platt, R.M., 1998. Free-living marine nematodes part III - Monhysterids. Pictorial key to world genera and notes for the identification of British species.
- Wei, C.-L., Rowe, G.T., Escobar-Briones, E., Boetius, A., Soltwedel, T., Caley, M.J., Soliman, Y., Huettmann, F., Qu, F., Yu, Z., Pitcher, C.R., Haedrich, R.L., Wicksten, M.K., Rex, M.A., Baguley, J.G., Sharma, J., Danovaro, R., MacDonald, I.R., Nunnally, C.C., Deming, J.W., Montagna, P., Levesque, M., Weslawski, J.M., Włodarska-Kowalczyk, M., Ingole, B.S., Bett, B.J., Billett, D.S.M., Yool, A., Bluhm, B.A., Iken, K., Narayanaswamy, B.E., 2010. Global Patterns and Predictions of Seafloor Biomass Using Random Forests. *PLoS One* 5. doi:e1532310.1371/journal.pone.0015323
- Werbrouck, E., Van Gansbeke, D., Vanreusel, A., De Troch, M., 2016. Temperature Affects the Use of Storage Fatty Acids as Energy Source in a Benthic Copepod (*Platychelipus littoralis*, Harpacticoida). *PLoS One* 11, e0151779. doi:10.1371/journal.pone.0151779
- Whitehouse, M.J., Priddle, J., Symon, C., 1996. Seasonal and annual change in seawater temperature, salinity, nutrient and chlorophyll a distributions around South Georgia, South Atlantic. *Deep. Res. Part I-Oceanographic Res. Pap.* 43, 425–443. doi:10.1016/0967-0637(96)00020-9
- Whittaker, R.H., 1960. Vegetation of the Siskiyou mountains, Oregon and California. *Ecol. Monogr.* 30, 279–338.
- Whittaker, R.J., Willis, K.J., Field, R., 2001. Scale and species richness: towards a general, hierarchical theory of species diversity. *J. Biogeogr.* 28, 453–470. doi:10.1046/j.1365-2699.2001.00563.x
- Wieser, W., 1953. Beziehungen zwischen Mundhöhlengestalt, Ernährungsweise und Vorkommen bei freilebenden marinen Nematoden. *Ark. für Zool.* 4, 439–484.
- Wigley, R.L., McIntyre, A.D., 1964. Some quantitative comparisons of offshore meiobenthos and macrobenthos south of Martha's Vineyard. *Limnol. Oceanogr.* 9, 485–493. doi:10.2307/2833569

- Wilson, G., 1999. Some of the Deep-Sea Fauna Is Ancient. *Crustaceana* 72, 1019–1030. doi:10.1163/156854099503915
- Wilson, G.D., 1983. Variation in deep-sea Isopod *Eurycope iphthima* (ASELLOTA, EURYCOPIDAE) - Depth related clines in rostral morphology and in population structure. *J. Crustac. Biol.* 3, 127–140. doi:10.2307/1547858
- Wilson, G.D.F., Hessler, R.R., 1987. Speciation in the Deep Sea. *Annu. Rev. Ecol. Syst.* 18, 185–207. doi:10.1146/annurev.es.18.110187.001153
- Wiseman, J.D.H., Ovey, C.D., 1953. Definitions of Features on the Deep-Sea Floor. *Deep. Res.* 1, 11–16.
- Wolf-Gladrow, D., 2012. The expedition of the research vessel “Polarstern” to the Antarctic in 2012 (ANT-XXVIII/3) (Report), Berichte zur Polar- und Meeresforschung. Alfred Wegener Institute for Polar and Marine Research.
- Wolff, G.A., Billett, D.S.M., Bett, B.J., Holtvoeth, J., FitzGeorge-Balfour, T., Fisher, E.H., Cross, I., Shannon, R., Salter, I., Boorman, B., King, N.J., Jamieson, A., Chaillan, F., 2011. The Effects of Natural Iron Fertilisation on Deep-Sea Ecology: The Crozet Plateau, Southern Indian Ocean. *PLoS One* 6. doi:10.1371/journal.pone.0020697
- Woolley, S.N.C., Tittensor, D.P., Dunstan, P.K., Guillera-Arroita, G., Lahoz-Monfort, J.J., Wintle, B.A., Worm, B., O'Hara, T.D., 2016. Deep-sea diversity patterns are shaped by energy availability. *Nature* 533, 393–396.
- Wright, S.W., Jeffrey, S.W., 1997. High-resolution HPLC system for chlorophylls and carotenoids of marine phytoplankton, in: Jeffrey, S.W., Mantoura, R.F.C., Wright, S.W. (Eds.), *Phytoplankton Pigments in Oceanography*. UN Educational, Scientific and Cultural Organization, Paris, pp. 327–341.
- Würzberg, L., Peters, J., Schueller, M., Brandt, A., 2011. Diet insights of deep-sea polychaetes derived from fatty acid analyses. *Deep. Res. Part II-Topical Stud. Oceanogr.* 58, 153–162. doi:10.1016/j.dsr2.2010.10.014
- Würzberg, L., Zinkann, A.-C., Brandt, A., Janussen, D., Bohn, J.M., Schwabe, E., 2014. Intensity of pelagic–benthic coupling in different regions along the Antarctic Polar Front – Clues from abyssal megafauna. *Deep. Res. II* 108, 85–92. doi:http://dx.doi.org/10.1016/j.dsr2.2014.09.003
- Yoder, M., De Ley, I.T., King, I.W., Mundo-Ocampo, M., Mann, J., Blaxter, M., Poiras, L., De Ley, P., 2006. DESS: a versatile solution for preserving morphology and extractable DNA of nematodes. *Nematology* 8, 367–376. doi:10.1163/156854106778493448
- Zeppilli, D., Pusceddu, A., Trincardi, F., Danovaro, R., 2016. Seafloor heterogeneity influences the biodiversity–ecosystem functioning relationships in the deep sea. *Sci. Rep.* 6, 26352. doi:10.1038/srep26352
- Zeppilli, D., Vanreusel, A., Danovaro, R., 2011. Cosmopolitanism and biogeography of the genus *Manganonema* (Nematoda: Monhysterida) in the deep sea. *Animals* 1, 291–305. doi:10.3390/ani1030291



20,0 μm

List of publications

A1 Publications

Lins, L. Leliaert, F., Riehl, T., Ramalho, S., Cordova., E.A., Esteves, A., Vanreusel, A. Species variability and connectivity in the deep sea: evaluating effects of spatial heterogeneity and hydrodynamic effects. Biogeosciences Discussion, 2016.

Lins, L., da Silva, M.C., Hauquier, F., Esteves, A.M., Vanreusel, A. Nematode community composition and feeding shaped by contrasting productivity regimes in the Southern Ocean. Progress in Oceanography 134, p. 356-369, 2015.

Lins, L., Guilini, K., Veit-Köhler, G., Hauquier, F., Alves, R.M.S., Esteves, A.M., Vanreusel, A. The link between meiofauna and surface productivity in the southern ocean. Deep-Sea Research. Part 2. Tropical Studies in Oceanography. , v.108, p.60 - 68, 2014.

Brandt, A., Vanreusel, A., Bracher, A., Hoppe, C., **Lins, L.**, Meyer-Löbbecke, A., Altenburg Soppa, M., Würzberg, L. Are boundary conditions in surface productivity at the Southern Polar Front reflected in benthic activity?. Deep-Sea Research. Part 2. Tropical Studies in Oceanography. , v.108, p.51 - 59, 2014.

Lins, L., Vanreusel, A., Van Campenhout, J., Ingels, J.. Selective settlement of deep-sea canyon nematodes after resuspension - an experimental approach. Journal of Experimental Marine Biology and Ecology. , v.441, p.110 - 116, 2013.

Lima, R.C.C., **Lins, L.**, Silva, M. C., Esteves, A. M. Four new species of Syringolaimus De Man, 1888 (Nematoda, Ironidae) from the southeast Atlantic (Brazil), with redefinition of valid species and the proposal of a new key.. Zootaxa (Online). , v.2096, p.119 - 136, 2009.

C2 Publications (Dissertations, essays, internal reports, and conference abstracts)

Hauquier F., Mevencamp L., Great E., Bezerra T.N., **Lins L.**, Janssen F., Vonnahme T., Boetius A., Vanreusel A. Meiofauna response to physical disturbance at the DEA: the importance of scale to identify long-term effects. MIDAS Final meeting, 3-7 October 2016, Het Pand, Ghent, Belgium **(Contributed talk)**.

Mevenkamp L., Brown A., Guilini K., **Lins L.**, Moodley L., Stratmann T., Sweetman A., van Oevelen D., Westerlund S., Vanreusel A. Responses of nematodes to increased copper toxicity, tailings exposure and sediment deposition from *in situ* and laboratory experiments. MIDAS Final meeting, 3-7 October 2016, Het Pand, Ghent, Belgium **(Contributed talk)**.

Marcon Y., Purser A., Janssen, F., **Lins L.**, Brown, A., Boetius A. Megabenthic community structure within and surrounding the DISCOL experimental area 26 years after simulated manganese nodule mining disturbance. MIDAS Final meeting, 3-7 October 2016, Het Pand, Ghent, Belgium **(Contributed talk)**.

Guggolz T., Brandt A., Meißner K., **Lins L.** The Vema Fracture Zone – A bridge through the Mid-Atlantic Ridge? 12th International Polychaete Conference, 1-5 August 2016, National Museum Wales, Cardiff **(Contributed talk)**.

Lins, L., Leliaert, F. Riehl, T., Ramalho, Sofia P., Cordova, E. A., Esteves, A. M., Vanreusel, A. A multifaceted approach to understanding spatial turnover and connectivity in the deep sea. 16th International Meiofauna Conference, 3-8 July 2016, Heraklion, Crete, Greece **(Contributed talk)**.

Bezerra, T. N., Lima, R. C., **Lins, L.**, Silva, C., Passotti, F., Esteves, A., Vanreusel, A., Moens, T. Global-Scale distribution of *Microloaimus* de Man, 1880 with updated list of valid species. 16th International Meiofauna Conference, 3-8 July 2016, Heraklion, Crete, Greece **(Contributed talk)**.

Ramalho, S.P., **Lins, L.**, Lampadariou, N., Vanreusel, A., Cunha, M.R. Deep-sea megafaunal response to physical disturbance along the SW Portuguese continental slope. PeerJ PrePrints 4:e1745v1 <https://doi.org/10.7287/peerj.preprints.1745v1> **(Contributed talk)**.

Ramalho, S.P., **Lins, L.**, Pape, E., Lampadariou, N., Vanreusel, A., Cunha, M.R. Impact of trawling on benthic diversity and functioning in the SW Portuguese continental slope. 14th Deep-sea biology symposium, 31/08 – 04/09/2015, Aveiro, Portugal **(Poster)**.

Ingels J, Allcock L, Bourque J, Demopoulos ⁴, Kiriakoulakis K, **Lins L**, Martin D, Robertson C, Roman S, Rueggeberg A, Vanreusel A, Wolff G. The curious tale of *Astomonema* in the deep sea – a chemosynthetic worm feeling at home in submarine canyons. 14th Deep-sea biology symposium, 31/08 – 04/09/2015, Aveiro, Portugal **(Contributed talk)**.

Lins, L., Esteves, A.M., Vanreusel, A.. Differences in primary productivity regulating benthic standing stocks in the Southern Ocean, 2015. 2015 ASLO Aquatic Sciences Meeting (Granada, Spain). **(Contributed talk)**.

Lins, L., Vanreusel, A. How strong is the link between CO₂ carbon flux and benthic communities in the Southern Ocean? Young Marine Scientists' Day, 2015 (Brugge, Belgium). **(Poster)**.

Lins, L., Hauquier, F., Esteves, A.M., Vanreusel, A. Insights on the link between surface productivity and benthic communities in the deep sea. Young Marine Scientists' Day, 2014 (Brugge, Belgium). **(Contributed talk)**.

Lins, L., Hauquier, F., Esteves, A.M., Vanreusel, A. Primary Productivity regulating benthic standing stocks in the Southern Ocean. Mares Conference - Marine Ecosystems Health and Conservation, 2014 (Olhão, Portugal) **(Poster)**.

Lins, L., Ingels, J., Vanreusel, A. Distribution and habitat selectivity of deep-sea canyon nematodes. 13th International deep-sea biology Symposium, 2012 (Wellington, New Zealand). , 2012. (Contributed talk).

Lins, L., Lima, R.C.C., Santos, P. J.P., Silva, A. P.C., Genevois, V. F., Esteves, A. M. Padrões de distribuição vertical de Nematoda da praia arenosa de Maracaípe (Arraial do Cabo, Brazil). VIII Encontro de Bioincrustação, Ecologia Bêntica e Biocorrosão, 2009. **(Contributed talk)**.

Lima, R., **Lins, L.**, Esteves, A.M. *Syringolaimus* De Man, 1888 (Ironidae - Nematoda) at Campos Basin (Rio de Janeiro, Brazil): Is water depth a trend to body size?. Thirteenth International Meiofauna Conference, 2007 (Recife, Brazil)

Websites

Vanaverbeke, J., Bezerra, T.N., Braeckman, U., De Groote, A., de Meester, N., Deprez, T., Derycke, S., Gilarte, P., Guilini, K., Hauquier, F., **Lins, L.**, Maria, T., Moens, T., Pape, E., Smol, N., Taheri, M., Van Campenhout, J., Vanreusel, A., Wu, X., Vincx, M. Nemys: World Database of Free-living Marine Nematodes, 2015.